TECHNISCHE UNIVERSITÄT MÜNCHEN
Lehrstuhl für Mikrobielle Ökologie

Characterization of *Listeria sensu stricto* specific genes involved in colonization of the gastrointestinal tract by *Listeria monocytogenes*

Jakob Johannes Schardt

Vollständiger Abdruck der von der Fakultät Wissenschaftszentrum Weihenstephan für Ernährung, Landnutzung und Umwelt der Technischen Universität München zur Erlangung des akademischen Grades eines

Doktors der Naturwissenschaften

genehmigten Dissertation.

Vorsitzender: Prof. Dr. rer.nat. Siegfried Scherer

Prüfende der Dissertation: 1. apl.Prof. Dr.rer.nat. Thilo Fuchs

2. Prof. Dr.med Dietmar Zehn

Die Dissertation wurde am 18.01.2018 bei der Technischen Universität München eingereicht und durch die Fakultät Wissenschaftszentrum Weihenstephan für Ernährung, Landnutzung und Umwelt am 14.05.2018 angenommen.

Table of contents

List of figures

List of tables

List of abbreviations

1,2-PD	1,2-propanediol
ABC	ATP-binding cassette
ABM	Antibiotic biosynthesis monooxygenase
ADI	Arginine deiminase
AgDI	Agmatine deiminase
ANI	Average nucleotide identities
ANIb	BLAST average nucleotide identities
ATCC	American type culture collection
B_{12}	Vitamin B_{12} (cobalamin)
BCCM	Belgian coordinated collection of microorganisms
BHI	Brain heart infusion
BLAST	Basic local alignment search tool
bp	Base pairs
BSH	Bile salt hydrolase
Caco-2	Human epithelial colorectal adenocarcinoma cells
cfu	Colony forming units
CI	Competitive index
COG	Cluster of orthologous groups
DC	Dendritic cells
ddH_2O	Double distilled H_2O
DEPC	Diethylpyrocarbonate
DMEM	Dulbecco's Modified Eagle Medium
DPD	2,2'-dipyridyl
E. coli	*Escherichia coli*
e.g.	Exempli gratia (for example)
EC	Epithelial cells
EDTA	Ethylenediaminetetraacetic acid
EtOH	Ethanol
FCS	Fetal calf serum
FDR	False discovery rate
GAD	Glutamate decarboxylase
GI	Gastrointestinal
GIT	Gastrotintestinal tract
HEp-2	Human larynx squamous cell carcinoma cells
i.e.	Id est (that is)
i.g.	Intragastric
i.p.	Intraperitoneal
i.v.	Intravenous
IPA	Isotopologe profiling analysis
IPTG	Isopropyl β-D-1-thiogalactopyranoside
IVC	Individually ventilated cage
L.	*Listeria*
LB	Lysogeny broth
LIPI-1	Listeria pathogenicity island 1
Log_2FC	Logarithm base 2 fold-change

LP	Lamina propria
MLNs	Mesenteric lymph nodes
MM	Minimal medium
MOI	Multiplicity of infection
MQ-H_2O	Milli-Q water
MRCA	Most recent common ancestor
MRI	Max Rubner-Institute
NBD	Nucleotide binding domain
NGS	Next generation sequencing
NS	Not significant
nt	Nucleotides
p.i.	Post infection
PBS	Phosphate buffered saline
PCR	Polymerase chain reaction
PGAP	Prokaryotic Genome Annotation Pipeline
PrfA	Positive regulatory factor A
PTS	Phosphotransferase systems
qRT-PCR	Quantitative real-time reverse transcription PCR
R^2	Coefficient of determination
RAST	Rapid annotation using subsystem technology
RBS	Ribosome binding site
RPKM	Reads per kilobase per million mapped reads
RT	Room temperature
RTL	Relative transcription levels
S.	*Salmonella*
SBP	Solute binding protein
SOC	Super optimal broth
sp. nov.	Novel species
spp.	Species
ssp.	Subspecies
TAE	Tris-acetate-EDTA
TCA	Tricarboxylic acid
T_d	Doubling time
TMD	Transmembrane domains
TSS	Transcription start site
WGS	Whole genome shotgun
YE	Yeast extract

Abstract

Listeria monocytogenes is a Gram-positive bacterium and the causative agent of listeriosis. This foodborne pathogen can colonize the mammalian gastrointestinal tract and cause subsequent systemic disease by crossing the intestinal barrier. The genus *Listeria* is divided into two distinct clades: *Listeria sensu stricto* and *Listeria sensu lato*. *Listeria sensu stricto* includes the pathogenic species *L. monocytogenes* and *L. ivanovii,* as well as four other apathogenic species, all of which have been isolated from food or animal sources such as the gastrointestinal tract or feces. During recent years, several novel species have been discovered, which are supposedly environmental strains and form the *Listeria sensu lato.* In this thesis, *in vivo* colonization experiments with different representatives of the *Listeria sensu stricto* and *Listeria sensu lato* clades were performed for the first time. Using a novel oral infection model for BALB/c mice, it was shown that the former group is able to at least transiently colonize the gastrointestinal (GI) tract of mice, although only the pathogenic *L. monocytogenes* was able to invade the intestinal mucosa. In contrast, the environmental *Listeria sensu lato* were rapidly cleared from the intestines of infected mice, and thus, seemed to be less adapted to the conditions encountered during the GI passage. To gain further insight into the genomic determinants responsible for this discrepancy, a genome comparison between *Listeria sensu lato* species and the pathogenic *L. monocytogenes* was performed. Apparently, not only the classical virulence genes from the LIPI-1 and the *inlAB* locus are missing in the apathogenic strains, but also several genes that are key for surviving the harsh conditions encountered in the gut. Based on the colonization experiments, it was hypothesized that yet unknown genes associated with virulence and colonization are present in the clade *Listeria sensu stricto* but missing in the *Listeria sensu lato*. To verify this assumption, a genome comparison was conducted to identify factors from *L. monocytogenes* conserved in the former, but absent in the latter clade. Indeed, several of the 151 obtained genes have not yet been investigated for their potential role in virulence and colonization. Of these, two interesting candidates were selected, and in-frame deletion mutants were constructed to evaluate their contribution during the infection process using *in vitro* and *in vivo* methods. The operon lmo1131-1132 encoding for a putative ABC transporter was involved in adherence and invasion in cultures of Caco-2 cells. Further analysis revealed that regulation of this operon was dependent on temperature levels as well as oxygen and iron availability. Finally, the role of this transporter in colonization was assessed in mice after oral infection. Deletion of lmo1131-1132 led to decreased persistence in the ileal lamina propria and to reduced bacterial loads in the liver. Additional candidate genes from a cluster for the degradation of 1,2-propanediol (1,2-PD) were also analyzed. Enhanced anaerobic growth of *L. monocytogenes* EGDe by supplementation with 1,2-PD as a potential energy and carbon source was shown for the first time, and the induction of the corresponding *pdu* genes was proven. Deletion of *pduD* led to shortened survival of *L. monocytogenes* in the mouse GI tract after oral infection, thus confirming the relevance of 1,2-PD catabolism for listerial proliferation during infection.

Zusammenfassung

Das Gram-positive Bakterium *L. monocytogenes* ist der Auslöser der Krankheit Listeriose. Nach Kolonisierung des Darms ist das Lebensmittelpathogen in der Lage, die Darmbarriere zu überqueren und eine systemische Erkrankung auszulösen. Die Gattung *Listeria* besteht aus zwei individuellen monophyletischen Gruppen: *Listeria sensu stricto* und *Listeria sensu lato*. Die pathogenen *L. monocytogenes* und *L. ivanovii* sowie vier weitere apathogene Spezies bilden die *Listeria sensu stricto* und konnten in der Vergangenheit aus dem Darminhalt oder Kot von Tieren oder aus tierischen Lebensmitteln isoliert werden. Die meisten Mitglieder der *Listeria sensu lato* wurden erst in den letzten Jahren entdeckt und sind vermutlich reine Umweltspezies. In dieser Arbeit wurden zum ersten Mal verschiedene Vertreter beider Gruppen auf ihre Kolonisierungsfähigkeit in einem *in vivo* Mausmodell nach oraler Infektion untersucht. Es konnte gezeigt werden, dass die Mitglieder der *Listeria sensu stricto* zumindest vorübergehend in der Lage sind, den tierischen Darm zu kolonisieren, wenngleich *L. monocytogenes* als einzige Spezies in das Darmgewebe eindringen konnte. Im Gegensatz dazu zeigten die *Listeria sensu lato* Spezies eine schlechtere Anpassung an die Bedingungen im Gastrointestinaltrakt und wurden rasch beseitigt. Um die verantwortlichen genomischen Unterschiede zwischen beiden Gruppen aufzuklären, wurden die Genome der *Listeria sensu lato* mit der pathogenen Spezies *L. monocytogenes* verglichen. Neben klassischen Virulenzgenen wie LIPI-1 und *inlAB* fehlten eine Reihe von Genen, die am Überleben unter den Stressbedingungen des Darms beteiligt sind. Auf Grundlage der Kolonisierungsexperimente wurde die Hypothese aufgestellt, dass noch weitere, bisher unbekannte genetische Faktoren für die Virulenz und Kolonisierung des Darms in der *Listeria sensu stricto* Klade vorhanden sein müssen, die in der *Listeria sensu lato* Gruppe fehlen. Zur Überprüfung wurden ein Genomvergleich durchgeführt und 151 Gene identifiziert, die eine Beteiligung an den genannten Prozessen nahelegen. Aus dieser Liste wurden zwei vielversprechende Kandidaten ausgewählt und Deletionsmutanten erstellt, die mittels verschiedener *in vitro* und *in vivo* Methoden auf eine Beteiligung während der Infektion untersucht wurden. Das Operon lmo1131-1132, das für ein ABC Transportsystem kodiert, hatte Einfluss auf die Adhärenz- und Invasionsfähigkeit im Caco-2 Zellkulturmodell. Weitere Analysen offenbarten eine Regulation des Operons in Abhängigkeit von Temperatur sowie Sauerstoff- und Eisenverfügbarkeit. Die Bedeutung des Transporters für die orale Infektion wurde in Mäusen untersucht. Eine Deletion von lmo1131-1132 bewirkte eine verringerte Persistenz in der Lamina Propria des Ileums und verminderte Bakterienzahlen in der Leber. Ebenfalls wurden Kandidatengene aus der Genregion für den Abbau von 1,2-Propandiol (1,2-PD) untersucht. Zum ersten Mal konnte ein verbessertes anaerobes Wachstum von *L. monocytogenes* durch die Zugabe von 1,2-PD sowie eine Induktion der entsprechenden *pdu* Gene gezeigt werden. Die Deletion von *pduD* bewirkte ein verkürztes Überleben von *L. monocytogenes* im Mausdarm nach oraler Infektion und bestätigte die Bedeutung des Katabolismus von 1,2-PD für die listerielle Proliferation während der Infektion.

1 Introduction

1.1 The genus *Listeria*

Listeria are Gram-positive, facultative anaerobic, non-sporulating bacteria that form regular, short rods about 0.4-0.5 x 1-2 µm in size (McLauchlin & Rees, 2015). Together with the closely related genera *Bacillus*, *Staphylococcus*, *Enterococcus*, *Streptococcus* and *Clostridium*, the genus *Listeria* belongs to the division of Firmicutes, a large group of Gram-positive bacteria characterized by a low GC content (36-42 %) (Sallen *et al.*, 1996; Collins *et al.*, 1991). Currently, there are 17 characterized *Listeria* species (spp.), which are divided into two distinct clades, the *Listeria sensu stricto* and *Listeria sensu lato* (Chiara *et al.*, 2015; Orsi & Wiedmann, 2016).

1.1.1 *Listeria sensu stricto*

The most well-known member of the genus *Listeria* is *Listeria monocytogenes*, which causes the disease listeriosis in humans and animals (Farber & Peterkin, 1991). It was first isolated in the 1920s from infected laboratory animals (Murray *et al.*, 1926). For many years, *L. monocytogenes* was believed to be the only bacterium of the genus *Listeria* until the discovery of *L. grayi* in 1966, which is a member of the *Listeria sensu lato* group (Larsen & Seeliger 1966). During the 70s and 80s, scientists described four more species, *L. innocua* (Seeliger, 1981), *L. seeligeri*, *L. welshimeri* (Rocourt & Grimont, 1983) and *L. ivanovii* (Seeliger *et al.*, 1984), which are closely related to *L. monocytogenes*. It took more than 25 years until the next species, *L. marthii*, was discovered (Graves *et al.*, 2010). Together, they constitute the so-called *Listeria sensu stricto* group, Latin for "*Listeria* in the narrow sense", in opposition to the *Listeria sensu lato*, i.e. the "*Listeria* in the wider sense", which comprises a quite extensive number of *Listeria* spp. that have been discovered during recent years (Orsi & Wiedmann, 2016).

The *Listeria sensu stricto* spp. can be found ubiquitously in nature. They have been isolated from a variety of different ecological niches like soil, surface waters, sewage, food-processing environments and vegetation throughout the world (Sauders & Wiedmann, 2007; Orsi & Wiedmann, 2016). Several studies reported a high prevalence of these species in large-scale analyses of soil and water samples from both urban and rural environments ranging from 22.3 % to up to 72 %, with many samples harboring more than one species (Linke *et al.*, 2014; Sauders *et al.*, 2012; Stea *et al.*, 2015). In addition, there are numerous reports for the isolation of not only *L. monocytogenes,* but all other *Listeria sensu stricto* members from feces or the gastrointestinal tracts (GIT) of mostly symptom-free animals (Antoniollo *et al.*, 2003; Rocourt & Seeliger, 1985; Inoue *et al.*, 1991; Husu 1990; Skovgaard *et al.*, 1988; Lawan *et al.*, 2013) and from food of animal origin (Farber *et al.*, 1989; Osaili *et al.*, 2011; Soriano *et al.*, 2001; Huang *et al.*, 2007; Gebretsadik *et al.*, 2011; Nayak *et al.*, 2015; Dahshan *et al.*, 2016).

The only *Listeria sensu stricto* spp. regularly associated with pathogenicity in animals and humans are *L. monocytogenes* and *L. ivanovii*, the latter of which rarely affects humans (Cummins *et al.*, 1994; Guillet *et al.*, 2010) but mainly causes listeriosis in ruminants (Alexander *et al.*, 1992; Chand & Sadana, 1999; Sergeant *et al.*, 1991). Three genomic loci were identified to encode key virulence genes in these species: (i) The *Listeria* Pathogenicity Island 1 (LIPI-1) consists of six genes (*prfA*, *plcA*, *hly*, *mpl*, *actA*, *plcB*), which are responsible for intra- and intercellular motility and intracellular survival (Vázquez-Boland *et al.*, 2001a) (ii) The *inlAB* locus encodes the two internalins InlA and InlB. These surface proteins mediate the invasion of host cells (Pizarro-Cerda *et al.*, 2012) (iii) A third internalin locus *inlC* is required for cell-to cell spread (Rajabian *et al.*, 2009).

About 40 to 60 million years ago, the most recent common ancestor (MRCA) of the *Listeria sensu stricto* group acquired these genes via horizontal gene transfer (Schmid *et al.*, 2005; den Bakker *et al.*, 2010b). The pathogenicity loci were lost in several separate events, which coincide with the evolutionary transition of multiple *Listeria* spp. from a facultative pathogenic lifestyle to an obligate saprophytic lifestyle (den Bakker *et al.*, 2010b). *L. welshimeri* and *L. marthii* are non-pathogenic species, whose genomes lack LIPI-1, *inlAB* and *inlC* (den Bakker *et al.*, 2010a; den Bakker *et al.*, 2010b). Consequently, they provide negative results in hemolysis and phosphatidyl-inositol-phospholipase C activity test, which are used to assess the presence of *hly* (encoding for the Listeriolysin O) and *plcA* (encoding the phosphatidyl-inositol-phospholipase C). Isolates of *L. seeligeri* are typically hemolytic, since they possess the LIPI-1 but are missing *inlAB* and *inlC* (den Bakker *et al.*, 2010a; den Bakker *et al.*, 2010b). Although they are generally considered non-pathogenic, there are some possible cases of human listeriosis due to *L. seeligeri* (Rocourt *et al.*, 1986). Recent secondary losses occurred in a few non-hemolytic strains, which are missing the LIPI-1 (Volokhov *et al.*, 2006). *L. innocua* is generally considered non-pathogenic, although there are a small number of hemolytic strains containing the LIPI-1 but missing *inlAB* and *inlC* (Johnson *et al.*, 2004; den Bakker *et al.*, 2010a; den Bakker *et al.*, 2010b; Moreno *et al.*, 2014). One fatal case of human listeriosis caused by *L. innocua* has been reported (Perrin *et al.*, 2003), indicating that at least some strains have the potential to cause invasive disease (den Bakker *et al.*, 2010a). Interestingly, similar evolutionary paths of transition to obligate saprophytism can also be observed in several *L. monocytogenes* isolates, which show attenuated virulence after mutations in *prfA* or *inlA* (Maury *et al.*, 2017; Nightingale *et al.*, 2008).

1.1.2 *Listeria sensu lato*

During recent years, a quite extensive number of novel *Listeria* spp. have been discovered, which, together with *L. grayi* (Larsen & Seeliger, 1966), cluster in a distinct clade, the *Listeria sensu lato*. These species include *L. rocourtiae* (Leclercq *et al.*, 2010) *L. fleischmannii* (Bertsch *et al.*, 2013), *L. floridensis*, *L. aquatica*, *L. cornellensis, L. grandensis*, *L. riparia* (den Bakker *et al.*, 2014), *L. newyorkensis*, *L. booriae*

(Weller *et al.*, 2015) and *L. weihenstephanensis* (Lang Halter *et al.*, 2013). *Listeria sensu lato* strains have been isolated from cheese, running water, a seafood and a dairy processing plant, pre-cut lettuce and vegetation. All *Listeria sensu lato* spp. are considered to be non-pathogenic since they lack hemolytic and phosphoinositide phospholipase C activity (Bertsch *et al.*, 2013; den Bakker *et al.*, 2014; Lang Halter *et al.*, 2013; Weller *et al.*, 2015; Leclercq *et al.*, 2010). Additionally, their genomes encode only a small number of internalin-like proteins (Chiara *et al.*, 2016; den Bakker *et al.*, 2010b), which have been shown to be important for the interaction of *Listeria* with mammalian host cells (Pizarro-Cerda *et al.*, 2012). Consequently, the only *Listeria sensu lato* member tested for interaction with human intestinal epithelial cells, *L. fleischmannii*, was unable to invade Caco-2 cells (Bertsch *et al.*, 2013). Since all *Listeria sensu lato* spp. except for *L. grayi* have been discovered recently, further data on virulence *in vitro* and particularly *in vivo*, is missing.

1.2 The pathogenic *L. monocytogenes*

The most prominent member of the genus *Listeria* is the pathogenic species *L. monocytogenes*, a foodborne pathogen causing the disease listeriosis in humans and animals. It was first discovered by Gustav Hülphers in 1911 in the liver of infected rabbits, although he named the bacterium *Bacillus hepatis* and did not preserve the strains. The first isolation is therefore ascribed to Everitt Murray in 1923, who investigated six cases of sudden death in young rabbits. Infection experiments with laboratory animals led to monocytosis and lesions in the lungs, therefore he named the isolate *Bacterium monocytogenes* and published his findings three years later (Murray *et al.*, 1926) before Harvey Pirie changed the name to *Listeria monocytogenes* in 1940 (Pirie, 1940). The potential threat as a human pathogen was not realized until several cases of listeriosis in newborns were reported in the late 1940s and early 1950s in Germany, which lead to the start of listeriosis research resulting in one of the first comprehensive reports in 1961 by H.P.R Seeliger (Seeliger, 1961). Although Murray mentioned oral transmission as a possible infection route in his original publication, *L. monocytogenes* was not recognized as a foodborne pathogen until 1983 when an outbreak caused by coleslaw occurred in Halifax, Canada (Schlech *et al.*, 1983).

1.2.1 Human listeriosis

L. monocytogenes is the causative agent of human listeriosis and has been isolated from a variety of different foods, including meat and dairy products, vegetables, ready-to-eat food and seafood (Farber & Peterkin, 1991). In 2015, 2,206 cases were reported in the EU, a low incidence compared to infection numbers of *Campylobacter*, *Salmonella*, or *Yersinia*. Nevertheless, listeriosis is a major public health concern due to the high fatality rate of 17.7 % and because it mainly affects the elderly population (EFSA Journal 2016). Other risk groups include neonates or immunocompromised persons, as well as pregnant women. These susceptible populations are prone to the development of serious symptoms

such as meningitis, meningoencephalitis, septicemia and prenatal infection (Schuchat *et al.*, 1991; Cossart & Toledo-Arana, 2008). In contrast, infection of healthy adults mostly leads to self-limiting, febrile gastroenteritis, which can last up to two days. Symptoms may include fever, watery diarrhea, headache, nausea and pain in joints and muscles (Ooi & Lorber, 2005; Aureli *et al.*, 2000; Dalton *et al.*, 1997; Frye *et al.*, 2002). In addition, asymptomatic carriage of *L. monocytogenes* has been reported in 1-5 % of healthy adults (MacGowan *et al.*, 1994; Hof, 2001; Grif *et al.*, 2003) or even in up to 25 % of family members living in the same household as listeriosis patients (Schuchat *et al.*, 1991; Schuchat *et al.*, 1993). A study by Grif and colleagues examined 868 stool samples from three healthy volunteers over the course of one year and was able to prove an incidence of 5-9 exposures to *L. monocytogenes* and two episodes of asymptomatic carriage per person per year (Grif *et al.*, 2003). Contact with the foodborne pathogen is frequent, and it is estimated that immunocompetent healthy adults orally ingest ca. 10^5 *L. monocytogenes* cells approximately four times in one year (Notermans *et al.*, 1998). For these reasons, *L. monocytogenes* can be characterized as an opportunistic pathogen which can colonize the GIT of humans after oral ingestion and cause gastroenteritis in healthy individuals; however, it is also able to cause a systemic infection in risk groups leading to severe symptoms with a high fatality rate.

1.2.2 *L. monocytogenes* as an intracellular model pathogen

L. monocytogenes is capable of invading both professional phagocytes like macrophages or dendritic cells (DC) and non-professional phagocytes like fibroblasts, epithelial or endothelial cells. Therefore, it has become a model organism to study the lifestyle of intracellular pathogens. Most studies have been carried out *in vitro* in cell culture or *in vivo* via intravenous (i.v.) and intraperitoneal (i.p.) injection in animal models. The pathogen possesses a set of specialized virulence factors enabling the intracellular life cycle which consists of host cell adhesion and invasion, intracellular multiplication and motility, and intercellular spread (Camejo *et al.*, 2011). The genomic locus *inlAB*, encoding two surface proteins Internalin A and Internalin B, mediates entry into the non-phagocytic host cells by binding to receptors of the host cell. This leads to manipulation of the host cell signaling and subsequent actin polymerization and membrane remodeling, thereby resulting in phagocytosis of the bacterium (Seveau *et al.*, 2007). Inside the phagosome of non-phagocytic cells as well as phagocytic cells, *L. monocytogenes* prevents maturation and secretes the pore-forming listeriolysin O (LLO) and two phospholipases A (PlcA) and C (PlcB) to gain access to the host cell cytosol (Krawczyk-Balska & Bielecki, 2004; Hamon *et al.*, 2012). In the cytosol, it exploits the host cell's actin machinery for intracellular motility. The surface protein ActA mediates actin polymerization at one bacterial end, thus "pushing" the bacterium through the cytosol (Pillich *et al.*, 2017). This intracellular motility allows for the invasion of adjacent cells via cell-to-cell spread by protrusion into the neighboring cell and subsequent uptake into a double-membrane vacuole of non-infected cells. This membrane is lysed again by LLO and PlcB,

resulting in access to the cytosol of the neighboring cell (Dussurget, 2008; Vázquez-Boland *et al.*, 2001b). A novel study on the intercellular spread suggest that *L. monocytogenes* eventually stops producing ActA and becomes trapped in so-called *Listeria*-containing vacuoles, thus switching from an active motile lifestyle to a non-replicative state of persistence. This is thought to be responsible for the long incubation period in humans and to favor asymptomatic carriage (Kortebi *et al*., 2017).

Additional virulence factors for the intracellular life of *L. monocytogenes* have been investigated (Schultze *et al.*, 2015; Chatterjee *et al.*, 2006; Joseph *et al.*, 2006), especially with regard to its metabolism in the host cytosol (Joseph and Goebel, 2007; Schauer *et al.*, 2009; Schauer *et al.*, 2010; Grubmüller *et al.*, 2014; Fuchs *et al.*, 2012a; Chen *et al.*, 2017). The host cell cytosol is a complex environment with a variety of different carbon, nitrogen, phosphorus and sulfur sources (Brown *et al.*, 2008), to which *L. monocytogenes* specifically adapts (Eisenreich *et al.*, 2010). Transcriptomics and proteomics studies (Chatterjee *et al.*, 2006, Joseph *et al.*, 2006; van de Velde *et al.*, 2009) as well as isotopologe profiling analysis (IPA) (Eylert *et al.*, 2008) during intracellular growth have contributed to a better understanding of metabolism after invasion of host cells. Glucose, glucose-6-phosphate as well as glycerol and amino acids have been identified as possible carbon sources by IPA studies (Eylert *et al.*, 2008). While the genes involved in glycolysis have been shown to be downregulated in macrophages or epithelial cells, genes for the oxidative pentose phosphate pathway were upregulated, suggesting that the latter is the preferred pathway during sugar catabolism (Chatterjee *et al.*, 2006; Joseph *et al.*, 2006). Studies suggest that glucose-6-phosphate is oxidized by the pentose phosphate pathway and serves as a precursor for nucleotide biosynthesis and aromatic compounds, whereas glycerol is used for energy production and amino acids biosynthesis via glycolysis. Nevertheless, alternative carbon sources are likely to be present during intracellular replication (Grubmüller *et al*., 2014). Glycerol might be obtained from the breakdown of phosphatidylethanolamine in mammalian membranes by the listerial phosphatidylcholine phospholipase C, thus liberating glycerol and ethanolamine (Tsoy *et al*., 2009; Geoffroy *et al*., 1991). The latter could serve as an alternative carbon and nitrogen sources since Listeriae lacking genes from the *eut* gene cluster for the degradation of ethanolamine exhibited a defect in intracellular replication in epithelial cells (Joseph *et al*., 2006; Joseph & Goebel, 2007).

Worthy of note, the tricarboxylic acid (TCA) cycle in *L. monocytogenes* is interrupted since the genes for a 2-oxoglutarate dehydrogenase are missing (Eisenreich *et al.*, 2006; Glaser *et al.*, 2001). Therefore, the main function of 2-oxoglutarate is to serve as a precursor of glutamine, which plays a key role in connecting the carbon and nitrogen metabolism. Besides ethanolamine, ammonium, glutamine, and arginine have been discussed as possible intracellular nitrogen sources (Buchrieser *et al.*, 2003; Joseph *et al.*, 2006; Joseph & Goebel, 2007; Kutzner *et al.*, 2016). Depending on the nitrogen source, 2-

oxoglutarate levels have been hypothesized to regulate transcription of TCA cycle genes based on *in vitro* studies (Picossi *et al.*, 2007; Schardt, 2014). Intracellular nitrogen sources could act as an environmental cue influencing virulence gene expression as was observed for glutamine (Haber *et al.*, 2017). Oxaloacetate needs to be channeled into the tricarboxylic acid cycle via anaplerotic reactions since it is an important intermediate for the synthesis of asparagine, aspartate, lysine and threonine as well as arginine, histidine and purine. Lastly, oxaloacetate is the acceptor for acetyl-CoA in the initial step of the tricarboxylic acid cycle (Sauer & Eikmanns, 2005). This is performed by the pyruvate carboxylase PycA, since a *pycA* deletion mutant was unable to replicate in macrophages and epithelial cells and was highly attenuated in mice after i.v. infection (Schär *et al.*, 2010). IPA proved that the majority of bacterial amino acids is acquired from the host cell cytosol (Eylert *et al.*, 2008) and several transporters involved in uptake of amino acids or oligopeptides were shown to be involved in intracellular survival (Joseph *et al.*, 2006; Schauer *et al.*, 2010). *L. monocytogenes* requires several vitamins including biotin, riboflavin, cobalamin or thiamine as cofactors for enzymatic reactions. *De novo* biosynthesis of thiamine plays a vital role for intracellular metabolism and the transporter ThiT was shown to be involved in thiamine uptake and proliferation in epithelial cells (Schauer *et al.*, 2009). Biotin and riboflavin are probably taken up from the host cell cytosol via transporters (Dowd *et al*., 2011; Karpowich *et al*., 2015; Matern *et al*., 2016).

1.2.3 Animal models for *in vivo* studies on listeriosis

Most of the knowledge about the pathophysiology of *L. monocytogenes* is derived from the study of animal models. Since the incidence of listeriosis in humans is low and incubation periods can be long, epidemiological data and clinical case reports are often insufficient to illuminate the transmission routes, the number of consumed *L. monocytogenes* cells, or the original food vehicles (Hoelzer *et al.*, 2012). As an example, the dose-response relationship of listeriosis in humans, i.e. the likelihood of invasive disease after ingestion of a certain number of *L. monocytogenes* cells, has not been clearly established. The infection dose for healthy individuals has been estimated to be ca. 10^6-10^7 colony forming units (cfu) (FAO/WHO 2004; Farber *et al.*, 1996; Smith *et al.*, 2008).

Besides the ability to cause disease in humans, *L. monocytogenes* has a broad host range including at least domestic and wild ruminants like sheep, cattle, goats, deer, and antelopes. In addition, sporadic cases of listeriosis have been reported in non-human primates and birds. Rodents are frequently used as animal infection models since they are small, inexpensive and easy to breed and house. *L. monocytogenes* can infect, amongst others, mice, rats, guinea pigs and rabbits, which are the most common species for *in vivo* studies on listeriosis (Hoelzer *et al.*, 2012).

An ideal model should closely mimic the course, the infection dose and the transmission of human disease. In contrast to humans, most animal models seem to require much larger inocula to establish

infection (10^8-10^{10} cfu) (D'Orazio, 2014). This high resistance to oral inoculation led to the preferred use of i.v. and i.p. infection models, which were helpful for the elucidation of intracellular virulence factors and the innate and adaptive immune response to *L. monocytogenes* infection. As a major drawback, they do not represent the natural course of listeriosis since they bypass the gastrointestinal (GI) phase of infection (Bou Ghanem *et al.*, 2013a). Intragastric inoculation (i.g). methods usually require large infection doses and were not able to generate a reproducible period of GI infection prior to systemic spread in the past (Czuprynski *et al.*, 2003; Gajendran *et al.*, 2007; Pron *et al.*, 1998; Lecuit *et al.*, 2001; Wollert *et al.*, 2007, Bou Ghanem *et al.*, 2013a). It is possible that i.g. inoculation causes physical trauma in the esophagus that facilitates direct invasion of the bloodstream (D'Orazio, 2014). To circumvent this problem, a novel model for the oral infection of BALB/c mice was developed (Bou Ghanem *et al.*, 2012; Bou Ghanem *et al.*, 2013a; Bou Ghanem *et al.*, 2013b). Inoculation occurs via *L. monocytogenes*-contaminated bread pieces. This natural feeding method is non-traumatic and requires no specialized skills by the researchers. It causes a reproducible delay of systemic spread after GI colonization, which results in a distinct course of disease mimicking human listeriosis. This novel mouse model specifically enables studies focused on the GI phase of infection, crossing of the intestinal barrier and systemic dissemination during listeriosis (Bou Ghanem *et al.*, 2012; Bou Ghanem *et al.*, 2013a; Bou Ghanem *et al.*, 2013b).

Another major problem is the species-specific interaction of the internalins InlA and InlB with their host cell receptors (D'Orazio, 2014). While InlA has a high affinity for human, guinea pig and rabbit E-cadherin, murine and rat E-cadherin is not able to promote internalization of *L. monocytogenes* into host cells (Lecuit *et al.*, 1999). Similarly, InlB interacts with human, mouse and rat host receptor c-Met, but not with guinea pig and rabbit c-Met (Khelef *et al.*, 2006). Two mouse strains have been engineered to increase the interaction between InlA and E-cadherin. The first strain expresses both human and murine E-cadherin in enterocytes of the small intestine (Lecuit *et al.*, 2001), the second strain possesses a "humanized" E-cadherin, which was created by a knock-in with a single amino acid substitution in the murine polypeptide (Disson *et al.*, 2008). Another approach was chosen by Wollert and colleagues, who increased affinity of *L. monocytogenes* InlA by protein engineering. The modified "murinized" $InlA^m$ harbors two specific amino acid substitutions allowing for interaction with murine E-cadherin (Wollert *et al.*, 2007).

1.3 Pathophysiology of listeriosis

L. monocytogenes is an opportunistic pathogenic species, which is encountered in various environments. Foodborne infection of the host leads to colonization of the GIT causing gastroenteritis in healthy individuals. In immunocompromised risk groups, however, *L. monocytogenes* is able to cause a systemic infection leading to severe symptoms associated with high fatality rates. *In vitro*

experiments and *in vivo* infection studies in animal models have provided insight into the pathophysiology, although exact mechanisms still need to be illuminated. This is hindered by the differences in pathogenesis of the used animal models and application routes, and contradicting results in literature.

1.3.1 The transition between environmental and pathogenic lifestyle

Like the other *Listeria sensu stricto* members, *L. monocytogenes* can be found ubiquitously in nature, including aqueous environments, soil and vegetation, where it lives as a saprophyte on decaying plant material. It is regularly isolated from various food sources (Farber & Peterkin, 1991). Its widespread occurrence is ascribed to the capability to survive under diverse environmental conditions including a wide pH range (4.5-9.0), temperatures of 0°C-45°C, and high concentrations of salt (up to 10 % NaCl) (Thévenot *et al.*, 2006). This is reflected by the large number of regulatory and transport proteins as well as virulence associated and stress resistance genes in the *L. monocytogenes* genome (Glaser *et al.*, 2001). The bacterium is able to sense environmental signals like temperature, osmolarity, availability of nutrients, pH and oxygen levels in order to modify gene expression, e.g. metabolism, motility and virulence (Müller-Herbst *et al.*, 2014; Sue *et al.*, 2004; Kazmierczak *et al.*, 2003; Mekalanos, 1992; Weme-Kamphuis *et al.*, 2004).

Upon ingestion of contaminated food, *L. monocytogenes* must quickly switch from a saprophytic to a pathogenic lifestyle (Freitag *et al.*, 2009). It is believed that the physiological stresses encountered in food and the GIT serve as a signal for priming of the cell for invasion and intracellular lifestyle (Chaturongakul *et al.*, 2008; Gray *et al.*, 2006). For example, acidic and osmotic stress during passage of the stomach and intestine trigger the expression of the stress-responsive, stationary-phase sigma factor B (σB), which induces several stress response and virulence associated genes (Sue *et al.*, 2004; Kazmierczak *et al.*, 2003). It works synergistically with the positive regulatory factor A (PrfA), a thermo-regulated transcription factor active at 37°C, i.e. the body temperature of the host, but also at environmental temperatures upon induction by low pH (Neuhaus *et al.*, 2013), which controls the expression of most virulence genes (Vázquez-Boland *et al.*, 2001b; Hamon *et al.*, 2006; Cossart and Toledo-Arana, 2008; Camejo *et al.*, 2011; Ivy *et al.*, 2010).

1.3.2 The GI phase of infection

During colonization of the intestine, the so-called GI phase of infection, *L. monocytogenes* must overcome a plethora of different physical stresses like low pH values, high osmolarity or low oxygen tension as well as well as colonization resistance mediated by the gut microbiota (Gahan & Hill, 2014). After replication in the intestinal lumen or inside enterocytes, the pathogen can then cross the digestive barrier and subsequently cause systemic disease.

1.3.2.1 Survival under acidic conditions in the stomach

Upon ingestion of contaminated food, *L. monocytogenes* passages through the stomach. The gastric lumen is characterized by low pH values of about 4-5, which can even drop as low as 1-2 after a meal. Studies proved that treatment of people with antacid substances, which neutralize stomach acidity, led to reduced resistance to or increased fecal shedding of *L. monocytogenes* (Donnelly, 2001; Cobb *et al.*, 1996). These findings indicate that the low pH value of the stomach acts as a first barrier for *L. monocytogenes* infection. To battle acidic conditions, the glutamate decarboxylase (GAD) system, including GadD1, GadD2, and GadD3, is capable of converting glutamate to γ-aminobutyrate, which is then transported out of the cell in exchange for glutamate via an antiporter (GadT1, GadT2). Consumption of protons during the enzymatic reaction causes an increase of pH in the bacterial cytoplasm (Cotter and Hill, 2003). Deletion of genes encoding the decarboxylase enzymes results in reduced survival in porcine or human stomach fluid and attenuated virulence in mice after oral infection indicating that the GAD system contributes to survival in the stomach (Cotter *et al.*, 2001a; Cotter *et al.*, 2001b; Cotter *et al.*, 2005; Feehily *et al.*, 2014). In addition, *L. monocytogenes* possesses the arginine deiminase (ADI) and the agmatine deiminase (AgDI) systems, which, analogous to the GAD system, result in increase of the cytoplasmic pH by catabolism of arginine or agmatine. Disruption of these pathways led to reduced survival under acidic conditions and decreased virulence in a murine infection model (Chen *et al.*, 2011; Ryan *et al.*, 2009).

1.3.2.2 Osmotolerance

During colonization, *L. monocytogenes* encounters conditions of high osmolarity (0.3 M NaCl) in the small intestine (Chowdhury *et al.*, 1996). The osmotic shift during passage from the stomach to the small intestine triggers expression of genes for osmotic survival. Transporters for the uptake of compatible solutes protect the pathogen against turgor pressure (Sleator & Hill, 2010). Three membrane transporters, BetL (Sleator *et al.*, 1999), Gbu (Ko & Smith, 1999) and OpuC (Fraser *et al.*, 2000; Sleator *et al.*, 2001) have been identified to promote uptake of the osmolytes betaine and carnitine. Deletion of *opuC* resulted in reduced virulence in mice after oral infection (Sleator *et al.*, 2001), while deletion of *gbu* and *betL* had no influence (Wemekamp-Kamphuis *et al.*, 2002). Nevertheless, Gbu and BetL seem to play a role during survival in food (Sleator *et al.*, 2003).

1.3.2.3 Bile resistance

Bile, which is composed of bile acids, cholesterol, phospholipids and the pigment biliverdin, is produced by the liver, stored in the gallbladder and secreted into the duodenum. Not only is it involved in emulsification and solubilization of lipids during digestion, but it can also cause membrane or DNA damage as well as other detrimental effects in bacteria (Begley *et al.*, 2005a). Therefore, commensal bacteria and pathogens colonizing the GIT encode the enzyme bile salt hydrolase, which enables them to tolerate bile (Jones *et al.*, 2008). *L. monocytogenes* can cause cholecystitis, and thus, is resistant to

bile despite a varied amount of resistance among strains (Begley *et al.*, 2005a). The strain LO28 can survive even under high concentrations of bile, while strain EGDe is more bile sensitive (Begley *et al.*, 2002). *L. monocytogenes* also encodes a bile salt hydrolase Bsh, which confers resistance to bile *in vitro* (Dussurget *et al.*, 2002). It is required for GI colonization after oral infection of guinea pigs and mice as well as for systemic infection after i.v. injection in mice. *Bsh* is regulated by the virulence regulator PrfA (Dissurget *et al.*, 2002; Begley *et al.*, 2005b). Another gene, *bltB*, is weakly homologous to bile acid dehydratase genes, and was also shown to be necessary for colonization of the GIT of mice after oral infection (Begley *et al.*, 2005b). A two-gene operon named *bilE* is responsible for exclusion of cytoplasmatic bile and required for both intestinal colonization and listerial survival in spleen and liver after translocation of the gut barrier (Sleator *et al.*, 2005).

1.3.2.4 Colonization resistance

Besides the physico-chemical host defense, commensal bacteria constitute another barrier for *L. monocytogenes* during colonization. The mammalian GIT harbors a vast number of different bacterial species with estimates ranging from 500-1,000 to up to 36,000 species (Guarner and Malagelada, 2003; Sears, 2005; Frank *et al.*, 2007). The two dominant phyla are Firmicutes and Bacteroidetes, but other phyla commonly found are Proteobacteria, Actinobacteria and Cyanobacteria (Qin *et al.*, 2010). Microbial composition and bacterial density vary between different parts of the GIT. The stomach and the duodenum harbor 10^1 to 10^3 bacteria per gram of contents, the jejunum and ileum contain 10^4 to 10^7 bacteria per gram contents, and the caecum and colon are the most densely populated tissues with up to 10^{12} bacteria per gram contents (Sekirov *et al.*, 2010). Commensal bacteria have adapted to the environment of the intestines during millions of years of evolution. The host provides them with nutrients and a favorable environment. In return, the microbiota provides digestive functions, modulates the immune system and promotes the intestinal barrier forming a mutualistic symbiosis (Pickard *et al.*, 2017).

In addition, symbiotic bacteria can limit the growth of pathogenic bacteria and prevent colonization of the intestinal lumen, which are prerequisites for enteropathogens to establish infection. This so-called "colonization resistance" is mediated by several mechanisms (Stecher & Hardt, 2011; Pickard *et al.*, 2017). One indirect mode of action is the interplay between the immune system and the microbiota, which is essential for both the maintenance of tolerance to innocuous antigens and the induction of the host's immune response to pathogens. By releasing microbial patterns like flagella or peptidoglycan, which are sensed by intestinal epithelial cells, the innate immune defensive is activated. As a consequence, epithelial cells release α-defensins, goblet cells produce mucin and plasma B-cells located in the LP provide secretory IgA. All of these substances can directly inhibit luminal pathogens

and are important for minimizing the contact between pathogens and the epithelial surface (Belkaid & Hand, 2014).

As another mode of colonization resistance, the microbiota can directly inhibit the growth of pathogens. This is achieved by consuming oxygen, which limits the growth of facultative anaerobic bacteria like *L. monocytogenes* or by occupying physical niches on the epithelial surface or in the mucus layer. In addition, some commensals release inhibitory molecules like metabolic by-products including acetate and butyrate as well as bacteriocins, thus directly targeting enteropathogens. One of the major aspects of colonization resistance is competition of the endogenous gut microbiota with pathogenic bacteria for nutrients (Stecher & Hardt, 2011; Pickard *et al.*, 2017).

The barrier effect of commensal bacteria on *L. monocytogenes* infection has been analyzed in several *in vitro* and *in vivo* studies. Certain species of the genera *Lactobacillus* and *Bifidobacterium* are capable of inhibiting *L. monocytogenes* invasion and infection of eukaryotic host cells in cell culture by production of antimicrobial peptides and modulation of the immune response (Corr *et al.*, 2007b; Gomes *et al.*, 2012; Nakamura *et al.*, 2012). Numerous reports have revealed the protective effect of commensals after oral inoculation of mice or rats with *L. monocytogenes* (Corr *et al.*, 2007a; Czuprynski and Balish, 1981; Bambirra *et al.*, 2007; Archambaud *et al.*, 2012; Nakamura *et al.*, 2012). A novel study by Becattini and colleagues analyzed the influence of antibiotic-mediated depletion of the microbiota on *L. monocytogenes* infection. Pre-treatment of mice with antibiotics resulted in increased numbers of the pathogen in both the lumen and tissue of the GIT and in the liver and spleen. Their observation that infection doses as low as 10^2 cfu/mouse are sufficient to establish infection in microbiota dysbalanced mice is a strong indication that colonization resistance is a major contributor to the high level of resistance to orally acquired listeriosis in mice (Becattini *et al.*, 2017).

1.3.2.5 Oxygen availability in the gut and facultative anaerobic metabolism

All major pathogens of the GIT like *Salmonella enterica*, *Yersinia enterolitica*, *Campylobacter jejuni* and *L. monocytogenes* are facultative anaerobic bacteria, which must be able to adapt to varying oxygen concentrations during infection (Marteyn *et al.*, 2011). Oxygen levels decrease from the proximal to the distal GIT, and the colonic lumen is thought to be mainly hypoxic (He *et al.*, 1999), while diffusion of oxygen from the capillary network of intestinal villi causes a zone of relative oxygenation at the mucosal surface (Marteyn *et al.*, 2010). *L. monocytogenes* is able to switch between aerobic and anaerobic metabolism (Lungu *et al.*, 2009) and harbors an exceptionally large number of genes encoding for phosphotransferase systems (PTS) which are used for carbohydrate transport (Glaser *et al.*, 2001). Accordingly, glucose and other PTS sugars like fructose, mannose and cellobiose are the preferred carbon source in liquid media conditions (Tsai & Hodgson, 2003). Glucose is incompletely oxidized to acetate, lactate, and acetoin under aerobic conditions, while lactate is the major

fermentation product beside ethanol, formate, and carbon dioxide under anaerobic conditions (Lungu *et al.*, 2009). 139 genes were identified as being differentially regulated during anaerobiosis by DNA microarray analyses, including central metabolic genes, e.g. the *pdhABCD* operon encoding a pyruvate dehydrogenase or several genes encoding PTS systems for fructose, mannose and galactitol (Müller-Herbst *et al.*, 2014).

The intracellular metabolism of *L. monocytogenes* has been the subject of several studies (Eisenreich *et al.*, 2010; Fuchs *et al.*, 2012a; Fuchs *et al.*, 2012b; Schauer *et al.*, 2010), but the luminal metabolism during intestinal colonization has not received much attention. As a mechanism of colonization resistance, commensal bacteria, most of which are obligate anaerobes, compete with *L. monocytogenes* for nutrients (Stecher & Hardt, 2014; Pickard *et al.*, 2017). The proximal GIT is mainly responsible for the digestion of diet-derived simple carbohydrates, triglycerides and proteins. A significant portion of dietary carbohydrates cannot be utilized by the host and pass through the distal part of the small intestine (Wong *et al.*, 2006). These nutrients, e.g. complex plant-derived polysaccharides, are utilized by obligate anaerobic commensal bacteria in the colon (Hooper *et al.*, 2002). According to Freter's "nutrient niche" hypothesis, colonization of the intestinal lumen by a bacterial species requires a growth rate faster than the individual washout rate. Therefore, it must be able to utilize one or more growth-limiting nutrients more efficiently than all other competitors (Freter *et al.*, 1983). *L. monocytogenes* and other enteropathogens must therefore be able to metabolize carbon and energy sources which are either inefficiently or not at all utilized by the microbiota. For example, sugars derived from mucins like galactose, hexosamines, mannose or fucose have been shown to be an important nutrient source for colonization (Staib & Fuchs, 2014).

Toledo-Arana and colleagues investigated the transcriptome of *L. monocytogenes* in the GI lumen and during hypoxia. Several PTS systems for mannitol, mannose, galactitol, fructose and cellobiose and a dihydroxyacetone kinase for utilization of glycerol were upregulated during growth in the lumen compared to BHI (Toledo-Arana *et al.*, 2009). The pathogen also possesses genes for the degradation of *myo*-Inositol, fucose and rhamnose, although only the latter has been associated with virulence (Salazar *et al.*, 2013). Most notably, *L. monocytogenes* possesses a 53-kb genomic region consisting of three gene clusters for the utilization of ethanolamine and 1,2-propanediol (1,2-PD) as well as for the biosynthesis of vitamin B_{12} (cobalamin), which is a required co-factor in both degradation pathways. Ethanolamine is an abundant nutrient in the GIT, which is derived from the diet, luminal bacteria, or intestinal epithelial cells. Fermentation of mucin-derived rhamnose or fucose by commensal bacteria like *Bifidobacteria* and *Bacteroidetes* results in production of 1,2-PD (Gill *et al.*, 2006; Hooper *et al.*, 1999). Anaerobic utilization of ethanolamine and 1,2-PD was shown for *S. enterica* (Roth *et al.*, 1996) and seems to contribute to virulence *in vitro* and *in vivo* (Conner *et al.*, 1998; Heithoff *et al.*, 1999;

Harvey *et al.*, 2011; Hautefort *et al.*, 2008; Klumpp & Fuchs, 2007; Thiennimitr *et al.*, 2011; Winter *et al.*, 2010). The role of these catabolic pathways in *L. monocytogenes* is unclear. So far, upregulation of the corresponding gene clusters in the GIT compared to *in vitro* growth in BHI has been shown (Toledo-Arana *et al.*, 2009). Enzymatic activity of PduD, a diol dehydratase that participates in 1,2-PD catabolism, and transcriptional induction of several genes from the propanediol cluster in the presence of 1,2-PD have been shown *in vitro* for *L. innocua* (Xue *et al.*, 2008). Growth of *L. monocytogenes* on 1,2-PD as the sole carbon and energy source has not been proven yet. Knowledge about the enteropathogen's luminal nitrogen metabolism is scarce. *L. monocytogenes* can infect the nematode *Caenorhabditis elegans* and replicates extracellularly in the worm's intestine (Thomsen *et al*., 2006; Neuhaus *et al*., 2013; Kern *et al*., 2016). Using IPA to label this model host with stable ^{15}N-isotopes, a significant metabolic flux from nitrogenous compounds including oligopeptides and amino acids of the nematode to listerial proteins was shown (Kern *et al*., 2016).

Not only does low oxygen availability have implications for the metabolism of enteropathogens, oxygen is also an important signaling molecule, which affects virulence (Marteyn *et al.*, 2010; Lungu *et al.*, 2009). Anaerobic cultivation of *L. monocytogenes* increased the invasiveness in Caco-2 cells *in vitro* and virulence in guinea pigs after oral infection (Bo Andersen *et al.*, 2007). Furthermore, oxygen restriction induced acid tolerance in GI-simulated conditions (Sewell *et al.*, 2015). Deletion of *aroA*, *aroB* and *aroE*, which encode for enzymes involved in aromatic amino acid biosynthesis, led to anaerobic metabolism in *L. monocytogenes*. These strains showed posttranscriptional upregulation of *inlA* and *inlB* and subsequent enhanced invasiveness in epithelial and endothelial cells. In addition, mutants exhibit reduced virulence in mice after i.v. infection (Stritzker *et al.*, 2004; Stritzker *et al.*, 2005).

1.3.3 Crossing of the intestinal barrier and subsequent systemic disease

L. monocytogenes is capable of invading both professional phagocytes like macrophages or DCs and non-professional phagocytes like epithelial or endothelial cells. The significance of being able to cause invasive disease is still unclear, especially with regard to the specific role of the intracellular lifestyle during the GI phase of infection and the subsequent crossing of the intestinal barrier.

1.3.3.1 Invasion of the intestinal epithelium

L. monocytogenes is an intracellular pathogen, which can cause invasive disease and subsequent systemic infection by crossing the GI mucosa. The pathogen can directly invade non-professional phagocytes like epithelial cells via the "zipper mechanism". This requires specific interaction of the surface protein Internalin A and its receptor E-cadherin (Mengaud *et al.*, 1996, Lecuit *et al.*, 1997; Gaillard *et al.*, 1991). E-cadherin is a calcium-dependent cell adhesion glycoprotein located at the basolateral surface of enterocytes, but is transiently exposed at the tips of intestinal villi during the

extrusion of dying cells from the epithelium (Pentecost *et al.*, 2006). In addition, E-cadherin is luminally available at junctions between mucus-expelling goblet cells and this was shown to be the preferred site for translocation across the epithelium in mice after intestinal ligated loop infections (Nikitas *et al.*, 2011). The interaction between InlA and E-cadherin is species-specific, since InlA has a high affinity for E-cadherin from humans, rabbits and guinea pigs but only low interaction occurs in rodents (Lecuit *et al.*, 1999). This is thought to be the reason for the high resistance of mice against oral *L. monocytogenes* infection. InlA is not only required for entry of enterocytes at the tips of intestinal villi but also important for infection of spleen and liver after oral infection (Lecuit *et al.*, 2001). A second internalin, InlB, binds the hepatocyte growth factor receptor c-Met and mediates entry into multiple cell types including hepatocytes and endothelial cells (Dramsi *et al.*, 1995; Parida *et al.*, 1998; Shen *et al.*, 2000). A study by Pentecost and colleagues suggests that c-Met is also found at multicellular junctions between epithelial cells in the gut and that InlB cooperates with InlA to facilitate endocytosis of *L. monocytogenes* by accelerating internalization (Pentecost *et al.*, 2010). The interaction of InlB with its receptor c-Met is species-specific, as InlB can interact with human and murine c-Met, but not with guinea pig or rabbit c-Met (Khelef *et al.*, 2006).

An alternative InlA-independent pathway for *L. monocytogenes* to invade intestinal epithelial cells, especially in species deficient of functional E-cadherin, is by transcytosis of M cells. These cells are located in the follicle-associated epithelium of Peyer's patches in the small and large intestine. Their main function is the transport of antigens from the lumen to the mucosal lymphoid tissues, where the antigen gets processed and an immune response is initiated. This mechanism is exploited by many pathogens like *Salmonella*, *Yersinia* or *Vibrio cholerae* (Corr *et al.*, 2008). *L. monocytogenes* has been shown to transcytose through M cells for crossing of the intestinal barrier in animal models and in cell culture, although the importance of this mechanism is still unclear (MacDonald & Carter, 1980; Marco *et al.*, 1997; Pron *et al.*, 1998; Daniels *et al.*, 2000; Corr *et al.*, 2006; Chiba *et al.*, 2011; Bou Ghanem *et al.*, 2012).

1.3.3.2 Dissemination to distant organs

Currently, it is unclear how *L. monocytogenes* spreads from infected epithelial cells to distant organs like mesenteric lymph nodes (MLNs), the liver and spleen. The intracellular pathogen is capable of infecting adjacent cells via cell-to-cell spread without being exposed to the extracellular environment (Theriot *et al.*, 1992; Robbins *et al.*, 1999). This mechanism could be used to spread to cells in the underlying lamina propria (LP) and gain access to capillaries and lymphatic vessels. While bacterial replication inside and cell-to-cell spread in between enterocytes have been proven *in vivo* (Melton-Witt *et al.*, 2012), another study suggested that the basement membrane underlying epithelial cell layers constitutes an effective barrier for bacterial cell-to-cell spread (Robbins *et al.*, 2010), thus

preventing access to the LP. As an alternative mechanism, Nikitas *et al.* showed that preferential invasion of goblet cells from the intestinal lumen resulted in rapid transcytosis through the cell without *L. monocytogenes* being released from the vacuole (Nikitas *et al.*, 2011). Bacteria are subsequently released into the underlying LP where they replicate either in interstitial fluid or within phagocytes (Jones *et al.*, 2015).

Once in the LP, *L. monocytogenes* can cause systemic spread by gaining access to either capillaries, which is called the direct route of dissemination, or lymphatic vessels, i.e. the indirect route of dissemination (Melton-Witt *et al.*, 2012). Following the indirect route, bacterial cells from the LP are transported either extracellularly or inside migratory phagocytes to the MLNs via the lymphatic fluid (Bou Ghanem *et al.*, 2012; Jones *et al.*, 2015). From the lymph nodes, *L. monocytogenes* is transferred to the bloodstream via the thoracic duct. This leads to infection of the liver and spleen.

An alternative mechanism to gain access to the LP following the indirect route of dissemination via lymphatic vessels was proposed by Melton-Witt and colleagues. *L. monocytogenes* can invade epithelial cells in the small intestine shortly after oral infection and replicate inside these cells. From the cytosol, bacterial cells are shed back into the intestinal lumen and re-infect M cells, which transcytose the pathogen across the epithelial layer of the gut (Melton-Witt *et al.*, 2012). On the basolateral surface of M cells, an intraepithelial invagination containing B- and T-lymphocytes as well as macrophages and DCs is present (Corr *et al.*, 2008). Therefore, it was suggested that after transcytosis, *L. monocytogenes* is quickly phagocytosed by migratory leukocytes and transported inside these cells from the LP to the MLNs (Pron *et al.*, 1998; Pron *et al.*, 2001; Lelouard *et al.*, 2010; Lelouard *et al.*, 2012).

The direct route of dissemination allows for direct invasion of the bloodstream from the gut and colonization of the liver via the portal vein. The mechanisms for this type of bacterial spread are still unclear. It is known that *L. monocytogenes* can directly invade endothelial cells in an InlA-independent manner (Greiffenberg *et al.* 1997; Greiffenberg *et al.*, 1998; Parida *et al.*, 1998), which might grant access to intestinal blood vessels after reaching the LP. Direct access to the circulatory system can also be caused by physical trauma to the esophagus or stomach during oral infection of laboratory animals, thus skipping the GI route (D'Orazio, 2014). Although this lymphatic tissue-independent route has also been observed in *Salmonella enterica* serovar Typhimurium and *Yersinia pseudotuberculosis* (Vazquez-Torres *et al.*, 1999; Barnes *et al.*, 2006), it is possible that this pathway could be an unnatural consequence of administering large inocula, which are needed to cause infection in animal models like mice that are fairly resistant to oral infection by *L. monocytogenes*.

1.3.3.3 Liver and spleen as the main targets for dissemination

Most bacteria are quickly cleared from the circulatory system by the liver and inactivated by immune cells like Kupffer cells, neutrophils, DCs or natural killer cells (Gregory *et al.*, 1996a; Gregory *et al.*, 1996b; Gregory *et al.*, 2002; Broadley *et al.*, 2016; Zeng *et al.*, 2016). Surviving bacteria invade hepatocytes, either via interaction between InlB and c-Met or via cell-to-cell spread from infected Kupffer cells (Appelberg & Leal, 2000; Dramsi *et al.*, 1995; Braun *et al.*, 1998). Inside the cytosol, *L. monocytogenes* replicates and infects neighboring cells via cell-to-cell spread (Vázquez-Boland *et al.*, 2001b). Infected hepatocytes recruit neutrophils and macrophages, which results in apoptosis and the development of multifocal pyogranulomatous lesions (Conlan & North, 1991; Portney, 1992; Cousens & Wing, 2000; Vázquez-Boland *et al.*, 2001b). *L. monocytogenes* cells that have not been trapped by the liver are transported to the spleen, where they are cleared from the blood by macrophages, DCs and granulocytes in the marginal zone (Neuenhahn *et al.*, 2006; Aichele *et al.*, 2003; Conlan, 1996; Aoshi *et al.*, 2009). After translocation to the white pulp, *L. monocytogenes* induces apoptosis of splenic cells and causes depletion of both CD4+ and CD8+ lymphocytes leading to pyogranulomas. This enables exponential growth of the pathogen in the spleen (Conlan, 1996; Marco *et al.*, 1991; Carrero *et al.*, 2004a; Carrero *et al.*, 2004b).

The liver and spleen are the primary targets after dissemination from the gut and these organs support the intracellular replication of *L. monocytogenes*, however, infectious foci in these organs represent essentially subclinical infections, which are cleared in immunocompetent individuals mainly via CD8+ T cells. In immunocompromised hosts, however, bacteria from granulomatous lesions are released into the bloodstream, thus causing clinical listeriosis. This is characterized by septicemia and the breach of other host barriers like the blood-brain and the placental barrier, which leads to infection of secondary organs like the brain or placenta and therefore also the unborn fetus (Pamer, 2004).

1.4 Aim of this thesis

Advances in DNA sequencing methods, i.e. the uprising of next generation sequencing (NGS) (Goodwin *et al.*, 2016) and the subsequent plummeting of costs for genome analyses, have facilitated the discovery of novel bacterial species. In addition, new methods in phylogenetics like the calculation of average nucleotide identities (ANI) (Konstantinidis & Tiedje, 2005; Konstantinidis *et al.*, 2006; Goris *et al.*, 2007) improved species delineation and taxonomy of prokaryotic genera (Varghese *et al.*, 2015). This led to the discovery of several novel *Listeria* spp. during the last decade and the division of the genus into the two clades *Listeria sensu lato* and *Listeria sensu stricto* (Orsi & Wiedmann, 2016; Chiara *et al.*, 2015). Several studies have investigated the virulence potential of the latter group in cell culture or after i.v. infection and additional empirical evidence suggests association with the GIT of the mammalian host. Information about the potential of *Listeria sensu lato* members to colonize the GIT

or to cause invasive disease is scarce. Recently, *L. kieliensis* sp. nov., was isolated from a wastewater plant in Northern Germany. Genome sequencing via DNA NGS and genome comparison with the pathogenic *L. monocytogenes* was lacking at the beginning of this thesis and could help to assess the colonization and virulence potential of this novel environmental species.

So far, no controlled experiments on the colonization capabilities of different *Listeria* spp. after oral infection have been performed. Previous experiments on mouse models for foodborne listeriosis suffered from extensive lab-to-lab variation such as the infection dose used and the duration of the GI phase before systemic dissemination. Therefore, a novel oral infection model for BALB/c mice was intended to be established and used in this thesis (Bou Ghanem *et al.*, 2013a). The major advantage of this model is the defined and reproducible phase of GI infection, which should allow investigators to specifically analyze the colonization and invasion capabilities of *Listeria sensu lato* and *Listeria sensu stricto* spp. It was hypothesized that *Listeria sensu stricto* members have the potential to at least transiently colonize the intestines of mammals, unlike *Listeria sensu lato* spp., which seem to be less adapted to the conditions of the GIT.

In addition to the reassessment of this assumption via *in vivo* experiments, an *in silico* approach was envisaged to identify genetic determinants encoded within the former group that promote growth or survival in the mammalian GIT. With more than 2,000 sequenced listerial genomes deposited in the NCBI GenBank (Benson *et al.*, 2017) (as of: October 2017) and a plethora of novel bioinformatic tools for genome analyses, it should be possible to gain insights into the differences between both clades as well as into the evolution of virulence and colonization properties of the genus *Listeria*. While several studies have investigated the genomic relationship between pathogenic and apathogenic species of the *Listeria sensu stricto* (Buchrieser *et al.*, 2003, Glaser *et al.*, 2001; Hain *et al.*, 2006a; Hain *et al.*, 2006b; den Bakker *et al.*, 2010a; den Bakker *et al.*, 2010b), no comprehensive genome comparison between the two phylogenetic groups has been performed.

To identify novel listerial genes that could be involved in colonization of the intestines, several factors being encoded by all *sensu stricto* strains, but absent from the strains of the *sensu lato* group were planned to be analyzed in this thesis using different *in vitro* and *in vivo* methods.

2 Material & Methods

2.1 Material

2.1.1 Chemicals, enzymes, and commercial kits

All chemicals and enzymes used in this thesis are listed in **Supplementary Table 1**. Chemicals dissolvable in water are usually prepared using high-purity Milli-Q water (MQ-H_2O) from a Milli-Q water purification system (Merck Millipore) and are usually sterile filtered with a 0.22 µm filter (Merck).

2.1.2 Equipment and consumables

All equipment and consumables used in this thesis are listed in **Supplementary Table 2**.

2.1.3 Bacterial strains

Bacterial strains that are created and/or used in this thesis are listed in **Table 1**.

Table 1: Bacterial strains used in this study

Bacterial strains	Description and relevant features	Source
L. monocytogenes EGDe	*L. monocytogenes* Sv 1/2a, wild type (strain ATCC BAA-679), parental strain of deletion mutants	Strain collection ZIEL Weihenstephan (Glaser *et al.*, 2001)
E. coli DH5α	*deoR endA1 gyrA96 hsdR17*(r_k-m_{k+}) *recA1 relA1 supE44 λthi-1* Δ(*lacZYA-argFV169*)	Strain collection ZIEL Weihenstephan (Hanahan, 1983)
L. welshimeri	*L. welshimeri* wild type strain, isolated 1988 and listed as WS 2259	Strain collection ZIEL Weihenstephan
L. seeligeri	*L. seeligeri* wild type strain, isolated 1988 and listed as WS2253	Strain collection ZIEL Weihenstephan
L. aquatica	*L. aquatica* wild type strain, type strain FSL S10-1188	Belgian Coordinated Collection of Microorganisms (BCCM)
L. booriae	*L. booriae* wild type strain, type strain FSL A5-0281	BCMM
L. floridensis	*L. floridensis* wild type strain, type strain FSL S10-1187	BCMM
L. newyorkensis	*L. newyorkensis* wild type strain, type strain FSL M6-0635	BCMM
L. riparia	*L. riparia* wild type strain, type strain FSL S10-1204	BCMM
L. kieliensis sp. nov.	*L. kieliensis* sp. nov. wild type strain, isolated from a waste water plant	Max Rubner-Institute Kiel (MRI)
EGDe Δlmo1130	In-frame deletion of lmo1130 in EGDe	This thesis

EGDe Δlmo1131	In-frame deletion of lmo1131 in EGDe	This thesis
EGDe Δlmo1132	In-frame deletion of lmo1132 in EGDe	This thesis
EGDe Δlmo1131-1132	In-frame deletion of lmo1131-1132 in EGDe	This thesis
EGDe Δlmo1133	In-frame deletion of lmo1133 in EGDe	This thesis
EGDe Δlmo1134	In-frame deletion of lmo11314 in EGDe	This thesis
EGDe Δlmo1135	In-frame deletion of lmo1135 in EGDe	This thesis
EGDe Δlmo1136	In-frame deletion of lmo1136 in EGDe	This thesis
EGDe Δ*pduD*	In-frame deletion of *pduD* in EGDe	Kristina Schauer
EGDe::pIMC3kan	EGDe with pIMC3kan integrated at the $tRNA^{ARG}$	This thesis
EGDe Δlmo1131-1132::pIMC3ery	EGDe Δlmo1131-1132 with pIMC3ery integrated at the $tRNA^{ARG}$	This thesis
EGDe Δ*pduD*::pIMC3ery	EGDe Δ*pduD* with pIMC3ery integrated at the $tRNA^{ARG}$	This thesis

2.1.4 Plasmids

Plasmids used in this thesis are listed in **Table 2**.

Table 2: Plasmids used in this study

Plasmids	Description and relevant features	Source
pLSV101	Temperature-sensitive shuttle vector; erythromycin-resistant	(Joseph *et al.*, 2006)
pLSV101Δlmo1130	Deletion plasmid for lmo1130	This thesis
pLSV101Δlmo1131	Deletion plasmid for lmo1131	This thesis
pLSV101Δlmo1132	Deletion plasmid for lmo1132	This thesis
pLSV101Δlmo1131-1132	Deletion plasmid for lmo1131-1132	This thesis
pLSV101Δlmo1133	Deletion plasmid for lmo1133	This thesis
pLSV101Δlmo1134	Deletion plasmid for lmo1134	This thesis
pLSV101Δlmo1135	Deletion plasmid for lmo1135	This thesis
pLSV101Δlmo1136	Deletion plasmid for lmo1136	This thesis
pIMC3kan	Site-specific integrative vector. IPTG controlled expression of *aphA*-III; chloramphenicol-resistant.	(Monk *et al.*, 2008)
pIMC3ery	Site-specific integrative vector. IPTG controlled expression of *ermAM*; chloramphenicol-resistant.	(Monk *et al.*, 2008)

2.1.5 Oligonucleotides

Oligonucleotides used in this thesis are listed in **Table 3**. All primers are lyophilized and salt-free and are purchased from Eurofins Genomics (Ebersberg, Germany). Primers are dissolved in MQ-H_2O to a stock concentration of 100 pmol/µl, used at a working concentration of 10 pmol/µl and stored at -20°C. Oligonucleotides for quantitative real-time reverse transcription PCR (qRT-PCR) are dissolved in diethylpyrocarbonate (DEPC; Carl Roth)-treated dH_2O.

Table 3: Oligonucleotides used in this study (restriction enzymes used for cloning are shown in brackets and the corresponding recognition sequence is underlined)

Name of oligonucleotide (5'-3')	Sequence
	Construction of deletion mutants
lmo0721_A	GGTAAGGAATGAATAATCGGG
lmo0721_B	ATTATAAGATCTTGGCTCGATAAACTCTTTCAT (*Bgl*II)
lmo0721_C	GCCCATAGATCTTTAGATGAATTTATAGAGGTT (*Bgl*II)
lmo0721_D	AAACATCGGCTTCATTTGCCA
lmo0721_nestAB	GGAAAAGTCGACTGTTTAAGACGTCGGTTGTCA (*Sal*I)
lmo0721_nestCD	CTACGACCCGGGCAAATACCTCAATGACCTAGG (*Xma*I)
lmo1130_A	TCGTAATCGAATTCAGTTGCA
lmo1130_B	TTGCGCGGTACCGCCAGTGGAAAGAGTAAGCAT (*Kpn*I)
lmo1130_C	CTCGCCGGTACCGACGCAATGGTTTACACAATG (*Kpn*I)
lmo1130_D	ACTTGGTTGACTTCGTTTGCG
lmo1130_nestAB	AATAAAGTCGACATTGTTCAATCCCATCTACCG (*Sal*I)
lmo1130_nestCD	ATTTTTCCCGGGCGTTTAATTGTATCCACTCCA (*Xma*I)
lmo1131-1132_A	TGCTTTTAATGGAAAGGGTCA
lmo1131-1132_B	TTCAACGGTACCAAATAAACGCTTATCAATCAT (*Kpn*I)
lmo1131-1132_C	GAAGAAGGTACCTTTATAGAAAATGGTGCATTG (*Kpn*I)
lmo1131-1132_D	CGGCCAACTAATTCATTTGTA
lmo1131-1132_nestAB	GCGAATGTCGACTTTTTTGAATCGTTTTTTGAA (*Sal*I)
lmo1131-1132_nestCD	GTAATGCCCGGGAATTTTTAATGTTTGTTATTG (*Xma*I)
lmo1133_A	CCGAAACATCTGAAAACAACC
lmo1133_B	ATATAAGGTACCCGTGTTTTCTTTTAAATACAT (*Kpn*I)
lmo1133_C	GAACTTGGTACCGTTGAATTTTTCGAAAGCTCA (*Kpn*I)
lmo1133_D	AATACGCCAAGGAAGCGAGCT
lmo1133_nestAB	CAGCTTGTCGACGAATCAATTTTATCAGCACAT (*Sal*I)
lmo1133_nestCD	CTGATGCCCGGGTGGGATCCAGATGGTCAAGTT (*Xma*I)
lmo1134_A	TAAGGGTAAATGGCTTGGCAT
lmo1134_B	CCCCGTGGTACCGGCAAAATCTTTAATATACAT (*Kpn*I)
lmo1134_C	GCAGAAGGTACCTCTTTTGTGGCTAAAAAAGTG (*Kpn*I)
lmo1134_D	TCCCCAATCAAATCGAATGGT
lmo1134_nestAB	GGTTTAGTCGACTTATTCCTTCATGACGCACCG (*Sal*I)
lmo1134_nestCD	CATCTGCCCGGGACCAATTACAAGCCCGAAACC (*Xma*I)

lmo1135_A	TTATTCCTTCATGACGCACCG
lmo1135_B	GATCACGGTACCTATCTCGTTATTAATCATCAT (*Kpn*I)
lmo1135_C	AAACACGGTACCATTTTGGCTCAAAACATGTTA (*Kpn*I)
lmo1135_D	CCGAAATAGGATTGGCGCTAA
lmo1135_nestAB	AATCTGGTCGACGCACTTTCTAAAGGAACAATC (*Sal*I)
lmo1135_nestCD	AGCTTCCCCGGGTCCGCCACAACTTGCGCGAGT (*Xma*I)
lmo1136_A	ACAGTCGATTTACCACTTTTG
lmo1136_B	TAAACTGGTACCAATCTTGATAGTTTTTTTCAT (*Kpn*I)
lmo1136_C	GGGTTAGGTACCACTGTTACTAGCGCTATTTTA (*Kpn*I)
lmo1136_D	TTGATACACGCACAGTGTTAA
lmo1136_nestAB	GATTAGGTCGACCGCCAATTGCTGGATATTCAA (*Sal*I)
lmo1136_nestCD	GATGCGCCCGGGAATTAACCGCTTAATCGCCGA (*Xma*I)
lmo1829_A	CTACCACTTGTTCAGTGATTT
lmo1829_B	CATTGCGGTACCAAACATTGCATCAAACGCCAT (*Kpn*I)
lmo1829_C	AAACACGGTACCAAACCAAATGGTGCCAAGCCT (*Kpn*I)
lmo1829_D	GTTCATTAAAAGCAGTGGAAG
lmo1829_nestAB	TCCTTCGTCGACTCTCATCTCATCCAGTCGCTC (*Sal*I)
lmo1829_nestCD	AGCGACCCCGGGAGCTGGAACGGGAACGAATCC (*Xma*I)
pduD_A	CGCACTCGGATATTCG
pduD_B	GAAGATCTTCTTTTTCGTTAATTTCAACC (*Bgl*II)
pduD_C	GAAGATCTTGTTCAAGGGAAAAACG (*Bgl*II)
pduD_D	GCCACTTCCGTTGTAG
pduD_nestedAB	CGGGATCCCGACGGTGGGTTAACAC (*Bam*HI)
pduD_nestedCD	CGGAATTCCGCTGTGCTGCTTCACG (*Eco*RI)
LSV3	AGTACCATTACTTATGAG
LSV-4380rev	AGGGTTTTCCCAGTCACG
	qRT-PCR
lmo1131_qRT_F	CACGATTAGTATGACTGGCA
lmo1131-qRT_R	ACAATTTACTGCAAGCACTG
lmo1132_qRT_F	TGAAAAGCTCAATAGGCAGT
lmo1132_qRT_R	GTTTCAAGTGGCAATTGTGA
lmo1133_qRT_F:	TTGAACATTTGGAGGCGTTA
lmo1133_qRT_R:	CTGATTCTGCCAAATTTCCC
lmo1135_qRT_F:	ATGAATATGGTTTCGGGCTT
lmo1135_qRT_R:	TACGAATAACAAGCGGAACT
lmo1146_qRT_F	ATGTTGTCGGAGGAGAAATG
lmo1146_qRT_R	CGCTGGTTTGAGTTACTTTC
lmo1150_qRT_F	TTTTCAGTCCCTATCGTTGT
lmo1150_qRT_R	AAACGCGGAGATAAGATCC
lmo1153_qRT_F	GGAGATGATACACCTTGGTC
lmo1153_qRT_R	TTTTCCTTCTGCATAACCCA
lmo1190_qRT_F	GAATGATGGGCGTAACAATG
lmo1190_qRT_R	GTGCAAGTAATGATAATGGACA

lmo1199_qRT_F	AGCAACCCAGATTTAGAAGT
lmo1199_qRT_R	TTTCAATTACTTCCCACGGT
16S_LmonF1	AGACACGGCCCAGACTCCT
16S_LmonR1	GATCCGAAAACCTTCTTCATACA
lmo1759_qRT_F	AAACGAACGGACAATTGAAG
lmo1759_qRT_R	CTAACTTATCGACGTCAGCA
rpoB_qRT_F	ACACGTATCTGCGAAAGACT
rpoB_qRT_R	TTACTTCTTTGCCATCCACT

2.1.6 Media and Buffers

All media and buffers are prepared with double distilled H_2O (ddH_2O) and are autoclaved at 121°C for 21 min if not stated otherwise. If needed, supplements are added aseptically after cooling below 60°C. Media and buffers are stored at room temperature (RT) or at the temperature indicated. For agar plates, 1.5 % (w/v) bacteriological agar (Oxoid) is added to the medium. Plates are stored at 4°C.

Lysogeny broth (LB)	
Tryptone (Oxoid)	10 g/l
Yeast extract (YE) (Oxoid)	5 g/l
NaCl (Carl Roth)	10 g/l

Brain heart infusion broth (BHI)	
BHI (Merck)	37 g/l

Minimal medium (MM)
adapted from Premaratne *et al.* (1991)

KH_2PO_4 (Carl Roth)	6.56 g/l
$Na_2HPO_4 \cdot 2\ H_2O$ (Fluka)	16.4 g/l
$MgSO_4 \cdot 7\ H_2O$ (Merck)	0.41 g/l
Ferric citrate (Merck)	0.1 g/l
L-Leucine (Serva)	0.1 g/l
L-Valine (Merck)	0.1 g/l
L-Methionine (Sigma)	0.1 g/l
L-Arginine (Merck)	0.1 g/l
L-Cysteine (Merck)	0.1 g/l
L-Histidine (Carl Roth)	0.1 g/l
Riboflavin (Sigma)	0.5 mg/l
Thiamine (Fluka)	1 mg/l
Biotin (Sigma)	0.5 mg/l
DL-6,8-Thioctic acid (Sigma)	0.0015 mg/l

Filter sterilized (0.22 µm), stored at 4°C

Super optimal broth incl. glucose (SOC)	
Peptone (Merck)	20 g/l
YE (Oxoid)	5 g/l
NaCl (Carl Roth)	0.6 g/l
KCl (Carl Roth)	0.2 g/l

$MgSO_4 \cdot 7\ H_2O$ (Merck)	2.5 g/l
$MgCl_2 \cdot 6\ H_2O$ (Carl Roth)	2.1 g/l
Glucose (Fluka)	3.9 g/l

Filter sterilized (0.22 µm), stored at 4°C

Phosphate buffered saline (PBS)	
NaCl (Carl Roth)	8 g/l
KCl (Carl Roth)	0.2 g/l
$Na_2HPO_4 \cdot 2\ H_2O$ (Fluka)	1.44 g/l
KH_2PO_4 (Carl Roth)	0.24 g/l

adjusted to pH 7.4

Tris-acetate-EDTA (TAE) buffer (50x stock solution)	**1 L**
Tris base (Carl Roth)	242 g
Glacial acetic acid (Sigma-Aldrich)	57.1 ml
0.5 M EDTA (Carl Roth) pH 8.0	100 ml

Palcam agar	**500 ml**
Palcam Base (Sifin)	34 g
Bacteriological Agar (Oxoid)	2.5 g

Autoclave at 121°C for 21 min, after cooling below 60°C add one bottle of Palcam selective supplement (Sifin) dissolved in 2 ml Milli-Q H_2O

Tris-borate-EDTA (TBE) buffer (10x stock solution)	**1 L**
Tris base (Carl Roth)	108 g
Boric acid (Merck)	55 g
0.5 M EDTA (Carl Roth) pH 8.0	40 ml

2.1.7 Supplements

Supplements used in this study are listed in **Table 4**. Antibiotics and additives are sterile filtrated.

Table 4: Supplements

Additive	**Solvent**	**Stock concentration**	**Working concentration**
Erythromycin (Calbiochem or Sigma)	100% (v/v) EtOH	5-10 mg/ml 50 mg/ml	5-10 µg/ml (*Listeria*) 300 µg/ml (*E. coli*)
Kanamycin (Amresco)	dH_2O	50 mg/ml	50 µg/ml
Chloramphenicol (Sigma)	100% (v/v) EtOH	7.5 mg/ml	7.5 µg/ml
Yeast extract (YE) (Oxoid)	dH_2O	250 g/l	0.5 g/l
Isopropyl β-D-1-thiogalactopyranoside (IPTG)	dH_2O	1 M	1 mM
Cobalamin (vitamin B_{12}) (AppliChem)	MeOH	1 mM	25 nM
1,2-PD (Sigma-Aldrich)	dH_2O	1 M	1 mM
Glucose (Fluka)	dH_2O	1 M	50 mM

2.2 Microbiology

2.2.1 Culture conditions

2.2.1.1 Bacterial glycerol stocks

For long term storage, bacterial strains are stored at -80°C in 20% glycerol (Carl Roth) to prevent cell damage. Therefore, 800 µl of an overnight culture and 400 µl autoclaved 60% glycerol are thoroughly mixed in a 1.5 ml Eppendorf tube with a screw cap.

2.2.1.2 Growth on plates

Bacteria from glycerol stocks are streaked out on BHI (*Listeria*) or LB (*E. coli*) agar plates and incubated for 24-48 h at 24°C, 30°C or 37°C. Afterwards, agar plates are stored at 4°C for up to four weeks.

2.2.1.3 Overnight cultures

Growth in liquid culture is typically performed in the standard medium BHI (*Listeria*) or LB (*E. coli*) in either glass tubes or glass flasks. For overnight cultures, a single colony from plate is used to inoculate 3 ml BHI or LB medium in a capped glass tube and incubated at 24°C, 30°C or 37°C under shaking (150 rpm) for up to 24 h if not stated otherwise. Overnight cultures are then used for inoculation of growth analysis studies, infection purposes or other experiments.

2.2.1.4 Growth for RNA isolation

To cultivate *L. monocytogenes* cells for isolation of RNA, an overnight culture in BHI grown at 37°C 150 rpm is diluted 1:100 in BHI for a total volume of 50 ml and incubated in a 200 ml Erlenmeyer flask or a sealed 50 ml Falcon under varying conditions (temperature-, iron- and oxygen-dependent transcription analysis). For next generation RNA sequencing, overnight cultures are scaled up to 30 ml BHI, diluted 1:15 in a total of 3.75 ml BHI plus optional supplements and cultivated in 15 ml glass tubes at 37°C under shaking (150 rpm). In both cases, cells are harvested in mid-logarithmic phase (OD_{600} = 0.80 – 0.95) by centrifugation (8 min, 4,180 g, RT). Supernatant is discarded, and the cell pellet is shock frozen in liquid nitrogen and stored at -80°C.

2.2.2 Growth analysis

2.2.2.1 Growth in liquid media

Experiments for growth analysis are usually performed in BHI medium. If necessary, chemically defined MM is used based on Welshimer's broth (Premaratne *et al.*, 1991), whose composition has been published before (Kaspar *et al.*, 2014). MM is generally supplemented with 0.5 % (w/v) YE (Oxoid) to ensure anaerobic growth of *L. monocytogenes*. Additional carbon sources are added if necessary.

The optical density of bacterial cultures is determined at a wavelength of 600 nm (OD_{600}). Therefore 1 ml of a culture is transferred into a disposable cuvette (Brandt) and measured using a Lamda+ spectrophotometer (Perkin Elmer). In case of OD_{600} values above 1, samples are diluted 1:10 in fresh medium before measurement. This allows for analysis of growth behavior over time, which is

conducted in either 3 ml glass tubes or 100 ml or 200 ml Erlenmeyer flask containing varying amounts of BHI or MM and optional supplements.

2.2.2.2 Growth analysis using the Bioscreen C

Automated and simultaneous measurement of multiple strains in a micro-plate format is performed using the Bioscreen C Automated Microbiology Growth Curve Analysis System (Oy Growth Curves). OD_{600} of overnight cultures grown in BHI is determined and the cultures are centrifuged (8 min, 4,180 g, RT), washed with PBS and then diluted in PBS to obtain an OD_{600} of 1. The cell suspension is diluted 1:20 in BHI or MM to a final volume of 200 µl. For establishment of anaerobic conditions, wells are covered with 200 µl paraffin oil (Carl Roth). Plates are incubated with continuous medium shaking (shaking steps: 60), and the OD_{600} is automatically measured every 30 min. For growth comparison of *Listeria* spp., plates are incubated at 38°C microaerobically and anaerobically. For growth analysis with 1,2-PD and cobalamin, plates are incubated at 37°C anaerobically.

2.2.2.3 Growth analysis on selective agar plates

For determination of cfu on BHI and selective Palcam agar, overnight cultures of different *Listeria* spp. grown in BHI at 30°C are centrifuged (8 min, 4,180 g, RT), washed with PBS and diluted in PBS to an OD_{600} of 0.1. Cell suspensions are further diluted (10^{-4} to 10^{-7}) in PBS and then plated on BHI and Palcam agar plates simultaneously. Plates are incubated at 37°C for 24h and the ratio of cfu $\frac{cfu_{BHI}}{cfu_{Palcam}}$ is calculated for each species.

2.3 Molecular biology

2.3.1 Preparation of nucleic acids

2.3.1.1 Plasmid isolation

Plasmids are isolated from *E. coli* small-scale (5 ml) or large-scale (50-100 ml) overnight cultures in selective LB media using the GenElute HP plasmid miniprep kit (Invitrogen) or the PureLink HiPure plasmid midiprep kit (Sigma-Aldrich) according to the manufacturers' instructions. Elution of plasmids is carried out using MQ-H_2O.

2.3.1.2 Isolation of genomic DNA

For preparation of genomic DNA (gDNA), cells of *L. monocytogenes* from a 3 ml overnight culture are harvested (2 min, 13,200 rpm, RT) and resuspended in 0.5 ml AKI solution (6.7 % (w/v) sucrose (Carl Roth), 50 mM Tris-HCl pH 8.0 (Carl Roth), 1 mM Na_2-EDTA (Carl Roth)). To disrupt the cell wall, lysozyme (Sigma-Aldrich) is added to a final concentration of 10 mg/ml. To remove RNAs, RNAse A (Sigma-Aldrich) is added to a final concentration of 100 µg/ml. The mixture is thoroughly vortexed and incubated for 60-90 min at 37°C, while inverting the tubes once in a while to improve cell lysis. 12.5 µl of Proteinase K (20 mg/ml; AppliChem) is added afterwards to degrade cell proteins and the solution is incubated for 20 min at 50°C. 200 µl 5 % (v/v) sodium dodecylsulfate (SDS; Carl Roth) is added to the

sample and the tube is incubated for 10 min at 70°C. After cooling, 200 µl neutral Roti-Phenol (Carl Roth) is added and the sample is homogenized by inverting the tubes. The tubes are then centrifuged for 20 min at 13,200 rpm RT to separate the phenol and aqueous upper phase. The latter (containing the DNA) is transferred into a new 1.5 ml Eppendorf tube and the phenol-chloroform extraction is repeated. To precipitate the dissolved DNA, 60 µl 3 M Na-Acetate pH 8.0 (Carl Roth) and 600 µl isopropanol (Carl Roth) are added and the tubes are inverted several times. The DNA filament is washed with 500 µl 70% ethanol (J.T. Baker) two times and then transferred into a new 1.5 ml Eppendorf tube. The DNA is air-dried and afterwards resuspended in MQ-H_2O (if necessary, the solution is heated to 37°C for 30 min to facilitate dissolution of the DNA). DNA is stored at -20°C.

DNA for NGS

For next generation DNA sequencing, bacteria are grown on BHI agar plates overnight at 30°C. gDNA is isolated using the QIAamp DNA Mini Kit (Qiagen) according to the manufacturer's instructions with an additional lysozyme treatment at 37°C overnight to digest peptidoglycan from the bacterial cell wall. Therefore, 1-2 inoculation loops from the culture plate are treated with a lysozyme solution (20 mg/ml lysozyme (Sigma-Aldrich), 20 mM Tris-HCl pH 8.0 (Carl Roth), 2 mM EDTA (Carl Roth), 1.2 % (v/v) Triton X-100 (Carl Roth)) in a thermoshaker (1,300 rpm) at 37°C. Lysozyme is inactivated at 95°C for 15 min and DNA isolation is continued following the Qiagen protocol.

2.3.1.3 Isolation of bacterial RNA

Cultivation of cells for RNA isolation is performed as described in 2.2.1.4 Growth for RNA isolation. The cell pellet is thawed on ice and thoroughly resuspended in 1 ml TRI-Reagent (Sigma-Aldrich). Cell suspension is transferred to screw-capped 2 ml microcentrifuge tube (Sarstedt) filled with 0.5 cm silica beads (Ø 0.1 mm; Sigma-Aldrich). Tubes are incubated for 5 min at RT and afterwards cells are mechanically lysed using the FastPrep-24 Tissue and Cell Homogenizer (MP Biomedicals) (3x45 sec with 6.5 m/s and 1 min on ice in between cycles). To remove beads and cell debris, tubes are centrifuged at 13,200 rpm for 3 min at RT and the supernatant is transferred into a fresh 2 ml Eppendorf tube. After 200 µl chloroform (Carl Roth) is added and tubes are manually shaken for 15 s, solution is incubated at RT for 3 min and subsequently centrifuged at 12,000 g for 15 min at 4°C. This step causes separation of proteins (accumulating in the lower organic phase), DNA (concentrated in the white interphase) and RNA in the upper aqueous phase. This phase is transferred into a fresh 1.5 ml Eppendorf tube, 0.5 ml ice cold isopropanol (Carl Roth) is added, followed by inversion of the tubes by hand and incubation at RT for 10 min. Samples are centrifuged (12,000 g, 10 min, 4°C), the supernatant discarded, and the pellet is washed with 1 ml ice cold 70 % (v/v) ethanol (J.T. Baker) and subsequently centrifuged (7,500 g, 5 min, 4°C). After removal of supernatant, the pellet is air dried at RT for 20 min before it is resuspended in 80 µl DEPC-treated (0.1 % (v/v)) dH_2O (DEPC-H_2O).

To remove remaining DNA contaminations, RNA samples are digested with 10µl RNase-free DNaseI (1 U/µl; Promega) and 10 µl 10x RQ1 RNase-free DNase buffer (Promega) for 45 min at 37°C in a heat block (Thermoblock, Biometra). To stop digestion, 100 µl chloroform is added. Then, the tubes are inverted by hand and centrifuged at 15,000 g for 15 min at 4°C allowing for the separation of DNase and buffer components. RNA dissolved in the upper aqueous phase is transferred into a new 1.5 ml Eppendorf tube and filled up to 100 ml with DEPC-H_2O.

The RNA is then purified via the RNeasy mini kit (Qiagen). This column-based technology causes binding of RNA molecules larger than 200 bp to a silica-based membrane while smaller RNAs are excluded. This leads to diminishment of small RNAs < 200 bp (e.g. 5S rRNAs and tRNAs) and enrichment of desired mRNA. The manufacturer's instructions are followed, and an additional on-column digestion step is performed by DNaseI (2 U/µl; Qiagen) for 15 min at RT. RNA is eluted in 2x 15 µl DEPC-H_2O and stored at -80°C.

RNA for NGS

For NGS, whole RNA isolation is performed as described above using nuclease-free water (Ambion) instead of DEPC-H_2O. After DNase digestion and chloroform extraction, 60 µg RNA are applied onto the RNeasy column to prevent overloading.

Since the majority of RNAs in the microbial cell are ribosomal RNAs, the MICROBExpress Bacterial mRNA Enrichment Kit (Ambion) is used for the removal of 16S and 23S rRNAs. Therefore, 5 µg total RNA is treated following the manufacturer's instructions (without initial RNA precipitation). After rRNA depletion, samples are resuspended in 25 µl nuclease-free water and the concentration and integrity are checked again to ensure sufficient rRNA removal.

To obtain RNA fragments of ca. 150 nucleotides (nt) for subsequent cDNA library preparation, 300 ng RNA in 50 µl nuclease-free H_2O are fragmented using the S220 focused-ultrasonication system (Covaris) (180 s, 10 % duty factor, 175 W, 200 cycles/burst) in a microTUBE (Covaris).

RNA is chemically modified to ensure strand specific sequencing by dephosphorylation and re-phosphorylation to create a 5'-phosphate and a 3'-OH group. This enables back-to-back 3' and 5' adapter ligation in the subsequent steps before cDNA synthesis and PCR amplification. Therefore, RNA is dephosphorylated using antarctic phosphatase (New England Biolabs; 5 U/µl) with the addition of SUPERase In RNA inhibitor (Ambion) in a total volume of 65.5 µl for 1 h at 37°C.

Dephosphorylation reaction mix	**65.5 µl**
Fragmented RNA	50 µl
Antarctic phosphatase (5 U/µl)	3 µl
Antarctic phosphatase buffer (10x)	6.5 µl
Superase In RNA inhibitor (20 U/µl)	3.25 µl
Nuclease-free H_2O	2.75 µl

Afterwards, sample volume is filled up to 70 µl by addition of nuclease-free H_2O and 700 µl QIAzol (Qiagen) is added. RNA is purified with the miRNeasy mini kit following the manufacturer's protocol without homogenization steps. After elution in 35.5 µl nuclease-free H_2O, RNA is re-phosphorylated by adding T4 polinucleotide kinase (New England Biolabs; 10 U/µl) and SUPERase In RNA inhibitor. The solution is incubated for 1 h at 37°C, purified again by using the miRNeasy mini kit and eluted in 30 µl nuclease-free H_2O.

Phosphorylation reaction mix	**50 µl**
Dephosphorylated RNA	35.5 µl
T4 Polinucleotide Kinase (10 U/µl)	2 µl
PNK Buffer (10x)	5 µl
Superase In RNA inhibitor (20 U/µl)	2.5 µl
10 mM ATP	5 µl

2.3.1.4 cDNA synthesis

Isolated single stranded RNA is reverse transcribed into cDNA using the qScript cDNA supermix (Quanta Biosciences). This mix provides all necessary components for first strand cDNA synthesis, including 5x buffer, $MgCl_2$, dNTPs, oligo(DT) primers, random primers, a recombinant RNase inhibitor protein, stabilizers and the qScript reverse transcriptase. RNA is thawed on ice and the concentration is determined via NanoDrop (Thermo Fisher Scientific) and adjusted to a stock concentration of 100 ng/µl in 25 µl DEPC-H_2O. 1 µg of RNA is used as a template and incubated in a PCR cycler. After the reaction is finished, 80 µl DEPC-H_2O are added to obtain a final volume of 100 µl.

cDNA synthesis reaction mix	**20 µl**
Isolated RNA (100 ng/µl)	10 µl
qScript cDNA supermix (Quanta)	4 µl
DEPC-H_2O	6 µl

cDNA synthesis program	
25°C	5 min
42°C	30 min
85°C	5 min
8°C	hold

2.3.1.5 Determination of nucleic acid concentrations, purity and integrity

The concentration and purity of DNA or RNA samples is determined using the NanoDrop ND-1000 spectrophotometer (Thermo Fisher Scientific) by measuring optical densities at various wavelengths (230, 260 and 280 nm). Using the Lambert-Beer law, 1.5 µl of nucleic acid is applied on the sample column and the OD_{260}, being proportional to the nucleic acid concentration, is measured. The ratios OD_{260}/OD_{280} and OD_{260}/OD_{230} are also determined in order to identify impurities with proteins or other organic compounds, e.g. ethanol. For NGS, DNA and RNA concentrations are measured using the Qubit 2.0 Fluorometer (Thermo Fisher Scientific) which achieves a higher sensitivity and accuracy by fluorometric quantitation.

RNA integrity is validated by analysis of RNA samples on a 2 % agarose gel by electrophoresis. Distinct band of 16S and 23S rRNAs on the stained gel indicate integer RNA. Absence of DNA is verified by PCR with 0.5 µl RNA as template and 0.5 µl genomic listerial DNA as positive control. As primers, lmo0721_nestAB and lmo0721_B are used to amplify a fragment of ≈ 400 base pairs (bp). For NGS, RNA and cDNA integrity is analyzed using the 2100 Bioanalyzer (Agilent Technologies) and the RNA 6000 Nano Kit, RNA 6000 Pico Kit or High sensitivity DNA kit (all Agilent Technologies) by following the manufacturer's instructions. This automated chip-based electrophoresis system enables sizing, quantification, and purity assessments for RNA and DNA samples.

2.3.1.6 DNA sequence analysis

20 – 80 ng/µl PCR product or 80 – 100 ng/µl plasmid DNA with the respective primers are sequenced at GATC Biotech using the Lightrun Sanger sequencing method. DNA sequences are aligned to the genome sequence of *L. monocytogenes* EGDe using NCBI Nucleotide BLAST (Altschul *et al.*, 1990).

2.3.1.7 Purification of DNA

PCR products or restriction preparations are purified using the E.Z.N.A. Cycle Pure Kit (Omega Bio-Tek) according to the instructions in the manual. To purify DNA from agarose gels, the desired bands are visualized under an UVsolo TS Imaging System (Biometra) and cut out of the gel with a scalpel. The DNA fragment is purified using the E.Z.N.A. Gel Extraction Kit (Omega Bio-Tek) according to the manufacturer's instructions.

2.3.2 Agarose gel electrophoresis

The length of DNA fragments is analyzed by agarose gel electrophoresis. Due to the negative charge of the DNA molecules, application of voltage leads to migration of the fragments in an electrical field through the agarose gel matrix to the positively charged pole (anode). A DNA ladder with molecules of defined lengths allows estimation of fragment size. Depending on the fragment size, 1 % or 2 % (w/v) LE agarose (Biozym) dissolved in 1x TAE buffer is used. The GeneRuler 1 kb DNA Ladder (Fermentas) is used for 1 % gels separating DNA fragments larger than 600 base pairs (bp) and the GeneRuler 100 bp

DNA Ladder (Fermentas) for 2 % gels for DNA fragments smaller than 600 bp. Prior to loading the gel pockets, DNA samples (2-5 µl) are mixed with 6x DNA loading dye (Fermentas). Gel electrophoresis is carried out in a PerfectBlue Gelsystem mini electrophoresis chamber (Peqlab) with the PeqPower 300 power supply unit (Peqlab) filled with 1x TAE buffer at 100-120 V for 30 up to 90 min. Afterwards, DNA is stained with GelRed (Biotium) for approximately 20 min and bands visualized under UV light on the UVsolo TS Imaging System.

2.3.3 Polymerase chain reaction

The polymerase chain reaction (PCR) is used for the *in vitro* enzymatic amplification of DNA fragments via a thermostable DNA polymerase. In the first step, the reaction mix is heated to cause separation of the two complementary DNA strands (denaturation). The temperature is then lowered to allow binding of specific primers to the target DNA sequence (annealing) before temperature is elevated again in order to let the DNA-polymerase elongate the primers by adding dNTPs to the nascent strand which is complementary to the template strand (elongation).

2.3.3.1 Standard PCR

For generation of PCR products for cloning, Pfu Polymerase (Thermo Fisher Scientific) is used. This high-fidelity polymerase exhibits a 3'-5' exonuclease (proofreading) activity, thus creating PCR products with lower mutagenesis rate. For conventional gene amplification (e.g. screening or sequencing), a Taq polymerase (self-produced) with a lower replication fidelity is used. A PCR mix containing primers, appropriate buffer, required cofactors, dNTPs and thermostable polymerase is prepared and transferred into 0.2 ml PCR tubes.

Taq Polymerase	**25 µl**	**Pfu Polymerase**	**50 µl**
Forward primer (10 pmol/µl)	1 µl	Forward primer (10 pmol/µl)	2 µl
Reverse primer (10 pmol/µl)	1 µl	Reverse primer (10 pmol/µl)	2 µl
10x Taq Buffer (Thermo Scientific)	2.5 µl	10x Pfu Buffer + $MgSO_4$ (Fermentas)	5 µl
$MgCl_2$ (25 mM) (Thermo Scientific)	2.5 µl	dNTPs (20 mM) (Fermentas)	0.5 µl
dNTPs (20 mM) (Fermentas)	0.5 µl	Pfu Polymerase (Fermentas)	0.5 µl
Taq Polymerase (self-produced)	0.1 µl	Template	1 µl
Template	1 µl	MQ-H_2O	39 µl
MQ-H_2O	16.4 µl		

For amplification of gene fragments, a 1:10 dilution of *L. monocytogenes* EGDe genomic DNA is used. For colony-PCR, cell material is picked off an agar plate with a sterile pipette tip and directly placed into a PCR tube with the PCR mix. Furthermore, reaction volumes are downscaled to 25 µl and the initial denaturation is elongated to 10 min to lyse the cells and release the template DNA. Annealing temperatures are adjusted to primer specificity and elongation time is adjusted to the amplicon size.

Reactions are carried out in a thermal cycler (Primus 96 advanced (Peqlab), MJ Mini Personal Therma Cycler (Bio-Rad)). PCR products are purified using the E.Z.N.A. cycle pure kit.

PCR Program		
Initial denaturation	95°C	3 min or 10 min (colony PCR)
	PCR cycles (30x)	
Denaturation	95°C	30 sec
Annealing	50-54°C	30 sec
Elongation	72°C	1 min / 1 kb (Taq)
		2 min / 1 kb (Pfu)
	End of cycles	
Final elongation	72°C	5 min
Holding	15°C	forever

2.3.3.2 qRT-PCR

qRT-PCR is performed with PerfeCTA SYBR Green FastMix (Quanta Biosciences), a 2x ready to use solution containing all components necessary for qRT-PCR, including a 2x reaction buffer, $MgCl_2$, dNTPs, SYBR Green I dye, AccuFast Taq DNA polymerase and stabilizers. 5 µl of the diluted cDNA template (100 ng/µl) or DEPC-H_2O as negative control are added to 15 µl of the qRT-PCR mix (including primers and 3 µl DEPC-H_2O). Each cDNA sample (corresponding to one specific condition) from three independent biological experiments is measured twice, cDNA for measurement of the reference gene 16S RNA (coding for the 16S ribosomal RNA of the small subunit of the ribosome) is diluted 1:100 since 16S RNA is abundant in bacterial cells.

qRT-PCR reaction mix	**20 µl**
2x PerfeCTA SYBR Green FastMix (Quanta)	10 µl
Forward Primer (10 pmol/µl)	1 µl
Reverse Primer (10 pmol/µl)	1 µl
DEPC-H_2O	3 µl
cDNA (100 ng/µl)	5 µl

The reaction mix is pipetted into low-profile PCR-tube strips (Bio-Rad) or single PCR tubes (BioRad) and measured using the CFX96 Touch (Bio-Rad) or the Smartcycler System (Cepheid). After the PCR cycles, an additional melt curve is created to check specificity of primers.

qRT-PCR Program		
Initial denaturation	95°C	10 min
	PCR cycles (40x)	
Denaturation	95°C	20 sec
Annealing	53°C	30 sec
Elongation	72°C	30 sec
	End of cycles	
Melt Curve	53°C - 97°C	0.2°C/sec

Data evaluation

Relative transcription levels (RTL) are calculated using the $2^{-\Delta\Delta C_T}$ method (Livak & Schmittgen, 2001). Thereby, expression of target genes is compared to a non-regulated reference gene between one or more sample conditions and a control conditions (Equation 1). In this thesis, the established house-keeping gene 16S rRNA encoding a component of the 30S small subunit of a prokaryotic ribosome or the gene lmo1759 (*pcrA*) encoding an ATP-dependent DNA helicase are used as reference genes. RTL are calculated in % compared to the control conditions which is preassigned at 100 % transcription.

$$RTL = 2^{-\Delta\Delta C_T}$$

$$\Delta\Delta C_T = Avg.\Delta C_{T,sample\ condition} - Avg.\Delta C_{T,control\ condition}$$

$$\Delta C_T = Avg.target\ gene\ C_T - Avg.reference\ gene\ C_T$$

Equation 1: Formula of the $2^{-\Delta\Delta C_T}$ method
Formula for the calculation of RTL using the $2^{-\Delta\Delta C_T}$ method. Avg. = average; C_T = cycle threshold; Adapted from Livak & Schmittgen, 2001.

2.3.4 Enzymatic modification of nucleic acids

2.3.4.1 DNA digestion by restriction endonucleases

Site-specific restriction endonucleases are used to digest DNA fragments and plasmids. All restriction enzymes and buffers listed in **Table 5** are purchased from Thermo Fisher Scientific.

Table 5: Restriction enzymes used in this study

Enzyme	Restriction site	Reaction buffer
*Eco*RI	GAATTC	*Eco*RI buffer
*Bam*HI	GGATCC	*Bam*HI buffer
*Kpn*I	GGTACC	*Kpn*I buffer
*Xma*I (*Cfr*9I)	CCCGGG	*Xma*I buffer
*Bgl*II	AGATCT	Orange buffer

The following reaction mixes are usually incubated at 37°C for 2-3 h. DNA fragments and plasmids are purified using the E.Z.N.A. cycle pure kit following the manufacturer's instruction. When necessary, fragments are recovered by gel electrophoresis and subsequent purification with the E.Z.N.A. gel extraction kit.

Restriction reaction mix	**100 µl**
DNA fragment / plasmid	up to 10 µg
10x Buffer	10 µl
Restriction enzyme	4 µl
MQ-H_2O	filled up to 100 µl

2.3.4.2 Dephosphorylation of plasmids

In order to prevent religation of plasmids after restriction digestion, plasmids are dephosphorylated using shrimp alkaline phosphatase (SAP; Thermo Fisher Scientific). After gel electrophoresis of the

digested plasmid and purification, the whole eluate is used in the following reaction mix and incubated for 1h at 37°C. Afterwards, the dephosphorylated plasmid is purified using the E.Z.N.A. cycle pure kit.

Dephosphorylation reaction mix	**100 µl**
Eluted plasmid	88 µl
SAP buffer (Thermo Fisher Scientific)	10 µl
SAP (Thermo Fisher Scientific)	2 µl

2.3.4.3 DNA ligation

Ligation of DNA fragments and plasmids is performed using T4 DNA ligase (Thermo Scientific). Typically, a molar vector to insert ratio of 1:3 to 1:7 is used and the appropriate amounts are calculated by an online ligation calculator. The reaction mix is incubated at 22°C for up to 1 h or at 15°C overnight. The reaction mix is directly used to transform or electroporate target bacterial cells.

Ligation reaction mix	**10 µl**
Vector	varying
Insert	varying
T4 DNA ligase buffer (Thermo Fisher Scientific)	1 µl
T4 DNA ligase (Thermo Fisher Scientific)	1 µl
MQ-H_2O	fill up to 10 µl

2.3.5 Genetic modification of bacteria

2.3.5.1 Preparation of $CaCl_2$-competent cells

For preparation of calcium chloride ($CaCl_2$) competent *E. coli* cells, 100 ml LB medium is inoculated with 1 ml of an *E. coli* overnight culture and grown to the logarithmic growth phase (correlating to OD_{600} = 0.3 – 0.6) under continuous shaking at 150 rpm and 37°C. The cells are centrifuged (10 min, 4,000 rpm, 4°C), the supernatant is removed, and the pellet is resuspended in 10 ml ice-cold 0.1 M $CaCl_2$ (Merck). After resting on ice for 30 min, cells are harvested again (10 min, 4,000 rpm, 4°C) and resuspended in ice-cold 0.1 M $CaCl_2$ containing 20 % (v/v) glycerol (Carl Roth). The cell suspension is divided in 100 µl aliquots, shock frozen in liquid nitrogen and stored at -80°C.

2.3.5.2 Transformation

100 µl $CaCl_2$ competent *E. coli* cells are thawed on ice and 10 µl ligation mix is added. The mixture is incubated on ice for 30 min, afterwards cells are heat shocked at 42°C for 90 s (TB1 Thermoblock, Biometra). Again, tubes are placed on ice for 2 min and 1 ml LB medium is added. The cells are incubated at 37°C under continuous shaking (150 rpm) for 4 – 6 h allowing for the antibiotic resistance genes encoded on the plasmid to be expressed. Afterwards, 100 µl of the cell suspension is plated on LB agar plates containing 300 µg/ml erythromycin. The remaining cell suspension is centrifuged (13,200 rpm, 1 min, RT), the supernatant decanted, and the cell pellet is resuspended in the remaining medium (approximately 100 µl). This suspension is plated on LB agar plates containing 300 µg/ml

erythromycin. The plates are incubated at 37°C for 1 – 2 days until colonies reach a suitable size to be picked. Successfully transformed *E. coli* colonies are screened via colony-PCR.

2.3.5.3 Preparation of electrocompetent cells

For preparation of electrocompetent *L. monocytogenes* cells, 0.5 ml of a 50 ml overnight culture is used to inoculate 50 ml BHI containing 0.1 g glycine (Merck). Cells were grown to logarithmic growth phase (OD_{600} = 0.5) at 37°C and induced with 20 µl Penicillin G (12.5 mg/ml; Biochrom). Cultures are grown to OD_{600} = 0.65 at 37°C and subsequently harvested (4°C, 1,200 g, 10 min). Supernatant is discarded, and the cell pellet resuspended in 5 ml pre-chilled SMHEM (952 mM sucrose, 3.5 mM $MgCl_2$, 7 mM HEPES (all Carl Roth)) buffer. After repeated centrifugation and removal of buffer, the washed cell pellet is resuspended in 0.5 ml pre-chilled SMHEM buffer and dispensed in 100 µl aliquots, shock frozen in liquid nitrogen and stored at -80°C.

2.3.5.4 Electroporation

100 µl electrocompetent *L. monocytogenes* cells are thawed on ice and mixed with 1 – 5 µg plasmid DNA in an ice cold 2 mm gap electroporation cuvette (Peqlab). The cells are then exposed to an electrical pulse in the Gene Pulser (Bio-Rad) at 25 µF, 12.5 kV/cm and 200 Ω. Afterwards, 1 ml SOC-Medium is added immediately, and the suspension is transferred into a 1.5 ml Eppendorf tube and incubated at 30°C for 6 h with continuous shaking (150 rpm). 100 µl are plated out on BHI plates containing an appropriate selective antibiotic. The remaining cells are centrifuged (1 min, 13,200 g, RT), the medium discarded and the pellet is resuspended in the remaining medium. This cell suspension is again plated out on BHI plates containing appropriate selective antibiotic. Plates are incubated at 30°C for 2 days. Colonies are screened for the vector with correct insert via colony-PCR.

2.3.5.5 Construction of in-frame deletion mutants

Stable in-frame deletion mutants of several chromosomal genes in the parental *strain L. monocytogenes* EGDe are constructed using homologous recombination strategies (**Supplementary figure 1**). LmoX represents the gene sequence which is supposed to be deleted. The used primers are listed in **Table 3**.

As a first step, the flanking regions of the gene (approximately 1,000 bp) are amplified using the proof-reading Pfu polymerase and the primer pairs lmoX_A/B (upstream region) and lmoX_C/D (downstream region). The amplified fragment AB and CD are purified, digested with *Bgl*II and ligated. The resulting ligation product AD serves as a template for a nested PCR using the primer pair lmoX_nestAB and lmoX_nestCD, thus amplifying an approximately 1,200 bp fragment which contains restriction sites at both ends (*Bam*HI + *Eco*RI or *Kpn*I + *Xma*I) for cloning. After digestion with *Bam*HI + *Eco*RI or *Kpn*I + *Xma*I, the fragment is ligated into the likewise cut vector pLSV101, a temperature sensitive shuttle vector derived from pLSV1 (Joseph *et al.*, 2006). The resulting vector pLSV101-ΔlmoX is transformed

into $CaCl_2$-competent *E. coli* DH5α cells for plasmid amplification. Transformed cells are selected on LB agar plates with 300 µg/ml erythromycin at 37°C. Positive clones are screened via colony-PCR, using the pLSV101-specific primer pair LSV3 and LSV-4380rev yielding an approximately 1,500 bp size fragment. Plasmids of a positive clone are isolated and sequenced to check the correct insertion of the AD fragment. The plasmid is transferred vial electroporation into electrocompetent EGDe cells that are plated on BHI agar plates containing 10 µg/ml erythromycin. Plates are incubated at 30°C. Three clones are picked and streaked out onto a BHI agar plate supplemented with 10 µg/ml erythromycin and clones harboring the insert containing plasmid are validated via colony-PCR using one plasmid-specific and one insert-specific primer (LSV-4380rev and lmoX_nestAB, respectively). To select for cells with successful integration of the vector into the bacterial chromosome via homologous recombination, positive clones are incubated at 42°C on BHI agar plates with 10 µg/ml erythromycin. Clones are checked for successful integration with the primer pairs lmoX_A/LSV-4380rev and lmoX_D/LSV3 in a colony-PCR. Positive mutants are subcultured in BHI medium without antibiotics at 30°C several times allowing for a second recombination event and excision of the plasmid. Dilutions of each subculture are plated on BHI without erythromycin and incubated at 30°C overnight. Grown colonies are picked and streaked out on BHI agar plates with and without erythromycin. Strains lacking the gene are identified via colony-PCR using the primer pairs lmoX_nestAB and lmoX_nestCD. The respective gene locus is sequenced to rule out frame shifts.

2.3.6 NGS methods

2.3.6.1 *De novo* genome sequencing of *L. kieliensis* sp. nov.

NGS sample preparation and sequencing

Genomic DNA isolation of *L. kieliensis* sp. nov. is conducted as described (2.3.1.2) and concentration and purity are determined by using the Qubit Fluorometer (2.3.1.5). The concentration is normalized to 75 ng/µl and 52.5 µl are transferred to a microTUBE (Covaris). gDNA is sheared using the S220 focused-ultrasonication system (Covaris) (25 s, 175 W, 10 % duty factor, 200 cycles/burst). For library preparation, the TruSeq DNA PCR-free LT library preparation Kit (Illumina) is used with a modified protocol (Huptas *et al.*, 2016). In short, sheared gDNA is size selected using AMPure XP beads from the Kit. Afterwards, blunt-ends are created, followed by a second size selection. After 3'-adenylation, single index adapters are ligated to the fragments. The library is then sequenced on the MiSeq platform (Illumina) using the MiSeq Reagent Kit v2 (Illumina) and paired-end sequencing with 50 cycles.

2.3.6.2 Transcriptomics of *L. monocytogenes* EGDe

NGS sample preparation and sequencing

Sample preparation and NGS of total mRNA in *L. monocytogenes* under different conditions is performed as recently described (Landstorfer *et al.*, 2014, Ferrari *et al.*, 2017) and outlined below. RNA is isolated as described before 2.3.1.3 Isolation of bacterial RNA

Library preparation

Concentration and quality of the modified RNA is checked using the Qubit and the Bioanalyzer. 100 ng RNA is isolated and concentrated to a final volume of 5 µl using the Concentrator 5301 (Eppendorff).

The TruSeq Small RNA Library preparation kit (Illumina) is used according to the manufacturer's protocol to ligate 3' and 5' adapters to the RNA fragments which are subsequently reverse transcribed into double-stranded cDNA and amplified via PCR. cDNA concentration is checked using the Qubit and the mean of peak distribution is determined using the Bioanalyzer. The cDNAs from the three tested conditions (BHI, BHI + 1,2-PD, BHI + 1,2-PD + B_{12}) for each of the two time points (exponential and stationary phase) are mixed with Novex TBE urea sample buffer (Life Technologies) and loaded onto 6 % Novex polyacrylamide gel (Life Technologies) in 1x TBE buffer for size selection. The fragments are stained in 1x TBE buffer containing 0.0001 % (v/v) SYBR gold nucleic acid gel stain (Life Technologies) and visualized under a UV table (Syngene). Fragment sized between 200 and 350 bp are selected using the custom RNA ladder and the high resolution ladder (Illumina) as orientation. cDNA is extracted from the gel by centrifugation with 0.22 µm Costar Spin-X plastic centrifuge tube filters (Corning) and purified by ethanol precipitation. The combined and indexed libraries for the exponential and the stationary phase are quantified using the Qubit and are diluted to a concentration of 2 nM in Buffer EB (Qiagen) using the following equation:

$$nM = ([\frac{ng}{\mu l}] \cdot 10^6)/(mean\ of\ peak\ distribution\ \cdot 650 \frac{g}{mol})$$

10 µl of the 2 nM libraries is mixed with 10 µl 0.1 M NaOH (VWR) and incubated for 5 min at RT for denaturation. Afterwards, libraries are diluted to the final concentration of 10 pM in 1 mM NaOH using pre-chilled HT1 buffer (Illumina).

Sequencing

Libraries are sequenced on the MiSeq System (Illumina) using the MiSeq reagent kit v2 50 cycles (Illumina) resulting in 50 nt single-end reads.

2.3.7 Bioinformatics

2.3.7.1 Genome assembly and annotation

Following the DNA sequencing of *L. kieliensis* sp. nov., raw reads are filtered using the NGS QC Toolkit (Patel & Jain, 2012) for a cut-off read length of 80 % having a mean sequence quality score (Phred) ≥20. After filtering, reads are trimmed resulting in a final read length of 170 nt. Draft genome sequences are assembled using SPAdes 2.5.1 (Bankevich *et al.*, 2012) with automatic k-mer selection (21, 33, 55, 77, 99, 127 size). The assembly is submitted for automated annotation to the NCBI Prokaryotic Genome Annotation Pipeline (PGAP) (Tatusova *et al.*, 2013). Additional functional annotation is performed by the RAST (Rapid Annotation using Subsystem Technology) server (Overbeek *et al.*, 2014). The *L. kieliensis* sp. nov. Whole Genome Shotgun (WGS) project is submitted at DDBJ/EMBL/GenBank under the accession number LARY00000000 (BioProject: PRJNA276498; Biosample: SAMN03376159).

2.3.7.2 Phylogenetic analysis

Pairwise comparison between the *L. kieliensis* sp. nov. assembled draft genome and publicly available genome sequences from type strains of all 17 up to date known *Listeria* spp. is conducted to calculate BLAST average nucleotide identities (ANIb). This is accomplished by using JSpecies, more precisely the JSpecies Web Service (Richter and Rosselló-Móra, 2009). A phylogenetic tree based on the resulting ANIb values is constructed with the help of MEGA6 software (Tamura *et al.*, 2013) and the Neighborhood-Joining-Method.

2.3.7.3 Genome comparison of different *Listeria* spp.

For a genome comparison between *Listeria sensu stricto* and *Listeria sensu lato* members, FASTA files of type strain genomic sequences of the 16 up to date known *Listeria* spp. (without *L. grayi*) are downloaded from NCBI GenBank (Benson *et al.*, 2017). The sequences as well as the genome of the newly sequenced *L. kieliensis* are uploaded to the RAST server and functionally annotated. The percentage of the predicted amino acid sequences identity for each protein coding gene of *L. monocytogenes* against the proteins of the other *Listeria* spp. within both clades is calculated.

To analyze the presence of selected *L. monocytogenes* genes involved in virulence and colonization in the genomes of *L. kieliensis* and other *Listeria sensu lato* members, the percentage of amino acid sequence identity of the corresponding genes against the proteins of *Listeria sensu lato* spp. is calculated. Well conserved gene products with at least 70 % sequence homology to these species are considered as functionally homologous, whereas genes below 40 % are not considered to be functionally conserved. A table is created, and genes are grouped in functional categories.

Additionally, the complete list of *L. monocytogenes* proteins with the respective homology percentage values against each species is filter for genes with at least 70 % sequence homology amongst the

Listeria sensu stricto spp. and less than 40 % sequence homology amongst the *Listeria sensu lato* group. The corresponding genes of this list serve as candidates for involvement in the colonization process of the host during *L. monocytogenes* infection.

2.3.7.4 Analysis of transcriptome sequencing data

After successful sequencing, the reads of each of the 6 conditions are stored in separate Illumina output files called FASTQ files. The analysis of transcriptome sequencing data is conducted as described recently (Landstorfer *et al.*, 2014, Ferrari *et al.*, 2017).

Galaxy

Galaxy (Afgan *et al.*, 2016; Blankenberg *et al.*, 2010; Goecks *et al.*, 2010) is an online server containing a large collection of bioinformatic tools which can be used for analysis of RNA sequencing data. FASTQ files are converted from an Illumina format to a sanger format using FASTQ groomer. This is necessary for mapping of the FASTQ files to the *L. monocytogenes* EGDe reference genome FASTA file (NCBI accession number NC_003210) with the help of Bowtie for Illumina (Langmead *et al.*, 2009) using the default settings (20 nt seed length, 0 mismatches in the seed). The resulting SAM file is filtered using the NGS: SAM tools eradicating unmapped reads. Using the same tools, the filtered SAM files are converted to BAM format. The BAM files are subsequently sorted by coordinates and indexed using the Java-based command-line program Picard tools (version 1.107; Li *et al.*, 2009).

Artemis

Using the Artemis program (version 15), the number of reads overlapping a gene on the same strand (counts) are calculated (Rutherford *et al.*, 2000; Carver *et al.*, 2012). Therefore, a GenBank file of the *L. monocytogenes* reference genome (NCBI accession number NC_003210) is used. The resulting read counts for each coding sequence are saved as a .txt file and converted to a .xlsx Microsoft Excel file.

RPKM calculations

The read counts of each library are normalized to the smallest library for more accurate comparison. RPKM (reads per kilobase per million mapped reads) values for each gene are calculated using the following formula to correct for differences in both sequencing depth and gene length:

$$RPKM = number\ of\ reads\ /\ (\frac{length\ of\ gene}{10^3} \cdot \frac{total\ number\ of\ reads}{10^6})$$

The fold changes of RPKM values of the conditions BHI + 1,2-PD and BHI + 1,2-PD + cobalamin (sample conditions) in comparison to the reference condition BHI are calculated. Fold changes of the *pdu*/*cob*/*cbi*/*eut* genomic island are visualized using a two-color scheme, with blue colors expressing positive and red colors negative fold changes and the color intensity referring to the magnitude of fold

change. For comparison of RNA sequencing data with qRT-PCR data, mRNA expression of a specific gene under sample conditions in percent is calculated based on its RPKM values with the reference condition being set to 100 % expression.

$$RNA-sequencing\ mRNA\ expression\ (\%) = \frac{RPKM_{sample\ condition}}{RPKM_{reference\ condition}} \cdot 100$$

Differential gene expression analysis

Read counts of all protein coding genes are analyzed for differential gene expression by conducting pairwise comparisons between conditions by using the Bioconductor (Gentleman *et al.*, 2004) package edegR (Robinson *et al.*, 2010) as described previously (Mühlig *et al.*, 2014). Genes with less than 1 count per million (cpm) at both conditions are filtered and the library sizes are further normalized by the trimmed mean of M-values (TMM) method (Robinson and Oshlack, 2010). Exact-test function with a common dispersion of 0.1 is used to perform differential expression analysis. The Benjamini-Hochberg (BH) method (Benjamini and Hochberg, 1995) is used to adjust the false discovery rate (FDR) and genes with FDR ≤ 0.3 and p-value ≤ 0.05 are considered as differentially expressed. Log_2FC (logarithm base 2 fold-change) values >1 represent upregulation and values < -1 downregulation of a specific gene under the two different conditions.

2.3.7.5 Bioinformatic protein analyses

Proteins are analyzed using TOPCONS (Tsirigos *et al*., 2015), a tool for consensus prediction of membrane protein topology and signal peptides, which predicts transmembrane helices as well as cytosolic and extracellular amino acids sequences. The domain structure of proteins is analyzed using ExPASy PROSITE (Sigrsit *et al*., 2013; Sigrist *et al*., 2002). The online tool ExPASy MyDomains is used to graphically depict protein domains (Hulo *et al*., 2008). A 3D model of proteins is constructed using ExPASy SWISS-MODEL (Guex *et al*., 2009; Arnold *et al*., 2006; Kiefer *et al*., 2006; Biasini *et al*., 2014) and the ProMod3 Version 1.0.2.

2.4 Cell culture

2.4.1 Cell lines

For *in vitro* cell culture experiments, Caco-2 (human epithelial colorectal adenocarcinoma cells, ATCC HTB-37) and HEp-2 (human larynx squamous cell carcinoma cells, ATCC CCL-23) cells from the American Type Culture Collection (ATCC) are used. Cells are used up to passage number 40 for experiments.

2.4.2 Culture conditions

All materials and media used are listed in **Supplementary Table 3**. Cells are cultured at 37°C and 5 % CO_2 in Dulbecco's Modified Eagle Medium (DMEM) (Biochrom) supplemented with 10 % (v/v) fetal calf serum (FCS; Pan Biotech) (DMEM + FCS). A HeraCell incubator (Heraus) or a CO_2- incubator Serie

CB (Binder) is used for incubation. Typically, 75 cm^2 or 175 cm^2 cell-culture flasks for adherent cells with a ventilated cap (Sarstedt) are used. Medium is changed three times a week. For washing, Dulbecco's PBS (Biochrom) is used.

2.4.3 Subcultivation of cells

When reaching ca. 90 % confluency, cells are split into new cell culture flasks. Therefore, medium is removed, and cells are washed with pre-warmed Dulbecco's PBS (Biochrom) supplemented with 1 mM ethylenediaminetetraacetic acid (EDTA) (PBS-EDTA). Pre-warmed 1x 0.25 % Trypsin + 0.02 % EDTA (Biochrom) is added and the flask is incubated at 37°C 5 % CO_2 for 10 min or until all cells are detached. The enzymatic reaction is stopped by adding pre-warmed DMEM + FCS. Cells are resuspended and transferred into a 15 ml Falcon tube. The cell suspension is centrifuged at 500 rpm for 5 minutes. The supernatant is discarded, and cells are resuspended in an appropriate amount of DMEM + FCS and split into two new cell culture flasks.

2.4.4 Freezing of cells

For long term storage, cells are detached with trypsin as described before. After addition of DMEM + FCS, centrifugation and aspiration of the supernatant, the cells are resuspended in freezing medium (FCS + 10 % (v/v) dimethyl sulfoxide (DMSO; Carl Roth)). Approximately 1 ml freezing medium is used for a 75 cm^2 flask with 90 % confluent cells and is transferred into a 2 ml cryotube (Sarstedt). The tubes are put in a Mr. Frosty freezing container (Thermo Fisher Scientific) filled with isopropanol (Carl Roth) to ensure a constant and slow freezing rate. The freezing container is stored at -80°C for 24 h, afterwards the cryo tubes are transferred into a tank filled with liquid nitrogen for long term storage.

2.4.5 Thawing and seeding of cells

Cryo tubes from liquid nitrogen are thawed in a 37°C water bath. The cells are transferred into 10 ml pre-warmed DMEM + FCS in a 15 ml falcon tube. The tube is centrifuged at 500 rpm for 5 min and the supernatant is discarded. Cells are resuspended in 15 ml DMEM + FCS and transferred into a 75 cm^2 flask for incubation.

2.4.6 Cell counting

Cells are detached with trypsin as described before. After addition of DMDM + FCS, centrifugation and aspiration of supernatant, the cells are resuspended in DMEM+FCS. 50 µl cell suspension is transferred to a 1.5 ml Eppendorf tube and mixed with 50 µl trypan blue (AppliChem). 10 µl are pipetted into a Neubauer-improved counting chamber (Brandt) and the number of cells in the 4 large corner squares is counted under a microscope. The following formula is used to calculate the number of cells.

$$cell\ concentration\ (cells/ml) = \frac{number\ of\ cells\ \cdot\ 10^4/ml}{number\ of\ squares\ \cdot\ dilution}$$

2.4.7 Mycoplasma detection

Cells are checked at regular intervals for contamination with mycoplasma. Therefore, supernatant of cultures is tested via PCR using the MYCOPLASMACHECK barcodes at GATC Biotech. Results can be checked online after 48 h. Alternatively, cells to be checked are seeded in a petri dish for adherent cells (Sarstedt) and incubated to allow attachment of cells. The next day, cells are washed twice with PBS and fixed using a 5 ml solution of methanol (Carl Roth) and acetic acid (Sigma-Aldrich) (3:1 ratio) with subsequent incubation for 10 min at RT. Fixative is aspirated, and cells are stained with 5 ml DAPI solution (5 mg/ml, diluted 1:100 in McIvaine buffer pH 7.0 (4.2 g/l citric acid (Carl Roth), 22.7 g/l Na_2HPO_4 (Fluka))). DAPI solution is discarded and the petri dish is dried. Cells are checked under a fluorescence microscope. Stained cell nuclei become visible, dotted stains around the nuclei would be indicators for mycoplasma contamination.

2.4.8 Glycerol stocks for infection

To create glycerol stocks of *L. monocytogenes* strains for infection, cells from a 3 ml BHI overnight culture (37°C, 150 rpm, 16 h) are diluted 1:25 in 30 ml of BHI medium and grown at 37°C shaking (150 rpm) to mid-log phase (OD_{600} = ~0.85-0.95). 20 ml culture is harvested by centrifugation in a 50 ml falcon tube at 6,000 rpm for 8 min at RT. The supernatant is aspirated, and cells are washed with 20 ml warm PBS. After centrifugation (6,000 rpm, 8 min, RT) and aspiration of supernatant, cells are resuspended in 20 ml warm PBS containing 15 % (v/v) glycerol. The cell suspension is diluted to OD_{600} = 0.5 and 1 ml aliquots are shock frozen in liquid nitrogen and stored at -80°C. Prior to infection, two aliquots per strain are thawed, and the number of viable bacteria is determined as colony forming units (cfu) per ml by plating on BHI agar.

2.4.9 Adhesion assay

For the assessment of adhesion capabilities of different *L. monocytogenes* strains, a total of 2.5×10^5 Caco-2 or HEp-2 cells per well are seeded in a 24-well culture plate (Sarstedt) and cultivated for 48 h until infection to receive an intact eukaryotic cell monolayer. Cells are washed twice with PBS/$Mg^{2+}Ca^{2+}$ (Biochrom) and covered for 35 min with 500 µl DMEM containing approximately 2.5×10^6 bacteria (multiplicity of infection, MOI =10) from a glycerol stock. For assessment of adhesion, the Caco-2 cells are washed thrice with PBS/$Mg^{2+}Ca^{2+}$ after a 35 min incubation period. Cell layers are lysed in 1 ml of cold Triton X-100 (0.1% (v/v)) (Carl Roth) and vortexed for 1 min to disrupt the cells. The number of adherent bacteria is determined by plating dilutions of the lysed eukaryotic cells on BHI agar and incubating the plates at 37°C for 24 h. Mean values of three independent biological experiments in technical duplicates are used for the calculation of the percentage of adherent cells from the infection titer.

2.4.10 Intracellular replication assay

Similar to the adhesion assay, 2.5×10^5 Caco-2 or HEp-2 cells per well are seeded in a 24-well culture plate and cultivated for 48 h until infection. Cells are then infected with an MOI of 10. Afterwards, cells are washed twice with PBS/$Mg^{2+}Ca^{2+}$ after 1 h of incubation. Extracellular bacteria are removed by adding 0.5 ml DMEM containing 100 µg/ml gentamycin (Biochrom) for 1 h, and the medium is then replaced by DMEM with 10 µg/ml gentamycin. At appropriate time points of incubation in the presence of 10 µg/ml gentamycin, the infected cells are washed again with PBS/$Mg^{2+}Ca^{2+}$ and then lysed in 1 ml of cold Triton X-100 and vortexed. Cell lysates are plated on BHI to enumerate the number of intracellular bacteria. Mean values of three independent biological experiments in technical duplicates are used for the calculation of the percentage of intracellular bacteria from the infection titer.

2.4.11 Comparative analysis of adhesion and invasion

To determine to percentage of adhesive bacterial cells which are able to invade to host cell, adhesion assay (2.4.9 Adhesion assay) and intracellular replication assay (2.4.10 Intracellular replication assay) were performed in parallel with the following exceptions: Incubation time of *L. monocytogenes* strains for the adhesion to Caco-2 cells was prolonged to 1 h to match the incubation time for intracellular replication. Afterwards, cells are washed twice with PBS/$Mg^{2+}Ca^{2+}$and either overlaid with 0.5 ml DMEM containing 100 µg/ml gentamycin (Biochrom) (assessment of intracellular cells) or with 0.5 ml DMEM without gentamycin (assessment of both adhesive and intracellular cells). By subtracting the number of intracellular cells from the number of adhesive and intracellular cells combined, the cfu of adhering *L. monocytogenes* cells can be calculated. The number of adhesive cells being able to invade to host cell is calculated using the following formula:

$$invading\ cells\ [\%] = \frac{cfu_{intracellular\ cells}}{cfu_{adhesive\ cells}} \times 100$$

2.5 Mouse infections

The animal experiments conducted in Germany have been approved by the district government of Upper Bavaria under the permit number 55.2-1-54-2532-194-2015. Animal experiments performed in the USA are in accordance with the recommendations in the Guide for the Care and Use of Laboratory Animals published by the National Institutes of Health and the corresponding procedures have been approved by the Institutional Animal Care and Use Committee (IACUC) at the University of Kentucky. All material and equipment used is listed in **Supplementary Table 4**.

2.5.1 Mouse strain

Four-week-old female specific pathogen free (SPF) BALB/cByJ mice from The Jackson Laboratory (Bar Harbor, ME, USA) or BALB/cAnNCrl mice from Charles River Laboratories (Sulzfeld, Germany) were purchased and used for experiments at the age of 6-8 weeks.

2.5.2 Basic mouse care and maintenance

2.5.2.1 Accommodation

Mice are maintained in a specific-pathogen-free facility at the University of Kentucky or the Zentralinstitut für Ernährungs- und Lebensmittelforschung (ZIEL) of the Technical University Munich with a 14-h light and 10-h dark cycle at least two weeks prior to experiments to acclimate them to the new conditions. Three to four mice are housed in Sealsafe Plus individually ventilated cages (IVCs) (Tecniplast), covered in bedding and enriched with a plastic mouse house (Tecniplast) impervious to light and nesting material. Filled cages are autoclaved before use and are changed once a week. Rooms have air-conditioning (22°C constant temperature) and approximately 55% air humidity.

2.5.2.2 Food and water

Mice have access to food and water *ad libitum*. As mouse chow, complete feed for mice breeding (Ssniff) is used, which has been sterilized by radiation (25 kGy). So-called “soft water” is provided, which contains low concentrations of ions (especially calcium and magnesium) to ensure proper functioning of the water bottles (Tecniplast). These dispensers are filled according to manufacturer’s instruction and autoclaved.

2.5.3 Infection experiments

Mice are infected using a model for food borne infection as described previously (Bou Ghanem *et al.*, 2013a). In short, mice are orally infected with *Listeria*-contaminated bread pieces and killed after a defined period of time. Bacterial loads in the lumen and tissue of the GIT as well as in the organs liver, spleen, gallbladder and MLNs are determined.

2.5.3.1 Infection inocula

To prepare frozen aliquots for infection, 20 ml BHI in a 100 ml flask is inoculated with a single colony of *Listeria* spp. or *L. monocytogenes* strains and incubated at 30°C under shaking (225 rpm) for 21 h. Bacteria are vortexed, divided into 550 µl aliquots and stored at -80°C. The next day, at least two aliquots are thawed and recovered in BHI medium for 1.5 h at 30°C without shaking. Serial dilutions are plated on BHI (plus potential antibiotics in the case of tagged strains) to determine the bacterial titers of aliquots.

For co-infection experiments, *L. monocytogenes* EGDe and the corresponding deletion mutants are chromosomally tagged with pIMC3kan (EGDe) *and* pIMC3ery (mutants) containing the IPTG-inducible antibiotic resistance markers kanamycin (3'-aminoglycoside phosphotransferase type III *aphA3*) or erythromycin (rRNA methyltransferase *ermAM*). This allows differentiation of these strains after infection by parallel plating of samples on BHI plates containing 7.5 µg/ml chloramphenicol, 1 mM IPTG as well as 50 µg/ml kanamycin or 5 µg/ml erythromycin.

2.5.3.3 Infection

Mice are placed in a cage with raised wire flooring to prevent coprophagy and denied food for 18-22 h before the infection. For infection of mice, a frozen Aliquot of *Listeria* is thawed and recovered in BHI medium for 1.5 h at 30°C without shaking. The desired inoculum is transferred to a 50 ml falcon tube and centrifuged (10,000g, 10 min, 20°C). The cell pellet is resuspended in 1 ml PBS, transferred to a 1.5 ml Eppendorf tube and centrifuged again (14,000 g, 7 min, RT). After aspiration of the supernatant, the pellet is resuspended in 2 µl of PBS mixed with 3 µl of salted butter (Kroger or REWE). The cell suspension is used to saturate a 2- to 3-mm piece of bread (Kroger or REWE). After the onset of the dark cycle, mice are transferred to an empty cage and fed the *Listeria*-contaminated bread pieces with sterile forceps. Afterwards, the mice are returned to their raised wire flooring cages and food is replenished. One piece of *Listeria*-contaminated bread is dissolved in 1 ml PBS and used to determine the actual infection dose. Oral infection doses of 4-9 × 10^8 cfu/mouse of *L. monocytogenes, L. welshimeri, L. aquatica*, or L. *booriae* are used for comparison of the *Listeria* phylogenetic groups. For co-infection experiments, a 1:1 ratio of *L. monocytogenes* EGDe and its mutants totaling 1–3 × 10^9 cfu/mouse is used.

2.5.3.4 Sampling

For *Listeria* sampling from mouse organs, mice are killed by cervical dislocation and colon and ileum are harvested aseptically, squeezed with sterile forceps, and flushed with 8 ml of PBS to collect the intestinal contents in a 50 ml Falcon tube. Flushed contents are centrifuged at 12,000 g for 20 min and the pellet is then resuspended in 1 ml of sterile water. The washed tissue is cut both longitudinally and laterally with a sterile scalpel, placed into a 50 ml Falcon tube containing 2 ml of sterile water, and homogenized for 1 min using a homogenizer (PowerGen 1000 from IKA Works or homogenizer from Südlabor) at 60 % power. Liver and spleen are harvested aseptically and homogenized for 30 s in 2.5 or 4 ml of sterile water. MLNs are collected in a 1.5-ml Eppendorf tube, mashed through sterile steel screens, and rinsed twice with 750 µl of sterile water. About three to five stool pellets (weighing ~50-100 mg) are collected every 24 h as well as 3 h post-infection, weighed, and suspended in sterile water (150 mg/ml). They are mashed with a sterile toothpick, vortexed for 1 min, and spun down for a short time to sediment debris. Serial dilutions of the intestinal contents and tissues, liver, spleen, and stool are plated on BHI agar with the appropriate antibiotics containing 1 mM IPTG or on Palcam agar.

2.5.3.5 Fractionation

As an alternative sampling method for the GI tissue, it can be fractionated into the mucus layer, the intestinal epithelium and the cells within the underlying LP. Therefore, intestinal tissues are flushed with 8 ml Hanks balanced salt solution supplemented with 2 % (v/v) fetal bovine serum (HB-2) to collect the intestinal contents and cut longitudinally.

HB-2	100 ml
1x Hanks balanced salt solution (HBSS), Ca^{2+}- and MG^{2+}-free, tissue culture, sterile	98 ml
Fetal bovine serum (FBS), tissue culture, sterile	2 ml

Isolation of mucus

Tissue is treated with N-acetylcysteine (NAC) (Sigma) to remove the mucus layer. Therefore, the flushed and longitudinally cut pieces are placed in a series of three 10 ml tubes containing 3 ml PBS + 6 mM NAC. Each step involves incubation for 2 min, vigorous swirling and transfer into the next tube. As a last step, tissue pieces are places in a 10 ml tube containing 3 ml PBS to remove excessive NAC. The NAC and PBS tubes are pooled and centrifuged at 10,000 g for 20 min at 4°C. The supernatant is aspirated, and the mucus pellet is resuspended in 0.5 ml sterile water. Appropriate dilutions are plated on BHI agar plates containing the suitable antibiotics to distinguish between *L. monocytogenes* EGDe and its isogenic mutants.

Isolation of epithelial cells

Tissue pieces are transferred into a petri dish and cut into smaller pieces for 1,4-Dithiothreitol (DTT) treatment which will yield the epithelial fraction. The small cut pieces are placed into a series of 50 ml tube containing 4 ml RPMI 1640 supplemented with 5 % (v/v) fetal bovine serum, 20mM HEPES, 5 mM EDTA and 1 mM DTT (RP5/HEPES/EDTA/DTT). The first tube is incubated at 37°C 250 rpm for 20 min and vortexed for 10 s. Afterwards, the contents of the tubes are decanted onto a sterile mesh filter on top of an empty 50 ml falcon tube. Using a steril forceps, the intestinal pieces are transferred to a fresh tube containing 4 ml RP5/HEPES/EDTA/DTT and incubated at 37°C 250 rpm for 10 min. After anew vortexing and decantation, the whole procedure is repeated one more time in a fresh RP5/HEPES/EDTA/DTT tube with an incubation period of 10 min. After a final washing step of the tissue in a 50 ml tube containing 15 ml RPMI 1640 supplemented with 5 % (v/v) fetal bovine serum (RP5/HEPES) and 20 mM HEPES (RP5/HEPES) to remove EDTA and DTT, the decanted solutions are pooled, centrifuged (10,000 g, 20 min, 4°C) and the generated cell pellet is resuspended in 0.5 ml sterile water and plated are plated on BHI agar plates containing the suitable antibiotics.

RP5/HEPES	100 ml
RPMI 1640	91.9 ml
Fetal bovine serum (FBS), tissue culture, sterile	5 ml
HEPES (1 M)	2 ml
EDTA (0.5 M)	1 ml
DTT (1 M)	0.1 ml

RP5/HEPES	100 ml
RPMI 1640	93 ml
Fetal bovine serum (FBS), tissue culture, sterile	5 ml
HEPES (1 M)	2 ml

Isolation of LP cells

The intestinal pieces are transferred into a 50 ml falcon tube containing 4 ml RP5/HEPES and collagenase IV (1 mg/ml; Worthington) and DNAse I (40 µg/ml; Worthington) to digest tissue and to release the LP cells. Therefore, tissue pieces are incubated under shaking (250 rpm) together with a stir bar at 37°C for 30 min. Several short vortex steps are executed, and the cell solution is decanted onto a mesh filter on top a 50 ml tube. Tissue pieces and stir bar are transferred into a new tube containing RP5/HEPES + collagenase IV and DNase I and the whole procedure is repeated until there are no visible tissue pieces left. The tubes are pooled, centrifuged (10,000 g, 20 min, 4°C) and the cell pellet is resuspended in 0.5 ml sterile water and plated are plated on BHI agar plates containing the suitable antibiotics.

2.5 Statistical methods

Statistical analyses for all experiments were performed using the Student's t-Test in Prism6 (GraphPad, La Jolla, CA, USA). If necessary, Welch's correction is used when two samples have unequal variances and/or unequal sample sizes. P values less than 0.05 were considered significant and are indicated as follows: *, ($P < 0.05$); **, ($P < 0.01$); ***, ($P < 0.001$); NS (not significant, $P \geq 0.05$).

3 Results

Listeriosis in humans and animals is divided into a GI phase, characterized by colonization of the lumen and tissue of the small intestine, caecum and colon, and the systemic phase. The latter, a far more severe form of infection, occurs when *L. monocytogenes* successfully crossed the intestinal barrier and subsequently spread from the mesenteric lymph nodes via the blood to the spleen, liver, gall bladder and brain (Vázquez-Boland *et al.*, 2001b). While the systemic infection and the virulence factors involved are well characterized, oral transmission and the GI phase of infection still need to be illuminated (D'Orazio *et al.*, 2014). Aspects that remain to be deciphered concern the two distinct clades of the genus, especially the evolution, genomic differences and potential colonization abilities of the *Listeria sensu stricto* and *Listeria sensu lato* groups. In this thesis, novel genetic determinants, which have been derived from a genome comparison of different *Listeria* spp., were analyzed for their involvement in the colonization process of the intestines. Therefore, *in vitro* methods including cell culture, transcriptomics, and growth analyses as well as *in vivo* oral infection experiments in mice were applied in this thesis.

3.1 Colonization abilities of *Listeria* spp. after oral infection in an *in vivo* mouse model

The genus *Listeria* consists of two distinct clades, the *Listeria sensu stricto* group including the two pathogens *L. monocytogenes* and *L. ivanovii*, and the *Listeria sensu lato* group, whose members have mostly been discovered only recently (Orsi & Wiedmann, 2016). While the *Listeria sensu lato* are believed to be environmental species, there are numerous reports that support the incidence of *Listeria sensu stricto* spp. in either samples of the GIT or feces of mostly symptom free animals or in food samples of animal origins (Rocourt & Seeliger, 1985; Nayak *et al.*, 1985; Dahshan *et al.*, 2016; Huang *et al.*, 2007; Husu *et al.*, 1990; Gebretsadik *et al.*, 2011; Soriano *et al.*, 2011). To verify the hypothesis of a strictly environmental lifestyle of the *Listeria sensu lato* spp. in contrast to the *Listeria sensu stricto* spp., which are able to survive at least temporarily in the GIT, colonization experiments in mice using species of both groups were conducted.

3.1.1 Use of a novel oral infection model for analysis of colonization

Bou Ghanem and colleagues recently published a novel method for the oral infection of BALB/c mice using *L. monocytogenes*-contaminated bread pieces for inoculation (Bou Ghanem *et al.*, 2013a). One advantage of this new listeriosis model is the defined GI phase of infection (about 24 to 36 h) before the bacteria spread to the organs. This closely mimics the course of human illness and is therefore suitable for gathering information about the colonization capabilities of different *Listeria* spp.

To establish an infection dose adequate to monitor bacterial numbers in the lumen and tissue of the GIT and to optimize sample handling, this oral infection model was tested in preliminary experiments. Six SPF-raised BALB/c mice were infected with *L. monocytogenes* EGDe. The infection doses ranged from 1.73 x 10^7 to 1.37 x 10^9 cfu/mouse (**Figure 1 A**). Mice were sacrificed 36 h post infection (p.i.) and the bacterial loads in the lumen of the three parts of the small intestine (duodenum, jejunum, ileum) as well as of the caecum and the colon were determined (**Figure 1 D**). The number of tissue-associated bacteria, that were present in the mucus, the epithelial layer, or the LP of the GIT, was also derived (**Figure 1 E**). In addition, infection numbers in the organs liver and spleen (**Figure 1 B**) and the shedding of *L. monocytogenes* in feces over time (**Figure 1 C**) were assessed.

Mouse numbers (No.) 1 and 2, which were infected with 1.73 x 10^7 and 2.53 x 10^7 cfu/mouse, respectively, did not show signs of colonization. No cells were detected when plating aliquots of the undiluted samples of the intestinal contents on Palcam agar. Cfu values for samples without detectable bacteria were therefore set as half the detection limit. Mouse No. 3 was infected with a ca. 10-fold higher inoculum (1.91 x 10^8 cfu/mouse). This led to colonization of the colon, caecum, and ileum lumen (ca. 10^2 – 10^3 cfu/compartment) but not of the jejunum and duodenum, the two proximal parts of the small intestine. The cfu numbers of tissue-associated bacteria were below the detection limit. This finding indicates that the listerial cells resided in the lumen but were unable to invade the epithelial cells. A fourth mouse, No. 4, received a slightly higher infection dose (7.10 x 10^8 cfu/mouse). The numbers of luminal bacteria in the colon, caecum and ileum were comparable to those obtained from mouse No. 3. In contrast to mouse No. 3, the mouse also harbored bacteria in the jejunum (ca. 6 x 10^2 cfu). Additionally, *L. monocytogenes* was able to invade the tissue of colon, caecum and jejunum (ca. 10^1 – 10^2 cfu/tissue) in mouse No. 4. Although no tissue-associated bacteria for mouse No. 3 were detected, both No. 3 and 4 showed signs of a systemic infection, since ca. 10^1 – 10^2 bacteria were found in the spleen and the liver (**Figure 1 B**). Mouse No. 5 and 6 were infected with ca. 1.37 x 10^9 cfu/mice. Consistent with the higher dose, the numbers of luminal *L. monocytogenes* cells were higher in these mice, ranging from 10^2 in the ileum to 10^4 in the colon. Mouse No. 6 even exhibited colonization in the duodenum (ca. 4 x 10^2 cfu). In mouse No. 6, the number of invading bacteria in the colon and caecum were higher (ca. 10^2 – 10^3 cfu/tissue) and ileum and jejunum were also infected (ca. 2 – 4 x 10^2 cfu/tissue). Surprisingly, mouse No. 5 did not show signs of splenic and hepatic infection while mouse No. 6 exhibited cfu numbers of 2.90 x 10^2 and 6.97 x 10^3, respectively, in these organs. Numbers of fecal *L. monocytogenes* in both mice showed the highest numbers 12 h p.i. and a subsequent decline of fecal spreading over the next 24 h (**Figure 1 C**).

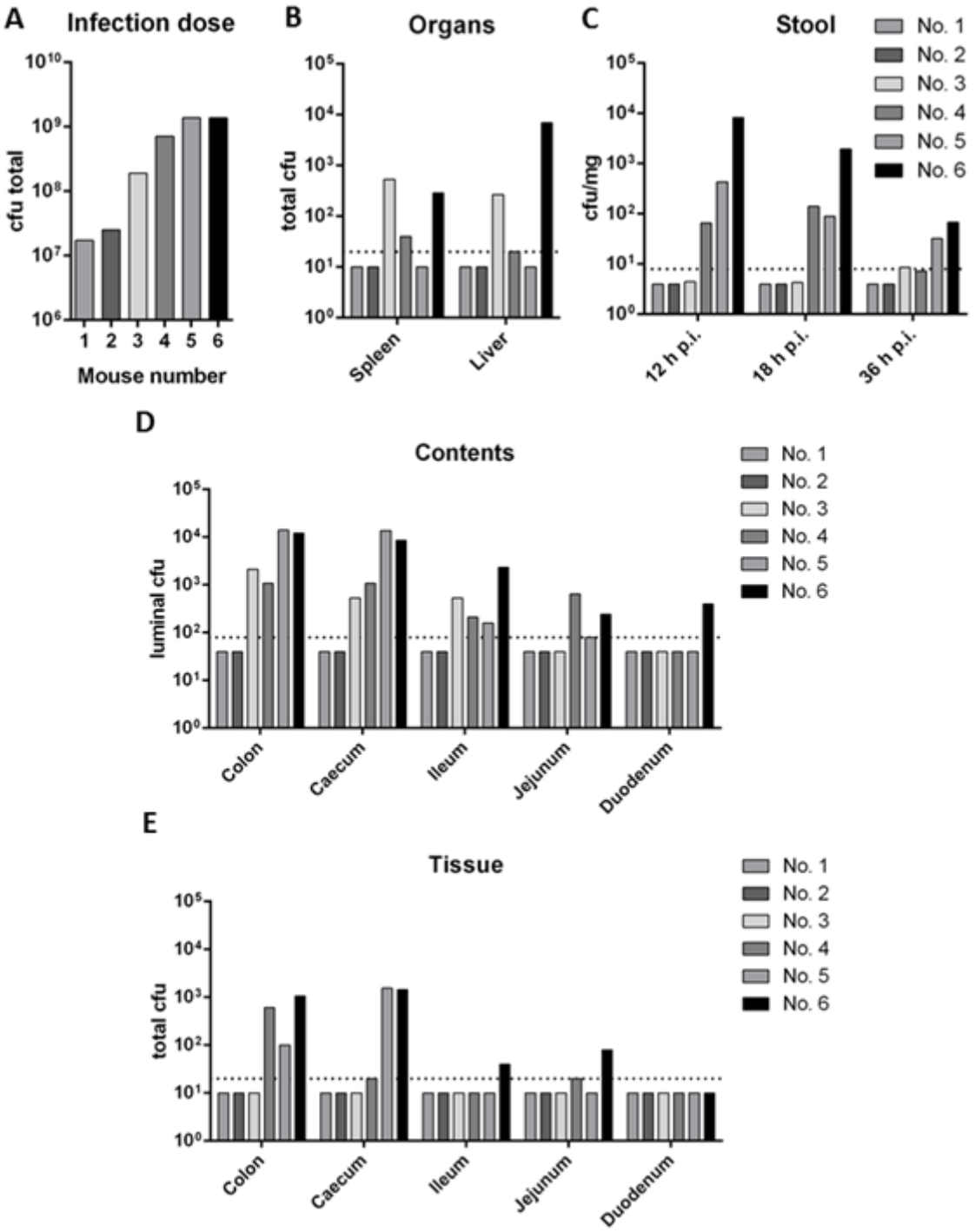

Figure 1: Numbers of colonizing listerial cells dependent on the infection dose.
Six female BALB/c mice were orally infected with varying numbers of *L. monocytogenes* (A). After 36 h, the bacterial loads in the organs spleen and liver (B), the lumen (D) and the tissue of the GIT were determined. Stool samples (C) were collected 12 h, 18 h and 36 h p.i. and the number of cfu/mg feces was calculated. Bars represent cfu values for individual mice. Dashed lines indicate the detection limit for each sample. Cfu values for samples without detectable bacteria were set as half the detection limit.

Linear regression analysis was applied to elucidate the relationship between the infection dose and the number of cfu in different sample types by calculating the coefficient of determination R^2 (**Figure 2**). The number of administered pathogens correlated well with the number of *L. monocytogenes*

colonizing the lumen and tissue of colon and caecum (**Figure 2 ABDE**) as indicated by R^2 values ≥ 0.61. The number of listeriae shed into in the feces at different time points also showed a high degree of linear relation to the infection dose (R^2 = 0.70-0.71) (**Figure 2 GHI**). The ileum, especially its tissue, exhibited lower R^2 values since five of six mice showed cfu numbers below the detection limit (**Figure 2 CF**).

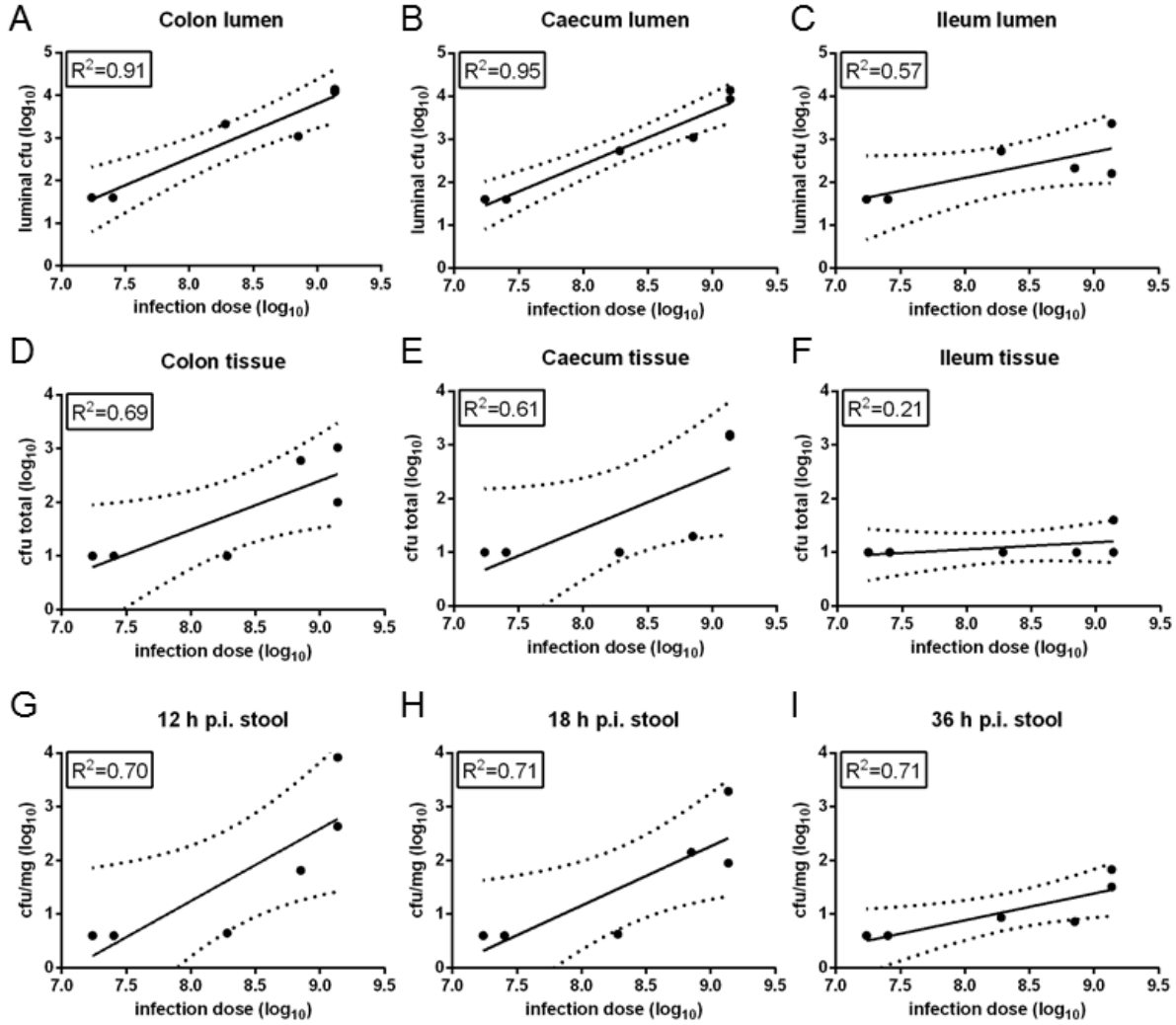

Figure 2: Correlation of infection dose and cfu in the lumen, tissue and stool.
Log_{10} transformed infection doses (x-axis) and luminal (A-C), tissue-associated (D-F) or fecal (G-I) cfu (y-axis) of *L. monocytogenes* isolated female BALB/c mice after 36 h p.i. were plotted on a XY-graph (●). Linear regression was performed. Solid lines depict the best fit lines and dashed lines indicate the 95% confidence bands. The coefficients of determination R^2 are listed on the top left corner of each graph.

As a summary, *L. monocytogenes* seems to require infection doses above 10^8 cfu/mouse to be able to consistently colonize the intestines and to infect spleen and liver. Therefore, an infection dose of at least 10^8 cfu/mouse for the following experiments was chosen to guaranty sufficient bacterial loads in the intestines. Only colon and ileum were selected for sampling of the GIT in the following

experiments, since both colon and caecum generally exhibit similar cfu numbers. Duodenum and jejunum are barely colonized in mice and were therefore not considered (**Figure 1 DE**; Sarah D'Orazio, personal communication).

3.1.2 Selection of suitable *Listeria* species for colonization experiments

Based on the oral infection model in BALB/c mice, a colonization experiment should be performed and the bacterial numbers in the colon and ileum as well as in the feces of individual mice 36 h after infection with 10^8 cfu/mouse of a single *Listeria* species should be analyzed. Besides highly pathogenic *L. monocytogenes*, a closely related apathogenic species should be tested for differences in the colonization ability within the *Listeria sensu stricto*. Two species from the *Listeria sensu lato* group, which so far have not been isolated from feces or GI samples of animals, should also be tested for GI survival. To select suitable *Listeria* spp., preliminary experiments were performed. The species had to meet three requirements to be considered for oral infection experiments:

a) The growth capabilities must be similar to *L. monocytogenes* under condition resembling the GIT (body temperature of mice: 38°C; mostly anaerobic conditions; nutrient deprived environment)
b) The species must be able to grow on selective Palcam plates
c) The species should represent genetically divers members of both clades

3.1.2.1 *In vitro* growth experiments

The publicly available *Listeria sensu stricto* spp. *L. seeligeri* and *L. welshimeri* as well as the *Listeria sensu lato* spp. *L. booriae, L. aquatica, L. riparia, L. floridensis*, and *L. newyorkensis* were selected for growth experiments in comparison to *L. monocytogenes*. Since the body temperature of mice ranges from 36.5°C to 38°C, 38°C was chosen as growth temperature. BHI or MM supplemented with 0.5 % (v/v) YE and 50 mM glucose were used as media under microaerobic or anaerobic conditions.

During microaerobic growth in nutrient rich BHI medium, *L. monocytogenes* reached an $OD_{600}^{max} = 0.79$. The *Listeria sensu stricto* spp. *L. seeligeri* and *L. welshimeri* reached a lower OD_{600}^{max} during stationary phase (**Figure 3 A**). *L. booriae*, *L. aquatica* and *L. riparia* from the *Listeria sensu lato group* exhibited growth patterns similar to *L. monocytogenes. L. floridensis* reached a far lower $OD_{600}^{max} = 0.60$ and the onset of stationary phase for *L. newyorkensis* was delayed for several hours (**Figure 3 B**). Under growth conditions without oxygen, *L. monocytogenes* reached a lower $OD_{600}^{max} = 0.56$ compared to microaerobic conditions. While *L. seeligeri* again exhibited a lower OD_{600}^{max}, *L. welshimeri* surpassed *L. monocytogenes* after 5 hours and reached a higher OD_{600}^{max} (**Figure 3 C**). All *Listeria sensu lato* spp. reached the stationary phase after 6 h and exhibited a significantly higher OD_{600} than *L. monocytogenes* at that time point with the exception of *L. newyorkensis* (**Figure 3 D**).

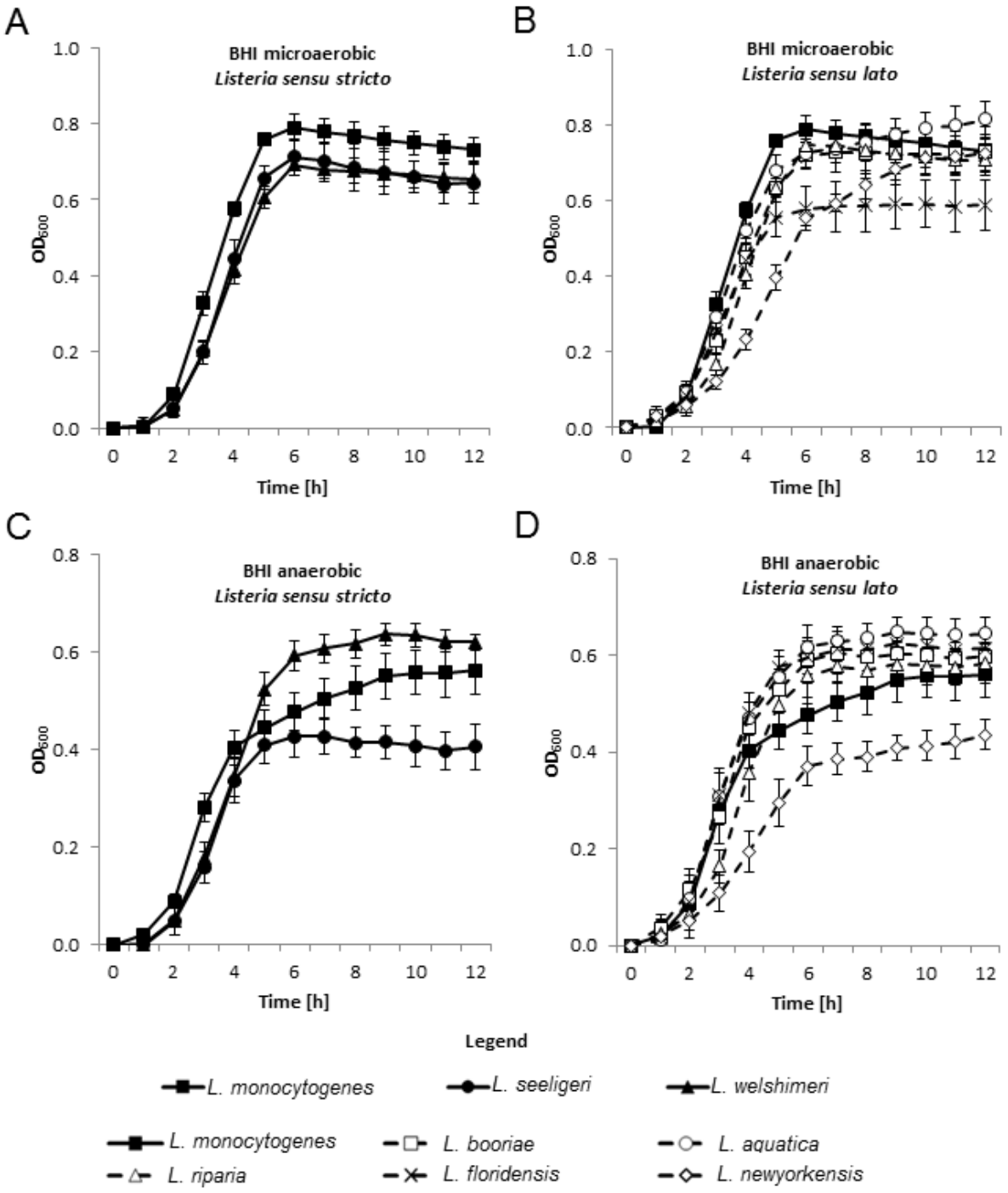

Figure 3: Growth of *Listeria* spp. in BHI medium.

Growth curves of the *Listeria sensu stricto* spp. (A+C) *L. monocytogenes* (■), *L. seeligeri* (●) and *L. welshimeri* (▲) as well as the *Listeria sensu lato* spp. (B+D) *L. booriae* (□), *L. aquatica* (○), *L. riparia* (△), *L. floridensis* (╳) and *L. newyorkensis* (◇) in BHI under microaerobic (A+B) and anaerobic conditions (C+D) at 38°C. OD_{600} was measured at the indicated intervals using the Bioscreen C. Growth curves depict the calculated mean value of three independent biological experiments with technical duplicates, while error bars indicate the standard deviation.

Growth in chemically defined MM under microaerobic conditions revealed significantly inferior growth of *L. monocytogenes* and a strongly reduced $OD_{600}{}^{max}$ compared to the other *Listeria sensu stricto* as well as to the *Listeria sensu lato* spp., with the exception of *L. newyorkensis* (**Figure 4 AB**). During

anaerobic growth, *L. welshimeri* and *L. seeligeri* reached a slightly but significantly higher OD_{600}^{max} than *L. monocytogenes* (**Figure 4 C**). Among the *Listeria sensu lato* spp., *L. riparia* and *L. newyorkensis* reached stationary phase later than the other species tested but reached OD_{600}^{max} values comparable to *L. monocytogenes* (**Figure 4 D**). *L. booriae* showed no significant differences to *L. monocytogenes*, and both *L. floridensis* and *L. aquatica* had a significant growth advantage.

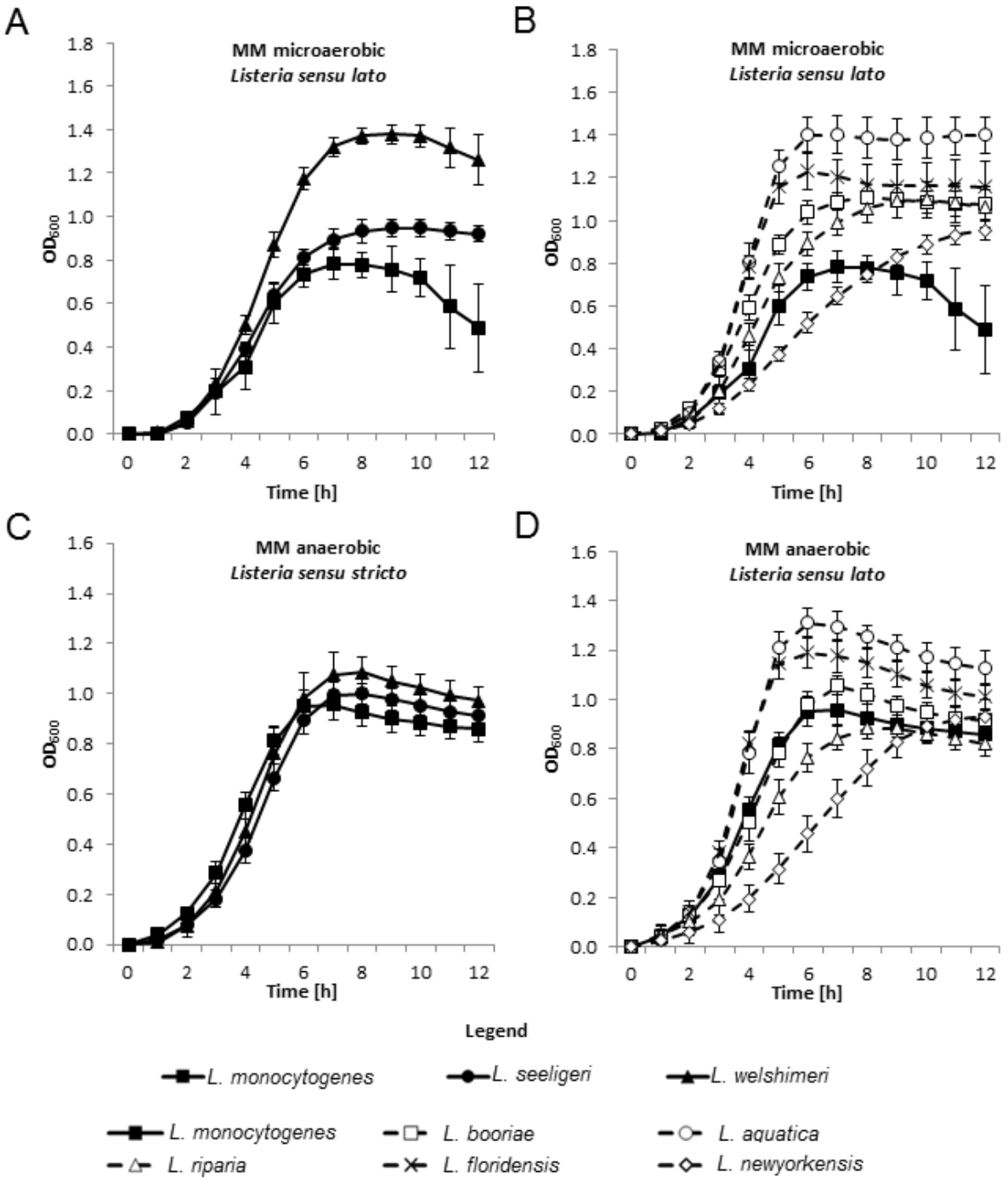

Figure 4: Growth of *Listeria* spp. in MM medium.

Growth curves of the *Listeria sensu stricto* spp. (A+C) *L. monocytogenes* (■), *L. seeligeri* (●) *and L. welshimeri* (▲) as well as the *Listeria sensu lato* spp. (B+D) *L. booriae* (□), *L. aquatica* (○), *L. riparia* (△), *L. floridensis* (╳) and *L. newyorkensis* (◇) in

MM supplemented with 0.5 % (w/v) YE and 50 mM glucose under microaerobic (A+B) and anaerobic conditions (C+D) at 38°C. OD_{600} was measured at the indicated intervals using the Bioscreen C. Growth curves depict the calculated mean value of three independent biological experiments with technical duplicates, while error bars indicate the standard deviation.

All in all, most species except *L. newyorkensis* exhibited growth phenotypes similar to those of *L. monocytogenes* under the conditions tested. Especially the *Listeria sensu lato* spp. outcompeted *L. monocytogenes* under conditions resembling the GIT, e.g. anaerobiosis or microaerobiosis and limited concentrations of nutrients.

3.1.2.2 Growth on selective agar plates

The mamalian GIT harbors a vast number of different bacterial species. Estimates range from 500-1,000 to up to 36,000 species (Frank *et al.*, 2007). Therefore, samples from feces or the GIT need to be plated on selective agar plates to determine the number of *Listeria* in the intestine after oral infection. This is archieved using Palcam agar, a *Listeria*-selective formula containing lithium chloride, ceftazidime, polymyxin B and acriflavine. It was described by Van Netten *et al.* in 1989 and is used for the isolation of *L. monocytogenes* from food samples. Growth of *Listeria* results in black halos around colonies due to the hydrolysation of aesculin. In addition mannitol and phenol red are added which allows for easy discrimination against contaminants like enterococci and streptocococi. These bacteria ferment mannitol, thus causing a change from red to yellow of the pH indicator phenol red. Since the authors reported enrichment of not only *L. monocytogenes* but also *L. ivanovii, L. seeligeri, L. welshimeri* and *L. innocua* (Van Netten *et al*., 1989), this agar formula can be used for enumeration of different *Listeria* spp. in murine samples to compare their colonization abilities. The selected *Listeria* spp. were therefore tested for growth on Palcam agar to ensure correct and accurate measurement of cell numbers in these sample types. Overnight cultures of different *Listeria* spp. were diluted in PBS and plated on on both Palcam and BHI agar simoultaneously. After 24 h, the ratio of cfu recovered from both agar types was calculated using the following formula:

$$Palcam/BHI\ cfu\ ratio\ [\%] = \frac{cfu_{Palcam}}{cfu_{BHI}} \cdot 100$$

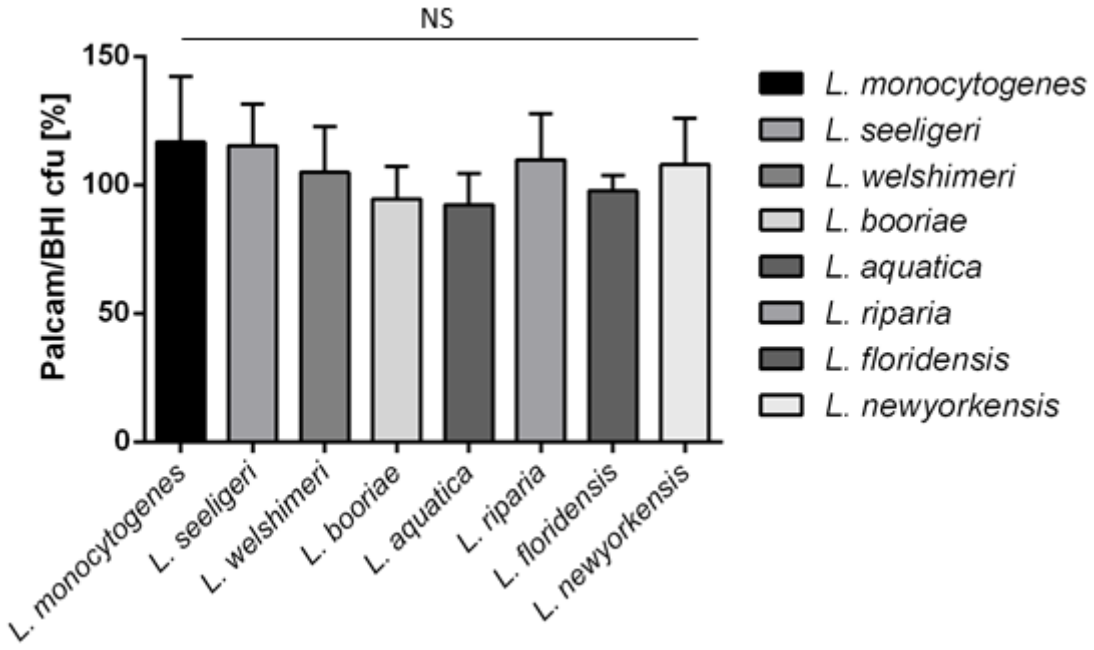

Figure 5: *Listeria* spp. show comparable cfu numbers on BHI and Palcam agar.
The percentage change of cfu grown on Palcam agar compared to BHI agar after 24-48 h incubation at 37°C is shown for the *Listeria sensu stricto* spp. *L. monocytogenes*, *L. seeligeri* and *L. welshimeri* as well as the *Listeria sensu lato* spp. *L. booriae*, *L. aquatica*, *L. riparia*, *L. floridensis* and *L. newyorkensis*. Mean values of four independent biological experiments are depicted and error bars indicate the standard deviation. Statistical significance was assessed using a two-tailed student's t-test. NS = not significant.

All *Listeria* spp. tested showed comparable cfu numbers on Palcam and BHI agar as indicated by the Palcam/BHI cfu ratio (**Figure 5**). The ratios ranged from 92.26 % (*L. aquatica*) to 116.76 % (*L. monocytogenes*). Due to the high standard deviations, no significant differences between the cfu of *Listeria* spp. in the two media were observed. In addition, GI samples of uninfected mice were plated on Palcam agar to ensure elimination of commensal bacteria like *Bacteroides* spp., *Clostridium* spp. or *Bifidobacterium* spp. Since none of these bacteria were able to grow on the plates, Palcam agar was proven to be a suitable selective medium for colonization experiments (data not shown).

3.1.2.3 Genetic diversity of *Listeria* spp.

Both *Listeria sensu stricto* members tested, *L. seeligeri* and *L. welshimeri*, were suitable candidates for colonization experiments because they exhibited growth characteristics in liquid media similar to *L. monocytogenes* and were able to grow on selective Palcam agar. Therefore, the genetic background and evolutionary history of both species were considered to select an appropriate candidate. It is generally accepted that the MRCA of the *Listeria sensu stricto* group acquired the LIPI-1 as well as the *inlAB* locus via horizontal gene transfer (Schmid *et al.*, 2005; den Bakker *et al.*, 2010a). These virulence genes, which are important for intracellular survival and host cell invasion, were lost in at least five separate events at different time points during the evolution of the *Listeria sensu stricto* clade. Loss

occurred in all sequenced *L. welshimeri* strains, while LIPI-1 and *inlAB* are preserved in most of the *L. seeligeri* strains (den Bakker *et al.*, 2010a). In addition, strains of *L. welshimeri* harbor a lower number of internalins than all other *Listeria sensu stricto* spp. Due to the low virulence potential, *L. welshimeri* was selected as a second representative of the clade *Listeria sensu stricto* for the *in vivo* infection experiments. As it is a strictly non-pathogenic species, this strain is an ideal reference for comparison of colonization properties with the highly virulent *L. monocytogenes*.

All *Listeria sensu lato* spp., which were tested in BHI or MM, exhibited similar or even improved growth behavior compared to *L. monocytogenes* with the exception of *L. newyorkensis.* Therefore, they proved to be suitable candidates for oral infection experiments. The clade *Listeria sensu lato* actually represents three distinct monophyletic groups, which have been proposed to be recognized as separate genera called *Murraya*, *Mesolisteria* and *Paenilisteria* (Stuart & Welshimer, 1974; Orsi and Wiedmann, 2016). Therefore, *L. booriae* and *L. aquatica* were chosen as representatives of the two latter groups for the mouse experiments.

3.1.3 *Listeria sensu lato* and *Listeria sensu stricto* exhibit differences in colonization ability

The *Listeria sensu stricto* spp. *L. monocytogenes* and *L. welshimeri* as well as the *Listeria sensu lato* members *L. aquatica* and *L. booriae* were tested for their ability to colonize the GIT and cause a systemic infection. Therefore, female BALB/c mice were orally infected with 4-9 x 10^8 cfu of an individual *Listeria* species. Two days p.i., the numbers of luminal listeriae in the ileum and colon were determined (**Figure 6 AB**).

Significantly lower cfu numbers of the three non-pathogenic species in both compartments were obtained in comparison with the cfu numbers of *L. monocytogenes* strain EGDe. The cfu values of *L. aquatica* and *L. welshimeri* were similar in the ileum. *L. booriae* was barely detectable in both compartments and showed significantly lower mean values in comparison to *L. welshimeri* in the colon, but not in the ileum.

The cfu/mg feces from stool samples taken 3 h p.i., 1 day p.i., and 2 days p.i. of the same mice were additionally analyzed (**Figure 6 E**). No significant difference in the cfu/mg feces was observed either immediately after infection or within 24 h of infection. In all cases, the number of cfu decreased 1000-fold, suggesting a species-independent initial clearance of listeriae shed in the feces. After an additional 24 h, *L. monocytogenes* persisted in stool pellets, but the number of cfu decreased significantly for the three non-pathogenic species. This effect was more pronounced in the *Listeria sensu lato* spp. For example, for half of the mice infected with *L. aquatica*, no cfu were detected, and only one of six mice fed *L. booriae* were still shedding.

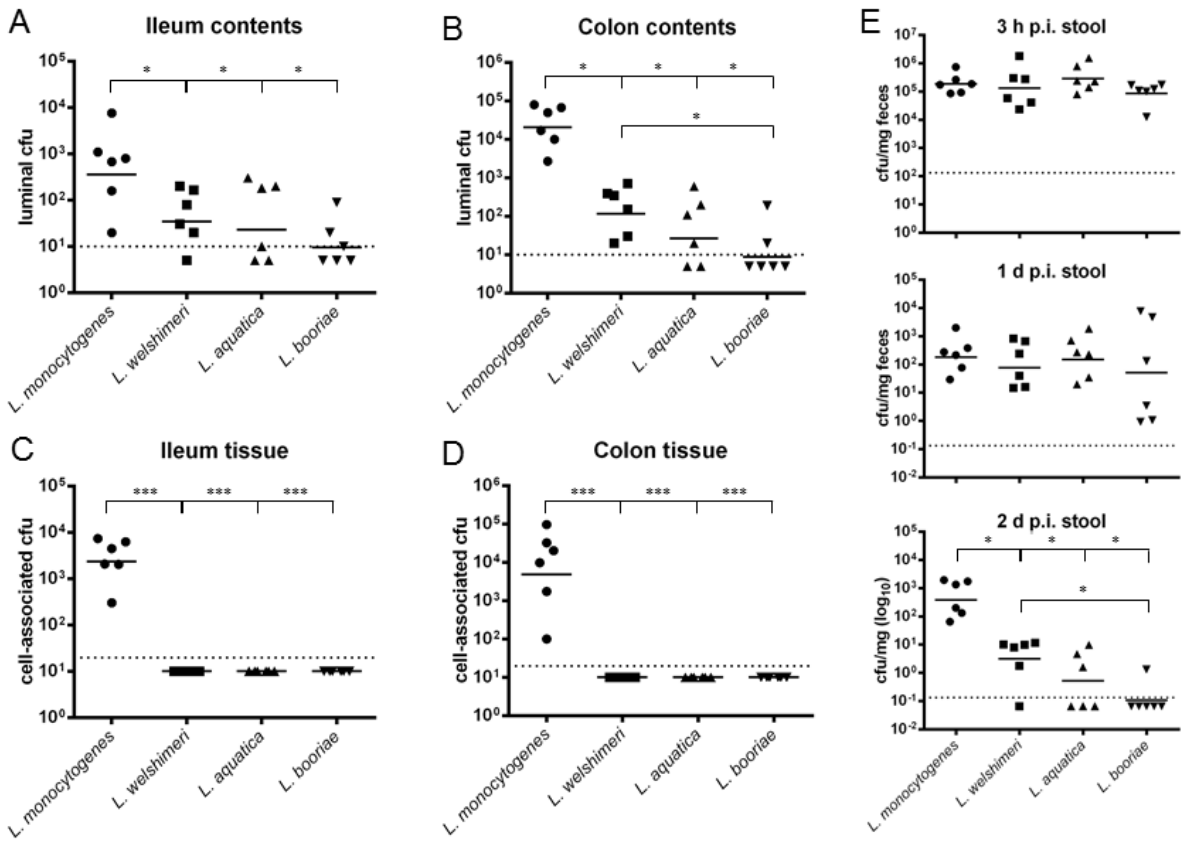

Figure 6: Members of the two listerial phylogenetic groups exhibit different cell numbers in the ileum and colon lumen.

Female BALB/c mice were orally infected with 4-9 × 10^8 cfu of the *Listeria sensu stricto* spp. *L. monocytogenes* (●) and *L. welshimeri* (■), as well as of the *Listeria sensu lato* spp. *L. aquatica* (▲) and *L. booriae* (▼). After 2 days, cfu numbers for each species were determined in the ileum (A) and colon lumen (B), as well as in the ileum (C) and colon tissue (D). Stool samples (E) were collected at 3 h p.i., 1 day p.i. and 2 days p.i., and the number of cfu per mg feces was calculated. Symbols represent values for individual mice, while horizontal lines indicate the mean value that was pooled from two separate experiments (n = 3 mice per group). Dashed lines represent the detection limit for each sample. Cfu values for samples without detectable bacteria were set as half the detection limit. Statistical significance was assessed using two-tailed student's t-test with Welch's correction. P values less than 0.05 were considered significant and are indicated as follows: * = $p < 0.05$; ** = $p < 0.01$; *** = $p < 0.001$. If not indicated otherwise, values are not significantly different.

The number of tissue-associated bacteria, e.g. in the mucus, the epithelial layer, or the LP of the GIT, was also analyzed (**Figure 6 CD**). While *L. monocytogenes* was found in high numbers of 2.5-6.9 × 10^3 cfu, the three other species were not detectable in these tissues, confirming their non-pathogenic behavior as reported previously for *L. welshimeri* in mice after i.v. injection (Kluge & Hof, 1986; Hof & Hefner, 1988). As expected, *L. monocytogenes* was able to reach the mesenteric lymph nodes and spread to the liver and spleen of infected mice (**Figure 7**).

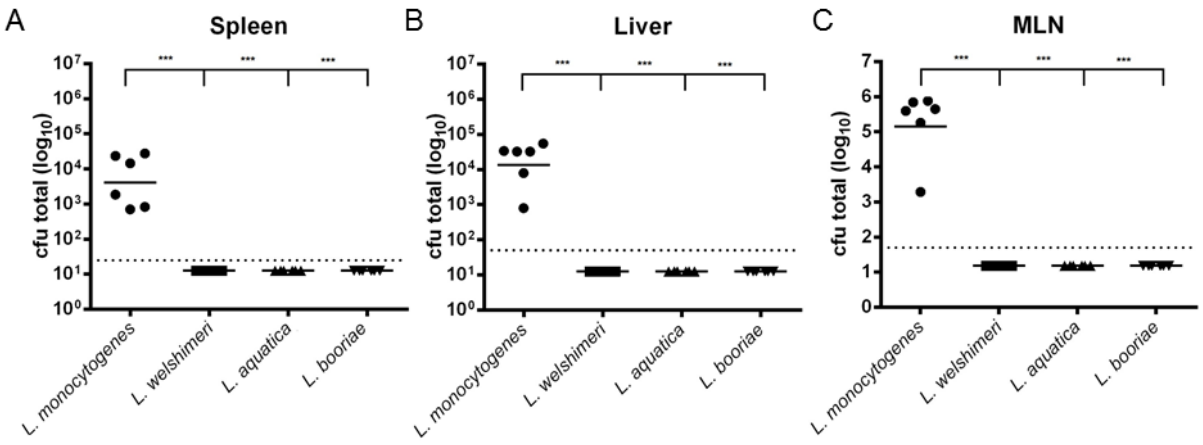

Figure 7: Only *L. monocytogenes* is able to cause systemic infection after oral infection.
Female BALB/c mice were orally infected with 4-9 × 10^8 cfu of the *Listeria sensu stricto* spp. *L. monocytogenes* (●) and *L. welshimeri* (■), as well as of the *Listeria sensu lato* spp. *L. aquatica* (▲) and *L. booriae* (▼). After 2 days, cfu numbers for each species were determined in the spleen, liver and MLNs. Symbols represent values for individual mice, while horizontal lines indicate the mean value that was pooled from two separate experiments (n = 3 mice per group). Dashed lines represent the detection limit for each sample. Cfu values for samples without detectable bacteria were set as half the detection limit. Statistical significance was assessed using two-tailed student's t-test with Welch's correction. P values less than 0.05 were considered significant and are indicated as follows: * = $p < 0.05$; ** = $p < 0.01$; *** = $p < 0.001$.

Taken together, these data confirm that the *Listeria sensu stricto* members including *L. welshimeri* have the potential to at least transiently colonize the intestines of mammals, whereas the *Listeria sensu lato* spp. seem to be less adapted to the conditions of the GIT.

3.2 Genome analyses of *Listeria sensu stricto* and *Listeria sensu lato* spp.

To further analyze the hypothesis of an inferior adaption of the *Listeria sensu lato* to the GIT of the host, genomic analyses of *Listeria sensu stricto* as well as newly discovered *Listeria sensu lato* species were conducted to identify key factors for colonization and virulence in *Listeria* spp.

3.2.1 Genomic sequencing of *L. kieliensis* and classification into the genus *Listeria*

In recent years, a quite substantial number of novel *Listeria* spp. has been discovered in various ecological niches like cheese, raw milk, running waters or vegetation (reviewed in: Orsi & Wiedmann, 2016). In 2015, another so far unknown *Listeria* species was isolated from a wastewater plant in Northern Germany and named *Listeria kieliensis* sp. nov. (Jan Kabisch, MRI Kiel, personal communication). To classify *Listeria kieliensis* sp. nov. into the phylogeny of the genus *Listeria* and to analyze the genomic differences to the pathogenic species *L. monocytogenes*, *de novo* NGS via the MiSeq platform was performed. A total number of eleven contigs with an average length of 237,476 bp was obtained. The assembled genome had a total length of 2,612,237 bp and a GC content of 45.67 %. The genome was annotated and 2,431 protein coding genes, 81 pseudogenes as well as 54 tRNAs and

eight rRNAs were identified. The *L. kieliensis* WGS project was submitted at DDBJ/EMBL/GenBank under the accession number LARY00000000 (BioProject: PRJNA276498; Biosample: SAMN03376159).

Pairwise comparison between the genomic sequences of *L. kieliensis* and 22 type strains of other known and sequenced *Listeria* spp. was performed to calculate ANIb using JSpecies (**Supplementary Table 5**). A phylogenetic tree based on these data was constructed using the software MEGA6 and the Neighbor-Joining method (**Figure 8**). *L. kieliensis* belongs to the *Listeria sensu lato* group and is most closely related to *L. aquatica* (ANIb = 85.44 %). The cut-off value for species delineation in bacterial taxonomy is generally defined as 95-96 %, which responds to the 70 % DNA-DNA hybridization cut-off (Richter and Rosselló-Móra, 2009), therefore *L. kieliensis* can be classified as a novel species. Both *L. kieliensis* and *L. aquatica* form a cluster with the closely related species *L. floridensis* and *L. fleischmannii*. This cluster has recently been proposed to be classified into a novel genus called *Mesolisteria*. The name refers to the mesophilic nature of these species since they are not able to grow at temperatures below 7°C (Orsi & Wiedmann, 2016).

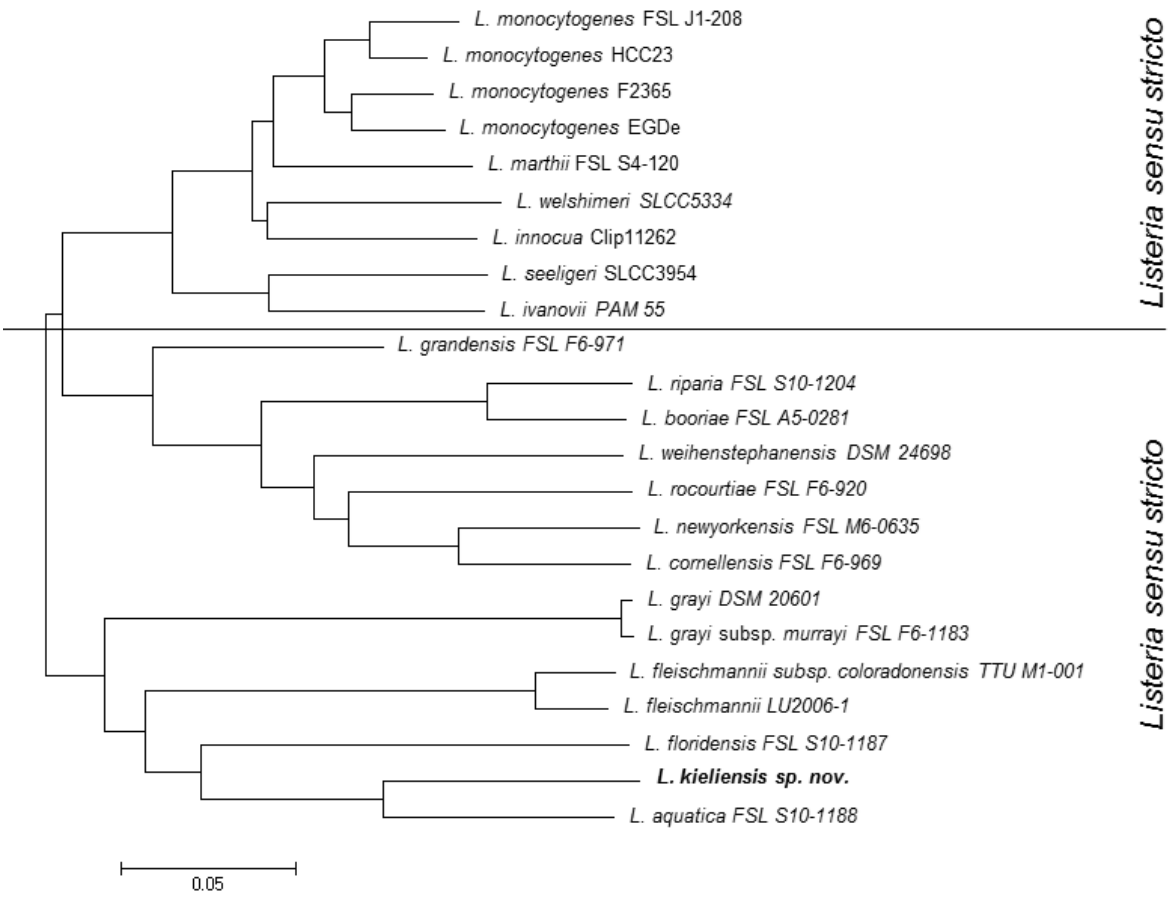

Figure 8: Phylogenetic tree of the genus *Listeria* including *L. kieliensis*
A Neighbor-Joining method phylogenetic tree based on the percentage of average nucleotide differences (100 % - ANIb; Chan *et al.*, 2012) was constructed. Horizontal bar indicates the number of inferred nucleotide substitutions per site.

3.2.2 *Listeria sensu lato* spp. are missing not only key virulence genes but also genes associated with survival in the GIT

The *Listeria sensu lato* spp. are considered to be non-pathogenic since they provided negative results in hemolytic and phosphatidylinositol-specific phospholipase C activity tests (Bertsch *et al.*, 2013; den Bakker *et al.*, 2013; den Bakker *et al.*, 2014; Lang Halter *et al.*, 2013; Leclercq *et al.*, 2010; Weller *et al.*, 2015). Results from the *in vivo* colonization experiments conducted in mice confirmed the apathogenic properties of these species since *L. aquatica* and *L. booriae* were not able to invade the tissue of the GIT (**Figure 6 CD**) or to spread to the MLNs, liver and spleen (**Figure 7**). The lower cfu numbers in the luminal samples (**Figure 6 AB**) and feces (**Figure 6 E**) of infected mice in comparison to *L. monocytogenes* and *L. welshimeri* indicated an insufficient ability to colonize the GIT. Therefore, the genomic sequences of *L. kieliensis* and other sequenced *Listeria sensu lato* members were analyzed for the presence of *L. monocytogenes* proteins, which are known to be involved in colonization and/or virulence from literature (**Table 6**). For this purpose, the percentage of amino acid sequence identity of selected *L. monocytogenes* proteins against the proteins of *Listeria sensu lato* spp. was calculated. Well conserved gene products with at least 70 % sequence homology to these species were considered as functionally homologous, whereas genes below 40 % were not considered to be functionally conserved.

Analysis of several known *listerial* virulence and colonization genes revealed that both *L. kieliensis* and the other *Listeria sensu lato* spp. contain none of the classical *prfA*-regulated virulence genes (*prfA, plcA, hly, mpl, actA, plcB*) encoded on the LIPI-1 (Vázquez-Boland *et al.*, 2001b). The *inlAB* locus encoding the two internalins InlA and InlB is only weakly conserved in *L. kieliensis* as well as in the other members of the clade. All in all, none of the 25 known internalins of *L. monocytogenes* EGDe are functionally conserved in *L. kieliensis* (data not shown).

L. monocytogenes possesses several stress resistance genes for the survival in the food environment and during the passage of the GIT. Two systems for the survival under acidic conditions are the ADI and AgDI systems (Ryan *et al.*, 2009; Chen *et al.*, 2011). The responsible gene locus lmo0036-0043 is missing in a number of *Listeria sensu lato* spp. but is present in *L. kieliensis*, *L. aquatica*, *L. floridensis* and *L. grayi*. In contrast, the GAD system (Cotter *et al.*, 2001a; Cotter *et al.*, 2001b; Cotter *et al.*, 2005), which is another acid stress survival system, is partly missing in *L. kieliensis.* The corresponding genes *gadD1* and *gadT1* (lmo0447-0448), *gadD2* and *gadT2* (lmo2362-2363) as well as *gadD3* (lmo2434) are weakly conserved or missing in *L. kieliensis* and *L. aquatica*, while other *Listeria sensu lato* members show varying degrees of conservation of the *gadD* and *gadT* genes. The genes lmo0447-0448 are part of a five-gene stress survival islet (SSI-1) responsible for survival of *L. monocytogenes* under low pH and high salt concentration (Ryan *et al.*, 2010), which is partly absent or only weakly conserved in a number of *Listeria sensu lato* spp. including *L. kieliensis*. Other important genes for stress survival are

bile protection genes (Begley *et al.*, 2005a; Dussurget *et al.*, 2002; Sleator *et al.*, 2005). While *bilE* (lmo1421-1422) is conserved in all *Listeria sensu lato* including *L. kieliensis*, *bsh* (lmo2067) and *bltB* (lmo0754) are weakly conserved or missing in these species. Compatible solutes, small molecules which act as osmolytes, help *L. monocytogenes* to overcome osmotic stress encountered in the environment outside and inside the host (Sleator & Hill, 2001). The carnitine and betaine transport systems OpuA/Gbu (encoded by lmo1014-1016), OpuC (encoded by lmo1425-1428) and BetL (encoded by lmo2092) (Ko & Smith, 1999; Fraser *et al.*, 2000; Sleator *et al.*, 2001; Wemekamp-Kamphuis *et al.*, 2002; Mendum & Smith, 2002) are well conserved in *L. kieliensis* but are absent in most other *Listeria sensu lato* spp. Only *opuAB* and *opuAC* are at least partly conserved in seven species.

Table 6: Genome comparison of selected virulence and colonization associated protein-coding genes in *L. monocytogenes* with *L. kieliensis* and other *Listeria sensu lato* spp.

	Gene	lmo number	Function	Percent identity in *L. kieliensis* [no. of *Listeria sensu lato* (except *L. grayi*) with conservation < 40 %]*
GAD system	*gadD1*	lmo0447	Glutamate decarboxylase	0 % [2/13]
	gadT1	lmo0448	Probable glutamate/gamma-aminobutyrate antiporter	25.68 % [10/13]
	gadT2	lmo2362	Probable glutamate/gamma-aminobutyrate antiporter	0 % [2/13]
	gadD2	lmo2363	Glutamate decarboxylase	0 % [2/13]
	gadD3	Lmo2424	Glutamate decarboxylase	25.86 % [10/13]
ADI / AgDI system	*arcB*	lmo0036	Putrescine carbamoyltransferase	80.71 %[6/13]
	arcD	lmo0037	Agmatine/putrescine antiporter, associated with agmatine catabolism	84.1 % [10/13]
	aguA1	lmo0038	Agmatine deiminase	79.94 % [10/13]
	arcC	lmo0039	Carbamate kinase	71.38 % [3/13]
	aguA2	lmo0040	Agmatine deiminase	66.95 % [10/13]
		lmo0041	phosphosugar-binding protein	81.1 % [10/13]
		lmo0042	DedA family protein	86.3 % [0/13]
	arcA	lmo0043	Arginine deiminase	0 % [10/13]
SSI-1		lmo0444	hypothetical protein	42.78 % [1/13]
		lmo0445	hypothetical protein	33.68 % [10/13]
	pva	lmo0446	Choloylglycine hydrolase	38.66 % [7/13]
	gadD1	lmo0447	Glutamate decarboxylase	0 % [2/13]
	gadT1	lmo0448	Probable glutamate/gamma-aminobutyrate antiporter	25.68 % [10/13]
Bile protection	*bsh*	lmo2067	Choloylglycine hydrolase	32.21 % [13/13]
	pva	lmo0446	Choloylglycine hydrolase	38.66 % [5/13]
	bltB	lmo0754	hypothetical protein	0 % [13/13]
	bilE	lmo1421	glycine betaine/L-proline ABC transporter, ATP-binding protein	67.08 % [0/13]
	bilE	lmo1422	Glycine betaine ABC transport system, permease protein OpuAB/ Glycine betaine ABC transport system, glycine betaine-binding protein OpuAC	81.75 % [0/13]

LIPI-1	*prfA*	lmo0200	Virulence regulatory factor PrfA / Transcriptional regulator, CrP/Fnr family	32.8 % [13/13]
	plcA	lmo0201	Phosphatidylinositol-specific phospholipase C	0 % [13/13]
	hly	lmo0202	Thiol-activated cytolysin / listeriolysin O (LLO)	0 % [13/13]
	mpl	lmo0203	Zinc metalloproteinase precursor	0 % [13/13]
	actA	lmo0204	Actin-assembly inducing protein ActA precursor	0 % [13/13]
	plcB	lmo0205	Broad-substrate range phospholipase C	0 % [13/13]
		lmo0206	Distant similarity with viral glycoprotein gp160 of HIV type 1	0 % [13/13]
LIPI-2	*inlA*	lmo0433	Internalin A (LPXTG motif)	30.22 % [13/13]
	inlB	lmo0434	Internalin B (GW modules)	42.62 % [3/13]
Osmo protection	*opuAA*	lmo1014	Glycine betaine ABC transport system, ATP-binding protein OpuAA	85.39 % [0/13]
	opuAB	lmo1015	Glycine betaine ABC transport system, permease protein OpuAB	90.07 % [7/13]
	opuAC	lmo1016	Glycine betaine ABC transport system, glycine betaine-binding protein OpuAC	81.48 % [7/13]
	opuCD	lmo1425	Osmotically activated L-carnitine/choline ABC transporter, permease protein OpuCD	87.89 % [0/13]
	opuCC	lmo1426	Osmotically activated L-carnitine/choline ABC transporter, substrate-binding protein OpuCC	82.08 % [0/13]
	opuCB	lmo1427	Osmotically activated L-carnitine/choline ABC transporter, permease protein OpuCB	87.10 % [0/13]
	opuCA	lmo1428	Osmotically activated L-carnitine/choline ABC transporter, ATP-binding protein OpuCA	84.87 % [0/13]
	betL	lmo2092	Glycine betaine transporter OpuD	73.18 % [1/13]

* The percentage of amino acid sequence identity of selected *L. monocytogenes* proteins against the proteins of *L. kieliensis* and other *Listeria sensu lato* spp. was calculated. Well conserved genes with an identity score above 70 % are shaded green and considered as functionally homologous, whereas genes below 40 % are shaded red and not considered to be functionally conserved. Square brackets indicate the number of 13 *Listeria sensu lato* spp. (except *L. grayi*) with percentage identities below 40 % for the respective gene.

3.2.3 Genome comparisons between *Listeria* phylogenetic groups reveal candidate genes for infection

The *Listeria sensu lato* group is lacking many genes present in *L. monocytogenes* which are involved in virulence and survival in the GIT, and the *in vivo* oral infection experiments pointed to a reduced colonization ability of *L. booriae* and *L. aquatica*. The *Listeria sensu stricto* spp. *L. welshimeri* and the pathogenic *L. monocytogenes*, on the other hand, seem to be more adapted to the conditions of the intestines. These findings prompted us to identify as yet unknown genes associated with *listerial* virulence and colonization that are present in the clade *Listeria sensu stricto* but missing in the *Listeria sensu lato*. Therefore, a genome sequence comparison of the 17 known *Listeria* members of both clades (except *L. grayi*) and the newly described *L. kieliensis* was conducted using type strain sequences. For this purpose, the percentage of amino acid sequence identity of each *L. monocytogenes* protein against the proteins of all other species was calculated. This list was filtered for gene products with at least 70 % sequence homology in the *Listeria sensu stricto* spp. as a highly stringent criterion for protein homology, and filtered against gene products with less than 30 % sequence homology in the *Listeria sensu lato* spp. as an indication for a missing functional conservation. The resulting **Table**

7 comprises 151 genes and gene products that might be involved in the colonization and infection process of Listeriae. Many of these candidate genes are involved in metabolism, motility, cell wall and membrane biogenesis, transport processes, transcription, and signaling according to their Cluster of Orthologous Groups (COG) categories (**Figure 9**) and could represent candidate genes which contribute to the virulence properties of *L. monocytogenes*.

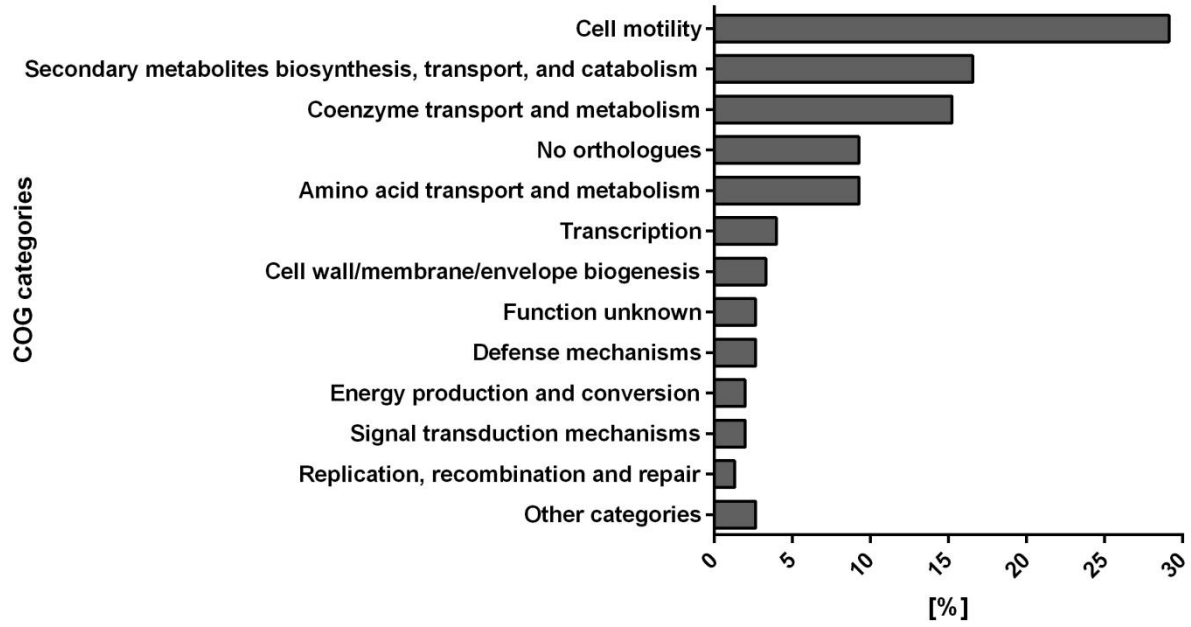

Figure 9: COG categories of *Listeria sensu stricto* specific genes.
151 genes unique *to Listeria sensu stricto* strains and absent in *Listeria sensu lato* strains were classified into COG categories. The percentage of genes falling into a specific category is depicted.

Many genes belong to a large genomic region comprising three gene clusters for the cobalamin (vitamin B_{12})-dependent utilization of ethanolamine and 1,2-PD (lmo1141-lmo1209). The gain of these clusters via horizontal gene transfer has already been described as an evolutionary event that contributed to the taxonomic definition of the *Listeria sensu stricto* group (Chiara *et al.*, 2015; Orsi & Wiedmann, 2016). The importance of this cluster was investigated in section 3.5 Characterization of the gene clusters for biosynthesis of cobalamin and degradation of 1,2-PD. Another large coherent set of genes missing in the *Listeria sensu lato* spp. encodes for flagellar genes (lmo0675-lmo0718). Motility as well as the two regulatory proteins MogR and DegU are known to contribute to successful infection by *L. monocytogenes* (Bigot *et al.*, 2005; Gründling *et al.*, 2004; Dons *et al.*, 2004; Bergmann *et al.*, 2013; Schauer *et al.*, 2010; Knudsen *et al.*, 2004; Shen & Higgins, 2006).

The sortase B (lmo2181) is a surface transpeptidase involved in cell wall anchoring of the transport proteins SvpA (lmo2185) and lmo2186 (Bierne *et al.*, 2004). Both transporters have putative iron transport capacity (Xiao *et al.*, 2011). SpvA is a *listerial* virulence factor that promotes escape from

phagosomes of macrophages (Borezee *et al.*, 2001) and/or enables crossing of the digestive barrier (Newton *et al.*, 2005). The ATPase synthase encoded by lmo0090-lmo0093 is known to play a role in intracellular survival (Schauer *et al.*, 2010), and deletion of the gene *pdeD* contributes to a decrease in listerial invasiveness in enterocytes and virulence after oral infection in mice (Chen *et al.*, 2014). Some of the candidates have no known function or no orthologues and can therefore not be characterized.

The presence of several experimentally validated virulence factors indicates that in general the genome based comparison approach is useful for identification of genes which contribute to colonization and infection properties of the *Listeria sensu stricto* clade. Several genes from this list were selected based on the following criteria:

- No hard evidence for the involvement of the gene during infection is present in the literature
- The predicted function of candidates or protein homologies to characterized genes suggest a potential role in colonization
- Genes exhibit transcriptional reads at 37°C, the body temperature of the host. This information was derived from a previous transcriptomics study of *L. monocytogenes* EGDe at varying temperatures (Elena Ferrari, personal communication)

These candidate genes were experimentally analyzed for their contribution to virulence in *L. monocytogenes* using *in vitro* and *in vivo* approaches to further validate the distinction between *Listeria sensu stricto* and *Listeria sensu lato* in successful colonization of the mammalian host.

Table 7: Genes unique to *Listeria sensu stricto* strains and absent in *Listeria sensu lato* strains.

gene name/lmo number	Function, protein name, or protein homology/similarity to	COG number	gene name/lmo number	protein name, or protein homology/similarity to	COG number
Metabolism			**Miscellaneous**		
lmo0661	Carboxymuconolactone decarboxylase family protein involved in protocatechuate catabolism	COG0599	lmo0090, 0091, 0093	ATP synthase α-/γ-chain, ε-subunit; upregulated in Caco-2 cells and relevant for intracellular replication (Joseph *et al.*, 2006; Schauer *et al.*, 2010)	COG0056, 0224, 0355
cobU-pduO (lmo1141-1142, 1146-1148, 1169, 1190-1199,1203-1209)	Cobalamin biosynthesis	COG2087	*pdeD* (lmo0111)	c-di-GMP-specific phosphodiesterase, EAL domain	COG2200
pduS-pduQ (lmo1143-1145, 1151-1171)	1,2-PD degradation pathway	COG4656	lmo0368	Putative Nudix hydrolase YfcD catalyzing the hydrolysis of nucleoside diphosphates	COG1443
eutA-eutQ (lmo1174-1187)	Ethanolamine utilization pathway	COG4819	lmo0481	Myosin-Cross-Reactive Antigen, oleate hydratase; upregulated *in vivo* (Camejo *et al.*, 2009)	COG4716
Cell motility and chemotaxis			lmo0511	Glutamine amidotransferase; DegU regulated	COG0518
fliN–fliS (lmo0675-lmo0718)	Flagellar biosynthesis	-	lmo0617	Putative lipoprotein with DUF4352 domain, immunoprotective extracellular protein0212	-
lmo0723, lmo1699	Methyl-accepting chemotaxis proteins	COG0840	lmo0625	Lipolytic protein GDSL family	COG2755
Cell wall/membrane/envelope biogenesis			lmo0635	2-Haloalkanoic acid dehalogenase with phosphatase activity	COG1011
lmo0703	UDP-N-acetylenolpyruvoylglucosamine reductase involved in peptidoglycan biosynthesis; regulated by DegU and MogR (Williams *et al.*, 2005; Shen and Higgins, 2006)	COG1728	lmo1415	Hydroxymethylglutaryl-CoA synthase involved in isopentenyl pyrophosphate synthesis via the mevalonate pathway; possibly influences Vγ9/Vδ2 T cells (Begley *et al.*, 2004)	COG3425
lmo0717	Murein transglycosylase with N-acetyl-D-glusoamine binding site, SLT family; DegU and MogR regulated (Williams *et al.*, 2005; Shen and Higgins, 2006)	COG0741	lmo1638	Microcin C7 self-immunity protein MccF; its absence results in listerial accumulation in the liver (Iurov *et al.*, 2012)	COG1619
lmo0724	Peptidase	COG4990	lmo2424	Thioredoxin	COG3118
Transporter			**No orthologues**		
lmo0269	Oligopeptide transport system permease protein	COG1173	lmo0615	Hypothetical protein	-
lmo0987	ABC transporter, permease protein, induced in CodY mutant (Bennett *et al.*, 2007); related to CylB of *Streptococcus agalactiae* involved in hemolysin production	COG1511	lmo0622	Hypothetical protein	-
lmo1131, 1132	ABC transporter, ATP-binding/permease protein	COG4988	lmo0657	Hypothetical protein	-
lmo2181	NPQTN specific sortase B; surface protein transpeptidase involved in anchoring of SvpA and Hbp1	COG4509	lmo0793	Putative transport protein	COG1811
svpA /*hbp2*(lmo2185), *hbp1* (lmo2186)	NPQTN cell wall anchored proteins with similarity to IsdA, IsdC of *Staphylococcus aureus* (Mariscotti *et al.*, 2009); heme-binding NEAT domain associated with iron/heme transport (Xiao *et al.*, 2011); Fur and MecA regulated virulence factor (Newton *et al.*, 2005; Borezee *et al.*, 2001)	COG5386	lmo0819	Hypothetical protein	-
lmo2669	Type IV ABC-transporter, upregulated under anaerobic conditions (Müller-Herbst *et al.*, 2014)	COG4905	lmo1626	Hypothetical protein	-
Transcription			lmo1779	Hypothetical protein	-
lmo0212	Acetyltransferase, GNAT family	COG0456	lmo2063	Hypothetical protein	-
lmo1309, 1310	Co-activators of prophage gene expression IbrB, IbrA	COG1475, COG3969	lmo2065	Hypothetical protein	-
lmo1311	SNF2 family domain protein	COG0553	lmo2066	Hypothetical protein	-
lmo2234	Sugar phosphate isomerase	COG1082	lmo2169	Hypothetical protein	-
			lmo2432	Hypothetical protein; Fur-box (Newton *et al.*, 2005)	-
			lmo2803	Hypothetical protein	-
			lmo2843	Hypothetical protein	COG5279

3.3 The putative fibronectin protein Lmo0721 is involved in adhesion to Caco-2 cells

In-frame deletion mutants of selected candidate genes in the parental strain *L. monocytogenes* EGDe were constructed using homologous recombination and a temperature-sensitive shuttle vector. These mutants were verified by PCR and sequencing of the respective gene locus to rule out frame shifts. Cultures of Caco-2 (human colon carcinoma) cells were used to assess adhesion, invasion and intracellular replication capabilities of in-frame deletion mutants of the candidate genes lmo0651, lmo2669, lmo0723-0724, lmo1699 and lmo0721 from **Table 7**. While no influence of the genes lmo0651 (encoding a putative transcriptional regulator), lmo2669 (encoding a hypothetical protein), lmo0723-0724 (encoding a methyl-accepting protein and a hypothetical protein), and lmo1699 (encoding a chemotaxis protein) (data not shown) was detected, the deletion of lmo0721 influenced adhesion to Caco-2 cells (**Figure 10 A**).

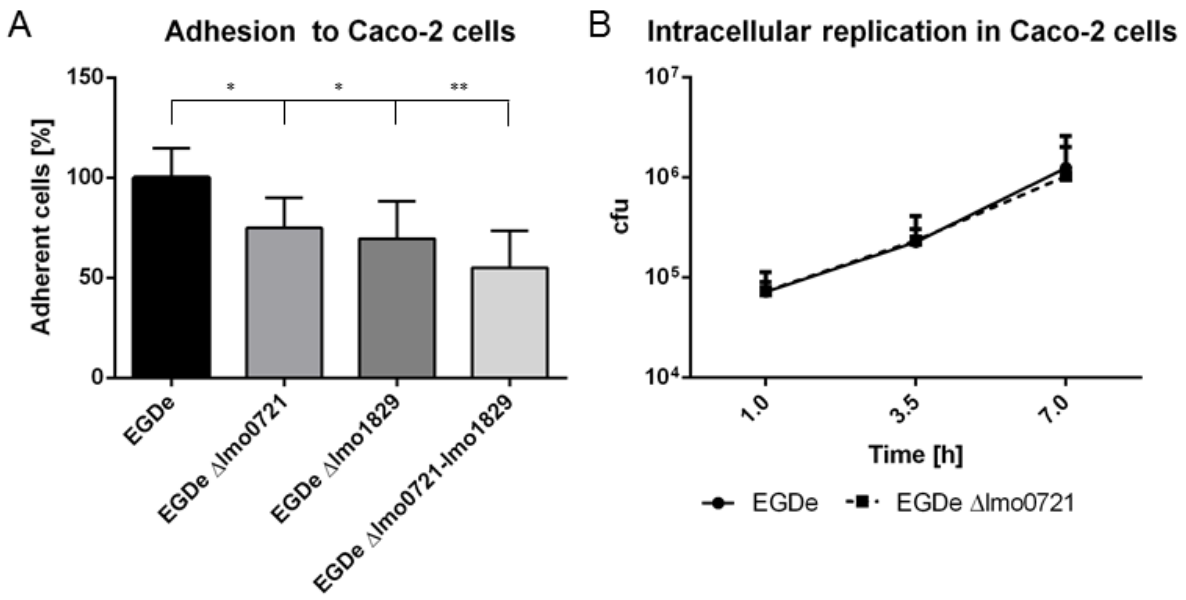

Figure 10: Deletion mutants of genes encoding fibronectin-binding proteins exhibit reduced adhesion to Caco-2 cells.

The percentage of adherent cells of *L. monocytogenes* EGDe, EGDe Δlmo0721, EGDe Δlmo1829 (*fbpA*) and EGDe Δlmo0721-lmo1829 to approximately 2.5×10^5 eukaryotic Caco-2 cells (A) was analyzed for a MOI of 10. The number of adherent EGDe cells was set to 100 %. (B) The percentage of invasive and replicating cells of *L. monocytogenes* EGDe (●) and EGDe Δlmo0721 (■) was determined. Approximately 2.5×10^5 eukaryotic Caco-2 or HEp2 cells were infected with a MOI of 10, and the numbers of intracellular bacterial cells were determined 1, 3.5 and 7 h p.i. Error bars indicate the standard deviation of three biologically independent experiments including technical replicates. Statistical significance was assessed using two-tailed student's t-test with Welch's correction. P values less than 0.05 were considered significant and are indicated as follows: * = $p < 0.05$; ** = $p < 0.01$.

The gene lmo0721 encodes a putative fibronectin-binding protein in *L. monocytogenes*, and its deletion led to a reduction of adhesion to Caco-2 cells of 25.09 % compared to the parental strain. Fibronectin is a component of the extracellular matrix of eukaryotic cells and *L. monocytogenes* can bind fibronectin to facilitate adhesion to the host cell. *L. monocytogenes* possesses five fibronectin-binding proteins (Gilot *et al.*, 1999). One of these proteins, FbpA (lmo1829), has been proven to be involved in adhesion in and invasion of human epithelial cells and its deletion led to decreased virulence in an oral and i.v. mouse model (Gilot *et al.*, 2000; Dramsi *et al.*, 2004; Osanai *et al.*, 2013). Therefore, as a control, we created a deletion mutant of lmo1829 and additionally a double deletion mutant Δlmo0721-lmo1829, which were also tested for adhesion capabilities in a Caco-2 assay. EGDe Δlmo1829 showed comparable results to EGDe Δlmo0721 since adhesion was reduced 30.39 % compared to the parental strain. The double mutant exhibited an even further reduced adhesion of 44.97 % (**Figure 10 A**). In addition, the invasion and intracellular replication of the EGDe Δlmo0721 mutant in comparison to EGDe were tested, but no significant differences 1 h, 3.5 h and 7 h after the infection were apparent (**Figure 10 B**).

To prove *in vitro* binding of lmo0721 to fibronectin, a microtiter assay with immobilized human fibronectin was conducted. It was not possible to detect a difference between EGDe Δlmo0721 and the parental strain in binding to the microtiter plate since the values fluctuated extensively (data not shown). Therefore, it remains to be deciphered whether or not the protein encoded by lmo0721 is able to bind to fibronectin.

3.4 The operon lmo1131-1132 encodes a putative ABC transporter involved in the infection process

Two genes from *L. monocytogenes* with a high conservation only in the *Listeria sensu stricto* spp. and therefore candidates for being involved in the colonization process are lmo1131 (1,713 bp) and lmo1132 (1,644 bp). These genes are encoded in an operon and the two protein coding sequences are separated by a single base pair. No functional role has been established, but according to the Basic Local Alignment Search Tool (BLAST) on the NCBI homepage, the operon encodes a putative ATP-binding cassette (ABC) ABC transporter. The amino acid sequences of both Lmo1131 and Lmo1132 showed homologies of up to 60 % to uncharacterized ABC transporters of *Enterococcus* spp. Furthermore, Lmo1131 showed weak homologies of about 40 % to cysteine ABC transport proteins or ATP-binding/permease CydD proteins. Lmo1132 exhibited homologies of about 40 % to thiol reductant ABC exporter subunit CydC proteins and specific hits to MdlB ABC-type multidrug transport system domains. These homologues mostly belonged to species from the order Clostridiales, which are closely related to the genus *Listeria*. A typical prokaryotic ABC transporter is composed of two hydrophobic

transmembrane domains (TMD) and two water soluble nucleotide binding domains (NBD) at the cytosolic side of the cell membrane (Wilkens, 2015). Each protein lmo1131 and lmo1132 contains a fused TMD and NBD domain (**Figure 11 A**), making up a "half-size" transporter, which eventually form a heterodimeric full-size transporter. According to TOPCONS (Tsirigos *et al.*, 2015), a tool for consensus prediction of membrane protein topology and signal peptides, lmo1131 and lmo1132 each contain six transmembrane helices, a typical feature of TMD domains in ABC transporters (**Figure 11 B**). In recent years, the tertiary structure of several prokaryotic ABC transporters has been analyzed by x-ray crystallography or electron microscopy, which can be used for homology modeling of transporter proteins with unknown structure. A 3D model of lmo1131-1132 was constructed using ExPASy SWISS-MODEL (Guex *et al.*, 2009; Arnold *et al.*, 2006; Kiefer *et al.*, 2006; Biasini *et al.*, 2014) and the ProMod3 Version 1.0.2. Since lmo1131 and lmo1132 encode for half-size transporters and form a heterodimeric ABC transporter with similarities to multidrug family permeases, the *Thermus thermophilus* heterodimeric multidrug ABC transport complex TmrAB (Kim *et al.*, 2015) served as a template to generate the 3D structure (**Figure 11 C**).

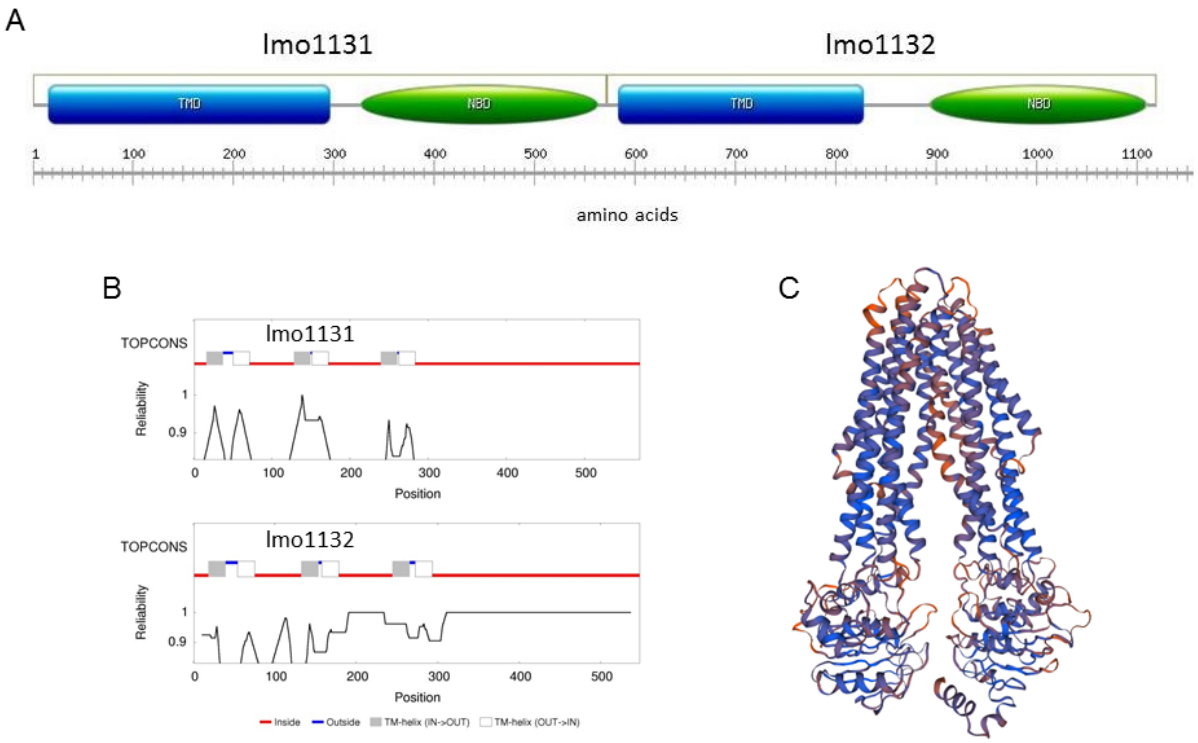

Figure 11: Domain and protein structure of lmo1131-1132.
(A) Domain structure of lmo1131 and lmo1132 predicted by ExPASy PROSITE (Sigrsit *et al.*, 2013; Sigrist *et al.*, 2002). The picture was generated with the online tool ExPASy MyDomains (Hulo *et al.*, 2008). Grey line with ticks indicates the number of amino acids starting at the first amino acid N-formylmethionine of lmo1131. TMD = ABC transporter integral membrane type-1 fused domain (transmembrane domain). NBD = ATP-binding cassette, ABC transporter-type domain (nucleotide binding domain). (B) Prediction of the membrane protein topology of lmo1131 and lmo1132 by TOPCONS (Tsirigos *et al.*, 2015). Predicted transmembrane helices are shown as grey and white squares, amino acids predicted to be on either the cytosolic or the extracellular side of the cell membrane are shown in red and blue, respectively. The reliability of the predictions and the position of the amino acids are indicated below. (C) Heterodimeric protein structure of lmo1131 and lmo1132 generated by homology-modelling using ExPASy SWISS-MODEL (Guex *et al.*, 2009; Arnold *et al.*, 2006; Kiefer *et al.*,

2006; Biasini *et al.*, 2014) and the ProMod3 Version 1.0.2. The *Thermus thermophilus* heterodimeric multidrug ABC transport complex TmrAB (Kim *et al.*, 2015) served as a template to generate the 3D structure.

Using BPROM (Solovyev and Salamov, 2011), a program for the prediction of bacterial promoters, a possible promoter sequence with a -35 and a -10 element was found 135 bp upstream of the ATG start codon of lmo1131 (**Figure 12**). A previous study on the repressor protein Fur (Shao, 2007) detected a recognition consensus sequence, a so-called Fur box, in the promoter region of lmo1131-1132. This Fur box is located 158 bp upstream of the start codon and overlaps with the -35 box. The overlap of the Fur consensus sequence with the -35 box agrees with the repressive nature of the protein. A genome-wide transcription start site (TSS) map created by strand-specific cDNA sequencing (Wurtzel *et al.*, 2012) revealed a TSS 128 bp upstream of the start codon.

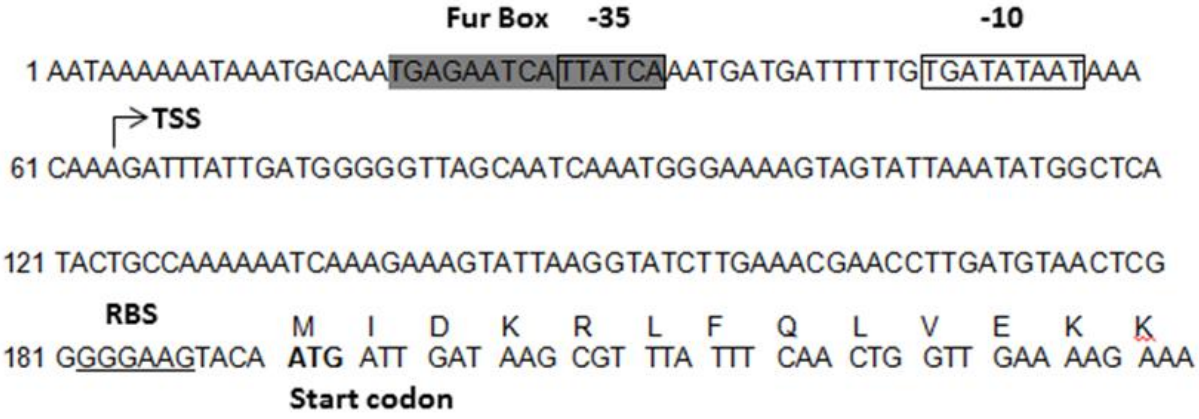

Figure 12: Promoter region of the operon lmo1131-1132.
The nucleotide sequence of the promoter region upstream of the lmo1131-1132 operon is shown. Black boxes depict the -35 and -10 region (determined by BPROM; Solovyev and Salamov, 2011), the arrow depicts the TSS (determined by Wurtzel *et al.*, 2012). The grey shaded nucleotides represent a putative Fur-Box (Shao, 2007). A potential ribosome binding site (RBS) is underlined, the start codon is shown in bold and the abbreviations for the amino acids encoded by the first few codons are shown above the DNA sequence.

3.4.1 Transcription of lmo1131-1132 is temperature-, oxygen- and iron dependent

The transcription of lmo1131 and lmo1132 in *L. monocytogenes* EGDe at 24°C and 37°C under both aerobic and anaerobic growth conditions was analyzed via qRT-PCR (**Figure 13 A**). The two transporter genes exhibited similar transcription levels under all four conditions, suggesting transcription of the operon from a common promoter located upstream of lmo1131 as predicted via BPROM (**Figure 12**). Setting the transcriptional level of both genes at 37°C with oxygen as 100 %, a decrease of the lmo1131 and lmo1132 mRNA levels at 37°C to 4.77 % and 6.15 %, respectively, was observed upon oxygen depletion. At 24°C, the transcription of the transporter genes was reduced to 55.80 % and 64.02 %, respectively, under aerobic conditions and to 3.18 % and 4.53 % in the absence of oxygen.

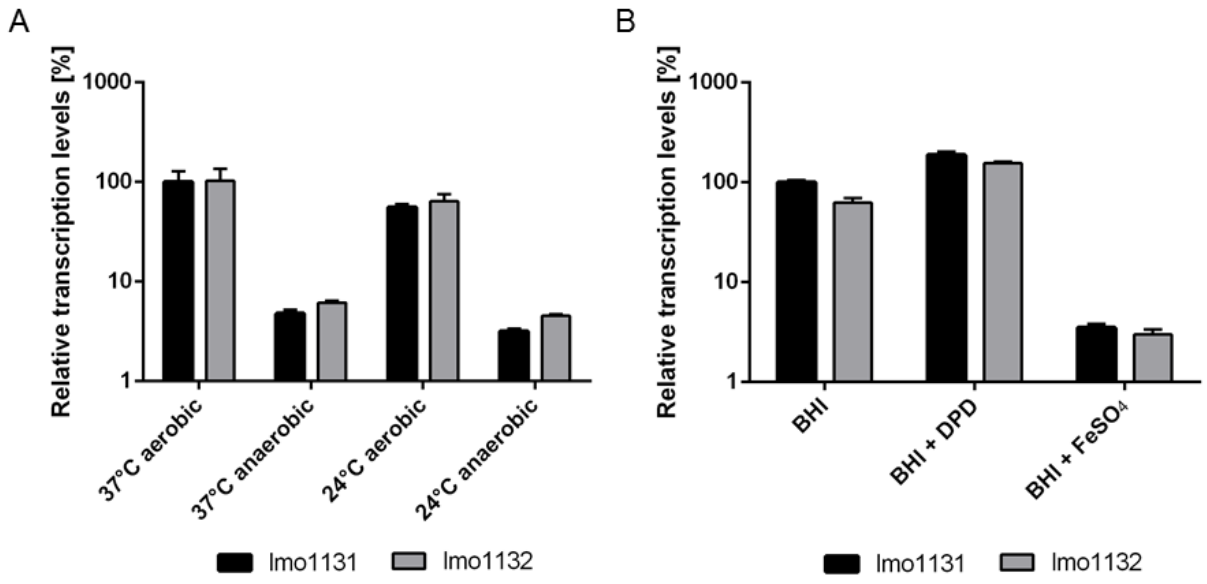

Figure 13: Temperature-, oxygen- and iron-dependent transcription of lmo1131 and lmo1132.
(A) Relative transcription of genes lmo1131 (black bars) and lmo1132 (gray bars) for the conditions 37°C anaerobic, 24°C aerobic, and 24°C anaerobic was compared to that at 37°C aerobic (preassigned as 100 % gene expression for lmo1131). (B) Relative transcription of genes lmo1131 (black bars) and lmo1132 (gray bars) for the conditions BHI + DPD or BHI + $FeSO_4$ was compared to BHI (preassigned as 100 % gene expression for lmo1131) at 37°C under shaking (150 rpm). The results were calculated using the $2^{-\Delta\Delta CT}$ method (Livak and Schmittgen, 2001) and lmo1759 (*pcrA*) was used as reference gene for normalization. Error bars indicate the standard error of three biologically independent experiments including technical duplicates for each condition.

The protein Fur is the main regulator of iron metabolism, homeostasis and uptake in many bacteria (Andrews *et al.*, 2003). Since a potential Fur box is present in the promoter region, an involvement of lmo1131-1132 in iron homeostasis and/or transport of ferrous compounds is possible. Therefore, transcription of lmo1131-1132 in media with different iron concentrations was analyzed (**Figure 13 B**). *L. monocytogenes* was cultivated in either 10 ml BHI or 10 ml BHI + 0.3 mM 2,2'-dipyridyl (DPD) or 10 ml BHI + 0.1 mM ferrous sulfate ($FeSO_4$) at 37°C under shaking (150 rpm) in a 100 ml Erlenmeyer flask. BHI, an iron rich medium, was supplemented with DPD, a metalloprotease inhibitor and a high-affinity iron chelator, to deplete iron. This caused an about two-fold increase of transcription levels for both lmo1131 (188.34 %) and lmo1132 (155.01 %) compared to BHI growth conditions (100.00 % and 62.71 %, respectively). In contrast, the addition of $FeSO_4$ renders excessive iron conditions that caused a strong repression of the transporter genes and a more than 20-fold decrease of transcription (3.49 % and 3.00 %, respectively).

Since both iron and oxygen are potential signals mediating the switch to a pathogenic lifestyle upon entrance of the GIT, this oxygen- and iron dependent transcriptional regulation of the genes lmo1131 and lmo1132 might play a role for the colonization process of *L. monocytogenes*.

3.4.2 The operon lmo1131-1132 facilitates adhesion to and invasion of Caco-2 cells

To analyze the functional role of the operon lmo1131-1132, the in-frame deletion mutant *L. monocytogenes* EGDe Δlmo1131-1132 was constructed and tested for adhesive and invasive capabilities in cell culture assays using Caco-2 and HEp2 (human larynx squamous cell carcinoma) cells (**Figure 14**).

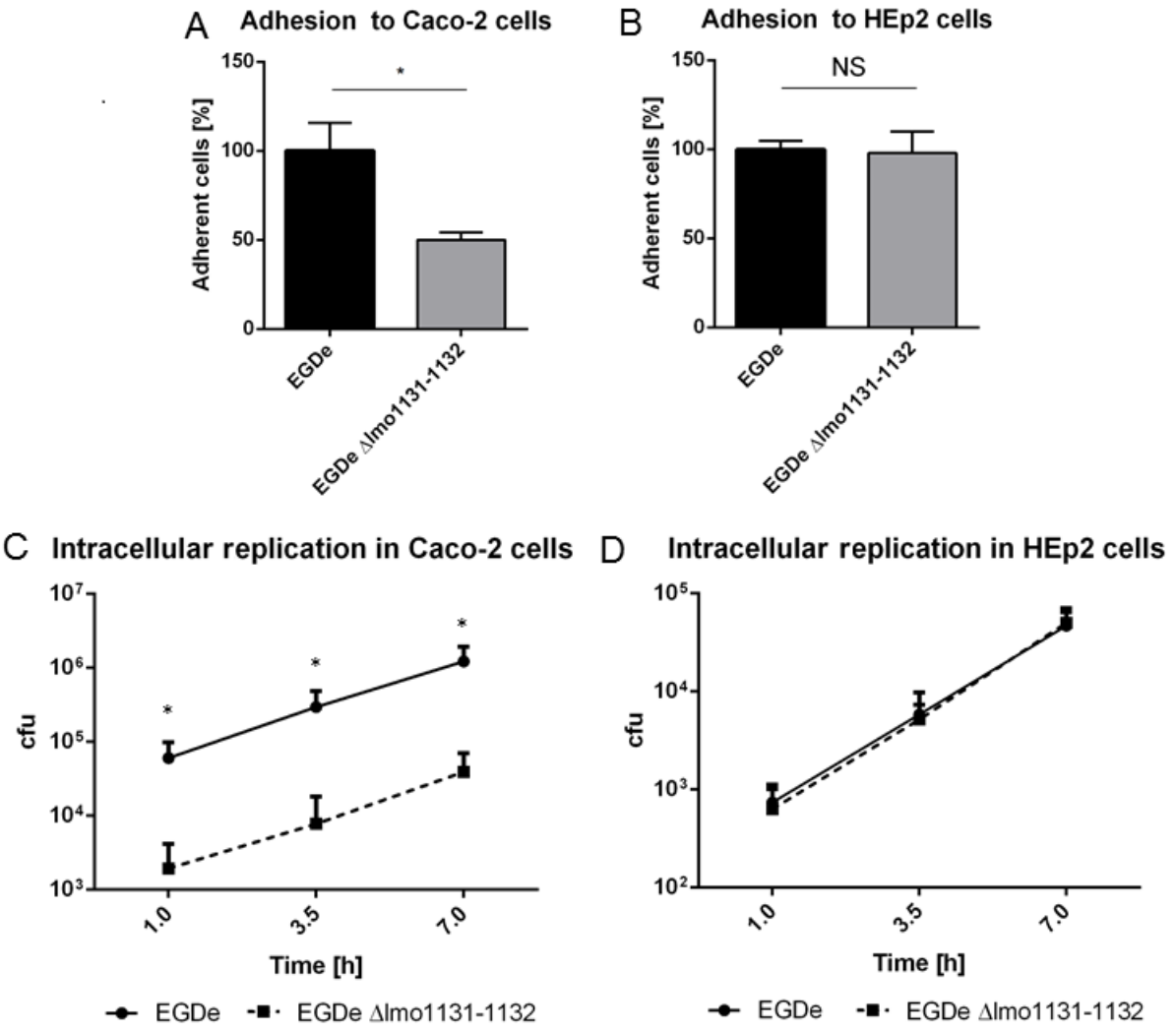

Figure 14: Adhesion to and invasion of Caco-2 and HEp2 cells by a transporter mutant.
The percentage of adherent cells of *L. monocytogenes* EGDe and EGDe Δlmo1131-1132 to approximately 2.5 × 10^5 eukaryotic Caco-2 cells (A) or HEp2 cells (B) was analyzed for a MOI of 10. The number of adherent EGDe cells was set to 100 %. (C+D) The percentage of invasive and replicating cells of *L. monocytogenes* EGDe (●) and EGDe Δlmo1113-1132 (■) was determined. Approximately 2.5 × 10^5 eukaryotic Caco-2 or HEp2 cells were infected with a MOI of 10, and the numbers of intracellular bacterial cells were determined 1, 3.5 and 7 h p.i. Error bars indicate the standard deviation of three biologically independent experiments including technical replicates. Statistical significance was assessed using two-tailed student's t-test with Welch's correction; P values less than 0.05 were considered significant and are indicated as follows: * = $p < 0.05$; ** = $p < 0.01$; *** = $p < 0.001$; NS = not significant.

Adhesion to Caco-2 cells by the deletion mutant cells was reduced by a factor of 2 in comparison with the parental strain EGDe (**Figure 14 A**). In contrast, cell culture assays with HEp2 cells revealed no significant adhesion differences between EGDe and EGDe Δlmo1131-1132 (**Figure 14 B**), suggesting a specific role of the putative ABC transporter in the interaction with Caco-2 cells. A gentamycin protection assay was performed to test the invasion and the intracellular replication properties of the deletion mutant in Caco-2 and HEp2 cells. The number of intracellular cells detected 1 h after cell culture infection is a measure of the capacity of a strain to enter cells. A more than 20-fold reduction of invasion in Caco-2 cells, but not in HEp2 cells, for EGDe Δlmo1131-1132 in comparison to the parental strain was observed (**Figure 14 CD**). The intracellular replication rates of EGDe [doubling time T_d (EGDe) = 83 min] and EGDe Δlmo1131-1132 [T_d (EGDe Δlmo1131-1132) = 83 min] however, were identical in the Caco-2 cells, indicating a specific role of the putative transporter in adhesion and/or invasion of this cell type.

To evaluate the role for each of the genes in adhesion to Caco-2 cells, the single gene deletion mutants *L. monocytogenes* EGDe Δlmo1131 and EGDe Δlmo1132 were constructed. Both mutants showed a significant reduction of adhesion properties compared to the parental strain (**Figure 15 A**), although the percentage of adhesive cells in relation to EGDe (set as 100 %) was slightly increased to 65.47 % (lmo1131) and 72.50 % (lmo1132) compared to the double mutant EGDe Δlmo1131-1132 (53.69 %). The number of invading cells compared to EGDe was similar in both mutants (**Figure 15 B**) and the intracellular replication rates differed only slightly (T_d (EGDe) = 61 min; T_d (EGDe Δlmo1131) = 69 min; T_d (EGDe Δlmo1132) = 75 min).

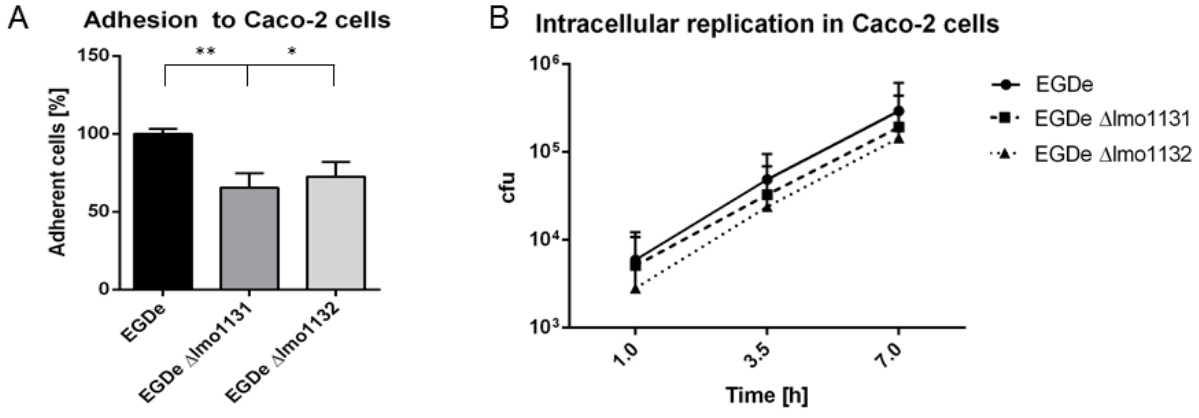

Figure 15: Adhesion to and intracellular replication in Caco-2 cells of single transporter mutants.
The percentage of adherent cells of *L. monocytogenes* EGDe, EGDe Δlmo1131 and EGDe Δlmo1132 to approximately 2.5×10^5 eukaryotic Caco-2 cells (A) was analyzed for a MOI of 10. The number of adherent EGDe cells was set to 100 %. (B) The percentage of invasive and replicating cells of *L. monocytogenes* EGDe (●), EGDe Δlmo1131 (■) and EGDe Δlmo1132 (▲) was determined. Approximately 2.5×10^5 eukaryotic Caco-2 cells were infected with a MOI of 10, and the numbers of intracellular bacterial cells were determined 1, 3.5 and 7 h p.i. Error bars indicate the standard deviation of three biologically independent

experiments including technical replicates. Statistical significance was assessed using two-tailed student's t-test with Welch's correction; P values less than 0.05 were considered significant and are indicated as follows: * = $p < 0.05$; ** = $p < 0.01$.

An experiment was conducted to directly compare the number of adhesive and invasive *L. monocytogenes* cells in Caco-2 cells after a 1 h incubation period (**Figure 16**). As expected, the number of adhesive EGDe Δlmo1131-1132 cells was about 10-fold lower compared to EGDe. Surprisingly, there was no significant difference between adherent EGDe, EGDe Δlmo1131 and EGDe Δlmo1132 cells after 1 h of incubation in contrast to the results from previous experiments with 35 min incubation (**Figure 15 A**). The number of invasive bacterial cells (**Figure 16**) for the parental strain and all three mutants was comparable to the previous results (**Figure 15 B**). While invading EGDe Δlmo1131-1132 cells were reduced 28-fold compared to EGDe, similar numbers of invading cells for the parental strain and the single deletion mutants were observed. The ratio of adhesive and invasive *Listeria* cells was calculated and revealed a 5-fold reduction for EGDe Δlmo1131-1132 (0.11 %) compared to the other strains (0.51 – 0.78 %). This indicates that a deletion of the operon lmo1131-1132 causes not only impaired adhesion but also a decreased ability of adherent cells to enter the host cell.

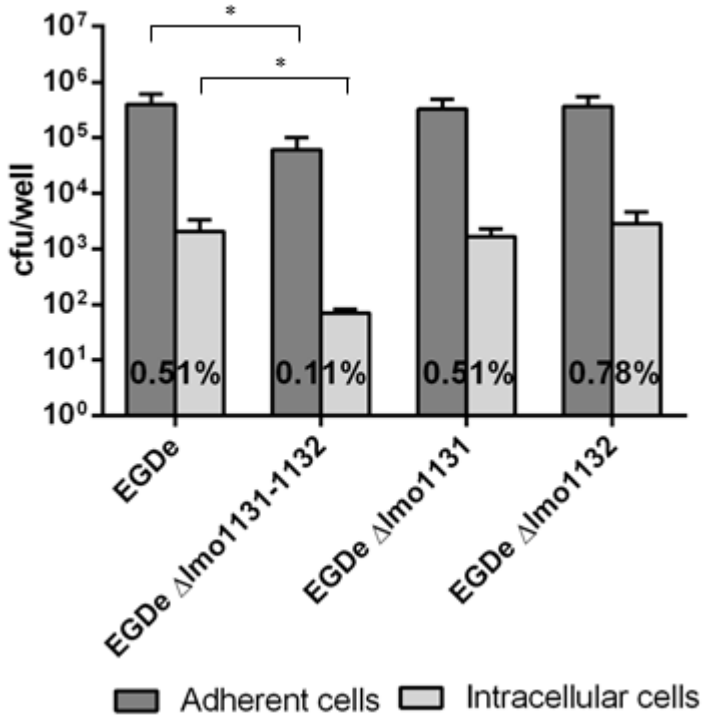

Figure 16: Comparison of adhesive and invasive *L. monocytogenes* cells reveals defect for adherent EGDe Δlmo1131-1132 cells in invasion of Caco-2 cells.

The number of adherent (dark grey) and intracellular (light grey) *L. monocytogenes* EGDe, EGDe Δlmo1131-1132, EGDe Δlmo1131 and EGDe Δlmo1132 cells per well was determined after 1 h of infection and an additional 1 h of treatment with (intracellular cells) or without (adherent cells) gentamycin. The percentage of adherent cells which invaded the host cells is depicted at the bottom of the columns. Error bars indicate the standard deviation of three biologically independent

experiments including technical replicates. Statistical significance was assessed using two-tailed student's t-test with Welch's correction. P values less than 0.05 were considered significant and are indicated as follows: * = $p < 0.05$. If not indicated otherwise, values are not significantly different.

3.4.3 Possible functions of lmo1131-1132-surrounding genes

In general, genes adjacent to ABC transporter gene regions may encode regulatory proteins or proteins involved in the same metabolic pathway or function. As an example, most prokaryotic importers encode solute binding proteins (SBP) which are either soluble, lipid-anchored or membrane-associated proteins responsible for capturing the substrate and delivering it to the TMD (Wilkens *et al.*, 2015). The genomic region of the operon lmo1131-1132 contains several neighboring genes (**Figure 17**), which might be involved in the adhesion and invasion deficient phenotype of the deletion mutant EGDe Δlmo1131-1132, although no possible candidate gene encoding a SBP was found.

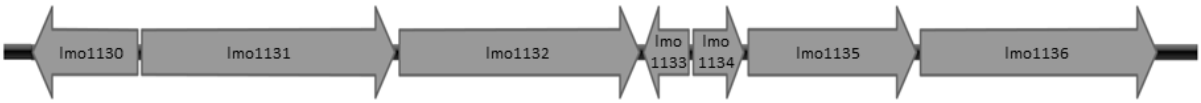

Figure 17: Schematic representation of the lmo1131-1132 genomic region.
The genetic organization of lmo1131-1132 and adjacent genes is depicted. Arrows indicate the direction of transcription and sizes correspond the number of nucleotides of each gene. lmo1130: encoding a protein similar to transcription regulators; lmo1131: encoding a protein similar to ABC transporters, ATP-binding proteins; lmo1132: encoding a protein similar to ABC transporters, ATP-binding proteins; lmo1133: encoding a protein similar to *B. subtilis* YjcS protein; lmo1134: encoding a protein similar to regulatory proteins; lmo1135: encoding a protein similar to immunity and potential surface protein; lmo1136: encoding a protein similar to internalin, putative peptidoglycan bound protein (LPXTG motif).

Two putative regulatory proteins, lmo1130 and lmo1134, are closely located in proximity to lmo1131-1132. Lmo1130 is transcribed in the opposite direction with respect to lmo1131. A putative Fur box is located upstream of lmo1130 (Shao, 2007). In the downstream region of lmo1131-1132, the gene lmo1133 is encoded, which has no known function but possesses an antibiotic biosynthesis monooxygenase (ABM) domain as revealed by BLAST protein search. These ABM domains were shown to be part of heme-degrading enzymes in *Staphylococcus aureus* (Wu *et al.*, 2005) and *Mycobacterium tuberculosis* (Chim *et al.*, 2010), therefore creating another possible link to iron homeostasis. Lmo1135 encodes for an immunity and potential surface protein and lmo1136 encodes for a putative internalin according to BLAST protein search (**Table 8**).

Table 8: Adjacent genes in the genomic region of lmo1131-1132.

lmo number	Protein homology
lmo1130	similar to transcription regulators
lmo1131	similar to ABC transporters, ATP-binding proteins
lmo1132	similar to ABC transporters, ATP-binding proteins
lmo1133	similar to *B. subtilis* YjcS protein
lmo1134	similar to regulatory proteins
lmo1135	similar to immunity and potential surface protein
lmo1136	similar to internalin, putative peptidoglycan bound protein (LPXTG motif)

To analyze the role of these genes during adhesion and invasion of host cells in cell culture, in-frame deletion mutants of the corresponding genes were constructed and tested for their phenotypes during adhesion to Caco-2 cells (**Figure 18**). The deletion mutants *L. monocytogenes* EGDe Δlmo1130, EGDe Δlmo1135 and EGDe Δlmo1136 showed no significant reduction in adhesion to Caco-2 cells in comparison to the parental strain. Only EGDe Δlmo1133 and EGDe Δlmo1134 showed decreased adhesion properties of 63.23 % and 72.89 %, respectively, in comparison to EGDe set as 100 %. This might indicate a possible role for these two genes in the phenotype of the deletion mutant *L. monocytogenes* EGDe Δlmo1131-1132.

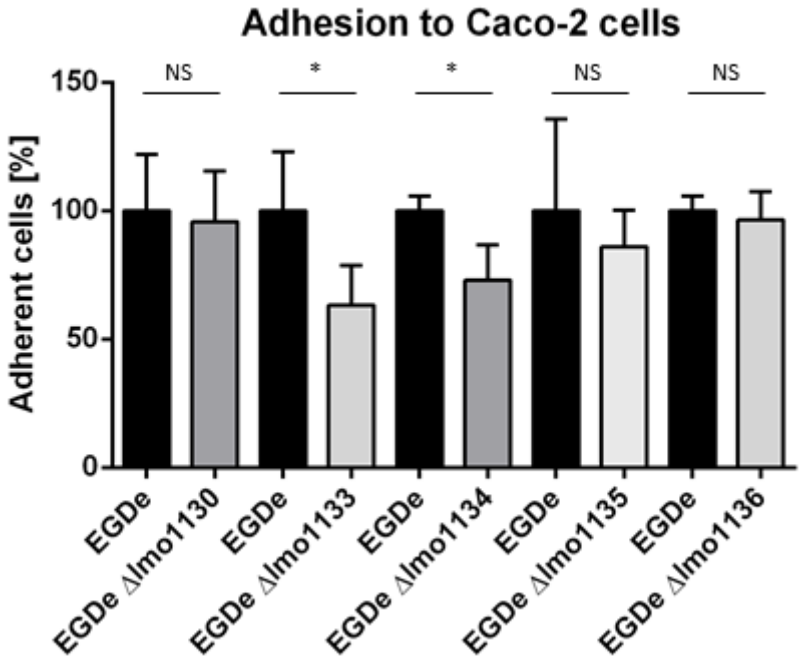

Figure 18: Adhesion capabilities of different transporter related deletion mutants.
The percentage of adherent cells of *L. monocytogenes* EGDe, EGDe Δlmo1130, EGDe Δlmo1133, EGDe Δlmo1134, EGDe Δlmo1135 and EGDe Δlmo1136 to approximately 2.5×10^5 eukaryotic Caco-2 cells after 35 min was analyzed for a MOI of 10. The number of adherent EGDe cells was set to 100 %. Error bars indicate the standard deviation of three biologically independent experiments including technical replicates. Statistical significance was assessed using two-tailed student's t-test with Welch's correction; NS, not significant. P values less than 0.05 were considered significant and are indicated as follows: * = $p < 0.05$; NS = not significant.

Transcription of lmo1131 and lmo1132 at 37°C under aerobic or anaerobic conditions was compared between *L. monocytogenes* EGDe and the two deletion mutants EGDe Δlmo1130 and EGDe Δlmo1134. The deletion of the two putative regulatory proteins had no significant impact on transcription levels of the ABC transporter genes under the conditions tested (data not shown).

3.4.4 Deletion of lmo1131-1132 leads to attenuated colonization in mice

To verify the relevance of the candidate genes lmo1131-1132 for the *in vivo* infection process, a food-borne transmission model in mice was used to study the GI phase of listeriosis. Co-infection experiments with female BALB/c mice aged 6-8 weeks were conducted using a 1:1 ratio of EGDe and its mutant EGDe Δlmo1131-1132 lacking the putative transporter genes. The strains were chromosomally tagged with pIMC3kan (EGDe) and pIMC3ery (mutant). Mice were fed a total of 1×10^9 cfu/mouse and the number of *Listeria* in the lumen and tissue of either the ileum or the colon was analyzed at different time points. In addition, the systemic spread to the MLNs, liver and spleen was also assessed.

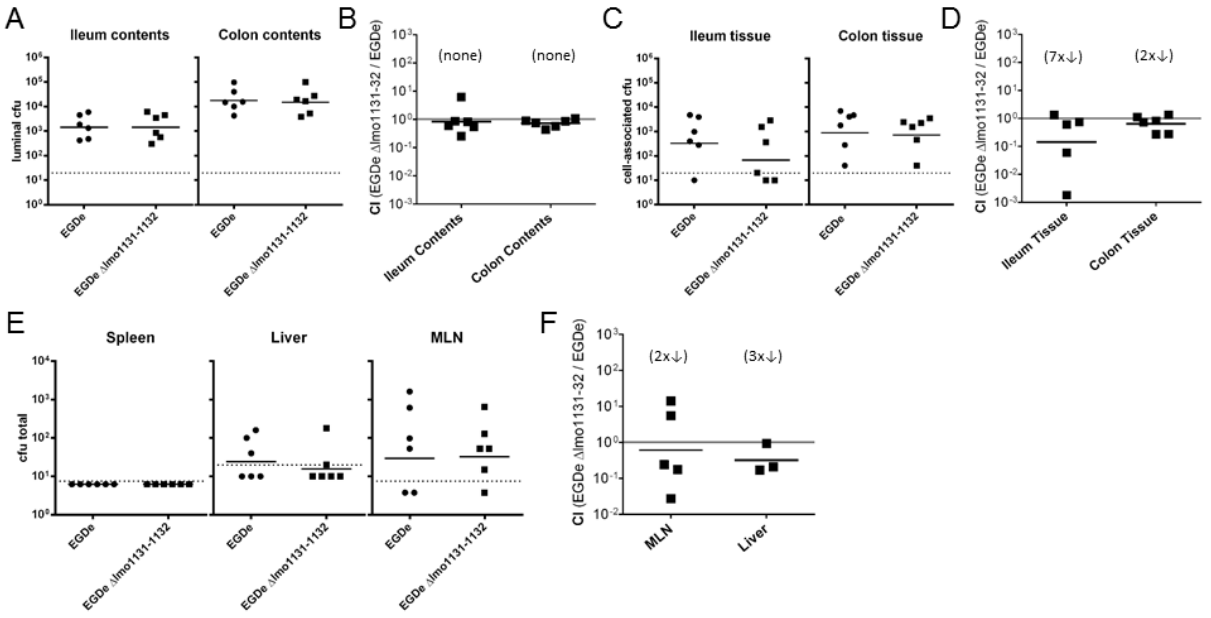

Figure 19: Deletion of lmo1131-1132 leads to a minor defect in the invasion of the ileum tissue in BALB/c mice after 1 day p.i.

Female BALB/c mice were orally infected with a 1:1 ratio of *L. monocytogenes* EGDe and EGDe Δlmo1131-1132 for a total inoculum of 1×10^9 cfu. After 24 h, the cfu of luminal (A) or cell-associated (C) strains in the ileum and colon were determined, and the CI was calculated (B+D). (E) The cfu numbers of both strains in the spleen, liver and MLNs are shown. The numbers of EGDe (circles) or EGDe Δlmo1131-1132 (squares) recovered in each mouse after co-infection are depicted. Solid horizontal lines indicate mean values from a group of mice (n = 6), while dashed lines represent the detection limit for each sample. Cfu values for samples without detectable bacteria were set as half the detection limit. (F) The CIs of the strains recovered from the organs are depicted. The geometric mean for each group was compared to the theoretical value of 1.0, and the fold change difference is indicated in parentheses. Statistical significance was assessed using two-tailed student's t-test with Welch's correction. P values less than 0.05 were considered significant and there was no indication of statistically significant differences between EGDe and EGDe Δlmo1131-1132.

24 h p.i., the infected mice harbored 10-fold more luminal *L. monocytogenes* in the colon than the ileum, but no significantly different amount of both strains was recovered (**Figure 19 A**), which was also reflected by the Competitive Index (CI) (**Figure 19 B**). The numbers of cfu associated with the flushed tissue was assessed, including *L. monocytogenes* cells trapped in the mucus layer, bacteria adhered to or inside intestinal epithelial cells (ECs), and bacteria that have reached the underlying LP (**Figure 19 C**). A similar ratio of EGDe and EGDe Δlmo1131-1132 was recovered from the colon tissue. In the ileum, the deletion mutant exhibited a lower mean cfu value than the parental strain and the CI value (**Figure 19 D**) enunciated a 7-fold reduction of the mutant, although this difference was not statistically significant.

To assess the systemic spread of both strains, the bacterial load in the MLNs, spleen and liver was determined (**Figure 19 E**). While the MLNs of most mice were already infected by equal numbers of both strains, only three mice showed signs of hepatic infection with three out of six mice harboring EGDe and two out of three mice harboring EGDe Δlmo1131-1132. No pathogens were detected in the spleen. The CI values were calculated showing a 2-fold and 3-fold reduction of EGDe Δlmo1131-1132 in the MLNs and liver (**Figure 19 F**).

In the following experiments, the incubation period after oral infection was increased to 2 days. The colon contained 25-fold more *L. monocytogenes* than the ileum (**Figure 20 A**), as was previously reported (Bou Ghanem *et al.*, 2013a; Becattini *et al.*, 2017). However, there was no significant difference in the ratio of the two strains recovered from the intestinal contents of either tissue (**Figure 20 B**).

When assessing the numbers of cfu associated with the flushed tissue, a bimodal distribution was observed in both the ileum and the colon, with little or no *L. monocytogenes* recovered in approximately half of the mice, and up to 10^4 cfu recovered in the other half (**Figure 20 C**). In the ileum, the average number of cfu for the latter group was six-fold higher for wildtype EGDe compared with the mutant. Overall, the CI revealed that the wild type strain outcompeted the mutant strain six-fold in the ileum (**Figure 20 D**). Interestingly, there was no significant difference between EGDe and EGDe Δlmo1131-1132 in the colon.

To assess the systemic spread of both strains, the bacterial load in the MLNs, spleen and liver 2 days p.i was determined (**Figure 20 E**). As shown in **Figure 20 F**, five-fold fewer EGDe Δlmo1131-1132 were recovered from the liver compared to the wild type strain. The MLNs and spleen contained equal numbers of the two strains.

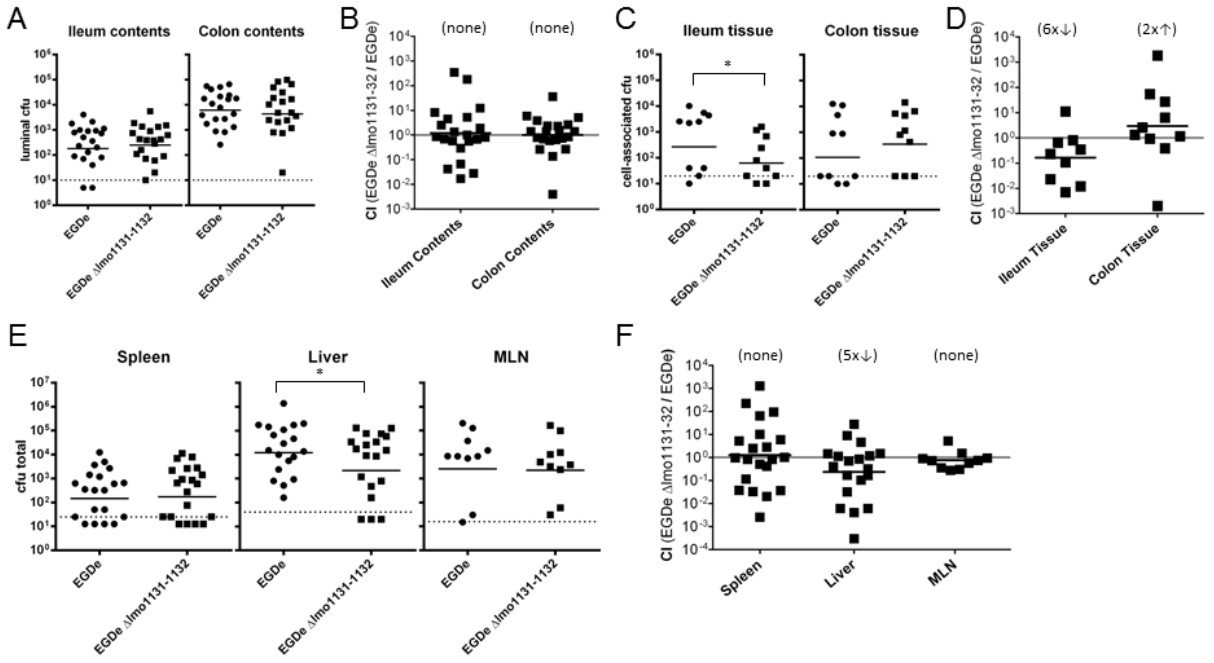

Figure 20: Deletion of lmo1131-1132 leads to attenuated colonization of BALB/c mice after 2 days p.i.

Female BALB/c mice were orally infected with a 1:1 ratio of *L. monocytogenes* EGDe and EGDe Δlmo1131-1132 for a total inoculum of 1 × 10^9 cfu. After 2 days, the cfu of luminal (A) or cell-associated (C) strains in the ileum and colon were determined, and the CI was calculated (B+D). (E) The cfu numbers of both strains in the spleen, liver and MLNs are shown. The numbers of EGDe (circles) or EGDe Δlmo1131-1132 (squares) recovered in each mouse after co-infection are depicted. Solid horizontal lines indicate mean values, which were pooled from at least two separate experiments, while dashed lines represent the detection limit for each sample. Cfu values for samples without detectable bacteria were set as half the detection limit. (F) The CIs of the strains recovered from the organs are depicted. The geometric mean for each group was compared to the theoretical value of 1.0, and the fold change difference is indicated in parentheses. Statistical significance was assessed using two-tailed student's t-test with Welch's correction. P values less than 0.05 were considered significant and are indicated as follows: * = $p < 0.05$. If not indicated otherwise, values are not significantly different.

To further investigate this difference in intestinal colonization, the gut tissues of infected mice 2 days p.i. were fractionated, and the number of cfu in either the mucus layer, ECs or the LP were determined (**Figure 21**). The number of wild type and EGDe Δlmo1131-1132 in the mucus and the epithelial layer of the ileum did not differ significantly (**Figure 21 A**). However, when looking at the CIs in the ileum, wild type *L. monocytogenes* outnumbered the deletion mutant by five-fold in underlying LP (**Figure 21 B**), similar to what was observed for whole tissue. As expected, there were no significant differences in the cfu numbers or CIs for any of the colon fractions (**Figure 21 CD).** This result suggests that the lmo1131-1132 gene products may be involved in efficient translocation across the intestinal mucosa in the small intestine, but not the large intestine.

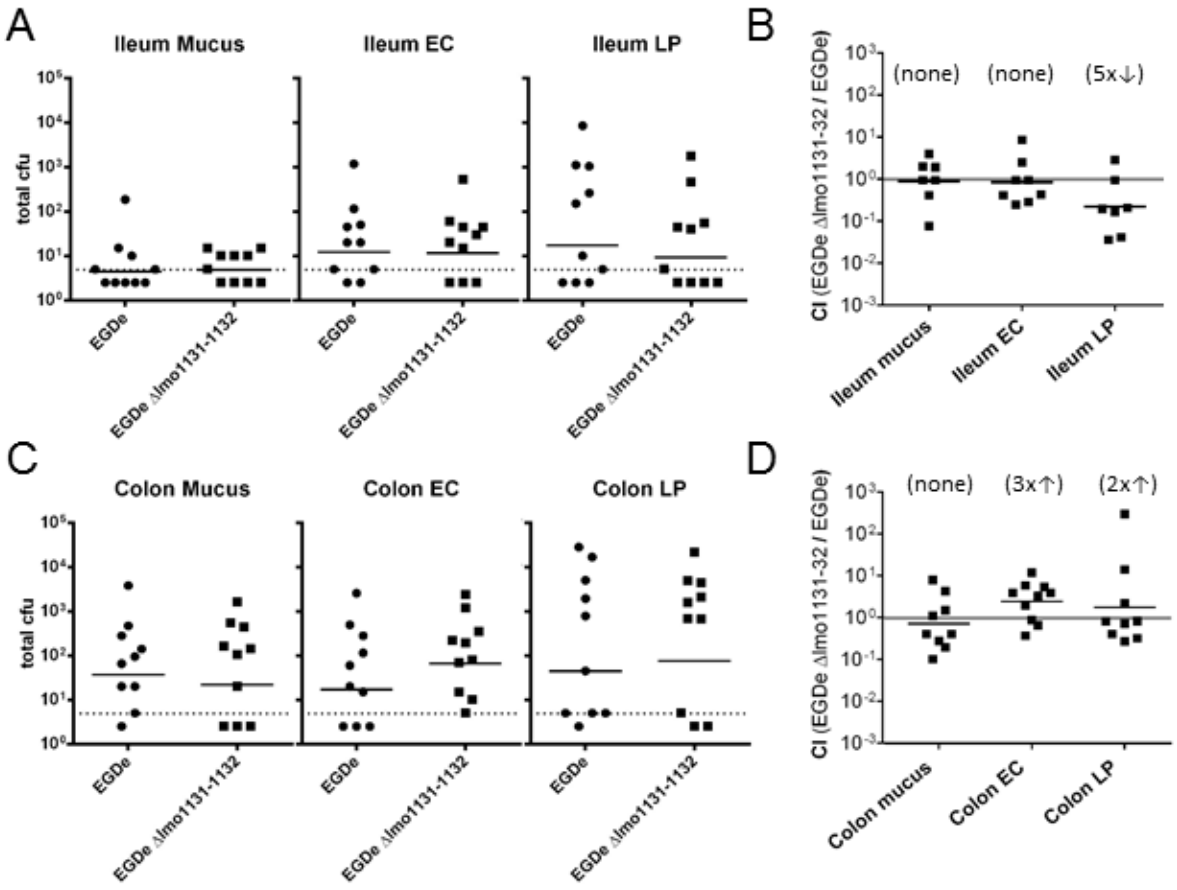

Figure 21: Fractionation of intestinal tissue hints to involvement of lmo1131-1132 for the infection of the ileal LP.

Female BALB/c mice were orally infected with a 1:1 ratio of *L. monocytogenes* EGDe and EGDe Δlmo1131-1132 for a total inoculum of 1 × 10^9 cfu. 2 days p.i., the numbers of listeriae in the mucus, ECs and the LP of the ileum (A) and the colon (B) were determined. The numbers of EGDe (circles) or EGDe Δlmo1131-1132 (squares) recovered in each mouse after co-infection are depicted. Solid horizontal lines indicate mean values, which were pooled from at least two separate experiments (n = 4 or 6 mice per group), while dashed lines represent the detection limit for each sample. Cfu values for samples without detectable bacteria were set as half the detection limit. (C+D) The CIs of both strains recovered from the ileum and colon are shown. The geometric mean for each group was compared to the theoretical value of 1.0, and the fold change difference is indicated in parentheses. Statistical significance was assessed using two-tailed student's t-test with Welch's correction. P values less than 0.05 were considered significant and there was no indication of statistically significant differences between EGDe and EGDe Δlmo1131-1132.

Additionally, fractionation of GI tissues was performed 6 h p.i. to assess the initial invasion of the gut mucosa shortly after oral infection (**Figure 22**). As seen before, equal numbers of both strains were recovered from the ileum and colon lumen (**Figure 22 AC**). The mucus and epithelial cells of the ileum harbored only small numbers of EGDe and EGDe Δlmo1131-1132 or were devoid of bacteria. Deletion mutant and parental strain were detected in similar numbers in the LP (**Figure 22 B**). All colonic fractions exhibited considerably higher cfu numbers than the ileum and were equally colonized by both strains (**Figure 22 D**). Therefore, the deletion of lmo1131-1132 did not influence the invasion of GI tissues or access to the LP in the first few hours p.i.

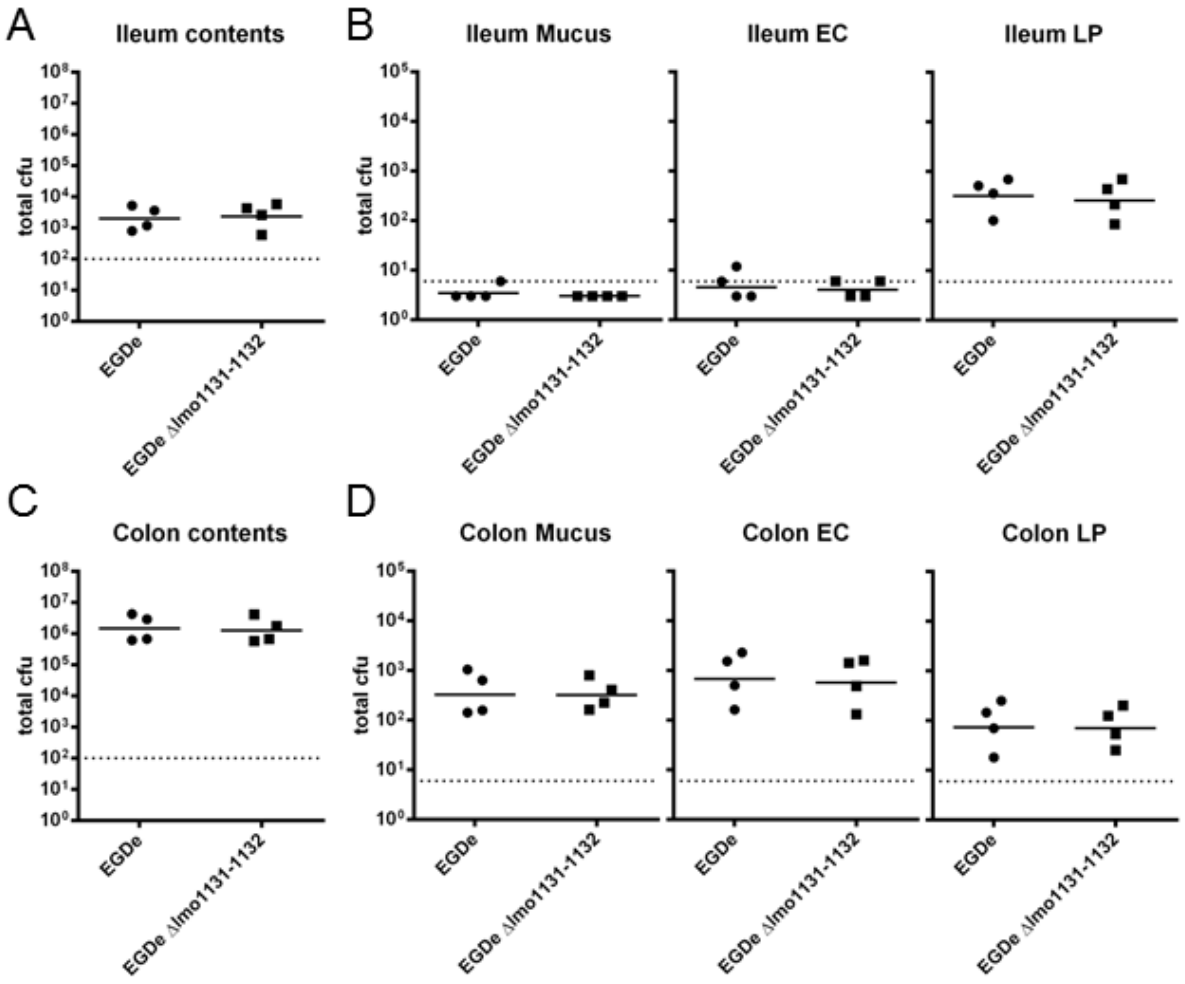

Figure 22: Initial invasion of GI tissues is not affected by the deletion of lmo1131-1132

Female BALB/c mice were orally infected with a 1:1 ratio of *L. monocytogenes* EGDe and EGDe Δlmo1131-1132 for a total inoculum of 1×10^9 cfu. 6 hours p.i., the cfu of luminal strains in the Ileum (A) and the colon (C) were determined. Gut tissues were fractionated and the numbers of listeriae in the mucus, ECs and the LP of the ileum (B) and the colon (D) were determined. The numbers of EGDe (circles) or EGDe Δlmo1131-1132 (squares) recovered in each mouse after co-infection are depicted. Solid horizontal lines indicate mean values from a single experiment (n = 4 mice), while dashed lines represent the detection limit for each sample. Cfu values for samples without detectable bacteria were set as half the detection limit. Statistical significance was assessed using two-tailed student's t-test with Welch's correction. P values less than 0.05 were considered significant and there was no indication of statistically significant differences between EGDe and EGDe Δlmo1131-1132.

To test whether dissemination of the transporter mutant to peripheral organs was impaired or if the mutant strain had a specific growth defect in the liver, mice were i.v. injected with a 1:1 mixture of EGDe and EGDe Δlmo1131-1132 and the total cfu in liver and spleen were determined 2 days p.i. Approximately equal numbers of both strains were recovered from the liver when the transmission route bypassed the gut (**Figure 23 A**) and the CI values were equal to 1 (**Figure 23 B**). Together, these data suggest that the transporter lmo1131-1132 contributes to crossing of the intestinal barrier.

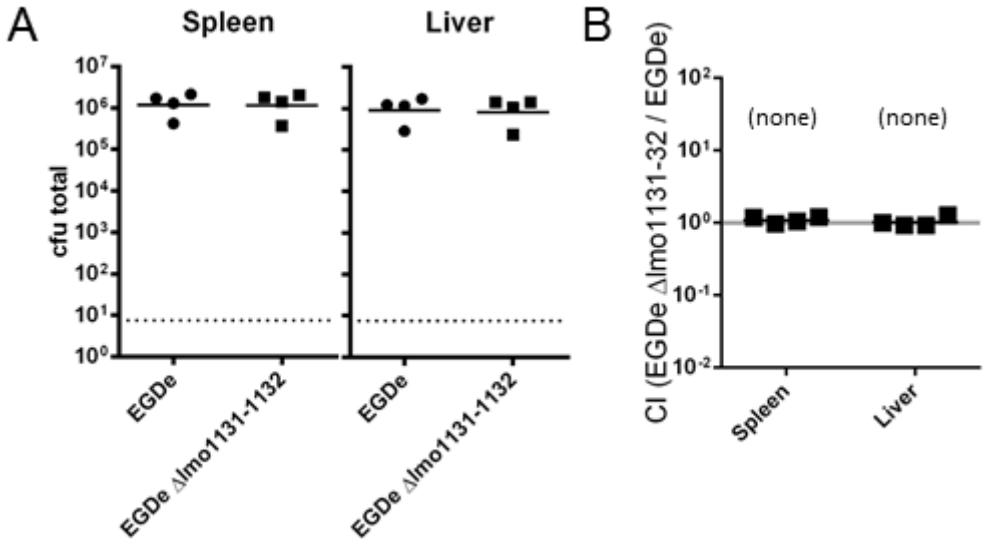

Figure 23: The operon lmo1131-1132 does not influence infection numbers in spleen and liver after i.v. injection.

Female BALB/c mice were i.v.-infected with a 1:1 ratio of *L. monocytogenes* EGDe and EGDe Δlmo1131-1132 for a total inoculum of 1 × 104 cfu. (A) Liver and spleen were harvested 2 days p.i., and the cfu numbers of listeriae in these organs was analyzed. The numbers of EGDe (circles) or EGDe Δlmo1131-1132 (squares) recovered in each mouse after co-infection are depicted. Solid horizontal lines indicate mean values, while dashed lines represent the detection limit for each sample. (B) CIs depict the ratio of EGDe Δlmo1131-1132/EGDe. The geometric mean for each group was compared to the theoretical value of 1.0 and the fold change difference is indicated in parentheses. Statistical significance was assessed using two-tailed student's t-test with Welch's correction. P values less than 0.05 were considered significant and there was no indication of statistically significant differences between EGDe and EGDe Δlmo1131-1132.

3.5 Characterization of the gene clusters for biosynthesis of cobalamin and degradation of 1,2-PD

L. monocytogenes possesses a 53-kb genomic region consisting of three gene clusters for the utilization of ethanolamine (*eut* genes) and 1,2-PD (*pdu* genes) as well as for the biosynthesis of vitamin B_{12} (cobalamin) (*cob*/*cbi* genes), which is a required co-factor in these degradation pathways. This large *eut/pdu/cbi/cob* genomic island is highly conserved in all *Listeria sensu stricto* spp., but is mostly absent or only weakly conserved in the *Listeria sensu lato* group. The three clusters are also present in *S.* Typhimurium enabling the use of 1,2-PD as carbon and energy source (Badia *et al.*, 1985; Bobik *et al.*, 1999; Price-Carter *et al.*, 2001). The corresponding catabolic pathways have been shown to play a role for *Salmonella* in *in vitro* and *in vivo* (Winter *et al.*, 2010; Srikumar & Fuchs, 2011; Faber *et al.*, 2017). The ethanolamine cluster has been shown to be important for pathogenesis of *L. monocytogenes* after i.v. injection in BALB/c mice (Mellin *et al.*, 2014) while necessity of the *pdu* cluster is still ambiguous. To analyze the role of the 1,2-PD as a possible carbon- and energy source during colonization, the phenotype of a *pduD* deletion mutant during *in vitro* and *in vivo* growth was analyzed.

3.6.1 The *pduD* gene is required for growth with 1,2-PD

1,2-PD is the product of rhamnose or fucose catabolism, which are abundant in plant matter and in the mammalian GIT in the form of glycoconjugates. To investigate the role of 1,2-PD as a potential carbon and energy source for *L. monocytogenes* under *in vitro* conditions, the in-frame deletion mutant EGDe Δ*pduD* was constructed. The gene encodes a homolog of the ß subunit of the diol dehydratase PduCDE, a hexameric vitamin B_{12}-dependent enzyme, which catalyzes the conversion of 1,2-PD to propionaldehyde in *Salmonella* (Daniel *et al.*, 1998).

The parental strain EGDe and its mutant EGDe Δ*pduD* were grown inMM with 0.5 % (w/v) YE under anaerobic conditions at 37°C (**Figure 24**). No significant differences in growth behavior between both strains were observed (OD_{600}^{max} = 0.25). However, when 1,2-PD and cobalamin, which is the essential cofactor of PduCDE, were added, EGDe grew to an optical density OD_{600}^{max} = 0.35, whereas the cell density of EGDe Δ*pduD* did not exceed that in the medium without 1,2-PD (**Figure 24 A**). These results suggest that all nutrients in the MM which are preferred over 1,2-PD are used up during the first 4 h, and that *L. monocytogenes* only then degrades 1,2-PD to reach a higher cell density. Experiments performed under microaerobic conditions did not result in an improved growth phenotype of EGDe by supplementation with 1,2-PD and cobalamin (**Supplementary figure 2**), suggesting that 1,2-PD can only be utilized under anaerobic conditions.

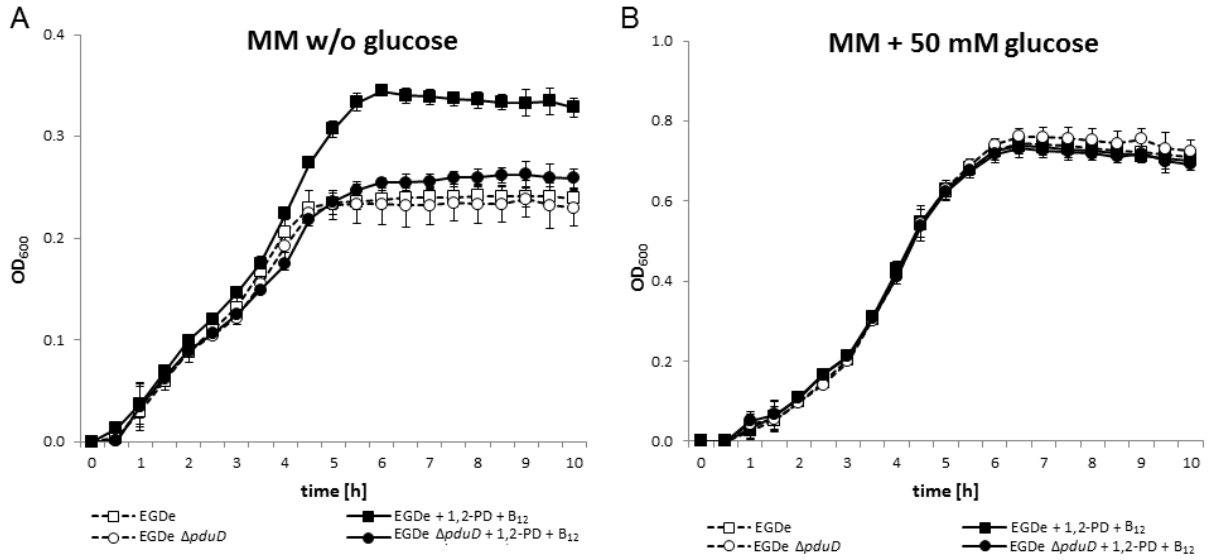

Figure 24: Improved growth of *L. monocytogenes* by addition of 1,2-PD.
Growth curves of *L. monocytogenes* EGDe (□) and *L. monocytogenes* EGDe Δ*pduD* (○) in MM and 0.5% (w/v) YE without glucose (A) or with 50 mM glucose (B) cultivated at 37°C under anaerobic conditions. MM was supplemented with 10 mM 1,2-PD and 25 nM cobalamin (filled symbols) or not supplemented (open symbols). OD_{600} was measured at the indicated intervals using Bioscreen C. Growth curves depict the calculated mean value of three independent biological experiments with technical duplicates, while error bars indicate the standard deviation.

As a control, the growth of both strains in MM supplemented with 50 mM glucose in the absence and presence of 1,2-PD and cobalamin was compared. Under these growth conditions with glucose as an energy source, cells reached far higher cell densities (OD_{600}^{max} = ≈0.75) and the addition of 1,2-PD had no significant effect on growth of either EGDe or EGDe Δ*pduD* (**Figure 24 B**), indicating that 1,2-PD is utilized by *L. monocytogenes* only in the absence of glucose.

3.6.2 Supplementation of 1,2-PD and/or cobalamin leads to induction of *pdu* and *cob*/*cbi* genes during stationary phase

A global transcriptome analysis of *L. monocytogenes* EGDe was conducted via NGS to investigate the transcriptional response of the *pdu*, *eut* and the *cob*/*cbi* gene clusters to the presence of 1,2-PD and/or cobalamin. During growth in BHI medium (BHI), in BHI medium with 10 mM 1,2-PD (BHI + 1,2-PD), or in BHI medium with 10 mM 1,2-PD and 25 nM cobalamin (BHI + 1,2-PD + B_{12}), cells were harvested in the mid-logarithmic (exponential) and stationary phases. RNA was isolated, sequenced on the MiSeq platform and the PRKM values for each condition were calculated (**Table 9**).

Table 9: Normalized RPKM values of *L. monocytogenes* EGDe for the conditions BHI, BHI with 10 mM 1,2-PD (BHI + 1,2-PD) and BHI with 10 mM 1,2-PD and 25 nM cobalamin (BHI + 1,2-PD + B_{12}) during stationary and exponential phases.

		Exponential Phase			Stationary Phase		
	Gene	BHI + 1,2-PD + B_{12}	BHI +1,2-PD	BHI	BHI + 1,2-PD + B_{12}	BHI +1,2-PD	BHI
Propanediol	*pduS* (lmo1142)	134	224	369	51,728	12,107	398
	pduT (lmo1143)	79	176	173	24,056	5,638	322
	pduU (lmo1144)	117	262	37	5,883	1,463	99
	pduV (lmo1145)	24	39	0	2,916	798	52
	pduA (lmo1151)	22	0	0	7,810	1,070	0
	pduB (lmo1152)	28	0	0	34,684	6,221	83
	pduC (lmo1153)	36	41	20	62,732	10,014	81
	pduD (lmo1154)	0	0	0	22,417	3,363	41
	pduE (lmo1155)	11	26	0	15,558	2,414	0
	pduG (lmo1156)	0	11	11	22,488	3,330	50
	pduH (lmo1157)	0	0	0	3,713	587	0
	pduK (lmo1158)	31	0	34	24,443	3,587	0
	pduJ (lmo1159)	0	0	10	6,981	1,463	13
	pduL (lmo1160)	0	0	0	28,847	6,123	137
	pduM (lmo1162)	29	130	64	32,136	5,527	130
	pduN (lmo1163)	0	0	0	8,371	1,256	75
	pduO (lmo1164)	29	21	0	19,977	3,574	71
	pduP (lmo1165)	50	37	0	28,766	5,801	50
	pduQ (lmo1166)	31	0	0	58,994	10,731	136
	pduF (lmo1167)	16	0	0	10,379	1,848	48
	pduW (lmo1168)	34	64	50	4,676	1,065	42
	pduX (lmo1170)	160	356	125	3,741	378	102
	pduL (lmo1182)	6	0	0	0	17	0
	pduT (lmo1185)	0	0	0	0	0	0

		Exponential Phase			Stationary Phase		
	Gene	BHI + 1,2-PD + B_{12}	BHI +1,2-PD	BHI	BHI + 1,2-PD + B_{12}	BHI +1,2-PD	BHI
Cobalamine	*cobU* (lmo1147)	46	0	50	2,126	552	0
	cobS (lmo1148)	19	0	0	1,526	336	28
	cobC (lmo1149)	0	0	24	282	32	0
	cobD (lmo1169)	173	160	63	12,428	2,185	128
	cbiA (lmo1191)	0	0	12	17	1,984	58
	cbiB (lmo1192)	0	0	0	24	3,050	46
	cbiC (lmo1193)	0	0	0	0	2,984	24
	cbiD (lmo1194)	0	13	0	37	1,354	0
	cbiE (lmo1195)	0	0	0	13	1,277	13
	cbiT (lmo1196)	0	28	0	197	3,672	19
	cbiF (lmo1197)	0	0	0	78	1,554	21
	cbiG (lmo1198)	0	0	0	167	1,906	20
	cbiH (lmo1199)	28	31	0	306	5,480	63
	cbiJ (lmo1200)	0	24	0	17	1,162	16
	cysG (lmo1201)	16	17	0	36	1,408	12
	cbiK (lmo1202)	11	25	0	17	600	0
	cbiL (lmo1203)	0	0	23	83	900	0
	cbiM (lmo1204)	0	0	0	17	359	8
	cbiN (lmo1205)	0	0	0	79	955	15
	cbiQ (lmo1206)	0	0	0	0	511	17
	cbiO (lmo1207)	22	0	0	135	1,713	162
	cbiP (lmo1208)	515	604	417	2,178	7,500	1,929
	pocR (lmo1150)	72	0	32	847	391	150
unknown	lmo1146	58	32	32	3,250	1,047	65
	lmo1171	0	0	0	0	0	0
	lmo1172	30	0	65	92	45	66
	lmo1173	55	20	20	71	55	136
	lmo1183	28	126	0	175	0	0
	lmo1188	1,799	1,380	1,912	501	621	459
	lmo1189	158	80	205	166	108	32
	lmo1190	73	121	0	12,748	4,635	161

During the exponential phase, the *pdu* and the *cob*/*cbi* gene clusters showed only weak or no transcription under all three growth conditions. RPKM values below 200 were obtained for all genes with the exception of the genes *pduS* (lmo1142), lmo1188, lmo1189 and *cbiP* (lmo1208). During growth in BHI medium in the stationary phase, six out of 24 *pdu* genes and five out of 22 *cob*/*cbi* genes showed no transcriptional activity according to the read numbers, while gene transcription increased slightly for the others, although levels were still very low. Again, RPKM values below 200 were observed for all genes except for *pduS* (lmo1142), *pduT* (lmo1143), and lmo1188. The gene *cbiP* (lmo1208) showed a more than 5-fold increase in transcription during growth in BHI compared to stationary phase.

However, when 1,2-PD was added to the cultures (BHI + 1,2-PD), RPKM values for both *pdu* and *cob*/*cbi* genes were strongly increased. By calculating the fold-changes in comparison to the read counts in plain BHI and visualizing them in a three-color scheme, a strong induction up to 1,605-fold was observed (**Figure 25**).

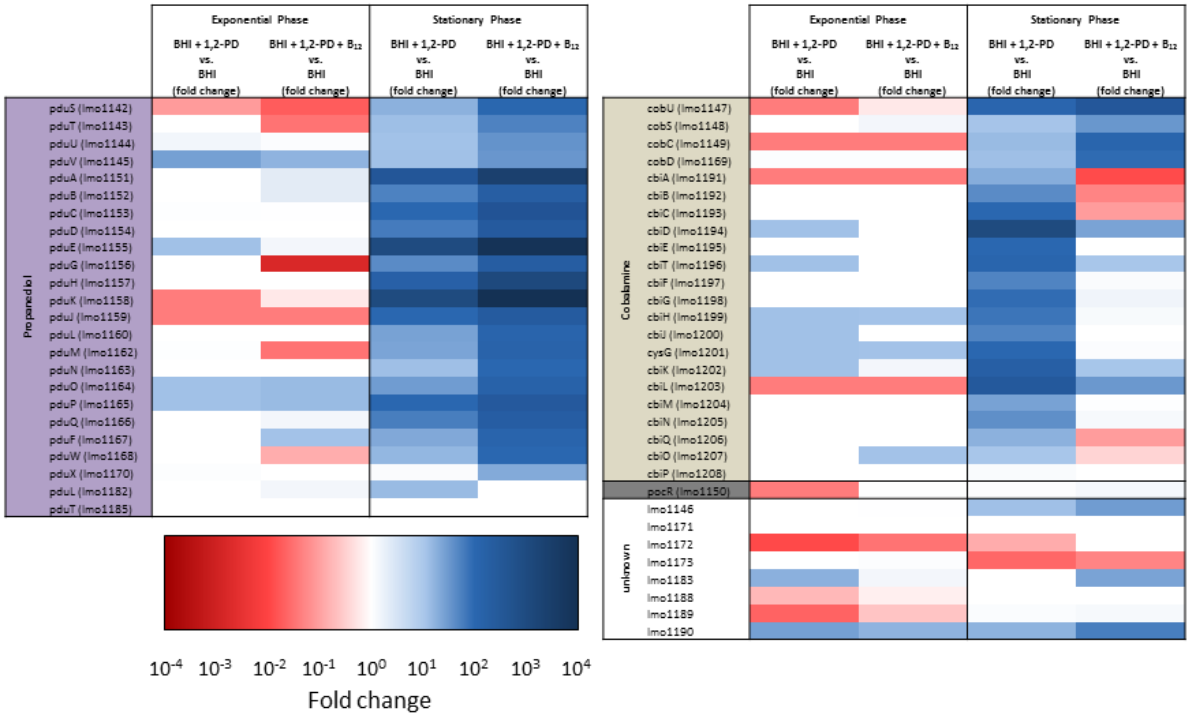

Figure 25: Transcriptomics of *L. monocytogenes* in response to 1,2-PD and B_{12}.
L. monocytogenes EGDe cells grown under different conditions was harvested during the exponential and stationary phases and the mRNA expression profile was analyzed via NGS using the Illumina MiSeq seqencing platform. Fold changes of normalized RPKM values under the conditions BHI with 10 mM 1,2-PD (BHI+1,2-PD) and BHI with 10 mM 1,2-PD and 25 nM cobalamin (BHI+1,2-PD+B_{12}) in comparison to BHI were calculated for both growth phases. The results were visualized using a three-color scheme with red colors indicating negative and blue colors indicating positive fold changes. The color intensity corresponds to the magnitude of fold change. Unknown genes refer to genes located in the region of propanediol, ethanolamine, and cobalamin clusters without any known function.

The logarithm base 2-fold changes (log_2FC) representing the log_2-transformed expression ratios of the conditions [BHI + 1,2-PD / BHI] or [BHI + 1,2-PD + B_{12} / BHI] or [BHI + 1,2-PD + B_{12} / BHI + 1,2-PD] in stationary phase were calculated using edgeR. No calculations were performed for growth conditions in exponential phase since RPKM values were low. Genes with a False Discovery Rate (FDR) ≤ 0.3 and a p-value ≤ 0.05 were considered as significantly differentially regulated. 37 genes (19 *pdu* genes, 16 *cob/cbi* genes, *eutJ* and lmo1190) were significantly upregulated during growth with 1,2-PD (**Table 10**).

Table 10: Gene upregulated during growth in BHI with 10 mM 1,2-PD (BHI + 1,2-PD) compared to BHI.

Gene	BHI + 1,2-PD vs. BHI log_2FC	Description
***pduS* (lmo1142)**	4.81	similar to *S. enterica* PduS protein
***pduT* (lmo1143)**	4.16	similar to *S. enterica* PduT protein
***pduV* (lmo1145)**	3.79	similar to *S. enterica* PduV protein
***pduA* (lmo1151)**	8.02	similar to *S.* Typhimurium PduA protein
***pduB* (lmo1152)**	6.07	similar to *S.* Typhimurium PduB protein
***pduC* (lmo1153)**	6.81	highly similar to propanediol dehydratase, α subunit
***pduD* (lmo1154)**	8.30	similar to diol dehydrase (diol dehydratase) γ subunit
***pduE* (lmo1155)**	9.10	similar to diol dehydrase (diol dehydratase) γ subunit (PddC)
***pduG* (lmo1156)**	6.14	similar to diol dehydratase-reactivating factor large subunit
***pduK* (lmo1158)**	9.22	similar to *S. enterica* PduK protein
***pduJ* (lmo1159)**	6.56	similar to carboxysome structural protein
***pduL* (lmo1160)**	5.32	similar to *S. enterica* PduL protein
***eutJ* (lmo1161)**	5.35	similar to ethanolamine utilization protein EutJ
***pduM* (lmo1162)**	5.75	similar to *S. enterica* PduM propanediol utilization protein
***pduN* (lmo1163)**	3.90	similar to carbon dioxide concentrating mechanism protein
***pduO* (lmo1164)**	5.81	highly similar to *S. enterica* PduO protein
***pduP* (lmo1165)**	6.62	similar to ethanolamine utilization protein EutE
***pduQ* (lmo1166)**	6.65	similar to NADPH-dependent butanol dehydrogenase
***pduF* (lmo1167)**	5.11	similar to glycerol uptake facilitator protein
***pduW* (lmo1168)**	4.81	similar to acetate kinase
***cobD* (lmo1169)**	3.99	similar to *S.* Typhimurium CobD protein and to histidinol-phosphate aminotransferase
lmo1190	4.71	similar to ECF transporter S component

***cbiA* (lmo1191)**	5.19	similar to cobyrinic acid a,c-diamide synthase
***cbiB* (lmo1192)**	5.80	similar to cobalamine synthesis protein CbiB
***cbiC* (lmo1193)**	8.90	similar to precorrin isomerase
***cbiD* (lmo1194)**	9.22	similar to cobalamin biosynthesis protein CbiD
***cbiE* (lmo1195)**	8.62	similar to precorrin methylase
***cbiT* (lmo1196)**	9.56	similar to precorrin decarbocylase
***cbiF* (lmo1197)**	5.95	similar to precorrin-3 methylase
***cbiG* (lmo1198)**	8.53	similar to cobalamin biosynthesis protein G CbiG
***cbiH* (lmo1199)**	6.79	similar to precorrin methylase
***cbiJ* (lmo1200)**	8.15	similar to cobalamin biosynthesis J protein CbiJ
***cysG* (lmo1201)**	8.88	similar uroporphyrinogen-III methyltransferase/ uroporphyrinogen-III synthase
***cbiL* (lmo1203)**	7.78	similar to S-adenosyl-methionine: precorrin-2 methyltransferase
***cbiM* (lmo1204)**	7.44	similar to cobalamin biosynthesis protein CbiM
***cbiN* (lmo1205)**	7.93	similar to putative cobalt transport protein CbiN
***cbiO* (lmo1207)**	3.29	similar to cobalt transport ATP-binding protein CbiO

The transcription of *pdu* genes was even more elevated up to 10,942-fold when cobalamin was added (BHI + 1,2-PD + B_{12}) (**Figure 25**). For the cobalamin biosynthesis genes, the presence of this cofactor in the medium resulted in reduced RPKM values except for *cobU* (lmo1147), *cobS* (lmo1148), *cobC* (lmo1149) and *cobD* (lmo1169) (**Table 9**).According to statistical analysis with edgeR, 28 genes (22 *pdu* genes, three *cob* genes, *eutJ*, lmo1146 and lmo1190) were significantly upregulated during growth with 1,2-PD + cobalamin compared to growth in plain BHI (**Table 11**).

Table 11: Gene upregulated during growth in BHI with 10 mM 1,2-PD + 25 nM cobalamin (BHI + 1,2-PD + B_{12}) compared to BHI.

Gene	BHI + 1,2-PD + B_{12} vs. BHI log_2FC	Description
pduS (lmo1142)	6.95	similar to *S. enterica* PduS protein
pduT (lmo1143)	6.30	similar to *S. enterica* PduT protein
pduU (lmo1144)	5.78	similar to *S. enterica* PduU protein
pduV (lmo1145)	5.71	similar to *S. enterica* PduV protein
lmo1146	6.04	hypothetical protein

cobU (lmo1147)	7.96	similar to bifunctional cobalamin biosynthesis protein CopB, (cobinamide kinase; cobinamide phosphatase guanylyltransferase)
cobS (lmo1148)	7.76	highly similar to cobalamin (5'-phosphatase) synthetase
pduA (lmo1151)	10.91	similar to *S.* Typhimurium PduA protein
pduB (lmo1152)	8.60	similar to *S.* Typhimurium PduB protein
pduC (lmo1153)	9.51	highly similar to propanediol dehydratase, α subunit
pduD (lmo1154)	11.06	similar to diol dehydrase (diol dehydratase) γ subunit
pduE (lmo1155)	11.81	similar to diol dehydrase (diol dehydratase) γ subunit (PddC)
pduG (lmo1156)	8.94	similar to diol dehydratase-reactivating factor large subunit
pduH (lmo1157)	9.66	similar to diol dehydratase-reactivating factor small chain
pduK (lmo1158)	12.01	similar to *S. enterica* PduK protein
pduJ (lmo1159)	8.86	similar to carboxysome structural protein
pduL (lmo1160)	7.60	similar to *S. enterica* PduL protein
eutJ (lmo1161)	7.88	similar to ethanolamine utilization protein EutJ
pduM (lmo1162)	8.34	similar to *S. enterica* PduM propanediol utilization protein
pduN (lmo1163)	6.69	similar to carbon dioxide concentrating mechanism protein
pduO (lmo1164)	8.34	highly similar to *S. enterica* PduO protein
pduP (lmo1165)	8.98	similar to ethanolamine utilization protein EutE
pduQ (lmo1166)	9.15	similar to NADPH-dependent butanol dehydrogenase
pduF (lmo1167)	7.65	similar to glycerol uptake facilitator protein
pduW (lmo1168)	6.99	similar to acetate kinase
cobD (lmo1169)	6.54	similar to *S.* Typhimurium CobD protein and to histidinol-phosphate aminotransferase
pduX (lmo1170)	5.12	similar to *S. enterica* PduX protein
lmo1190	6.22	similar to ECF transporter S component

This is also reflected in the $\log_2$FC values comparing the expression ratios BHI + 1,2-PD + B_{12} / BHI + 1,2-PD. While eight *pdu* genes were significantly upregulated, downregulation of eleven *cob*/*cbi* genes was observed when cobalamin was added (**Table 12**).

Table 12: Gene up- or downregulated during growth in BHI with 10 mM 1,2-PD + 25 nM cobalamin (BHI + 1,2-PD + B_{12}) compared to BHI + 10 mM 1,2-PD (BHI + 1,2-PD)

Gene	BHI + 1,2-PD + B_{12} vs. BHI + 1,2-PD log_2FC	Description
pduA (lmo1151)	2.92	similar to *S.* Typhimurium PduA protein
pduC (lmo1153)	2.70	highly similar to propanediol dehydratase, α subunit
pduD (lmo1154)	2.79	similar to diol dehydrase (diol dehydratase) γ subunit
pduE (lmo1155)	2.74	similar to diol dehydrase (diol dehydratase) γ subunit (PddC)
pduG (lmo1156)	2.81	similar to diol dehydratase-reactivating factor large subunit
pduK (lmo1158)	2.82	similar to *S. enterica* PduK protein
pduN (lmo1163)	2.78	similar to carbon dioxide concentrating mechanism protein
pduX (lmo1170)	3.35	similar to *S. enterica* PduX protein
cbiA (lmo1191)	-6.68	similar to cobyrinic acid a,c-diamide synthase
cbiB (lmo1192)	-5.81	similar to cobalamine synthesis protein CbiB
cbiC (lmo1193)	-8.91	similar to precorrin isomerase
cbiD (lmo1194)	-5.11	similar to cobalamin biosynthesis protein CbiD
cbiE (lmo1195)	-5.43	similar to precorrin methylase
cbiT (lmo1196)	-4.18	similar to precorrin decarbocylase
cbiF (lmo1197)	-4.08	similar to precorrin-3 methylase
cbiH (lmo1199)	-4.13	similar to precorrin methylase
cbiJ (lmo1200)	-4.96	similar to cobalamin biosynthesis J protein CbiJ
cysG (lmo1201)	-4.77	similar uroporphyrinogen-III methyltransferase/uroporphyrinogen-III synthase
cbiO (lmo1207)	-3.61	similar to cobalt transport ATP-binding protein CbiO

The transcription levels of *pocR*, the regulator of both clusters, were only slightly elevated in medium supplemented with 1,2-PD and/or cobalamin. The *eut* genes of the ethanolamine degradation cluster, which are positioned between the *pdu* and *cbi*/*cob* clusters, were not significantly induced under the growth conditions applied. The unknown genes lmo1171, lmo1172 and lmo1189 exhibited low or no transcription levels in exponential and stationary phase. The gene lmo1188 showed strong expression in exponential phase and a reduced expression during stationary phase under all three conditions (**Table 9**). The expression of the genes lmo1146, lmo1183 and lmo1190 was strongly increased during

growth with 1,2-PD and even more elevated by supplementation with cobalamin, suggesting that these gene might be involved in propanediol utilization or cobalamin biosynthesis (**Figure 24**).

For validation of the transcriptome data, qRT-PCR for the selected genes lmo1146, *pocR* (lmo1150), *pduC* (lmo1153), lmo1190 and *cbiA* (lmo1199) was conducted. The RTL for each condition in comparison to the NGS results are shown. The transcriptional activity obtained in the stationary phase of growth with BHI was set as 100 % for each gene (**Table 13**).

Table 13: Relative transcription in percent of the genes lmo1146, *pocR* (lmo1150), *pduC* (lmo1153), lmo1190 and *cbiH* (lmo1199) during growth in BHI with 10 mM 1,2-PD (BHI + 1,2-PD), in BHI with 10 mM 1,2-PD and 25 nM cobalamin (BHI + 1,2-PD + B_{12}), or in BHI.

Gene		Stationary Phase			Exponential Phase		
		BHI	BHI + 1,2-PD	BHI + 1,2-PD + B_{12}	BHI	BHI + 1,2-PD	BHI + 1,2-PD + B_{12}
lmo1146	**qRT-PCR**	100	1,845	6,664	250	454	578
	NGS	100	1,623	5,038	49	50	90
***pocR* (lmo1150)**	**qRT-PCR**	100	421	1,137	84	111	108
	NGS	100	261	566	21	1	48
***pduC* (lmo1153)**	**qRT-PCR**	100	9,078	148,856	51	101	205
	NGS	100	12,377	77,536	25	50	45
lmo1190	**qRT-PCR**	100	20,583	52,177	70	216	288
	NGS	100	2,874	7,905	2	75	45
***cbiH* (lmo1199)**	**qRT-PCR**	100	7,291	697	536	915	184
	NGS	100	8,724	486	3	50	45

NGS and qRT-PCR provided comparable results. RTL of all five tested genes were low during exponential phase and during stationary phase in BHI medium. Addition of 1,2-PD led to a slight induction of *pocR* (lmo1150) and a strong induction of lmo1146, *pduC* (lmo1153), lmo1190 and *cbiH* (lmo1199) transcription in stationary phase. Transcription of all genes except *cbiH* (lmo1199) was even more increased by the addition of cobalamin. Generally, transcriptional changes were more pronounced in qRT-PCR than in NGS experiments, although the same tendencies were observed.

Correlation analysis of $\log_2$ transformed RTL from NGS sequencing and qRT-PCR was performed (**Figure 26**). The calculated Pearson's correlation coefficient of 0.89 (p-value < 0.0001) indicates a high correlation between the results from both methods, thus validating the results from NGS for the whole *eut*/*pdu*/*cbi*/*cob* gene cluster.

The results of both the transcriptome analysis and the qRT-PCR are well in line with the observation that the addition of 1,2-PD and cobalamin to *L. monocytogenes* EGDe in MM led to a growth advantage when other nutrients had been used up (**Figure 24**).

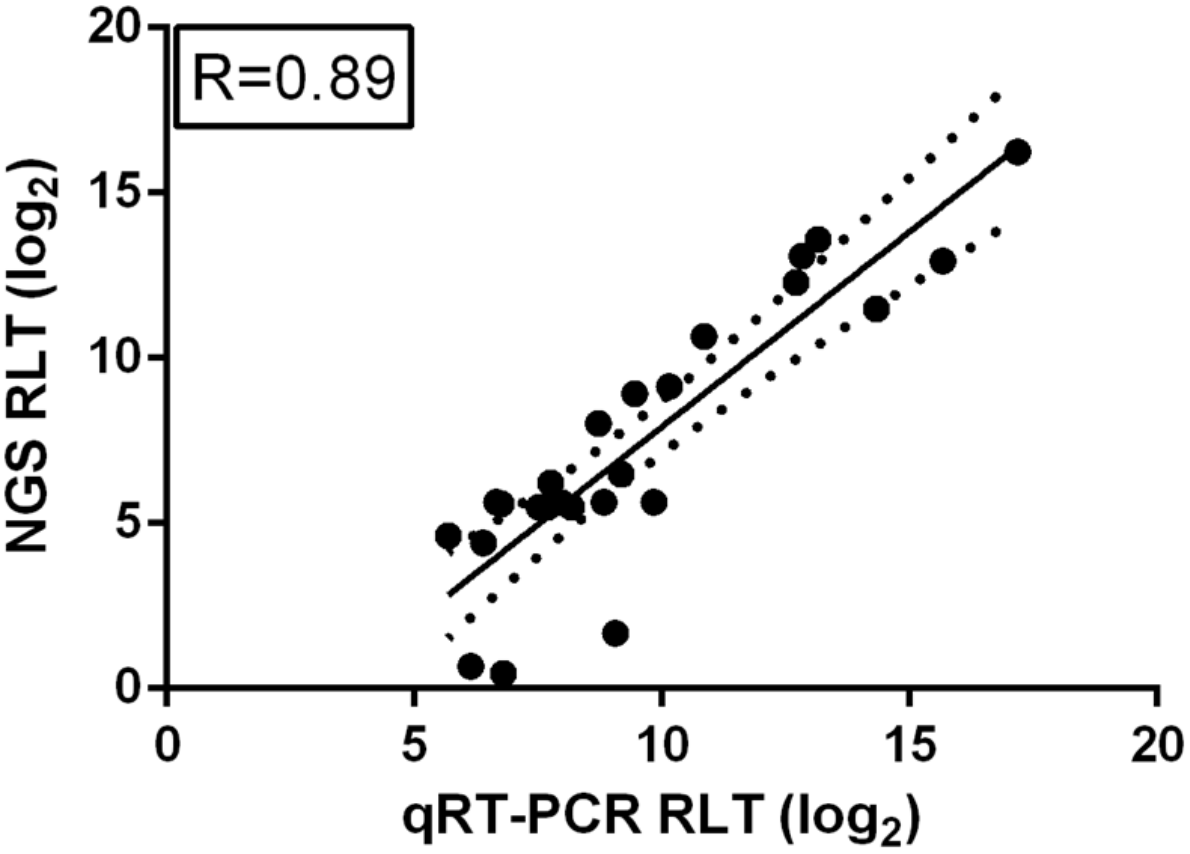

Figure 26: Correlation of log_2 RTL determined by qRT-PCR and NGS.
Log_2 transformed RTL of qRT-PCR (x-axis) and NGS (y-axis) for the selected genes lmo1146, lmo1150 (*pocR*), lmo1153 (*pduC*), lmo1190 and lmo1199 (*cbiH*) were plotted on a XY-graph (●).The Pearson's coefficient R was determined via correlation analysis. Linear regression was performed using the least square method. Solid lines depict the best fit lines and dashed lines indicate the 95% confidence bands.

3.6.3 Deletion of *pduD* leads to faster clearance in mice

It was hypothesized that the ability to metabolize 1,2-PD would enhance the ability of *L. monocytogenes* to compete with gut microbiota and to persist in the intestinal lumen following oral transmission. To test this, female BALB/c mice were co-infected with a 1:1 ratio of wild type EGDe and the isogenic Δ*pduD* mutant (total of 1×10^9 cfu/mouse), which were differentially tagged with antibiotic resistances. Stools were collected daily for up to 14 days p.i., and the total cfu numbers of strain per mg of feces were determined. As expected, a significant portion of the inoculum was shed in feces within 3 hours after feeding the mice, and the number of cfu detected 21 hours later had decreased considerably (**Figure 27 A**). At each time point after that, the average number of Δ*pduD* mutant bacteria recovered was less than the wildtype strain. By 10 days post-infection, the Δ*pduD* mutant had been cleared, but wildtype bacteria continued to be shed in the feces in at least some of the mice for up to 4 more days. Accordingly, the CI decreased steadily over the course of the experiment with a maximum difference on day 8 when the wild type bacteria outcompeted the mutant

bacteria by nearly 40-fold (**Figure 27 B**). Thus, the presence of the genes encoding the 1,2-PD utilization pathway prolonged the survival of *L. monocytogenes* EGDe in the mouse GIT.

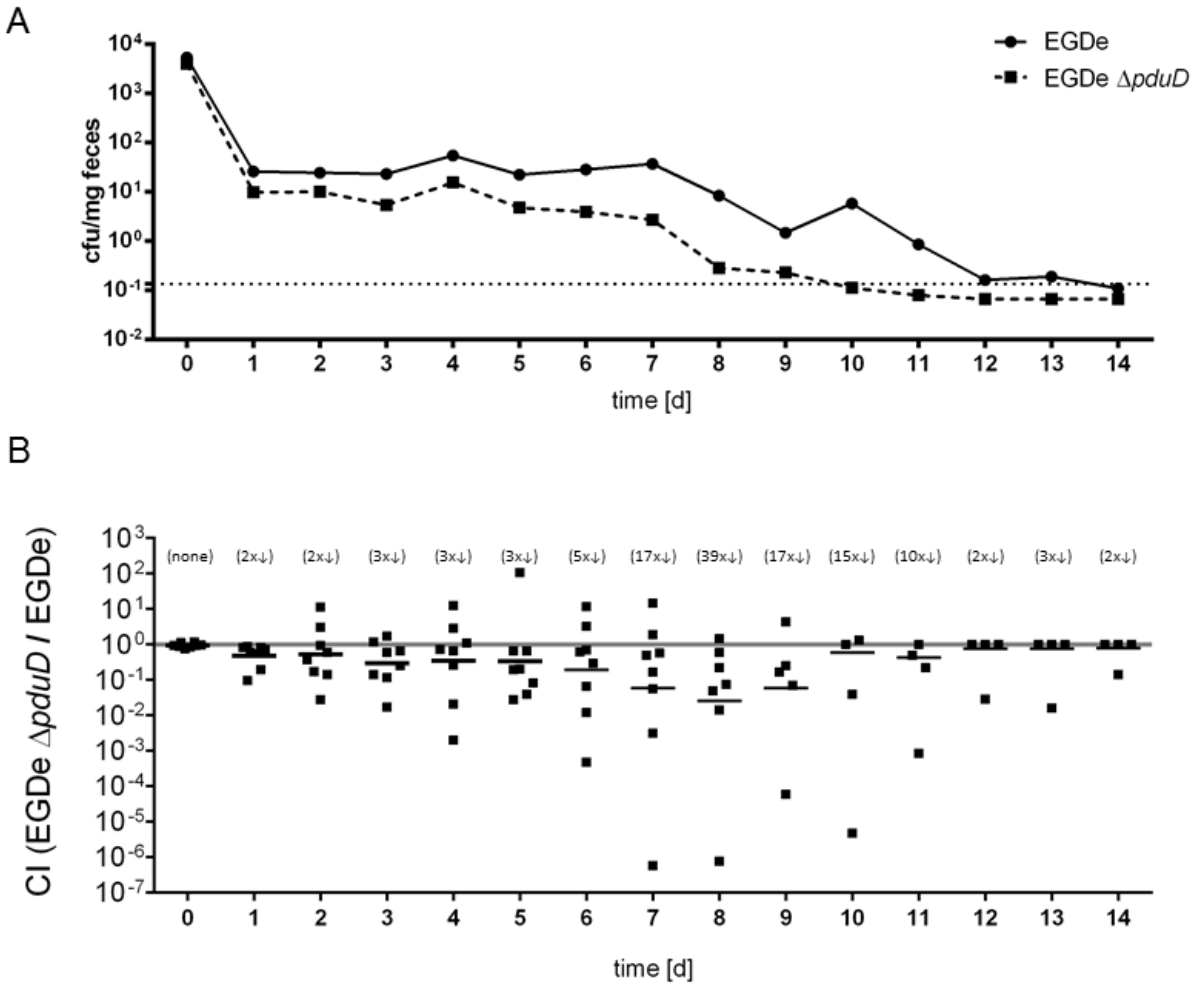

Figure 27: Deletion of *pduD* leads to faster clearance in BALB/c mice.
Female BALB/c mice were orally infected with a 1:1 ratio of *L. monocytogenes* EGDe and EGDe Δ*pduD* for a total inoculum of 1×10^9 cfu. Stool samples were collected 3 h p.i. as well as every 24 h up to 16 days and the mean value of cfu per mg feces was calculated (A). Symbols represent mean values from two separate experiments (n = 4 mice per group) for *L. monocytogenes* EGDe (circles) and EGDe Δ*pduD* (squares) and dashed line represents the limit of detection. Cfu values for samples without detectable bacteria were set as half the detection limit. (B) CIs depict the ratio of EGDe Δ*pduD*/EGDe. The geometric mean for each group was compared to the theoretical value of 1.0 and the fold change difference is indicated in parentheses.

4 Discussion

4.1 To be or not to be pathogenic: The evolution of virulence in the *Listeria sensu stricto* and *Listeria sensu lato*

The genus *Listeria* is divided into two distinct clades: The *Listeria sensu stricto* include the pathogenic species *L. monocytogenes* and *L. ivanovii* as well as the mostly apathogenic species *L. seeligeri*, *L. marthii*, *L. welshimeri* and *L. innocua*. During recent years, a quite extensive amount of novel environmental species has been discovered, which form the *Listeria sensu lato*: *L. rocourtiae, L. fleischmannii, L. floridensis, L. aquatica, L. cornellensis, L. grandensis, L. riparia, L. newyorkensis, L. booriae*, and *L. weihenstephanensis*. This clade also includes *L. grayi*, which was isolated in 1966 (reviewed in Orsi & Wiedmann, 2016).

A novel uncharacterized *Listeria* species was isolated from a wastewater plant in Northern Germany. In this thesis, *L. kieliensis* sp. nov. was sequenced and a phylogenetic tree was constructed for classification into the genus *Listeria*. The resulting tree showed the same subdivision of the genus *Listeria* into four distinct monophyletic clusters as derived by other groups via ANIb calculations before (Weller *et al.*, 2015; den Bakker *et al.*, 2014). These clusters have been proposed to represent separate genera: the six *Listeria sensu stricto* spp. (genus *Listeria*), and three genera in the *Listeria sensu lato* group, namely *L. grayi* (genus Murraya), *L. riparia*, *L. booriae*, *L. weihenstephanensis*, *L. rocourtiae*, *L. newyorkensis* and *L. cornellensis* (genus *Paenilisteria*), as well as *L. fleischmannii*, *L. floridensis*, and *L. aquatica* (genus *Mesolisteria*). This proposal (Stuart and Welshimer, 1974; Orsi & Wiedmann, 2016) still remains controversial (McLauchlin & Rees, 2009; Collins *et al.*, 1991; Rocourt *et al.*, 1992), mainly because cut-off values for genera are less well defined than for species (Qin *et al.*, 2014; Deloger *et al.*, 2009; Konstantinidis & Tiedje, 2005; Konstantinidis & Tiedje, 2007). *L. kieliensis* belongs to the *Listeria sensu lato* group and is most closely related to *L. floridensis*, *L. aquatica* and *L. fleischmannii* forming the newly proposed genus *Mesolisteria*. It is named after the mesophilic nature of its members since all three species have a temperature growth range of 22-42°C (den Bakker *et al.*, 2014; Bertsch *et al.*, 2013). *L. fleischmannii* was isolated from hard cheese in Switzerland in 2006 and grows well at 22°C – 42°C, while only very weak growth is observed at 4°C (Bertsch *et al.*, 2013). Both *L. floridensis* and *L. aquatica* have been isolated from running water in the United States and show no growth at 7°C or below, confirming their mesophilic nature (den Bakker *et al.*, 2014). *L. kieliensis* is also unable to grow at temperatures below 7°C (Jan Kabisch, personal communication), conforming the placement of this novel species into the *Mesolisteria*.

4.1.1 Two distinct clades in the genus *Listeria*: Differences in virulence and colonization properties

The evolution of virulence and the potential to cause disease in the *Listeria sensu stricto* has been the subject of several studies (Buchrieser *et al.*, 2003, Glaser *et al.*, 2001; Hain *et al.*, 2006a; Hain *et al.*, 2006b; den Bakker *et al.*, 2010a; den Bakker *et al.*, 2010b). Additionally, there are numerous reports for the isolation of not only *L. monocytogenes* but all other *Listeria sensu stricto* members from feces or GITs of mostly symptom-free animals (Antoniollo *et al.*, 2003; Rocourt & Seeliger, 1985; Inoue *et al.*, 1991; Husu 1990; Skovgaard *et al.*, 1988; Lawan *et al.*, 2013) and from food of animal origin (Farber *et al.*, 1989; Osaili *et al.*, 2011; Soriano *et al.*, 2001; Huang *et al.*, 2007; Gebretsadik *et al.*, 2011; Nayak *et al.*, 2015; Dahshan *et al.*, 2016). In contrast, information about the potential of *Listeria sensu lato* members to colonize the GIT or to cause invasive disease is missing. No controlled oral infection experiments for colonization of the animal GIT by *Listeria* spp. have been conducted so far.

In this thesis, a recently published oral infection model was applied using *Listeria*-contaminated bread pieces for infection (Bou Ghanem *et al.*, 2013a). This natural feeding method is advantageous over oral gavage since i.g. inoculation can cause minor physical trauma to the esophagus which may lead to direct bloodstream invasion of the pathogen. This has caused a discrepancy in prior i.g. inoculation studies in mice regarding the duration of the GI phase as well as reproducibility, likely due to inconsistencies in injection technique among investigators (D'Orazio, 2014). Since the oral model has a defined stage of GI infection before systemic spread of the pathogen (Bou Ghanem *et al.*, 2012), it is an ideal tool to study the colonization properties of *Listeria* spp.

As expected, *L. monocytogenes* was readily able to colonize the lumen of both the ileum and colon of mice. Cfu numbers were about 10-fold higher in the colon than the ileum, suggesting the colon is the primary site of colonization. This observation has been reported before (Bou Ghanem *et al.*, 2013a; Becattini *et al.*, 2017; Havell *et al.*, 1999). In contrast, although all infected mice were still colonized, *L. welshimeri* exhibited significantly lower numbers in the intestinal lumen compared to *L. monocytogenes*. Despite the already mentioned reports about the isolation of *Listeria sensu stricto* from food or feces, there is only one *in vivo* study analyzing oral infection by species other than *L. monocytogenes*. Inoculation of BALB/c mice with *L. innocua* led to colonization of the GIT, and similar bacterial loads compared to *L. monocytogenes* were observed (Lammdering *et al.*, 1992). However, gnotobiotic pregnant mice were used in that study. Unlike the BALB/c mice that were used in this thesis, these mice lack a diverse and protective intestinal microbiota, which might have facilitated colonization by *L. innocua.*

L. monocytogenes was able to invade the tissue of both the ileum and colon and to cause systemic infection, while *L. welshimeri* on the other hand did not cross the intestinal barrier. The evolution of

virulence in the *Listeria sensu stricto* spp. has been studied extensively (den Bakker *et al.*, 2010a; den Bakker *et al.*, 2010b; Schmid *et al.*, 2005; Hain *et al.*, 2006a; Hain *et al.*, 2006b; Hain *et al.*, 2007; Hain *et al.*, 2012; Buchrieser *et al.*, 2011). The genomes of the two pathogenic members are characterized by the presence of two major pathogenicity islands (Vázquez-Boland *et al.*, 2001a). The most well characterized and important virulence traits are encoded on the LIPI-1, which consists of a gene encoding for the virulence regulatory factor PfrA as well as six other genes (*plcA, hly, mpl, actA, plcB*, lmo0206) that are important for intracellular survival and inter- and intracellular motility (Vázquez-Boland *et al.*, 2001b). The second important locus is the pathogenicity cluster *inlAB*. The internalins InlA and InlB are essential for invasion of host cells *in vitro* and *in vivo* (Gaillard *et al.*, 1991; Gaillard *et al.*, 1996a). It is generally accepted that the MRCA of the *Listeria sensu stricto*, which can be dated to about 40 to 60 million years ago, possessed these two pathogenicity islands (Schmid *et al.*, 2005; den Bakker *et al.*, 2010b). The two genomic loci were then lost in several separate events during the evolution of the clade, yielding (i) the two pathogenic species *L. monocytogenes* and *L. ivanovii* with fully functional LIPI-1 and *inlAB* clusters, (ii) species in which the presence of these clusters and therefore also the virulence potential varies by strain, namely *L. innocua* and *L. seeligeri,* (iii) as well as the non-pathogenic species *L. marthii* and *L. welshimeri*, which lost both loci (den Bakker *et al.*, 2010b)

The virulence of *Listeria* spp. is usually assessed using four different *in vitro* and *in vivo* methods: Hemolysis is tested on blood or CAMP agar, and *L. welshimeri* proved to be non-hemolytic (Rocourt & Grimont, 1983). Caco-2 cells are used for evaluation of invasion and intracellular replication capabilities (Gaillard *et al.*, 1987). Only *L. monocytogenes* and *L. ivanovii* as well as some hemolytic *L. innocua* strains were shown to invade mammalian epithelial cells, while *L. welshimeri* and the other *Listeria sensu stricto* members failed to cause internalization due to missing *inlAB* and LIPI-1 genes (Gaillard *et al.*, 1987; Pine *et al.*, 1991; den Bakker *et al.*, 2010b). *In vivo* infection experiments in chicken embryos or mice via i.v. or i.p. injection further validated classification of *L. welshimeri*, *L. innocua* and *L. seeligeri* as avirulent species since they are cleared rapidly and are not able to multiply in spleen and liver (Mainou-Fowler *et al.*, 1988; Terplan & Steinmeyer, 1989; Notermans *et al.*, 1991; Lattmann *et al.*, 1989; Menudier *et al.*, 1991; Hof & Hefner, 1988; Klug & Hof, 1986).

The results from the oral infection experiments as well as numerous reports from literature suggest that *L. welshimeri* is a non-pathogenic species, which is not able to cross the intestinal barrier. Nevertheless, it can at least transiently colonize the GIT of mammals.

Since the members of the *Listeria sensu lato* group have only been discovered recently, reports for the occurrence of these species in the context of food or the animal/human host as well as their virulence potential are missing. To fill in the missing gaps in the knowledge about *Listeria sensu lato*, oral infection experiments in mice were conducted to test colonization abilities.

While mice exhibited high numbers of *L. monocytogenes* and were still persistently colonized by *L. welshimeri*, the two *Listeria sensu lato* spp. *L. aquatica* and *L. booriae* exhibited lower mean values of bacterial cfu in the ileum and colon. About half the mice were already devoid of *Listeria sensu lato*, suggesting that two days p.i. these species are already in the process of getting cleared from the intestines. This clearance was also apparent in the stool of mice, which was tracked over the course of two days. Since the *Listeria sensu lato* spp. have been discovered recently, only one publication mentions the presence of these species in fecal samples of animals. 341 intestinal fecal samples from the cecum and colon of wild rodents in China were analyzed. While the *Listeria sensu stricto* members *L. monocytogenes*, *L. ivanovii* and *L. innocua* were found in a total of 25 samples, *Listeria sensu lato* spp. were found in only three samples, namely *L. fleischmannii* and *L. floridensis* (Wang *et al.*, 2017). Both species are closely related to the examined *L. aquatica* and may point to a minor capability of the *Mesolisteria* in colonizing the GIT.

L. booriae and *L. aquatica* were not able to cross the gut mucosa during oral infection experiments in this thesis. While virulence of *Listeria sensu stricto* spp. has been assessed using different *in vitro* and *in vivo* methods in the past, data for virulence of *Listeria sensu lato* is mostly missing. The absence of both LIPI-1 and *inlAB* is a commonality of all *Listeria sensu lato* spp. and is used to distinguish them from the *Listeria sensu stricto* which at least partly possess these virulence traits. It is the major argument for the classification of the *Listeria sensu lato* as non-pathogenic bacteria. Subsequently, these species are all non-hemolytic as proven by blood agar or CAMP test since they are missing the gene *hly* encoding for the Listeriolysin O (LLO), which is responsible for ß hemolysis in *L. monocytogenes* (Gaillard *et al.*, 1986; Mengaud *et al.*, 1987; Cossart, 1988). The only *Listeria sensu lato* species which has been tested for other virulence properties than hemolysis is *L. fleischmannii*. Caco-2 invasion assays revealed a very low invasiveness, indicating that this species is not able to invade human epithelial cells (Bertsch *et al.*, 2013). Therefore, the absence of *inlAB* and LIPI-1 prevented tissue invasion of *L. booriae* and *L. aquatica* in mice in this thesis.

Beside these classical virulence genes, *L. monocytogenes* also contains a large set of additional genes for pathogenicity and extensive example lists for known virulence genes can be found in literature (Camejo *et al.*, 2009; den Bakker *et al.*, 2010b). However, invasion of host cells, intracellular survival and replication, systemic spread to organs like the liver, spleen and brain and subsequent tissue damage are only part of the virulence arsenal of *L. monocytogenes*. To be fully pathogenic, the bacterium needs to be able to survive under stressful conditions in the GIT and establish an ecological niche during the so-called GI phase of infection. This process is called “colonization” as opposed to “virulence”. Virulence is generally defined as the ability of bacteria to cause disease in a host by invasion of tissues and induction of damage. In contrast, colonization is part of or a prerequisite for

the infection process and defined as the presence of microorganisms at a particular site, e.g. the GIT, without causing disease. Stress resistance, motility, adhesion and metabolic genes are typical examples of colonization genes.

Since *L. aquatica* and *L. booriae* exhibited a minimum ability to colonize the murine GIT and since they were not able to invade the gut mucosa, the pathogenicity and colonization potential of another *Listeria sensu lato* species *L. kieliensis* sp. nov. was analyzed. To do this, the genomic sequences of *L. kieliensis* was scanned for the presence of known virulence and colonization genes from *L. monocytogenes.* Additionally, the conservation of these genes in the *other Listeria sensu lato* was checked to explain the insufficient colonization properties of *L. aquatica* and *L. booriae*. As expected, both LIPI-1 and *inlAB* are absent in *L. kieliensis*, a fact that was reported for all other *Listeria sensu lato* spp. before (Bertsch *et al.*, 2013; den Bakker *et al.*, 2013; den Bakker *et al.*, 2014; Lang Halter *et al.*, 2013; Leclercq *et al.*, 2010; Weller *et al.*, 2015). Consequentially, hemolysis test of the novel species provided negative results (Jan Kabisch, personal communication). All in all, *L. kieliensis* seems to be missing all 25 major internalins of *L. monocytogenes* EGDe. To be able to survive both in the food environment and during the passage of the GIT, *L. monocytogenes* possesses several genes to withstand a plethora of stresses including low pH values, high osmolarity and bile acids (Gahan & Hill, 2005; Gahan & Hill, 2014). The survival under acidic conditions is of special importance since the pathogen must passage the stomach after oral ingestion. Therefore, *L. monocytogenes* encodes the ADI and AgDI systems which confer resistance to acidic environments and are required for full virulence *in vivo* (Ryan *et al.*, 2009; Chen *et al.*, 2011). The corresponding genes lmo0036-0043 are missing in a number of *Listeria sensu lato* spp. but are present in *L. kieliensis*, *L. aquatica*, *L. floridensis* and *L. grayi*. Other genes for stress survival however, are (partly) missing in *L. kieliensis* These include the GAD system consisting of a glutamate antiporter (GadT1, GadT2) and a glutamate decarboxylase (GadD1, GadD2, GadD3) which protect *L. monocytogenes* against low pH conditions and allow for survival in gastric fluid (Cotter *et al.*, 2001a; Cotter *et al.*, 2001b; Cotter *et al.*, 2005). The corresponding genes lmo0447-0448, lmo2362-2363 and lmo2434 are weakly conserved or missing in *L. kieliensis* and *L. aquatica*, while other *Listeria sensu lato* members show varying degrees of conservation of the *gadD* and *gadT* genes. Lmo0447-0448 are part of a five-gene stress survival islet (SSI-1) responsible for survival of *L. monocytogenes* under low pH and high salt concentration (Ryan *et al.*, 2010), which is partly absent or only weakly conserved in a number of *Listeria sensu lato* spp. including *L. kieliensis.* This islet contains the gene *pva* (lmo0446) which is important for penicillin resistance (Begley *et al.*, 2005b). To inhibit bacterial overgrowth in the gut, the liver produces bile salts, which are stored in the gall bladder and released into the GIT upon food intake. These act as antimicrobial substances which need to be counteracted by pathogens to survive (Hofmann & Eckmann, 2006; Hay & Zhu, 2016; Begley *et al.*, 2005a). *L. monocytogenes* possesses several systems for protection against bile: *Bsh* (lmo2067),

bltB (lmo0754) and *bilE* (lmo1421-1422) are necessary for *in vitro* growth in sublethal or lethal bile concentrations and were proven to be involved in virulence in mice and guinea pigs after oral and i.p. infection (Begley *et al.*, 2005b; Dussurget *et al.*, 2002; Sleator *et al.*, 2005). While *bilE* is conserved in all *Listeria sensu lato* including *L. kieliensis*, *bsh* and *bltB* are weakly conserved or missing in these species. *L. monocytogenes* encounters stressful environmental conditions due to high osmolarity inside and outside the host. To overcome this osmotic stress, it accumulates compatible solutes inside the cytosol, which are small molecules like betaine or carnitine acting as osmoprotectants. Several uptake systems are encoded in its genome. The carnitine and betaine transport systems OpuA/Gbu (encoded by lmo1014-1016), OpuC (encoded by lmo1425-1428) and BetL (encoded by lmo2092) (Ko & Smith, 1999; Fraser *et al.*, 2000; Sleator *et al.*, 2001; Wemekamp-Kamphuis *et al.*, 2002; Mendum & Smith, 2002) are well conserved in *L. kieliensis* as well as many other *Listeria sensu lato* spp. All in all, *L. kieliensis* clearly seems to be a non-pathogenic species. As it is missing vital genes for survival under GI conditions, it might also be improperly adapted for colonization. Similar conclusions can be drawn for the other *Listeria sensu lato* spp.

4.1.2 *Listeria sensu stricto* specific genes might represent candidate genes for virulence and colonization

It was hypothesized that genetic determinants that are present in the *Listeria sensu stricto* but absent in the *Listeria sensu lato* promote growth or survival in the mammalian GIT, since the latter group seems to be less adapted to the intestinal environment. This is in line with a recent study on the dynamics of genome evolution in the *Listeria sensu lato* and *Listeria sensu stricto*. It was shown that the common ancestor of the latter clade acquired a large genomic cluster for flagellar biosynthesis as well as clusters for cobalamin biosynthesis and 1,2-PD and ethanolamine utilization. These genomic loci have been discussed to be involved in pathogenesis (Chiara *et al.*, 2015). Therefore, a genome comparison between the two clades was conducted to identify as yet unknown genes associated with gut colonization and infection. The resulting list of 151 genes, which are present in *Listeria sensu stricto* and absent or significantly divergent in *Listeria sensu lato*, contains several genes with experimental evidence to play a role in the mentioned processes.

Among these, the before mentioned clusters for flagellar biosynthesis and cobalamin-dependent catabolism of 1,2-PD and ethanolamine are present, acknowledging the results from Chiara *et al.*, who already described the gain of these clusters as an evolutionary event that contributed to the taxonomic definition of the *Listeria sensu stricto* (Chiara *et al.*, 2015; Orsi & Wiedmann, 2016). *S.* Typhimurium possesses a homologous genomic region of the catabolic clusters, which has been demonstrated to play a role in its proliferation *in vitro* and *in vivo* (Winter *et al.*, 2010; Srikumar & Fuchs, 2011; Faber *et al.*, 2017). The ethanolamine cluster has been investigated for its contribution to virulence in *L. monocytogenes* (Mellin *et al.*, 2014), whereas no such experimental data have been available for the

1,2-PD cluster. The importance of 1,2-PD utilization was investigated in section 3.5 Characterization of the gene clusters for biosynthesis of cobalamin and degradation of 1,2-PD. The other large coherent set of genes missing in the *Listeria sensu lato* spp. encodes for flagellar genes (lmo0675-lmo0718). This cluster for the flagellar biosynthetic pathway has most likely been acquired in a common ancestor of the *Listeria sensu stricto* and *L. grayi* from an ancestor of the *Bacillus cereus* complex via horizontal gene transfer (Chiara *et al.*, 2015). The acquisition of this cluster could have possibly played a role in the evolution of virulence in the *Listeria sensu stricto* clade since motility is well known to contribute to successful infection by *L. monocytogenes* (Bigot *et al.*, 2005; Gründling *et al.*, 2004; Dons *et al.*, 2004; Bergmann *et al.*, 2013; Schauer *et al.*, 2010; Knudsen *et al.*, 2004; Shen & Higgins, 2006). All *Listeria sensu lato* members (except *L. grayi*) are characterized as non-motile in laboratory experiments while the *Listeria sensu stricto* group exhibits flagellar motility (Orsi & Wiedmann, 2016). Two factors involved in peptidoglycan biosynthesis, lmo0703 and lmo0717, are also located in the genomic region of the flagellar cluster. These genes as well as lmo0723-0724 and lmo1699, which encode for chemotaxis proteins, are regulated by MogR and DegU (Williams *et al.*, 2005; Shen & Higgins 2006; Knudsen *et al.*, 2004; Gründling *et al.*, 2004), indicating that these genes might also be involved in motility. Other candidate genes are involved in cell wall and membrane biogenesis, transport processes, transcription, and signaling. Sortase B (lmo2181) is one of two transamidases linking proteins to the peptidoglycan of *L. monocytogenes*. While sortase A anchors the internalin InlA to the bacterial surface and its deletion leads to attenuated virulence (Garandeau *et al.*, 2002; Bierne *et al.*, 2002), a sortase B mutation does not influence virulence in mice or cell-culture (Bierne *et al.*, 2004). Nevertheless, sortase B is responsible for anchorage of SvpA (lmo2185) and lmo2186, encoded by two other candidate genes derived from genome comparison with putative haemin transport capacity (Newton *et al.*, 2005; Xiao *et al.*, 2011). While Borezee and colleagues showed decreased virulence after i.v. infection of mice and reduced escape from phagosome of macrophages (Borezee *et al.*, 2001), another group was able to show attenuated virulence of *srtB-svpA* mutants in an i.v. mouse model, but did report reduced crossing of the intestinal barrier after oral infection (Newton *et al.*, 2005). An ATP synthase encoded by lmo0090-lmo0093 is known to play a role in intracellular survival (Schauer *et al.*, 2010). PdeD (lmo0111) is a EAL domain protein with phosphodiesterase activity and plays a role in c-di-GMP signaling pathways, which have been shown to influence virulence in *L. monocytogenes*. Deletion of *pdeD* and two other phosphodiesterases encoding genes *pdeB* (lmo0131) and *pdeC* (lmo1914), both of which are also poorly conserved in *Listeria sensu lato* but just barely missed the 40 % homology cut-off, led to decreased invasiveness in enterocytes and lower infection numbers in the liver and spleen of orally-infected mice (Chen *et al.*, 2014).

4.1.3 Conclusion

This thesis represents the first study to compare colonization abilities and pathogenicity potential of *Listeria* spp. after oral infection in a controlled experiment. The knowledge gained will help to improve our understanding of virulence in the genus *Listeria*. Based on the obtained results, a comprehensive genome comparison between the two listerial clades with the specific goal of identifying yet unknown virulence and colonization genes was conducted for the first time. The literature research validated the approach of using comparative genome analyses since several already known pathogenicity genes were identified. Therefore, so far unknown candidate genes were selected for further functional characterization *in vivo* and *in vitro*. A putative ABC transporter lmo1131-1132 and the 1,2-PD utilization genes were analyzed in detail.

4.2 The role of lmo1131-1132 in virulence and colonization

Operon lmo1131-1132 encodes for a putative ABC transporter, that has been characterized *in vitro* and *in vivo* to study its role during intestinal colonization and virulence. Both genes exhibited increased expression at 37°C compared to environmental temperatures (Elena Ferrari, personal communication) indicating a possible role during infection. Additionally, 11.6 % of predicted genes in *L. monocytogenes* encode for transporter systems. Together with a large set of regulatory proteins, these transport proteins have been implicated to contribute to the adaptability of the pathogen to a wide range of environments including the GIT (Glaser *et al.*, 2001; Hain *et al.*, 2006b).

4.2.1 Potential function as an ABC export protein

A typical prokaryotic ABC transporter is composed of two hydrophobic TMD and two water soluble NBD at the cytosolic side of the cell membrane. ABC transporters can be composed of four separate polypeptides or two identical NBDs and/or TMDs can be present. NBDs and TMDs can also be fused together, thus making up either the complete transporter from a single polypeptide or from two homo- or heterodimeric polypeptides (Wilkens, 2015). The two main classes of ABC transporters are importers and exporters. Importers mediate the uptake of nutrients, including carbohydrates (Schneider, 2001), amino acids (Hosie & Poole, 2001), peptides (Detmers *et al.*, 2001) as well as iron and other metal ions (Köster, 2001; Claverys, 2001). Almost all importers are multimeric complexes composed of two TMDs and two NBDs as independent polypeptide chains (Davidson *et al.*, 2008). In addition, they almost always encode an additional extracellular SBP, which is either a soluble, lipid-anchored or membrane-associated protein with a high affinity for the respective substrate (Wilkens *et al.*, 2015). Exporters secrete various compounds like peptides, lipids, hydrophobic drugs, polysaccharides, and proteins, including toxins such as hemolysin (Davidson *et al.*, 2008).

Protein BLAST analyses revealed common structural motifs of ABC transporter systems for Lmo1131 and Lmo1132. The C-terminus of each protein contains a Walker A and Walker B motif as well as a

Q-loop, Switch H-loop and the signature motif, which are characteristic of the NBD of ABC transporters. The N-terminus includes a TMD with six transmembrane helices, thus making up "half-size" transporters, which eventually form a heterodimeric full-size transporter. This composition is a typical feature of exporters (Davidson *et al.*, 2008). Since no putative SBP was found in proximity of the genomic region of the operon, it can be assumed that lmo1131-1132 encodes for an ABC transporter with export function.

Protein blast was performed to identify possible homologues of Lmo1131-1132. Homologous proteins included uncharacterized ABC transporters of *Enterococcus* spp. Enterococci are Gram-positive bacteria of the phylum Firmicutes and belong to the same order as *Listeria*, the Bacilli. They include two common commensal bacteria, *E. faecalis* and *E. faecium*, but also the species *E. casseliflavus*, *E. gallinarum*, and *E. raffinosus*. Several multi-drug resistant, opportunistically pathogenic *Enterococcus* species have emerged over the years and pose a serious health threat (Ike, 2017). Furthermore, weak homologies to cysteine ABC transport, ATP-binding/permease CydD or thiol reductant ABC exporter subunit CydC proteins were identified. These homologues mostly belong to species from the order Clostridiales, e.g. the genus *Roseburia*, which includes butyrate-producing anaerobic bacteria colonizing the human colon (Tamanai-Shacoori *et al.*, 2017) or the genus *Clostridium*, which consists of several commensal species but also includes known enteropathogens like *Clostridium difficile* (Lopetuso *et al.*, 2013). Homologous proteins were also encoded by species from the family Ruminococcaceae, which can be found in the colon of herbivores and humans (Flint *et al.*, 2012). Since all these species are part of the intestinal microbiota, a function of the ABC transporter related to colonization of the gut seems possible.

The two proteins CydC and CydD have been studied in *E. coli* and *B. subtilis* (Poole *et al.*, 1993; Poole *et al.*, 1994; Winstedt *et al.*, 1998), but information from other species is missing. Each *E. coli* protein CydC and CydD possesses a C-terminal NBD and N-terminal TMD and together they form a heterodimeric transporter (Poole *et al.*, 1993), analogous to the structure of the ABC transporter presented here. It was shown that the CydDC transport system is required for the biosynthesis of the cytochrome bd-type quinol oxidase CydAB, which functions as a terminal electron acceptor in *E. coli*., It is likely that CydDC is responsible for the transport of heme across the cytoplasmic membrane into the periplasm of Gram-negative bacteria (Poole *et al.*, 1994). Recent studies suggest an export function of cysteine and/or glutathione, two important substances for redox control (Pittmann *et al.*, 2002; Pittmann *et al.*, 2005; Yamashita *et al.*, 2015; Shepherd, 2015). *L. monocytogenes* harbors two terminal oxidases, a cytochrome bd-type (CydAB) and a cytochrome menaquinol aa3-type (QoxAB) oxidase, which are required for respiration at different oxygen concentrations. The importance of CydAB in intracellular replication and of both CydAB and QoxAB after oral inoculation of mice has been proven

(Corbett *et al.*, 2017). *L. monocytogenes* possesses a CydDC ABC transporter that is encoded by the genes lmo2715 and lmo2716. The amino acid sequences of these two genes showed far weaker homologies to the sequences of Lmo1131 and Lmo1132 than to CydC and CyD proteins of *B. subtilis*. This indicates that Lmo2715-2716, and not Lmo1131-1132, is involved in cytochrome bd-type oxidase synthesis in *L. monocytogenes*. Potentially, a function of the latter in the export of cysteine or glutathione is conceivable. Lmo1132 also exhibited specific hits to MdlB ABC-type multidrug transport system domains. Lmo1131-1132 export function might include the efflux of antimicrobial substances, which is a common feature for this particular type of protein (Allikmets *et al.*, 1993; Chen *et al.*, 2007).

4.2.2 The role of lmo1131-1132 during adhesion and invasion of host cells

In this thesis, Caco-2 cells were used to assess adhesion and invasion capabilities of *L. monocytogenes* strains in cell culture. Caco-2 cells are human colon carcinoma cells and have been frequently used to study adhesion to and entry into non-phagocytic cells, e.g. the importance of InlA and InlB for these processes (Gaillard *et al.*, 1991; Gaillard *et al.*, 1996; Gaillard & Finlay, 1996; Dramsi *et al.*, 1997; Jaradat & Bhunia, 2003; Werbrouck *et al.*, 2006; Burkholder & Bhunia, 2010; Pizarro-Cerda *et al.*, 2012). Deletion of the operon lmo1131-1132 led to reduced adhesion to Caco-2 cells compared to the parental strain, however, adherence to HEp-2 cells remained unchanged. HEp-2 cells are human epithelial cells from the larynx, which have also been used to study adhesion of *L. monocytogenes* in the past (Milohanic *et al.*, 2001; Dramsi *et al.*, 1997; Pizarro-Cerda *et al.*, 2012). Thus, the reduced adhesion of *L. monocytogenes* EGDe Δlmo1131-1132 to Caco-2, but not HEp-2, cells might point to a specific role of the ABC transporter during adhesion to colonic epithelial cells. The single deletion mutants *L. monocytogenes* EGDe Δlmo1131 and EGDe Δlmo1132 were created to analyze the contribution of each protein to the phenotype observed in Caco-2 adhesion assays. Interestingly, deletion of a single gene from the operon led to a smaller decrease in adhesion than the deletion of the complete operon. Increase of the incubation period during adhesion assays caused complete restoration of the wildtype phenotype in EGDe Δlmo1131 and EGDe Δlmo1132 cells. This indicates that the deletion of one gene from the ABC transporter operon can be compensated over time. The implications of this observation for a possible function of the transport system are unclear.

Gentamycin protection assays were performed to assess the number of intracellular listeriae. Invasion of Caco-2 cells, but not intracellular replication, was significantly reduced in the EGDe Δlmo1131-1132 strain. Again, entry into HEp-2 cells were not influenced, pointing to a specific role of the transporter in the interaction with colonic cells. Deletion of a single gene from the operon did not affect invasion of Caco-2 cells. The invasion defect of EGDe Δlmo1131-1132 was not caused by the reduced numbers of adhering bacterial cells, since the percentage of adherent cells, which were able to invade the host cells, was significantly smaller in comparison to the parental strain. Not only does the deletion of

lmo1131-1132 cause impaired adhesion, the listerial cells that do adhere fail to mediate efficient uptake into the host cell. In contrast, the intracellular growth rates were not affected by the absence of the operon. Thus, the ABC transporter does not seem to be involved in bacterial replication in the cytosol but rather in the specific interaction with the cytoplasmic membrane of the host cell leading to internalization and/or in the escape from the vacuole.

ABC transporters facilitate the uptake of nutrients by several pathogenic species and have been frequently associated with virulence in animal models (Polissi *et al.*, 1998; Coulter *et al.*, 1998; Darwin & Miller, 1999; Karlyshev *et al.*, 2001), however, bacterial transporters that mediate host cell adhesion are rare. Transposon mutants of *Agrobacterium tumefaciens* were unable to adhere to plant cells, and interestingly, the mutated proteins showed homologies to ABC transport systems of Gram-negative bacteria (Matthysse *et al.*, 1999). Similarly, a *Streptococcus* deletion mutant lacking a glutamine transporter was unable to bind fibronectin and exhibited decreased adherence and invasion capabilities in cell culture assays of epithelial cells (Tamura *et al.*, 2002). In *L. monocytogenes*, the protein CtaP is the SBP of a cysteine ABC importer, and its deletion caused reduced adherence to host cells (Xayarath *et al.*, 2009), although this phenotype was not directly caused by an ABC transporter. Additionally, the respective operon lmo0135-0137 was shown to be attenuated in Caco-2 cells and in the liver and spleen of i.v.-infected mice (Schauer *et al.*, 2010).

4.2.3 Interdependence between ABC transporter function and environmental parameters

In order to adapt to different environments and to make the transition from a saprophytic to a pathogenic lifestyle, *L. monocytogenes* must modify gene expression in response to environmental changes including temperature, osmolarity, availability of nutrients, pH and oxygen levels (Müller-Herbst *et al.*, 2014; Sue *et al.*, 2004; Mekalanos, 1992; Weme-Kamphuis *et al.*, 2004; Becker *et al.*, 2000). Therefore, transcription of the genes lmo1131 and lmo1132 under different growth conditions was analyzed using qRT-PCR.

Increased transcription levels for lmo1131-1132 were observed at 37°C compared to 24°C. This result was significant because upon entry of the host via the oral route, *L. monocytogenes* encounters elevated temperatures due to the body temperature of the host. This represents one of the most important environmental cues for pathogenicity. Transcriptomic and proteomic analyses have indicated that the main virulence genes of *L. monocytogenes* including the LIPI-1, the internalins *inlAB* as well as numerous other genes, are directly or indirectly regulated by the PrfA protein (Milohanic *et al.*, 2003; Marr *et al.*, 2006; Port & Freitag, 2007). Maximal expression of these virulence genes is observed at 37°C. The 5’ UTR of *prfA* mRNA contains a thermoswitch that posttranscriptionally prevents translation at temperatures below 30°C (Johansson *et al.*, 2002). Regulation of lmo1131-1132

via PrfA has not been shown so far, but increased transcription at 37°C hints to the relevance of the operon during the infection process.

RTL of lmo1131-1132 were determined in *L. monocytogenes* cells grown with and without oxygen at 37°C and 24°C. Under anaerobic conditions, a strong decrease of transcription was observed at both temperatures. Oxygen is known the serve as a signal for enteropathogens during colonization (Marteyn *et al.*, 2011). Hypoxic conditions in the distal part of the GIT not only trigger the switch to anaerobic metabolism but also influence virulence properties and the expression of stress resistance genes in *L. monocytogenes*. Bo Andersen and colleagues compared bacteria cultivated with and without oxygen restriction and observed increased infection of Caco-2 cells as well as enhanced virulence in orally-infected guinea pigs for anaerobically grown bacteria (Bo Andersen *et al.*, 2007). Anaerobic growth of *L. monocytogenes* also increased invasion of human colonic epithelial cells and murine macrophages in another study, although intracellular replication was decreased, which was explained by decreased production of LLO (Wallace *et al.*, 2017). Improved bile resistance at low oxygen concentrations was also shown, which might be ascribed to the increased activity of BSH under these conditions (Wright *et al.*, 2016; Dussurget *et al.*, 2002). These findings point to increased colonization and virulence properties under anaerobic conditions. In contrast, decreased transcriptional levels of lmo1131-1132 were detected under anaerobic conditions in this thesis.

Although the lumen of the GIT is mainly anaerobic, a small zone of relative oxygenation exists near epithelial cells in the mucosa. This is caused by oxygen diffusion from the capillary network inside the intestinal villi (Marteyn *et al.*, 2011). The resulting oxygen gradient might serve as an attractant for enteropathogens. The intracellular pathogen *Shigella flexneri* exhibits precise modulation of virulence gene expression depending on oxygen availability. In the oxygen-deprived intestinal lumen, Fnr-dependent formation of surface needles for adhesion and invasion are formed, thus priming the cell for invasion. Under these conditions, secretion of Type III secretion system effectors is inhibited. Upon approaching the mucosal surface, effector secretion is activated, which mediates the entry into epithelial cells (Marteyn *et al.*, 2010). Since lmo1131-1132 seems to be important for adhesion and invasion, transcriptional upregulation of lmo1131-1132 under aerobic conditions encountered at the mucosal surface seems reasonable to prime *L. monocytogenes* for initial adhesion and invasion of host cells. Although the cytosol has a high oxygen tension, increased transcription of the operon under aerobic conditions does not seem to play a role during replication in this host compartment since the deletion mutant and EGDe exhibited similar intracellular growth rates in Caco-2 cells.

A potential Fur-box was discovered in the promoter region of lmo1131 (Shao, 2007). Fur is the main regulatory protein for iron homeostasis in most bacteria (Andrews *et al.*, 2003). Fur is complexed by iron under iron-sufficient conditions and binds a consensus nucleotide sequence called Fur-Box, that

is present in the promotor region of target genes causing transcriptional repression (Bsat *et al.*, 1998, Escolar *et al.*, 1999). Fur is also present in *L. monocytogenes,* where it acts in an analogous way by repressing several genes for the acquisition of iron (Newton *et al.*, 2005; Jin *et al.*, 2006; Ledala *et al.*, 2007; Ledala *et al.*, 2010). Repression of lmo1131 by Fur in growth medium with sufficient iron concentrations has been observed in microarray studies (Ledala *et al.*, 2010). To analyze the influence of iron on the expression of the operon lmo1131-1132, transcription levels in cells grown under different iron conditions were analyzed via qRT-PCR. In agreement with the results from Ledala *et al.*, listeriae grown in iron-depleted medium exhibited a ca. two-fold increase in transcription levels for both lmo1131 and lmo1132. Under iron-excessive conditions, a strong repression and a more than 20-fold decrease of transcription levels were observed.

These results might indicate a role of Lmo1131-1132 in the acquisition of iron during infection. Iron is an essential microelement for all living cells since it is involved in several important biological processes, e.g. energy production, regulation of gene expression, DNA biosynthesis and more. It is required as a co-factor for several cellular enzymes such as catalases, nitrogenases, peroxidases, and cytochromes (Lechowitz & Krawczyk-Balska, 2015). It exists in either the oxidized Fe^{3+} ferric or the reduced Fe^{2+} ferrous form. The former is predominant in the aerobic environment, but has a low solubility, therefore the availability of iron in the environment is low (Andrews *et al.*, 2003). In addition, by the means of nutritional immunity (Weinberg, 1974), the host limits the concentration of iron through sequestration proteins to inhibit growth of pathogenic bacteria (Latunde-Dada, 2009). Pathogens must adapt to iron limitations and have therefore evolved diverse mechanisms to assimilate iron during infection. Only a fraction of dietary iron is absorbed in the duodenum and jejunum, but nevertheless, the amount of available “unbound” iron is limited in the GI lumen. Most iron is present either in the low-soluble ferric form or bound by the high-affinity host proteins heme or lactoferrin (Kortman *et al.*, 2014). Commensal bacteria therefore either directly take up heme, reduce ferric to soluble ferrous iron via iron reductases or secrete high-affinity iron chelators called siderophores, which can be transported into the cell by specific transporters (Andrews *et al.*, 2003; Miethke & Marahiel, 2007; Cowart, 2002). *L. monocytogenes* does not produce siderophores (Glaser *et al.*, 2001). Instead, it can use the ferric hydroxamate uptake (Fhu) system and the hemin/hemoglobin uptake (Hup) system to take up xenosiderophores or heme (Jin *et al.*, 2006). Since the ABC transporter Lmo1131-1132 is repressed under anaerobic conditions, a role for the transport of iron in the intestinal lumen seems unlikely. Additionally, the proposed export function contradicts an involvement in iron acquisition.

The variation of iron concentrations in the host serves as an environmental cue and a regulatory signal for the expression of virulence genes in pathogenic bacteria (Litwin & Calderwood, 1993). Iron

deficiency increased transcription of *prfA* and *actA* and led to increased LLO production in listeriae in previous studies. Simultaneously, it caused reduced invasiveness in cell culture which might be ascribed to decreased expression of *inlAB* under these conditions (Cowart & Forster, 1981; Conte *et al.*, 1996; Böckman *et al.*, 1996; Conte *et al.*, 2000). Intracellular iron is stored by the protein ferritin in the cytoplasm (Lechowitz & Krawczyk-Balska, 2015). Therefore, the low concentrations of free iron encountered inside host cells are believed to be an important signal for enhanced expression of the proteins ActA and LLO, which are essential for intracellular survival. Transcription of lmo1131-1132 was also induced under iron-depleted conditions, but in contrast to ActA and LLO, the transporter seems to be important for invasion rather than intracellular replication as derived by Caco-2 assays.

4.2.4 Functional aspects of lmo1131-1132 during infection *in vivo*

Since the ABC transporter was involved in adhesion and invasion of human colonic epithelial cells, BALB/c mice were co-infected with EGDe and EGDe Δlmo1131-1132 to assess its role during the GI phase of infection and subsequent systemic spread.

After 24 h, a similar ratio of both strains was recovered from the lumen of both the colon and ileum. While the general dogma in literature suggests that the small intestine is the primary site for listeriosis and the colon is often not surveyed in animal studies, the total cfu numbers in the colon were actually ca. 10-fold higher than in the ileum. This is in line with recent findings, which acknowledge the colon as the major site for colonization and replication (Bou Ghanem *et al.*, 2012; Becattini *et al*, 2017). A small defect of EGDe Δlmo1131-1132 was observed in the tissues of the ileum but not the colon. In the following experiments, the infection period was extended by one day. This led to a reduction of EGDe Δlmo1131-1132 in the liver as well as the ileum but not the colon tissue, while the GI lumen, spleen and MLNs exhibited equal numbers of both strains.

Therefore, the ABC transporter Lmo1131-1132 was not involved in colonization of the intestinal lumen which is in accordance with the results from the qRT-PCR experiments. Because this is a hypoxic environment, transcription of the operon is strongly repressed. Upon contact with the mucosa, *L. monocytogenes* encounters conditions of relative oxygenation leading to increased transcription. Accordingly, a reduced number of cells lacking the lmo1131-1132 was observed in the intestinal tissue. As shown by the Caco-2 cell culture assays, the transporter is involved in adhesion and invasion of the host cell. Paradoxically, the invasion defect occurred in the small but not the large intestine. Caco-2 cells are colonic epithelial cells, but invasion of colonocytes was not affected in EGDe Δlmo1131-1132.

The exact mechanism how *L. monocytogenes* can cross the intestinal barrier is still unclear and contradicting results are published on this topic. On one hand, it can directly invade epithelial cells by binding of InlA to E-cadherin (Mengaud *et al.*, 1996; Lecuit *et al.*, 1997). E-cadherin becomes transiently accessible at the tips of intestinal villi during the extrusion of dying cells from the epithelium and at

junctions between mucus-expelling goblet cells (Pentecost *et al.*, 2006; Nikitas *et al.*, 2011). On the other hand, M cells are thought to represent an alternative route of passage by transcytosis of the pathogen (MacDonald & Carter, 1980; Marco *et al.*, 1997; Pron *et al.*, 1998; Daniels *et al.*, 2000; Corr *et al.*, 2006; Chiba *et al.*, 2011; Bou Ghanem *et al.*, 2012). M cells are found in the FAE of PP (Corr *et al.*, 2008). A second type of M cells, so called villous M cells, can be found at the tips of small intestinal villi (Jang *et al.*, 2004).

One major problem is the lack of suitable animal models to study infection. In mice, no specific interaction between InlA and its receptor E-cadherin occurs (Lecuit *et al.*, 1999) and transcytosis across M cells is thought to be the preferred route across the gut mucosa. Recent studies mainly used "murinized" listeriae that express an engineered $InlA^m$ with a high affinity for murine E-cadherin (Wollert *et al.*, 2007), although it is debated whether this causes altered cell tropism and host response (Tsai *et al.*, 2013). The required oral infection dose in this model is still higher than the assumed human dose, suggesting other mechanism that render mice relatively resistant to oral infection (Wollert *et al.*, 2007; Bou Ghanem *et al.*, 2012; Becattini *et al.*, 2017).

In this thesis, wild-type EDGe was used for oral infection experiments and as a background for the generation of deletions mutants. Since the specific interaction between InlA and E-cadherin is missing, transcytosis across M cells might be vital for invasion of the gut tissues. While M cells can also be found in the colon, they are more numerous in the small intestine, especially in the ileum. Therefore, the InlA-independent transcytosis across this cell type could be of special importance for wild-type EGDe and could explain the observed phenotype of EGDe Δlmo1131-1132 in the ileum. Nevertheless, the exact role of InlA during colonization and invasion is still unclear. Studies by the D'Orazio group were able to show that InlA is not essential to establish initial colonization but is instead needed for growth and persistence in the GIT and for dissemination from the gut to the MLNs (Bou Ghanem *et al.*, 2012). They also reported a similar course of disease for *L. monocytogenes* wildtype and $InlA^m$ strains, except for a ca. 10-fold higher infection dose required for infection by the former (Bou Ghanem *et al.*, 2012; Jones *et al.*, 2015). Experiments using a lmo1131-1132 deletion mutant in a $InlA^m$ background might be helpful to unravel the importance of this ABC transporter.

To further elucidate the cause for the impaired phenotype of the deletion mutant in the ileum, the tissue of infected mice was fractionated 2 days p.i. This allows separate analysis of the mucus layer, the epithelial cells and the underlying LP (Bou Ghanem *et al.*, 2013a). While the mucus and epithelial cells harbored equal numbers of bacteria, EGDe Δlmo1131-1132 cfu were slightly reduced in the LP. In an additional experiment, mice co-infected with EGDe and EGDe Δlmo1131-1132 were sacrificed 6 h p.i. and the ileal and colonic tissue were fractionated. Mucus and epithelial cells of the ileum were mostly devoid of bacteria and the LP harbored similar cfu numbers of both strains. The results of these

two experiments indicate two things: (i) The deletion of lmo1131-1132 did not influence the initial invasion and translocation of *L. monocytogenes* across the epithelial cells, as one might suggest from the cell culture experiments, since equal numbers of both strains were able to invade epithelial cells and reach the LP. (ii) The absence of the ABC transporter influenced the persistence in the LP of the ileum since the defect in cell numbers of the deletion mutant was apparent at 2 days p.i. but not at 6 hours p.i.

Previous studies identified extracellular *L. monocytogenes* as the majority of total bacterial burden in the LP of intestinal tissues and in the MLNs. Nevertheless, a small fraction of intracellular bacteria was essential not for establishment of infection but for persistence over time, especially in the ileum and for dissemination to the MLNs (Bou Ghanem *et al.*, 2012; Jones *et al.*, 2015). The fractionation experiments in this thesis point to an impaired persistence in the LP of listeriae lacking lmo1131-1132. After crossing the intestinal barrier via the InlA-dependent and -independent route, *L. monocytogenes* either exists extracellularly in the interstitial fluid or is phagocytosed by immune cells like DCs or macrophages in the LP (Pron *et al.*, 2001; Jones und D'Orazio 2017). Consistent with the previous hypothesis that Lmo1131-1132 might be involved in the entry to or the escape from the vacuole in Caco-2 cells after phagocytosis, the deletion of the operon might be detrimental for the survival in professional phagocytes of the LP. A similar hypothesis was proposed to explain the improved spread of *L. monocytogenes* $InlA^m$ from the LP to the MLNs by entry into migratory DCs (Bou Ghanem *et al.*, 2012; Jones *et al.*, 2015; Jones und D'Orazio 2017). Alternatively, although unlikely, extracellular *L. monocytogenes* might be dependent on the transporter function of Lmo1131-1132, e.g. for the acquisition of iron. Extracellular iron in the serum, the lymph or fluids of mucous membranes is sequestered by heme, transferrin or lactoferrin in the host. Therefore, *L. monocytogenes* possesses several systems, amongst these ABC transporters, to acquire iron during infection (Lechowitz & Krawczyk-Balska, 2015).

EGDe Δlmo1131-1132 numbers were decreased in the liver, but not the MLNs and spleen. Additional experiments showed no impaired phenotype for the deletion mutant during colonization of the liver and spleen after i.v. infection. Therefore, the ABC transporter is involved in the spread from the gut mucosa to the liver but not in survival and/or replication in hepatic tissues. This can be ascribed to the two different routes of dissemination. *L. monocytogenes* can spread from the intestinal mucosa via the lymphatic fluid to the MLNs and gain access to the blood, which causes infection of the liver and spleen. On the other hand, the pathogen can gain direct access to the circulatory system after crossing of the intestinal barrier, leading to exclusive infection of the liver via the portal vein (Melton-Witt *et al.*, 2012). Since the transporter deletion mutant was impaired only in liver colonization, it can be assumed that this was due to a defect in the direct route of dissemination via the blood. Since the LP harbored less

EGDe Δlmo1131-1132 compared to the parental strain, it might be possible that this host compartment represented a bottleneck for further dissemination, which has been assumed in an earlier study (Bou Ghanem *et al.*, 2012). The causation for the impaired subsequent spread via the blood might be explained by two hypotheses: (i) *Since L. monocytogenes* can directly invade endothelial cells in an InlA-independent manner (Greiffenberg *et al.* 1997; Parida *et al.*, 1998), a defect in the invasion of endothelial cells and therefore in the access to the bloodstream might be possible. (ii) A reduced invasion of or survival inside migratory phagocytes in the blood might cause the observed phenotype. It was shown that *L. monocytogenes* can disseminate via monocytes of the blood (Drevets *et al.*, 2004) and the ABC transporter might facilitate invasion of or survival in these professional phagocytes.

4.2.5 Conclusion

Together, it was shown that the *Listeria sensu stricto* specific operon lmo1131-1132 encodes for an ABC transporter with a possible export function, although it is unclear what the substrate is. Analyses via qRT-PCR showed transcriptional regulation based on temperature as well as on oxygen- and iron-availability, probably executed by the iron regulator Fur. These are important environmental cues governing the transition to an infectious lifestyle upon entry of the host. Cell culture experiments suggested an involvement of lmo1131-1132 in adhesion to and invasion of epithelial cells of the colon. Colonization capabilities of EGDe and EGDe Δlmo1131-1132 were assessed in oral co-infection experiments in mice. While a defect for the deletion mutant in persistence in the LP was observed, the exact mechanism remains unclear. The exclusive observation of this phenotype in the ileum, but not the colon, contradicts the results from cell culture. Further experiments in a $InlA^m$ background strain or cell culture experiments with gut-associated leucocytes like macrophages or DCs could help clarify the function of the ABC transporter during the colonization of the GIT.

4.3 From food to cell: Metabolic traits for proliferation in food and gut

L. monocytogenes is not only able to adapt to various environmental niches including soil, decaying plant material or water, but it is also a facultative pathogen that can infect mammalian hosts via contaminated food. Besides the already described stress resistance mechanisms, “pathometabolism” is a key feature of all foodborne pathogens. This term describes the metabolic adaptation to the various extra- and intracellular environments encountered during their infection processes, i.e. the circulatory system, the intracellular niche or the GIT (Fuchs *et al.*, 2012a; Fuchs *et al.*, 2012b; Eisenreich *et al.*, 2015; Dandekar & Eisenreich, 2015).

The intestinal microbiota protects the gut lumen from colonization by enteropathogens. This so-called colonization resistance is largely due to competition for nutrients (Stecher & Hardt, 2014; Pickard *et al.*, 2017). The majority of commensal bacteria are obligate anaerobes, which are well-adapted to the gut environment and the existing food supply, thus limiting the presence of high-energy nutrients

(Maier *et al.*, 2004; Hansson, 2012). Enteric pathogens must therefore develop metabolic strategies for exploitation of nutrients that are not efficiently utilized by the microbiota, including 1,2-PD, inositol, ethanolamine, fucose or sialic acid (Staib & Fuchs, 2014).

The presence of three large genomic clusters for the degradation of 1,2-PD and ethanolamine as well as for the biosynthesis of the required co-factor cobalamin in all genomes of the *Listeria sensu stricto* was derived by genome comparison between the two *Listeria* clades in this thesis, but has also been reported before (Chiara *et al.*, 2015). Besides *L. monocytogenes*, homologous genes are also present in the enteropathogens *Clostridium perfringens* and *S. enterica* and are associated with pathogenicity and food poisoning (Korbel *et al.*, 2005; Staib & Fuchs, 2014). According to the "from food to cell" hypothesis, certain metabolic traits of foodborne pathogens are not only useful during colonization of the GIT or intracellular replication but also during proliferation in food (Staib & Fuchs, 2014).

4.3.1 Ethanolamine utilization in food and host

The biological significance of cobalamin and the utilization of both 1,2PD and ethanolamine have been studied in *S. enterica* (Roth *et al.*, 1996). Ethanolamine can be derived from phosphatidylethanolamine, a membrane lipid component in both mammalian and bacterial cell membranes, and is present in the GI lumen (Randle *et al.*, 1969; Vance, 2008; Martin *et al.*, 2009). *Salmonella* can utilize ethanolamine via anaerobic respiration using tetrathionate as an alternative electron acceptor, which is a byproduct of inflammatory responses that occurs in mammalian hosts (Winter *et al.*, 2010; Thiennimitr *et al.*, 2011). This specific trait is discussed to be important for *in vivo* virulence (Harvey *et al.*, 2011; Srikumar & Fuchs, 2011; Thiennimitr *et al.*, 2011). Additionally, phosphatidylethanolamine is present in foods moderately rich in fat, and metabolism of ethanolamine has been shown to be important during proliferation of *S. enterica* in milk and egg yolk (Srikumar & Fuchs, 2010). Ethanolamine utilization and transcriptional regulation of corresponding *eut* genes have been studied in *L. monocytogenes* and have been shown to be important outside the GIT and possibly in the intracellular environment as derived by i.v. infection studies in mice (Mellin *et al.*, 2014).

4.3.2 1,2-PD as an alternative carbon and energy source

Most of the knowledge about 1,2-PD utilization is derived from *Salmonella*. This metabolic pathway has been demonstrated to be involved in virulence (Conner *et al.*, 1998; Heithoff *et al.*, 1999; Harvey *et al.*, 2001; Klumpp & Fuchs, 2007; Hautefort *et al.*, 2009). 1,2-PD is an abundant nutrient in the GIT, which is produced by the gut microbiota via fermentation of rhamnose and fucose (Badia *et al.*, 1985).

There is evidence that *pdu* genes for 1,2-PD degradation are transcribed in *L. monocytogenes*, a diol dehydratase is enzymatically active in *L. innocua,* and *pdu* genes are induced during growth in media supplemented with 1,2-PD *in vitro* as well as in the intestines of gnotobiotic mice *in vivo* (Xue *et al.*, 2008; Toledo-Arana *et al.*, 2009; Mellin *et al.*, 2013). However, it is unclear if *L. monocytogenes* utilizes

1,2-PD as a carbon and energy source, or if this pathway is involved in virulence. In this thesis, the importance of the listerial *pdu* gene cluster was studied. An in-frame deletion mutant of the gene *pduD* was constructed in *L. monocytogenes* EGDe. The protein PduD is a homolog of the ß subunit of the diol dehydratase PduCDE, a hexameric cobalamin-dependent enzyme, which catalyzes the conversion of 1,2-PD to propionaldehyde in *Salmonella* (Bobik *et al.*, 1997; Daniel *et al.*, 1998; Bobik *et al.*, 1999). Enzymatic activity of PduD has only been demonstrated in *L. innocua* (Xue *et al.*, 2008). Therefore, growth experiments in defined MM under anaerobic conditions were conducted. Supplementation with 1,2-PD and cobalamin led to significantly increased optical densities in *L. monocytogenes* EGDe, an effect which was abolished in the EGDe Δ*pduD* deletion mutant. Nevertheless, OD_{600}^{max} during growth supplemented with glucose was more than two-fold higher, indicating that 1,2-PD is not an ideal carbon and energy source and only provides a small growth advantage under the conditions tested. In *Salmonella*, 1,2-PD is catabolized to n-propanol and propionate under fermentation conditions. This results in ATP production, but no carbon source is provided under these circumstances. Nevertheless, 1,2-PD enhances growth under these conditions in the presence of poor carbon sources like YE (Bobik *et al.*, 1997; Daniel *et al.*, 1998; Bobik *et al.*, 1999; Price-Carter *et al.*, 2001; Havemann & Bobik, 2003; Liu *et al.*, 2007). In this thesis, MM required supplementation with YE since the strain EGDe is unable to grow anaerobically due to a deletion in the Class III NrdD ribonucleotide reductase (Ofer *et al.*, 2011). The low concentration of YE might provide just enough carbon for *L. monocytogenes* to gain a small advantage by using 1,2-PD for ATP production. Using aerobic or anaerobic respiration, 1,2-PD can serve as both an energy and a carbon source in *Salmonella* since propionyl-coenzyme A formed during degradation is converted to pyruvate via the methyl-citric acid cycle (Horswill & Escalante-Semerena, 1999; Palacios *et al.*, 2003). Since *L. monocytogenes* is not able to perform anaerobic respiration, 1,2-PD likely only serves as an energy source under the conditions tested (Glaser *et al.*, 2001; Müller-Herbst *et al.*, 2014). Improved growth by 1,2-PD was not observed in experiments under aerobic conditions. The methyl-citric acid cycle in *L. monocytogenes* is incomplete, suggesting that 1,2-PD is unable to be utilized as an energy or carbon source under oxic conditions (Xue *et al.*, 2008). As a control, MM containing glucose was used for growth experiments in this thesis. In the presence of glucose, additional supplementation with 1,2-PD had no effect on growth of listeriae since glucose was shown to inhibit *pdu* expression in both *L. monocytogenes* and *S*. Typhimurium (Nilsson *et al.*, 2005; Staib & Fuchs, 2015; Bobik *et al.*, 1992). Together, these results indicate that 1,2-PD and the co-factor cobalamin conferred only a small growth advantage under fermentative conditions, and alternative carbon sources must be present, e.g. in the form of YE, since this catabolic pathway does not provide a suitable carbon source itself.

The transcriptome of *L. monocytogenes* EGDe was analyzed under anaerobic conditions in BHI medium. Transcriptional changes upon supplementation with 1,2PD or 1,2-PD with cobalamin were

assessed. While transcription of *pdu* genes has been studied before (Xue *et al.*, 2008; Mellin *et al.*, 2013), data on *cob*/*cbi* genes for biosynthesis of cobalamin is missing. During exponential growth phase, both gene clusters showed only weak or no transcription under all three growth conditions tested. This indicates that the plentiful nutrients in BHI are sufficient to sustain growth without the need for 1,2-PD degradation. In exponential phase, transcription levels in plain BHI were still low. However, addition of 1,2-PD significantly increased the transcription of almost all *pdu* and *cob*/*cbi* genes. The transcription of *pdu* genes was even more elevated when cobalamin was added. Most *cbi*/*cob* genes exhibited less transcription under this condition. This finding confirms a regulatory model in which the presence of cobalamin represses its own synthesis post-transcriptionally via stabilization of an mRNA hairpin in *Salmonella* (Roth *et al.*, 1996). For *L. monocytogenes*, the existence of a cobalamin-dependent riboswitch was proven, which is transcribed as part of a noncoding antisense RNA. In the presence of cobalamin, a shorter transcript is produced, but in the absence of cobalamin, a full-length transcript is transcribed, which inhibits *pocR* expression (Mellin *et al.*, 2013). Indeed, maximal transcription levels for *pocR* in this thesis were observed under conditions with 1,2-PD and cobalamin compared to conditions with only 1,2-PD. The transcription factor PocR positively regulates expression of *pdu* and *cob*/*cbi* genes in *S. enterica* in the presence of 1,2-PD (Rondon & Escalante-Semerena, 1992). The interplay between a cobalamin-dependent riboswitch and PocR in *Listeria* ensure that *pdu* gene expression is maximal only during the presence of both cobalamin and 1,2-PD (Mellin *et al.*, 2013), which is consistent with the results in this thesis. Additionally, it was shown here that transcription of *cob*/*cbi* genes is repressed in the presence of cobalamin, a mechanism which is probably mediated by an additional cobalamin-dependent riboswitch in the *cob*/*cbi* region (Mellin *et al.*, 2013).

It has been shown that transcription of the 1,2-PD cluster is induced intracellularly in mammalian host cells as well as in the GIT of gnotobiotic mice after oral infection (Joseph *et al.*, 2006; Toledo-Arana *et al.*, 2009). The importance of the *cob*/*cbi* and *pdu* clusters for replication in macrophages has been demonstrated before in *S*. Typhimurium (Klumpp and Fuchs, 2007). To ultimately prove involvement of the *pdu* genes during *in vivo* infection, mice were co-infected with EGDe and EGDe Δ*pduD*. Stool pellets were collected every 24 h up to 14 days to quantify listerial shedding over time. The absence of *pduD* led to lower average cfu numbers of the deletion mutant in the stool compared to the parental strain. On average, EGDe Δ*pduD* was cleared 10 days post-infection, while the parental strain continued to be shed in the feces in at least some of the mice for up to 4 more days. Similar experiments were performed by Faber and colleagues with *S*. Typhimurium. Deletion of *pdu* genes resulted in reduced bacterial numbers in colon contents 14 days p.i. They demonstrated that microbiota-derived 1,2-PD was a critical carbon source facilitating expansion of the pathogen (Faber *et al.*, 2017).

The intestinal mucus layer not only represents a first line of defense in the GIT but also provides a vast source of nutrients for the proliferation of commensal and pathogenic bacteria (Staib & Fuchs, 2014; Pelaseyed *et al.*, 2014). It is composed of mucins, a family of highly glycosylated proteins produced by goblet cells. The sidechains of mucins contain carbohydrates like galactose, N-acetylglucosamine or fucose. Commensal bacteria such as *Bacteroides thetaiotaomicron*, which colonize the outer mucus layer of the colon, can cleave and degrade these glycans (Sicard *et al.*, 2017; Staib & Fuchs, 2014; Johansson *et al.*, 2008; Cummings & Macfarlane, 1991). Mucin-derived fucose is highly abundant in the intestinal lumen and can be fermented by Bacteroidetes and *Bifidobacteria*, resulting in the production of 1,2-PD (Robbe *et al.*, 2004; Xu *et al.*, 2003; Gill *et al.*, 2006; Hooper *et al.*, 1999; Faber *et al.*, 2017).

Interestingly, Toledo-Arana and colleagues observed upregulation of the *pdu*, *eut* and *cob*/*cbi* genes in the GIT of gnotobiotic mice compared to growth in BHI (Toledo-Arana *et al.*, 2009). Since the cleavage of fucose and the subsequent production of 1,2-PD is mediated by the microbiota, which is absent in these mice, it might be possible that other environmental cues induce transcription of these clusters in the gut. Alternatively, 1,2-PD might be derived from mouse chow, since it is used as a food additive in processed foods, or it could be that the nutrient-rich BHI medium inhibits transcription of these alternative degradation pathways. Another study analyzed the transcriptome of *L. monocytogenes* in either gnotobiotic or *Lactobacillus* monoassociated mice. The genes for biosynthesis of cobalamin and degradation of 1,2-PD and ethanolamine were induced in gnotobiotic mice, confirming the results by Toledo-Arana. The presence of Lactobacilli strongly increased transcription of these genes. These results suggest that during colonization of the GI lumen in gnotobiotic mice, *L. monocytogenes* is able to use various carbon and energy sources including ethanolamine and 1,2-PD. Colonization of mice by Lactobacilli results in competition for available carbon and nitrogen sources and a switch of listerial metabolism to 1,2-PD and ethanolamine utilization. While some *Lactobacillus* spp. can degrade both 1,2-PD and ethanolamine, the corresponding genes are missing in the species used in the study (Archambaud *et al.*, 2012; Zielinska *et al.*, 2017), thus these alternative catabolisms might confer an advantage for *L. monocytogenes*. Nevertheless, competition with *Lactobacillus* results in reduced invasion of intestinal tissues and dissemination by a number of different mechanisms (Archambaud *et al.*, 2012).

Besides the importance of 1,2-PD catabolism during colonization of the GIT, 1,2-PD is also present in food. It is used as a humectant, solvent, and preservative in various food products. In addition, the precursors fucose and rhamnose are commonly found in nature, e.g. in pectin, a plant cell wall polysaccharide. Interestingly, *L. monocytogenes* also possesses genes for the degradation of fucose and rhamnose (Staib & Fuchs, 2014). The transcription factor Lmo0753 has been shown to be essential

for utilization of rhamnose as an environmental carbon source and is specifically present in *L. monocytogenes* lineages LI and LII strains, which are associated with foodborne outbreaks (Salazar *et al.*, 2013). Another study was able to detect upregulation of the 1,2-PD, ethanolamine and cobalamin gene clusters during growth of *L. monocytogenes* on cold smoked salmon compared to growth in BHI medium. The authors speculated that 1,2-PD might become available through breakdown of salmon mucosal glycoconjugates containing rhamnose and fucose. Additional ethanolamine could be utilized via reduction of phosphatidylethanolamine to ethanolamine by the listerial phospholipase PlcB, which was also upregulated during growth on cold smoked salmon (Tang *et al.*, 2015).

4.3.3 Conclusion

As a conclusion, the metabolic pathway for the utilization of 1,2-PD seems to be beneficial for survival and proliferation in both the GIT and food in *L. monocytogenes*. The presence of three large gene clusters for the cobalamin-dependent catabolism of 1,2-PD and/or ethanolamine in the *Listeria sensu stricto* spp. might therefore confer an advantage for these species during colonization of the mouse gut, which was observed in oral infection experiments in this thesis. Additionally, reports from literature point to an association of *Listeria sensu stricto* with several food products, which might be explained by the presence of 1,2-PD, ethanolamine, fucose or rhamnose. These molecules might be used as alternative energy and/or carbon sources and enable survival and proliferation in the food matrix.

4.4 Outlook

The results from the oral colonization experiments performed in this thesis confirm the subdivision of the genus *Listeria* into two genotypically and phenotypically distinct clades, the *Listeria sensu lato* and the *Listeria sensu stricto* (Chiara *et al*., 2015; Orsi & Wiedmann, 2016). The former are environmental species and are insufficiently adapted to the GIT. The latter are able to at least transiently colonize the GIT, albeit only *L. monocytogenes* and *L. ivanovii* are considered to be enteropathogens. This is well in line with the hypothesis of a pathogenic MRCA and a subsequent loss of important virulence genes in the apathogenic members of the *Listeria sensu stricto* (Schmid *et al*., 2005; den Bakker *et al*., 2010a; den Bakker *et al*., 2010b). Nevertheless, the retention of certain virulence genes in these species and the presence of atypical strains of *L. innocua* and *L. seeligeri* that can cause disease in humans on rare occasions (Rocourt *et al.*, 1986; Perrin *et al.*, 2003) represent a challenge for virulence classification of these strains. The results from this thesis and the reports about the association of *Listeria sensu stricto* spp. with food from animal origins raise the question if these species pose a threat in food products and require monitoring.

Using the bioinformatic approach applied in this thesis, 151 candidate genes were identified that are present in the *Listeria sensu stricto* and absent in the *Listeria sensu lato*. The operon lmo1131-1132 encoding for an ABC transporter was shown to be involved in virulence of *L. monocytogenes in vitro* and *in vivo*. A role for bacterial ABC transporters in adherence to and invasion of intestinal ECs is an uncommon feature and needs further clarification in the future. Future advances in the knowledge about the pathophysiology of listeriosis could also help to illuminate the relevance of this transporter for persistence in the intestinal tissues and liver colonization.

The *pdu* gene cluster was necessary for the utilization of 1,2-PD as a potential energy and/or carbon source *in vitro* and prolonged the survival of *L. monocytogenes* in the GIT. This organic compound is not only present in the intestines but also in food. Further studies on the relevance of the catabolism of 1,2-PD for this foodborne pathogen and other *Listeria sensu stricto* spp. during proliferation in both food and host are needed.

Studies on other so far uncharacterized factors using NGS approaches and *in vitro* virulence assays from this list could help to gain further insight in the pathogenicity potential of the *Listeria sensu stricto*. The novel animal model for oral infection of BALB/c mice (Bou Ghanem *et al*., 2013) proved to be a useful tool for the identification of factors that play a role during the GI phase of infection and can be applied for future experiments.

5 References

Afgan, E., **Baker, D.**, **van den Beek, M.**, **Blankenberg, D.**, **Bouvier, D.**, **Čech, M.**, **Chilton, J.**, **Clements, D. & Coraor, N. & other authors (2016).** The Galaxy platform for accessible, reproducible and collaborative biomedical analyses: 2016 update. *Nucleic Acids Research* **44**, W3-W10.

Aichele, P., **Zinke, J.**, **Grode, L.**, **Schwendener, R. A.**, **Kaufmann, S. H. E. & Seiler, P. (2003).** Macrophages of the splenic marginal zone are essential for trapping of blood-borne particulate antigen but dispensable for induction of specific T cell responses. *Journal of Immunology (Baltimore, Md.: 1950)* **171**, 1148–1155.

Alexander, A. V., **Walker, R. L.**, **Johnson, B. J.**, **Charlton, B. R. & Woods, L. W. (1992).** Bovine abortions attributable to *Listeria ivanovii*. Four cases (1988-1990). *Journal of the American Veterinary Medical Association* **200**, 711–714.

Allikmets, R., **Gerrard, B.**, **Court, D. & Dean, M. (1993).** Cloning and organization of the *abc* and *mdl* genes of *Escherichia coli.* Relationship to eukaryotic multidrug resistance. *Gene* **136**, 231–236.

Altschul, S. F., **Gish, W.**, **Miller, W.**, **Myers, E. W. & Lipman, D. J. (1990).** Basic local alignment search tool. *Journal of Molecular Biology* **215**, 403–410.

Andrews, S. C., **Robinson, A. K. & Rodríguez-Quiñones, F. (2003).** Bacterial iron homeostasis. *FEMS Microbiology Reviews* **27**, 215–237.

Antoniollo, P. C., **Bandeira, F. d. S.**, **Jantzen, M. M.**, **Duval, E. H. & da Silva, W. P. (2003).** Prevalence of *Listeria* spp. in feces and carcasses at a lamb packing plant in Brazil. *Journal of Food Protection* **66**, 328–330.

Aoshi, T., **Carrero, J. A.**, **Konjufca, V.**, **Koide, Y.**, **Unanue, E. R. & Miller, M. J. (2009).** The cellular niche of *Listeria monocytogenes* infection changes rapidly in the spleen. *European Journal of Immunology* **39**, 417–425.

Appelberg, R. & Leal, I. S. (2000). Mutants of *Listeria monocytogenes* defective in In vitro invasion and cell-to-cell spreading still invade and proliferate in hepatocytes of neutropenic mice. *Infection and Immunity* **68**, 912–914.

Archambaud, C., **Nahori, M.-A.**, **Soubigou, G.**, **Bécavin, C.**, **Laval, L.**, **Lechat, P.**, **Smokvina, T.**, **Langella, P.**, **Lecuit, M. & Cossart, P. (2012).** Impact of lactobacilli on orally acquired listeriosis. *Proceedings of the National Academy of Sciences of the United States of America* **109**, 16684–16689.

Arnold, K., **Bordoli, L.**, **Kopp, J. & Schwede, T. (2006).** The SWISS-MODEL workspace. A web-based environment for protein structure homology modelling. *Bioinformatics (Oxford, England)* **22**, 195–201.

Aureli, P., **Fiorucci, G. C.**, **Caroli, D.**, **Marchiaro, G.**, **Novara, O.**, **Leone, L. & Salmaso, S. (2000).** An outbreak of febrile gastroenteritis associated with corn contaminated by *Listeria monocytogenes*. *The New England journal of Medicine* **342**, 1236–1241.

Badía, J., **Ros, J. & Aguilar, J. (1985).** Fermentation mechanism of fucose and rhamnose in *Salmonella* Typhimurium and *Klebsiella pneumoniae*. *Journal of Bacteriology* **161**, 435–437.

Bambirra, F. H. S., **Lima, K. G. C.**, **Franco, B. D. G. M.**, **Cara, D. C.**, **Nardi, R. M. D.**, **Barbosa, F. H. F. & Nicoli, J. R. (2007).** Protective effect of *Lactobacillus sakei* 2a against experimental challenge with *Listeria monocytogenes* in gnotobiotic mice. *Letters in Applied Microbiology* **45**, 663–667.

Bankevich, A., **Nurk, S.**, **Antipov, D.**, **Gurevich, A. A.**, **Dvorkin, M.**, **Kulikov, A. S.**, **Lesin, V. M.**, **Nikolenko, S. I. & Pham, S. & other authors (2012).** SPAdes: a new genome assembly algorithm and

its applications to single-cell sequencing. *Journal of Computational Biology: A Journal of Computational Molecular Cell Biology* **19**, 455–477.

Barnes, P. D., **Bergman, M. A.**, **Mecsas, J. & Isberg, R. R. (2006).** *Yersinia pseudotuberculosis* disseminates directly from a replicating bacterial pool in the intestine. *The Journal of Experimental Medicine* **203**, 1591–1601.

Becattini, S., **Littmann, E. R.**, **Carter, R. A.**, **Kim, S. G.**, **Morjaria, S. M.**, **Ling, L.**, **Gyaltshen, Y.**, **Fontana, E. & Taur, Y. & other authors (2017).** Commensal microbes provide first line defense against *Listeria monocytogenes* infection. *The Journal of Experimental Medicine* **214**, 1973–1989.

Becker, L. A., **Evans, S. N.**, **Hutkins, R. W. & Benson, A. K. (2000).** Role of sigma(B) in adaptation of *Listeria monocytogenes* to growth at low temperature. *Journal of Bacteriology* **182**, 7083–7087.

Begley, M., **Gahan, C. G. M. & Hill, C. (2002).** Bile stress response in *Listeria monocytogenes* LO28. Adaptation, cross-protection, and identification of genetic loci involved in bile resistance. *Applied and Environmental Microbiology* **68**, 6005–6012.

Begley, M., **Gahan, C. G. M. & Hill, C. (2005a).** The interaction between bacteria and bile. *FEMS Microbiology Reviews* **29**, 625–651.

Begley, M., **Gahan, C. G. M.**, **Kollas, A.-K.**, **Hintz, M.**, **Hill, C.**, **Jomaa, H. & Eberl, M. (2004).** The interplay between classical and alternative isoprenoid biosynthesis controls gammadelta T cell bioactivity of *Listeria monocytogenes*. *FEBS Letters* **561**, 99–104.

Begley, M., **Sleator, R. D.**, **Gahan, C. G. M. & Hill, C. (2005b).** Contribution of three bile-associated loci, *bsh*, *pva*, and *btlB*, to gastrointestinal persistence and bile tolerance of *Listeria monocytogenes*. *Infection and Immunity* **73**, 894–904.

Belkaid, Y. & Hand, T. W. (2014). Role of the microbiota in immunity and inflammation. *Cell* **157**, 121–141.

Benjamini, Y. & Hochberg, Y. (1995). Controlling the False Discovery Rate: A Practical and Powerful Approach to Multiple Testing. *Journal of the Royal Statistical Society. Series B (Methodological)* **57**, 289–300.

Bennett, H. J., **Pearce, D. M.**, **Glenn, S.**, **Taylor, C. M.**, **Kuhn, M.**, **Sonenshein, A. L.**, **Andrew, P. W. & Roberts, I. S. (2007).** Characterization of *relA* and *codY* mutants of *Listeria monocytogenes*. Identification of the CodY regulon and its role in virulence. *Molecular Microbiology* **63**, 1453–1467.

Benson, D. A., **Cavanaugh, M.**, **Clark, K.**, **Karsch-Mizrachi, I.**, **Lipman, D. J.**, **Ostell, J. & Sayers, E. W. (2017).** GenBank. *Nucleic Acids Research* **45**, D37-D42.

Bergmann, S., **Rohde, M.**, **Schughart, K. & Lengeling, A. (2013).** The bioluminescent *Listeria monocytogenes* strain Xen32 is defective in flagella expression and highly attenuated in orally infected BALB/cJ mice. *Gut Pathogens* **5**, 19.

Bertsch, D., **Rau, J.**, **Eugster, M. R.**, **Haug, M. C.**, **Lawson, P. A.**, **Lacroix, C. & Meile, L. (2013).** *Listeria fleischmannii* sp. nov., isolated from cheese. *International Journal of Systematic and Evolutionary Microbiology* **63**, 526–532.

Biasini, M., **Bienert, S.**, **Waterhouse, A.**, **Arnold, K.**, **Studer, G.**, **Schmidt, T.**, **Kiefer, F.**, **Gallo Cassarino, T. & Bertoni, M. & other authors (2014).** SWISS-MODEL. Modelling protein tertiary and quaternary structure using evolutionary information. *Nucleic Acids Research* **42**, W252-8.

Bierne, H., **Garandeau, C.**, **Pucciarelli, M. G.**, **Sabet, C.**, **Newton, S.**, **Garcia-del Portillo, F.**, **Cossart, P. & Charbit, A. (2004).** Sortase B, a new class of sortase in *Listeria monocytogenes*. *Journal of Bacteriology* **186**, 1972–1982.

Bierne, H., **Mazmanian, S. K.**, **Trost, M.**, **Pucciarelli, M. G.**, **Liu, G.**, **Dehoux, P.**, **Jänsch, L.**, **Garcia-del Portillo, F.**, **Schneewind, O. & Cossart, P. (2002).** Inactivation of the *srtA* gene in *Listeria monocytogenes* inhibits anchoring of surface proteins and affects virulence. *Molecular Microbiology* **43**, 869–881.

Bigot, A., **Pagniez, H.**, **Botton, E.**, **Fréhel, C.**, **Dubail, I.**, **Jacquet, C.**, **Charbit, A. & Raynaud, C. (2005).** Role of FliF and FliI of *Listeria monocytogenes* in flagellar assembly and pathogenicity. *Infection and Immunity* **73**, 5530–5539.

Bo Andersen, J., **Roldgaard, B. B.**, **Christensen, B. B. & Licht, T. R. (2007).** Oxygen restriction increases the infective potential of *Listeria monocytogenes in vitro* in Caco-2 cells and *in vivo* in guinea pigs. *BMC Microbiology* **7**, 55.

Bobik, T. A., **Ailion, M. & Roth, J. R. (1992).** A single regulatory gene integrates control of vitamin B_{12} synthesis and propanediol degradation. *Journal of Bacteriology* **174**, 2253–2266.

Bobik, T. A., **Havemann, G. D.**, **Busch, R. J.**, **Williams, D. S. & Aldrich, H. C. (1999).** The propanediol utilization (*pdu*) operon of *Salmonella enterica* serovar Typhimurium LT2 includes genes necessary for formation of polyhedral organelles involved in coenzyme B(12)-dependent 1,2-propanediol degradation. *Journal of Bacteriology* **181**, 5967–5975.

Bobik, T. A., **Xu, Y.**, **Jeter, R. M.**, **Otto, K. E. & Roth, J. R. (1997).** Propanediol utilization genes (*pdu*) of *Salmonella* Typhimurium. Three genes for the propanediol dehydratase. *Journal of Bacteriology* **179**, 6633–6639.

Böckmann, R., **Dickneite, C.**, **Middendorf, B.**, **Goebel, W. & Sokolovic, Z. (1996).** Specific binding of the *Listeria monocytogenes* transcriptional regulator PrfA to target sequences requires additional factor(s) and is influenced by iron. *Molecular Microbiology* **22**, 643–653.

Borezée, E., **Pellegrini, E.**, **Beretti, J. L. & Berche, P. (2001).** SvpA, a novel surface virulence-associated protein required for intracellular survival of *Listeria monocytogenes*. *Microbiology (Reading, England)* **147**, 2913–2923.

Bou Ghanem, E. N., **Jones, G. S.**, **Myers-Morales, T.**, **Patil, P. D.**, **Hidayatullah, A. N. & D'Orazio, S. E. F. (2012).** InlA promotes dissemination of *Listeria monocytogenes* to the mesenteric lymph nodes during food borne infection of mice. *PLoS Pathogens* **8**, e1003015.

Bou Ghanem, E. N., **Myers-Morales, T. & D'Orazio, S. E. F. (2013a).** A mouse model of foodborne *Listeria monocytogenes* infection. *Current Protocols in Microbiology* **31**, 9B.3.1-9B.3.16.

Bou Ghanem, E. N., **Myers-Morales, T.**, **Jones, G. S. & D'Orazio, S. E. F. (2013b).** Oral transmission of *Listeria monocytogenes* in mice via ingestion of contaminated food. *Journal of Visualized Experiments: JoVE*, e50381.

Braun, L., **Ohayon, H. & Cossart, P. (1998).** The InIB protein of *Listeria monocytogenes* is sufficient to promote entry into mammalian cells. *Molecular Microbiology* **27**, 1077–1087.

Broadley, S. P., **Plaumann, A.**, **Coletti, R.**, **Lehmann, C.**, **Wanisch, A.**, **Seidlmeier, A.**, **Esser, K.**, **Luo, S. & Rämer, P. C. & other authors (2016).** Dual-Track Clearance of Circulating Bacteria Balances Rapid Restoration of Blood Sterility with Induction of Adaptive Immunity. *Cell Host & Microbe* **20**, 36–48.

Brown, S. A., **Palmer, K. L. & Whiteley, M. (2008).** Revisiting the host as a growth medium. *Nature reviews. Microbiology* **6**, 657–666.

Bsat, N., **Herbig, A.**, **Casillas-Martinez, L.**, **Setlow, P. & Helmann, J. D. (1998).** *Bacillus subtilis* contains multiple Fur homologues. Identification of the iron uptake (Fur) and peroxide regulon (PerR) repressors. *Molecular Microbiology* **29**, 189–198.

Buchrieser, C., **Rusniok, C.**, **Garrido, P.**, **Hain, T.**, **Scortti, M.**, **Lampidis, R.**, **Kärst, U.**, **Chakraborty, T. & Cossart, P. & other authors (2011).** Complete genome sequence of the animal pathogen *Listeria ivanovii*, which provides insights into host specificities and evolution of the genus *Listeria*. *Journal of Bacteriology* **193**, 6787–6788.

Buchrieser, C., **Rusniok, C.**, **Kunst, F.**, **Cossart, P. & Glaser, P. (2003).** Comparison of the genome sequences of *Listeria monocytogenes* and *Listeria innocua*. Clues for evolution and pathogenicity. *FEMS Immunology and Medical Microbiology* **35**, 207–213.

Burkholder, K. M. & Bhunia, A. K. (2010). *Listeria monocytogenes* uses *Listeria* adhesion protein (LAP) to promote bacterial transepithelial translocation and induces expression of LAP receptor Hsp60. *Infection and Immunity* **78**, 5062–5073.

Camejo, A., **Carvalho, F.**, **Reis, O.**, **Leitão, E.**, **Sousa, S. & Cabanes, D. (2011).** The arsenal of virulence factors deployed by *Listeria monocytogenes* to promote its cell infection cycle. *Virulence* **2**, 379–394.

Carrero, J. A., **Calderon, B. & Unanue, E. R. (2004a).** Listeriolysin O from *Listeria monocytogenes* is a lymphocyte apoptogenic molecule. *Journal of Immunology (Baltimore, Md. : 1950)* **172**, 4866–4874.

Carrero, J. A., **Calderon, B. & Unanue, E. R. (2004b).** Type I interferon sensitizes lymphocytes to apoptosis and reduces resistance to *Listeria* infection. *The Journal of Experimental Medicine* **200**, 535–540.

Carver, T., **Harris, S. R.**, **Berriman, M.**, **Parkhill, J. & McQuillan, J. A. (2012).** Artemis: an integrated platform for visualization and analysis of high-throughput sequence-based experimental data. *Bioinformatics (Oxford, England)* **28**, 464–469.

Chan, J. Z.-M., **Halachev, M. R.**, **Loman, N. J.**, **Constantinidou, C. & Pallen, M. J. (2012).** Defining bacterial species in the genomic era. Insights from the genus Acinetobacter. *BMC Microbiology* **12**, 302.

Chand, P. & Sadana, J. R. (1999). Outbreak of *Listeria ivanovii* abortion in sheep in India. *The Veterinary Record* **145**, 83–84.

Chatterjee, S. S., **Hossain, H.**, **Otten, S.**, **Kuenne, C.**, **Kuchmina, K.**, **Machata, S.**, **Domann, E.**, **Chakraborty, T. & Hain, T. (2006).** Intracellular gene expression profile of *Listeria monocytogenes*. *Infection and Immunity* **74**, 1323–1338.

Chen, G. Y., **Pensinger, D. A. & Sauer, J.-D. (2017).** *Listeria monocytogenes* cytosolic metabolism promotes replication, survival, and evasion of innate immunity. *Cellular Microbiology* **19**.

Chen, J., **Cheng, C.**, **Xia, Y.**, **Zhao, H.**, **Fang, C.**, **Shan, Y.**, **Wu, B. & Fang, W. (2011).** Lmo0036, an ornithine and putrescine carbamoyltransferase in *Listeria monocytogenes*, participates in arginine deiminase and agmatine deiminase pathways and mediates acid tolerance. *Microbiology (Reading, England)* **157**, 3150–3161.

Chen, L.-H., **Köseoğlu, V. K.**, **Güvener, Z. T.**, **Myers-Morales, T.**, **Reed, J. M.**, **D'Orazio, S. E. F.**, **Miller, K. W. & Gomelsky, M. (2014).** Cyclic di-GMP-dependent signaling pathways in the pathogenic Firmicute *Listeria monocytogenes*. *PLoS Pathogens* **10**, e1004301.

Chen, S., **Cui, S.**, **McDermott, P. F.**, **Zhao, S.**, **White, D. G.**, **Paulsen, I. & Meng, J. (2007).** Contribution of target gene mutations and efflux to decreased susceptibility of *Salmonella enterica* serovar

Typhimurium to fluoroquinolones and other antimicrobials. *Antimicrobial Agents and Chemotherapy* **51**, 535–542.

Chiara, M., **Caruso, M.**, **D'Erchia, A. M.**, **Manzari, C.**, **Fraccalvieri, R.**, **Goffredo, E.**, **Latorre, L.**, **Miccolupo, A. & Padalino, I. & other authors (2015).** Comparative Genomics of *Listeria Sensu Lato*. Genus-Wide Differences in Evolutionary Dynamics and the Progressive Gain of Complex, Potentially Pathogenicity-Related Traits through Lateral Gene Transfer. *Genome Biology and Evolution* **7**, 2154–2172.

Chiba, S., **Nagai, T.**, **Hayashi, T.**, **Baba, Y.**, **Nagai, S. & Koyasu, S. (2011).** *Listeria*l invasion protein internalin B promotes entry into ileal Peyer's patches *in vivo*. *Microbiology and Immunology* **55**, 123–129.

Chim, N., **Iniguez, A.**, **Nguyen, T. Q. & Goulding, C. W. (2010).** Unusual diheme conformation of the heme-degrading protein from *Mycobacterium tuberculosis*. *Journal of Molecular Biology* **395**, 595–608.

Chowdhury, R., **Sahu, G. K. & Das, J. (1996).** Stress response in pathogenic bacteria. *Journal of Biosciences* **21**, 149–160.

Claverys, J. P. (2001). A new family of high-affinity ABC manganese and zinc permeases. *Research in Microbiology* **152**, 231–243.

Cobb, C. A., **Curtis, G. D.**, **Bansi, D. S.**, **Slade, E.**, **Mehal, W.**, **Mitchell, R. G. & Chapman, R. W. (1996).** Increased prevalence of *Listeria monocytogenes* in the faeces of patients receiving long-term H2-antagonists. *European Journal of Gastroenterology & Hepatology* **8**, 1071–1074.

Collins, M. D., **Wallbanks, S.**, **Lane, D. J.**, **Shah, J.**, **Nietupski, R.**, **Smida, J.**, **Dorsch, M. & Stackebrandt, E. (1991).** Phylogenetic analysis of the genus *Listeria* based on reverse transcriptase sequencing of 16S rRNA. *International Journal of Systematic Bacteriology* **41**, 240–246.

Conlan, J. W. (1996). Early pathogenesis of *Listeria monocytogenes* infection in the mouse spleen. *Journal of Medical Microbiology* **44**, 295–302.

Conlan, J. W. & North, R. J. (1991). Neutrophil-mediated dissolution of infected host cells as a defense strategy against a facultative intracellular bacterium. *The Journal of Experimental Medicine* **174**, 741–744.

Conner, C. P., **Heithoff, D. M.**, **Julio, S. M.**, **Sinsheimer, R. L. & Mahan, M. J. (1998).** Differential patterns of acquired virulence genes distinguish *Salmonella* strains. *Proceedings of the National Academy of Sciences of the United States of America* **95**, 4641–4645.

Conte, M. P., **Longhi, C.**, **Petrone, G.**, **Polidoro, M.**, **Valenti, P. & Seganti, L. (2000).** Modulation of *actA* gene expression in *Listeria monocytogenes* by iron. *Journal of Medical Microbiology* **49**, 681–683.

Conte, M. P., **Longhi, C.**, **Polidoro, M.**, **Petrone, G.**, **Buonfiglio, V.**, **Di Santo, S.**, **Papi, E.**, **Seganti, L.**, **Visca, P. & Valenti, P. (1996).** Iron availability affects entry of *Listeria monocytogenes* into the enterocytelike cell line Caco-2. *Infection and Immunity* **64**, 3925–3929.

Corbett, D., **Goldrick, M.**, **Fernandes, V. E.**, **Davidge, K.**, **Poole, R. K.**, **Andrew, P. W.**, **Cavet, J. & Roberts, I. S. (2017).** *Listeria monocytogenes* has both a bd-type and an aa3 -type terminal oxidase which allow growth in different oxygen levels and both are important in infection. *Infection and Immunity*.

Corr, S., **Hill, C. & Gahan, C. G. M. (2006).** An *in vitro* cell-culture model demonstrates internalin- and hemolysin-independent translocation of *Listeria monocytogenes* across M cells. *Microbial Pathogenesis* **41**, 241–250.

Corr, S. C., **Gahan, C. C. G. M. & Hill, C. (2008).** M-cells. Origin, morphology and role in mucosal immunity and microbial pathogenesis. *FEMS Immunology and Medical Microbiology* **52**, 2–12.

Corr, S. C., **Gahan, C. G. M. & Hill, C. (2007b).** Impact of selected *Lactobacillus* and *Bifidobacterium* species on *Listeria monocytogenes* infection and the mucosal immune response. *FEMS Immunology and Medical Microbiology* **50**, 380–388.

Corr, S. C., **Li, Y.**, **Riedel, C. U.**, **O'Toole, P. W.**, **Hill, C. & Gahan, C. G. M. (2007a).** Bacteriocin production as a mechanism for the antiinfective activity of *Lactobacillus salivarius* UCC118. *Proceedings of the National Academy of Sciences of the United States of America* **104**, 7617–7621.

Cossart, P. (1988). The listeriolysin O gene. A chromosomal locus crucial for the virulence of *Listeria monocytogenes*. *Infection* **16 Suppl 2**, S157-9.

Cossart, P. & Toledo-Arana, A. (2008). *Listeria monocytogenes*, a unique model in infection biology. An overview. *Microbes and Infection* **10**, 1041–1050.

Cotter, P. D., **Gahan, C. G. & Hill, C. (2001a).** A glutamate decarboxylase system protects *Listeria monocytogenes* in gastric fluid. *Molecular Microbiology* **40**, 465–475.

Cotter, P. D. & Hill, C. (2003). Surviving the acid test. Responses of gram-positive bacteria to low pH. *Microbiology and molecular biology reviews: Microbiology and Molecular Biology Reviews* **67**, 429-53.

Cotter, P. D., **O'Reilly, K. & Hill, C. (2001b).** Role of the glutamate decarboxylase acid resistance system in the survival of *Listeria monocytogenes* LO28 in low pH foods. *Journal of Food Protection* **64**, 1362–1368.

Cotter, P. D., **Ryan, S.**, **Gahan, C. G. M. & Hill, C. (2005).** Presence of GadD1 glutamate decarboxylase in selected *Listeria monocytogenes* strains is associated with an ability to grow at low pH. *Applied and Environmental Microbiology* **71**, 2832–2839.

Coulter, S. N., **Schwan, W. R.**, **Ng, E. Y.**, **Langhorne, M. H.**, **Ritchie, H. D.**, **Westbrock-Wadman, S.**, **Hufnagle, W. O.**, **Folger, K. R.**, **Bayer, A. S. & Stover, C. K. (1998).** *Staphylococcus aureus* genetic loci impacting growth and survival in multiple infection environments. *Molecular Microbiology* **30**, 393–404.

Cousens, L. P. & Wing, E. J. (2000). Innate defenses in the liver during *Listeria* infection. *Immunological Reviews* **174**, 150–159.

Cowart, R. E. (2002). Reduction of iron by extracellular iron reductases. Implications for microbial iron acquisition. *Archives of Biochemistry and Biophysics* **400**, 273–281.

Cowart, R. E. & Foster, B. G. (1981). The role of iron in the production of hemolysin by *Listeria monocytogenes*. *Current Microbiology* **6**, 287–290.

Cummings, J. H. & Macfarlane, G. T. (1991). The control and consequences of bacterial fermentation in the human colon. *The Journal of Applied Bacteriology* **70**, 443–459.

Cummins, A. J., **Fielding, A. K. & McLauchlin, J. (1994).** *Listeria ivanovii* infection in a patient with AIDS. *The Journal of Infection* **28**, 89–91.

Czuprynski, C. J. & Balish, E. (1981). Pathogenesis of *Listeria monocytogenes* for gnotobiotic rats. *Infection and Immunity* **32**, 323–331.

Czuprynski, C. J., **Faith, N. G. & Steinberg, H. (2003).** A/J mice are susceptible and C57BL/6 mice are resistant to *Listeria monocytogenes* infection by intragastric inoculation. *Infection and Immunity* **71**, 682–689.

Dahshan, H., **Merwad, A. M. A. & Mohamed, T. S. (2016).** *Listeria* Species in Broiler Poultry Farms. Potential Public Health Hazards. *Journal of Microbiology and Biotechnology* **26**, 1551–1556.

Dalton, C. B., **Austin, C. C.**, **Sobel, J.**, **Hayes, P. S.**, **Bibb, W. F.**, **Graves, L. M.**, **Swaminathan, B.**, **Proctor, M. E. & Griffin, P. M. (1997).** An outbreak of gastroenteritis and fever due to *Listeria monocytogenes* in milk. *The New England Journal of Medicine* **336**, 100–105.

Dandekar, T. & Eisenreich, W. (2015). Host-adapted metabolism and its regulation in bacterial pathogens. *Frontiers in Cellular and Infection Microbiology* **5**, 28.

Daniel, R., **Bobik, T. A. & Gottschalk, G. (1998).** Biochemistry of coenzyme B_{12}-dependent glycerol and diol dehydratases and organization of the encoding genes. *FEMS Microbiology Reviews* **22**, 553–566.

Daniels, J. J., **Autenrieth, I. B. & Goebel, W. (2000).** Interaction of *Listeria monocytogenes* with the intestinal epithelium. *FEMS Microbiology Letters* **190**, 323–328.

Darwin, A. J. & Miller, V. L. (1999). Identification of *Yersinia enterocolitica* genes affecting survival in an animal host using signature-tagged transposon mutagenesis. *Molecular Microbiology* **32**, 51–62.

Davidson, A. L., **Dassa, E.**, **Orelle, C. & Chen, J. (2008).** Structure, function, and evolution of bacterial ATP-binding cassette systems. *Microbiology and molecular biology reviews: MICROBIOLOGY AND MOLECULAR BIOLOGY REVIEWS* **72**, 317-64, table of contents.

Deloger, M., **El Karoui, M. & Petit, M.-A. (2009).** A genomic distance based on MUM indicates discontinuity between most bacterial species and genera. *Journal of Bacteriology* **191**, 91–99.

den Bakker, H. C., **Bundrant, B. N.**, **Fortes, E. D.**, **Orsi, R. H. & Wiedmann, M. (2010).** A population genetics-based and phylogenetic approach to understanding the evolution of virulence in the genus *Listeria*. *Applied and Environmental Microbiology* **76**, 6085–6100.

den Bakker, H. C., **Cummings, C. A.**, **Ferreira, V.**, **Vatta, P.**, **Orsi, R. H.**, **Degoricija, L.**, **Barker, M.**, **Petrauskene, O.**, **Furtado, M. R. & Wiedmann, M. (2010).** Comparative genomics of the bacterial genus *Listeria*. Genome evolution is characterized by limited gene acquisition and limited gene loss. *BMC Genomics* **11**, 688.

den Bakker, H. C., **Manuel, C. S.**, **Fortes, E. D.**, **Wiedmann, M. & Nightingale, K. K. (2013).** Genome sequencing identifies *Listeria fleischmannii* subsp. *coloradonensis* subsp. nov., isolated from a ranch. *International Journal of Systematic and Evolutionary Microbiology* **63**, 3257–3268.

den Bakker, H. C., **Warchocki, S.**, **Wright, E. M.**, **Allred, A. F.**, **Ahlstrom, C.**, **Manuel, C. S.**, **Stasiewicz, M. J.**, **Burrell, A. & Roof, S. & other authors (2014).** *Listeria floridensis* sp. nov., *Listeria aquatica* sp. nov., *Listeria cornellensis* sp. nov., *Listeria riparia* sp. nov. and *Listeria grandensis* sp. nov., from agricultural and natural environments. *International Journal of Systematic and Evolutionary Microbiology* **64**, 1882–1889.

Detmers, F. J., **Lanfermeijer, F. C. & Poolman, B. (2001).** Peptides and ATP binding cassette peptide transporters. *Research in Microbiology* **152**, 245–258.

Disson, O., **Grayo, S.**, **Huillet, E.**, **Nikitas, G.**, **Langa-Vives, F.**, **Dussurget, O.**, **Ragon, M.**, **Le Monnier, A. & Babinet, C. & other authors (2008).** Conjugated action of two species-specific invasion proteins for fetoplacental listeriosis. *Nature* **455**, 1114–1118.

Donnelly, C. W. (2001). *Listeria monocytogenes*. A continuing challenge. *Nutrition Reviews* **59**, 183–194.

Dons, L., **Eriksson, E.**, **Jin, Y.**, **Rottenberg, M. E.**, **Kristensson, K.**, **Larsen, C. N.**, **Bresciani, J. & Olsen, J. E. (2004).** Role of flagellin and the two-component CheA/CheY system of *Listeria monocytogenes* in host cell invasion and virulence. *Infection and Immunity* **72**, 3237–3244.

D'Orazio, S. E. F. (2014). Animal models for oral transmission of *Listeria monocytogenes*. *Frontiers in Cellular and Infection Microbiology* **4**, 15.

Dowd, G. C., **Joyce, S. A.**, **Hill, C. & Gahan, C. G. M. (2011).** Investigation of the mechanisms by which *Listeria monocytogenes* grows in porcine gallbladder bile. *Infection and Immunity* **79**, 369–379.

Dramsi, S., **Biswas, I.**, **Maguin, E.**, **Braun, L.**, **Mastroeni, P. & Cossart, P. (1995).** Entry of *Listeria monocytogenes* into hepatocytes requires expression of InIB, a surface protein of the internalin multigene family. *Molecular Microbiology* **16**, 251–261.

Dramsi, S., **Bourdichon, F.**, **Cabanes, D.**, **Lecuit, M.**, **Fsihi, H. & Cossart, P. (2004).** FbpA, a novel multifunctional *Listeria monocytogenes* virulence factor. *Molecular Microbiology* **53**, 639–649.

Dramsi, S., **Dehoux, P.**, **Lebrun, M.**, **Goossens, P. L. & Cossart, P. (1997).** Identification of four new members of the internalin multigene family of *Listeria monocytogenes* EGD. *Infection and Immunity* **65**, 1615–1625.

Drevets, D. A., **Dillon, M. J.**, **Schawang, J. S.**, **van Rooijen, N.**, **Ehrchen, J.**, **Sunderkötter, C. & Leenen, P. J. M. (2004).** The Ly-6Chigh monocyte subpopulation transports *Listeria monocytogenes* into the brain during systemic infection of mice. *Journal of Immunology (Baltimore, Md.: 1950)* **172**, 4418–4424.

Dussurget, O. (2008). New insights into determinants of *Listeria monocytogenes* virulence. *International Review of Cell and Molecular Biology* **270**, 1–38.

Dussurget, O., **Cabanes, D.**, **Dehoux, P.**, **Lecuit, M.**, **Buchrieser, C.**, **Glaser, P. & Cossart, P. (2002).** *Listeria monocytogenes* bile salt hydrolase is a PrfA-regulated virulence factor involved in the intestinal and hepatic phases of listeriosis. *Molecular Microbiology* **45**, 1095–1106.

EFSA Journal (2016). The European Union summary report on trends and sources of zoonoses, zoonotic agents and food-borne outbreaks in 2015. *EFS2* **14**, 148.

Eisenreich, W., **Dandekar, T.**, **Heesemann, J. & Goebel, W. (2010).** Carbon metabolism of intracellular bacterial pathogens and possible links to virulence. *Nature Reviews: Microbiology* **8**, 401–412.

Eisenreich, W., **Heesemann, J.**, **Rudel, T. & Goebel, W. (2015).** Metabolic Adaptations of Intracellullar Bacterial Pathogens and their Mammalian Host Cells during Infection ("Pathometabolism"). *Microbiology Spectrum* **3**.

Eisenreich, W., **Slaghuis, J.**, **Laupitz, R.**, **Bussemer, J.**, **Stritzker, J.**, **Schwarz, C.**, **Schwarz, R.**, **Dandekar, T.**, **Goebel, W. & Bacher, A. (2006).** ^{13}C isotopologue perturbation studies of *Listeria monocytogenes* carbon metabolism and its modulation by the virulence regulator PrfA. *Proceedings of the National Academy of Sciences of the United States of America* **103**, 2040–2045.

Escolar, L., **Pérez-Martín, J. & Lorenzo, V.** de **(1999).** Opening the iron box. Transcriptional metalloregulation by the Fur protein. *Journal of Bacteriology* **181**, 6223–6229.

Eylert, E., **Schär, J.**, **Mertins, S.**, **Stoll, R.**, **Bacher, A.**, **Goebel, W. & Eisenreich, W. (2008).** Carbon metabolism of *Listeria monocytogenes* growing inside macrophages. *Molecular Microbiology* **69**, 1008–1017.

Faber, F., **Thiennimitr, P.**, **Spiga, L.**, **Byndloss, M. X.**, **Litvak, Y.**, **Lawhon, S.**, **Andrews-Polymenis, H. L.**, **Winter, S. E. & Bäumler, A. J. (2017).** Respiration of Microbiota-Derived 1,2-propanediol Drives *Salmonella* Expansion during Colitis. *PLoS Pathogens* **13**, e1006129.

FAO/WHO (2004). Risk assessment of *Listeria monocytogenes* in ready-to-eat foods. *Microbiological Risk Assessment Series No. 5.*

Farber, J. M. & Peterkin, P. I. (1991). *Listeria monocytogenes*, a food-borne pathogen. *Microbiological Reviews* **55**, 476–511.

Farber, J. M., **Ross, W. H. & Harwig, J. (1996).** Health risk assessment of *Listeria monocytogenes* in Canada. *International Journal of Food Microbiology* **30**, 145–156.

Farber, J. M., **SANDERS, G. W. & JOHNSTON, M. A. (1989).** A Survey of Various Foods for the Presence of *Listeria* Species. *Journal of Food Protection* **52**, 456–458.

Feehily, C., **Finnerty, A.**, **Casey, P. G.**, **Hill, C.**, **Gahan, C. G. M.**, **O'Byrne, C. P. & Karatzas, K.-A. G. (2014).** Divergent evolution of the activity and regulation of the glutamate decarboxylase systems in *Listeria monocytogenes* EGD-e and 10403S. Roles in virulence and acid tolerance. *PloS One* **9**, e112649.

Ferrari, E., **Walter, M. C.**, **Huptas, C.**, **Scherer, S. & Müller-Herbst, S. (2017).** Complete Circular Genome Sequence and Temperature Independent Adaptation to Anaerobiosis of *Listeria weihenstephanensis* DSM 24698. *Frontiers in Microbiology* **8**, 1672.

Flint, H. J., **Scott, K. P.**, **Duncan, S. H.**, **Louis, P. & Forano, E. (2012).** Microbial degradation of complex carbohydrates in the gut. *Gut Microbes* **3**, 289–306.

Frank, D. N., **St Amand, A. L.**, **Feldman, R. A.**, **Boedeker, E. C.**, **Harpaz, N. & Pace, N. R. (2007).** Molecular-phylogenetic characterization of microbial community imbalances in human inflammatory bowel diseases. *Proceedings of the National Academy of Sciences of the United States of America* **104**, 13780–13785.

Fraser, K. R., **Harvie, D.**, **Coote, P. J. & O'Byrne, C. P. (2000).** Identification and characterization of an ATP binding cassette L-carnitine transporter in *Listeria monocytogenes*. *Applied and Environmental Microbiology* **66**, 4696–4704.

Freitag, N. E., **Port, G. C. & Miner, M. D. (2009).** *Listeria monocytogenes* - from saprophyte to intracellular pathogen. *Nature Reviews: Microbiology* **7**, 623–628.

Freter, R., **Brickner, H.**, **Botney, M.**, **Cleven, D. & Aranki, A. (1983).** Mechanisms That Control Bacterial Populations in Continuous-Flow Culture Models of Mouse Large Intestinal Flora. *Infection and Immunity* **39**, 676–685.

Frye, D. M., **Zweig, R.**, **Sturgeon, J.**, **Tormey, M.**, **LeCavalier, M.**, **Lee, I.**, **Lawani, L. & Mascola, L. (2002).** An outbreak of febrile gastroenteritis associated with delicatessen meat contaminated with *Listeria monocytogenes*. *Clinical infectious diseases: an official publication of the Infectious Diseases Society of America* **35**, 943–949.

Fuchs, T. M., **Eisenreich, W.**, **Heesemann, J. & Goebel, W. (2012a).** Metabolic adaptation of human pathogenic and related nonpathogenic bacteria to extra- and intracellular habitats. *FEMS Microbiology Reviews* **36**, 435–462.

Fuchs, T. M., **Eisenreich, W.**, **Kern, T. & Dandekar, T. (2012b).** Toward a Systemic Understanding of *Listeria monocytogenes* Metabolism during Infection. *Frontiers in Microbiology* **3**, 23.

Gahan, C. G. M. & Hill, C. (2005). Gastrointestinal phase of *Listeria monocytogenes* infection. *Journal of Applied Microbiology* **98**, 1345–1353.

Gahan, C. G. M. & Hill, C. (2014). *Listeria monocytogenes*. Survival and adaptation in the gastrointestinal tract. *Frontiers in Cellular and Infection Microbiology* **4**, 9.

Gaillard, J. L., **Berche, P.**, **Frehel, C.**, **Gouin, E. & Cossart, P. (1991).** Entry of *L. monocytogenes* into cells is mediated by internalin, a repeat protein reminiscent of surface antigens from gram-positive cocci. *Cell* **65**, 1127–1141.

Gaillard, J. L., **Berche, P.**, **Mounier, J.**, **Richard, S. & Sansonetti, P. (1987).** *In vitro* model of penetration and intracellular growth of *Listeria monocytogenes* in the human enterocyte-like cell line Caco-2. *Infection and Immunity* **55**, 2822–2829.

Gaillard, J. L., **Berche, P. & Sansonetti, P. (1986).** Transposon mutagenesis as a tool to study the role of hemolysin in the virulence of *Listeria monocytogenes*. *Infection and Immunity* **52**, 50–55.

Gaillard, J. L. & Finlay, B. B. (1996). Effect of cell polarization and differentiation on entry of *Listeria monocytogenes* into the enterocyte-like Caco-2 cell line. *Infection and Immunity* **64**, 1299–1308.

Gaillard, J. L., **Jaubert, F. & Berche, P. (1996).** The *inlAB* locus mediates the entry of *Listeria monocytogenes* into hepatocytes in vivo. *The Journal of Experimental Medicine* **183**, 359–369.

Gajendran, N., **Mittrücker, H.-W.**, **Bordasch, K.**, **Heinemann, E.**, **Koch, M. & Kaufmann, S. H. E. (2007).** Regional IFNgamma expression is insufficient for efficacious control of food-borne bacterial pathogens at the gut epithelial barrier. *International Immunology* **19**, 1075–1081.

Garandeau, C., **Réglier-Poupet, H.**, **Dubail, I.**, **Beretti, J.-L.**, **Berche, P. & Charbit, A. (2002).** The sortase SrtA of *Listeria monocytogenes* is involved in processing of internalin and in virulence. *Infection and Immunity* **70**, 1382–1390.

Gebretsadik, S., **Kassa, T.**, **Alemayehu, H.**, **Huruy, K. & Kebede, N. (2011).** Isolation and characterization of *Listeria monocytogenes* and other *Listeria* species in foods of animal origin in Addis Ababa, Ethiopia. *Journal of Infection and Public Health* **4**, 22–29.

Gentleman, R. C., **Carey, V. J.**, **Bates, D. M.**, **Bolstad, B.**, **Dettling, M.**, **Dudoit, S.**, **Ellis, B.**, **Gautier, L. & Ge, Y. & other authors (2004).** Bioconductor: open software development for computational biology and bioinformatics. *Genome Biology* **5**, R80.

Geoffroy, C., **Raveneau, J.**, **Beretti, J. L.**, **Lecroisey, A.**, **Vazquez-Boland, J. A.**, **Alouf, J. E. & Berche, P. (1991).** Purification and characterization of an extracellular 29-kilodalton phospholipase C from *Listeria monocytogenes*. *Infection and Immunity* **59**, 2382–2388.

Gill, S. R., **Pop, M.**, **Deboy, R. T.**, **Eckburg, P. B.**, **Turnbaugh, P. J.**, **Samuel, B. S.**, **Gordon, J. I.**, **Relman, D. A.**, **Fraser-Liggett, C. M. & Nelson, K. E. (2006).** Metagenomic analysis of the human distal gut microbiome. *Science (New York, N.Y.)* **312**, 1355–1359.

Gilot, P., **André, P. & Content, J. (1999).** *Listeria monocytogenes* possesses adhesins for fibronectin. *Infection and Immunity* **67**, 6698–6701.

Gilot, P., **Jossin, Y. & Content, J. (2000).** Cloning, sequencing and characterisation of a *Listeria monocytogenes* gene encoding a fibronectin-binding protein. *Journal of Medical Microbiology* **49**, 887–896.

Glaser, P., **Frangeul, L.**, **Buchrieser, C.**, **Rusniok, C.**, **Amend, A.**, **Baquero, F.**, **Berche, P.**, **Bloecker, H. & Brandt, P. & other authors (2001).** Comparative genomics of *Listeria* species. *Science (New York, N.Y.)* **294**, 849–852.

Goecks, J., **Nekrutenko, A. & Taylor, J. (2010).** Galaxy: a comprehensive approach for supporting accessible, reproducible, and transparent computational research in the life sciences. *Genome Biology* **11**, R86.

Goodwin, S., **McPherson, J. D. & McCombie, W. R. (2016).** Coming of age. Ten years of next-generation sequencing technologies. *Nature Reviews Genetics* **17**, 333.

Goris, J., **Konstantinidis, K. T.**, **Klappenbach, J. A.**, **Coenye, T.**, **Vandamme, P. & Tiedje, J. M. (2007).** DNA-DNA hybridization values and their relationship to whole-genome sequence similarities. *International Journal of Systematic and Evolutionary Microbiology* **57**, 81–91.

Graves, L. M., **Helsel, L. O.**, **Steigerwalt, A. G.**, **Morey, R. E.**, **Daneshvar, M. I.**, **Roof, S. E.**, **Orsi, R. H.**, **Fortes, E. D. & Milillo, S. R. & other authors (2010).** *Listeria marthii* sp. nov., isolated from the natural environment, Finger Lakes National Forest. *International Journal of Systematic and Evolutionary Microbiology* **60**, 1280–1288.

Gray, M. J., **Freitag, N. E. & Boor, K. J. (2006).** How the bacterial pathogen *Listeria monocytogenes* mediates the switch from environmental Dr. Jekyll to pathogenic Mr. Hyde. *Infection and Immunity* **74**, 2505–2512.

Gregory, S. H., **Cousens, L. P.**, **van Rooijen, N.**, **Döpp, E. A.**, **Carlos, T. M. & Wing, E. J. (2002).** Complementary adhesion molecules promote neutrophil-Kupffer cell interaction and the elimination of bacteria taken up by the liver. *Journal of Immunology (Baltimore, Md.:1950)* **168**, 308–315.

Gregory, S. H., **Jiang, X. & Wing, E. J. (1996b).** Lymphokine-activated killer cells lyse *Listeria*-infected hepatocytes and produce elevated quantities of interferon-gamma. *Journal of Infectious Diseases* **174**, 1073–1079.

Gregory, S. H., **Sagnimeni, A. J. & Wing, E. J. (1996a).** Bacteria in the bloodstream are trapped in the liver and killed by immigrating neutrophils. *Journal of Immunology (Baltimore, Md.: 1950)* **157**, 2514–2520.

Greiffenberg, L., **Goebel, W.**, **Kim, K. S.**, **Weiglein, I.**, **Bubert, A.**, **Engelbrecht, F.**, **Stins, M. & Kuhn, M. (1998).** Interaction of *Listeria monocytogenes* with human brain microvascular endothelial cells. InlB-dependent invasion, long-term intracellular growth, and spread from macrophages to endothelial cells. *Infection and Immunity* **66**, 5260–5267.

Greiffenberg, L., **Sokolovic, Z.**, **Schnittler, H. J.**, **Spory, A.**, **Böckmann, R.**, **Goebel, W. & Kuhn, M. (1997).** *Listeria monocytogenes*-infected human umbilical vein endothelial cells. Internalin-independent invasion, intracellular growth, movement, and host cell responses. *FEMS Microbiology Letters* **157**, 163–170.

Grif, K., **Patscheider, G.**, **Dierich, M. P. & Allerberger, F. (2003).** Incidence of fecal carriage of *Listeria monocytogenes* in three healthy volunteers. A one-year prospective stool survey. *European journal of clinical microbiology & infectious diseases: official publication of the European Society of Clinical Microbiology* **22**, 16–20.

Grubmüller, S., **Schauer, K.**, **Goebel, W.**, **Fuchs, T. M. & Eisenreich, W. (2014).** Analysis of carbon substrates used by *Listeria monocytogenes* during growth in J774A.1 macrophages suggests a bipartite intracellular metabolism. *Frontiers in Cellular and Infection Microbiology* **4**, 156.

Gründling, A., **Burrack, L. S.**, **Bouwer, H. G. A. & Higgins, D. E. (2004).** *Listeria monocytogenes* regulates flagellar motility gene expression through MogR, a transcriptional repressor required for virulence. *Proceedings of the National Academy of Sciences* **101**, 12318–12323.

Guarner, F. & Malagelada, J.-R. (2003). Gut flora in health and disease. *Lancet (London, England)* **361**, 512–519.

Guex, N., **Peitsch, M. C. & Schwede, T. (2009).** Automated comparative protein structure modeling with SWISS-MODEL and Swiss-PdbViewer. A historical perspective. *Electrophoresis* **30 Suppl 1**, S162-73.

Guillet, C., **Join-Lambert, O.**, **Le Monnier, A.**, **Leclercq, A.**, **Mechaï, F.**, **Mamzer-Bruneel, M. F.**, **Bielecka, M. K.**, **Scortti, M. & Disson, O. & other authors (2010).** Human listeriosis caused by *Listeria* ivanovii. *Emerging Infectious Diseases* **16**, 136–138.

Haber, A., **Friedman, S.**, **Lobel, L.**, **Burg-Golani, T.**, **Sigal, N.**, **Rose, J.**, **Livnat-Levanon, N.**, **Lewinson, O. & Herskovits, A. A. (2017).** L-glutamine Induces Expression of *Listeria monocytogenes* Virulence Genes. *PLoS Pathogens* **13**, e1006161.

Hain, T., **Chatterjee, S. S.**, **Ghai, R.**, **Kuenne, C. T.**, **Billion, A.**, **Steinweg, C.**, **Domann, E.**, **Kärst, U. & Jänsch, L. & other authors (2007).** Pathogenomics of *Listeria* spp. *International Journal of Medical Microbiology: IJMM* **297**, 541–557.

Hain, T., **Ghai, R.**, **Billion, A.**, **Kuenne, C. T.**, **Steinweg, C.**, **Izar, B.**, **Mohamed, W.**, **Mraheil, M. A. & Domann, E. & other authors (2012).** Comparative genomics and transcriptomics of lineages I, II, and III strains of *Listeria monocytogenes*. *BMC Genomics* **13**, 144.

Hain, T., **Steinweg, C. & Chakraborty, T. (2006).** Comparative and functional genomics of *Listeria* spp. *Journal of Biotechnology* **126**, 37–51.

Hain, T., **Steinweg, C.**, **Kuenne, C. T.**, **Billion, A.**, **Ghai, R.**, **Chatterjee, S. S.**, **Domann, E.**, **Kärst, U. & Goesmann, A. & other authors (2006).** Whole-genome sequence of *Listeria welshimeri* reveals common steps in genome reduction with *Listeria innocua* as compared to *Listeria monocytogenes*. *Journal of Bacteriology* **188**, 7405–7415.

Hamon, M., **Bierne, H. & Cossart, P. (2006).** *Listeria monocytogenes*. A multifaceted model. *Nature Reviews: Microbiology* **4**, 423–434.

Hamon, M. A., **Ribet, D.**, **Stavru, F. & Cossart, P. (2012).** Listeriolysin O. The Swiss army knife of *Listeria*. *Trends in Microbiology* **20**, 360–368.

Hanahan, D. (1983). Studies on transformation of *Escherichia coli* with plasmids. *Journal of Molecular Biology* **166**, 557–580.

Hansson, G. C. (2012). Role of mucus layers in gut infection and inflammation. *Current Opinion in Microbiology* **15**, 57–62.

Harvey, P. C., **Watson, M.**, **Hulme, S.**, **Jones, M. A.**, **Lovell, M.**, **Berchieri, A.**, **Young, J.**, **Bumstead, N. & Barrow, P. (2011).** *Salmonella enterica* serovar Typhimurium colonizing the lumen of the chicken intestine grows slowly and upregulates a unique set of virulence and metabolism genes. *Infection and Immunity* **79**, 4105–4121.

Hautefort, I., **Thompson, A.**, **Eriksson-Ygberg, S.**, **Parker, M. L.**, **Lucchini, S.**, **Danino, V.**, **Bongaerts, R. J. M.**, **Ahmad, N.**, **Rhen, M. & Hinton, J. C. D. (2008).** During infection of epithelial cells *Salmonella enterica* serovar Typhimurium undergoes a time-dependent transcriptional adaptation that results in simultaneous expression of three type 3 secretion systems. *Cellular Microbiology* **10**, 958–984.

Havell, E. A., **Beretich, G. R. & Carter, P. B. (1999).** The mucosal phase of *Listeria* infection. *Immunobiology* **201**, 164–177.

Havemann, G. D. & Bobik, T. A. (2003). Protein content of polyhedral organelles involved in coenzyme B_{12}-dependent degradation of 1,2-propanediol in *Salmonella enterica* serovar Typhimurium LT2. *Journal of Bacteriology* **185**, 5086–5095.

Hay, A. J. & Zhu, J. (2016). In Sickness and in Health. The Relationships Between Bacteria and Bile in the Human Gut. *Advances in Applied Microbiology* **96**, 43–64.

He, G., **Shankar, R. A.**, **Chzhan, M.**, **Samouilov, A.**, **Kuppusamy, P. & Zweier, J. L. (1999).** Noninvasive measurement of anatomic structure and intraluminal oxygenation in the gastrointestinal tract of living mice with spatial and spectral EPR imaging. *Proceedings of the National Academy of Sciences of the United States of America* **96**, 4586–4591.

Heithoff, D. M., **Conner, C. P.**, **Hentschel, U.**, **Govantes, F.**, **Hanna, P. C. & Mahan, M. J. (1999).** Coordinate intracellular expression of *Salmonella* genes induced during infection. *Journal of Bacteriology* **181**, 799–807.

Hoelzer, K., **Pouillot, R. & Dennis, S. (2012).** Animal models of listeriosis. A comparative review of the current state of the art and lessons learned. *Veterinary Research* **43**, 18.

Hof, H. (2001). *Listeria monocytogenes*. A causative agent of gastroenteritis? *European journal of clinical microbiology & infectious diseases: official publication of the European Society of Clinical Microbiology* **20**, 369–373.

Hof, H. & Hefner, P. (1988). Pathogenicity of *Listeria monocytogenes* in comparison to other *Listeria* species. *Infection* **16 Suppl 2**, S141-4.

Hofmann, A. F. & Eckmann, L. (2006). How bile acids confer gut mucosal protection against bacteria. *Proceedings of the National Academy of Sciences* **103**, 4333–4334.

Hooper, L. V., **Midtvedt, T. & Gordon, J. I. (2002).** How host-microbial interactions shape the nutrient environment of the mammalian intestine. *Annual Review of Nutrition* **22**, 283–307.

Hooper, L. V., **Xu, J.**, **Falk, P. G.**, **Midtvedt, T. & Gordon, J. I. (1999).** A molecular sensor that allows a gut commensal to control its nutrient foundation in a competitive ecosystem. *Proceedings of the National Academy of Sciences* **96**, 9833–9838.

Horswill, A. R. & Escalante-Semerena, J. C. (1999). *Salmonella* Typhimurium LT2 catabolizes propionate via the 2-methylcitric acid cycle. *Journal of Bacteriology* **181**, 5615–5623.

Hosie, A. H. & Poole, P. S. (2001). Bacterial ABC transporters of amino acids. *Research in Microbiology* **152**, 259–270.

Huang, B., **Eglezos, S.**, Heron B., **Smith, H.**, **Graham, T.**, **Bates, J. & Savill, J. (2007).** Comparison of multiplex PCR with conventional biochemical methods for the identification of *Listeria* spp. isolates from food and clinical samples in Queensland, Australia. *Journal of Food Protection* **70**, 1874–1880.

Hulo, N., **Bairoch, A.**, **Bulliard, V.**, **Cerutti, L.**, **Cuche, B. A.**, **Castro, E.** de, **Lachaize, C.**, **Langendijk-Genevaux, P. S. & Sigrist, C. J. A. (2008).** The 20 years of PROSITE. *Nucleic Acids Research* **36**, D245-9.

Huptas, C., **Scherer, S. & Wenning, M. (2016).** Optimized Illumina PCR-free library preparation for bacterial whole genome sequencing and analysis of factors influencing de novo assembly. *BMC Research Notes* **9**, 269.

Husu, J. R. (1990). Epidemiological studies on the occurrence of *Listeria monocytogenes* in the feces of dairy cattle. *Zentralblatt fur Veterinarmedizin. Reihe B. Journal of Veterinary Medicine. Series B* **37**, 276–282.

Ike, Y. (2017). Pathogenicity of Enterococci. *Nihon saikingaku zasshi. Japanese Journal of Bacteriology* **72**, 189–211.

Inoue, S., **Iida, T.**, **Tanikawa, T.**, **Maruyama, T. & Morita, C. (1991).** Isolation of *Listeria monocytogenes* from roof rats (Rattus rattus) in buildings in Tokyo. *The Journal of Veterinary Medical Science* **53**, 521–522.

Iurov, D. S., **Varfolomeev, A. F.**, **Tukhvatulin, A. I.**, **Logunov, D. I.**, **Naroditskiĭ, B. S. & Ermolaeva, S. A. (2012).** Contribution of L,D-carboxypeptidases in virulence of facultative intracellular pathogenic bacteria *Listeria monocytogenes*. *Zhurnal mikrobiologii, epidemiologii, i immunobiologii*, 15–20.

Ivy, R. A., **Chan, Y. C.**, **Bowen, B. M.**, **Boor, K. J. & Wiedmann, M. (2010).** Growth temperature-dependent contributions of response regulators, σB, PrfA, and motility factors to *Listeria monocytogenes* invasion of Caco-2 cells. *Foodborne Pathogens and Disease* **7**, 1337–1349.

Jang, M. H., **Kweon, M.-N.**, **Iwatani, K.**, **Yamamoto, M.**, **Terahara, K.**, **Sasakawa, C.**, **Suzuki, T.**, **Nochi, T. & Yokota, Y. & other authors (2004).** Intestinal villous M cells. An antigen entry site in the mucosal epithelium. *Proceedings of the National Academy of Sciences* **101**, 6110–6115.

Jaradat, Z. W. & Bhunia, A. K. (2003). Adhesion, invasion, and translocation characteristics of *Listeria monocytogenes* serotypes in Caco-2 cell and mouse models. *Applied and Environmental Microbiology* **69**, 3640–3645.

Jin, B., **Newton, S. M. C.**, **Shao, Y.**, **Jiang, X.**, **Charbit, A. & Klebba, P. E. (2006).** Iron acquisition systems for ferric hydroxamates, haemin and haemoglobin in *Listeria monocytogenes*. *Molecular Microbiology* **59**, 1185–1198.

Johansson, J., **Mandin, P.**, **Renzoni, A.**, **Chiaruttini, C.**, **Springer, M. & Cossart, P. (2002).** An RNA thermosensor controls expression of virulence genes in *Listeria monocytogenes*. *Cell* **110**, 551–561.

Johansson, M. E. V., **Phillipson, M.**, **Petersson, J.**, **Velcich, A.**, **Holm, L. & Hansson, G. C. (2008).** The inner of the two Muc2 mucin-dependent mucus layers in colon is devoid of bacteria. *Proceedings of the National Academy of Sciences of the United States of America* **105**, 15064–15069.

Johnson, J., **Jinneman, K.**, **Stelma, G.**, **Smith, B. G.**, **Lye, D.**, **Messer, J.**, **Ulaszek, J.**, **Evsen, L. & Gendel, S. & other authors (2004).** Natural atypical *Listeria innocua* strains with *Listeria monocytogenes* pathogenicity island 1 genes. *Applied and Environmental Microbiology* **70**, 4256–4266.

Jones, B. V., **Begley, M.**, **Hill, C.**, **Gahan, C. G. M. & Marchesi, J. R. (2008).** Functional and comparative metagenomic analysis of bile salt hydrolase activity in the human gut microbiome. *Proceedings of the National Academy of Sciences of the United States of America* **105**, 13580–13585.

Jones, G. S., **Bussell, K. M.**, **Myers-Morales, T.**, **Fieldhouse, A. M.**, **Bou Ghanem, E. N. & D'Orazio, S. E. F. (2015).** Intracellular *Listeria monocytogenes* comprises a minimal but vital fraction of the intestinal burden following foodborne infection. *Infection and Immunity* **83**, 3146–3156.

Jones, G. S. & D'Orazio, S. E. F. (2017). Monocytes Are the Predominant Cell Type Associated with *Listeria monocytogenes* in the Gut, but They Do Not Serve as an Intracellular Growth Niche. *Journal of Immunology (Baltimore, Md.: 1950)* **198**, 2796–2804.

Joseph, B. & Goebel, W. (2007). Life of *Listeria monocytogenes* in the host cells' cytosol. *Microbes and Infection* **9**, 1188–1195.

Joseph, B., **Przybilla, K.**, **Stühler, C.**, **Schauer, K.**, **Slaghuis, J.**, **Fuchs, T. M. & Goebel, W. (2006).** Identification of *Listeria monocytogenes* genes contributing to intracellular replication by expression profiling and mutant screening. *Journal of Bacteriology* **188**, 556–568.

Karlyshev, A. V., **Oyston, P. C.**, **Williams, K.**, **Clark, G. C.**, **Titball, R. W.**, **Winzeler, E. A. & Wren, B. W. (2001).** Application of high-density array-based signature-tagged mutagenesis to discover novel Yersinia virulence-associated genes. *Infection and Immunity* **69**, 7810–7819.

Karpowich, N. K., **Song, J. M.**, **Cocco, N. & Wang, D.-N. (2015).** ATP binding drives substrate capture in an ECF transporter by a release-and-catch mechanism. *Nature Structural & Molecular Biology* **22**, 565–571.

Kaspar, D., **Auer, F.**, **Schardt, J.**, **Schindele, F.**, **Ospina, A.**, **Held, C.**, **Ehrenreich, A.**, **Scherer, S. & Müller-Herbst, S. (2014).** Temperature- and nitrogen source-dependent regulation of GlnR target genes in *Listeria monocytogenes*. *FEMS Microbiology Letters* **355**, 131–141.

Kazmierczak, M. J., **Mithoe, S. C.**, **Boor, K. J. & Wiedmann, M. (2003).** *Listeria monocytogenes* sigma B regulates stress response and virulence functions. *Journal of Bacteriology* **185**, 5722–5734.

Kern, T., **Kutzner, E.**, **Eisenreich, W. & Fuchs, T. M. (2016).** Pathogen-nematode interaction. Nitrogen supply of *Listeria monocytogenes* during growth in *Caenorhabditis elegans*. *Environmental Microbiology Reports* **8**, 20–29.

Khelef, N., **Lecuit, M.**, **Bierne, H. & Cossart, P. (2006).** Species specificity of the *Listeria monocytogenes* InlB protein. *Cellular Microbiology* **8**, 457–470.

Kiefer, F., **Arnold, K.**, **Künzli, M.**, **Bordoli, L. & Schwede, T. (2009).** The SWISS-MODEL Repository and associated resources. *Nucleic Acids Research* **37**, D387-92.

Kim, J., **Wu, S.**, **Tomasiak, T. M.**, **Mergel, C.**, **Winter, M. B.**, **Stiller, S. B.**, **Robles-Colmanares, Y.**, **Stroud, R. M. & Tampé, R. & other authors (2015).** Subnanometre-resolution electron cryomicroscopy structure of a heterodimeric ABC exporter. *Nature* **517**, 396–400.

Kluge, R. & Hof, H. (1986). Zur Virulenz von *Listeria welshimeri*. *Zentralblatt fur Bakteriologie, Mikrobiologie, und Hygiene. Series A, Medical Microbiology, Infectious Diseases, Virology, Parasitology* **262**, 403–411.

Klumpp, J. & Fuchs, T. M. (2007). Identification of novel genes in genomic islands that contribute to *Salmonella* Typhimurium replication in macrophages. *Microbiology (Reading, England)* **153**, 1207–1220.

Knudsen, G. M., **Olsen, J. E. & Dons, L. (2004).** Characterization of DegU, a response regulator in *Listeria monocytogenes*, involved in regulation of motility and contributes to virulence. *FEMS Microbiology Letters* **240**, 171–179.

Ko, R. & Smith, L. T. (1999). Identification of an ATP-driven, osmoregulated glycine betaine transport system in *Listeria monocytogenes*. *Applied and Environmental Microbiology* **65**, 4040–4048.

Konstantinidis, K. T., **Ramette, A. & Tiedje, J. M. (2006).** The bacterial species definition in the genomic era. *Philosophical transactions of the Royal Society of London. Series B, Biological sciences* **361**, 1929–1940.

Konstantinidis, K. T. & Tiedje, J. M. (2005). Genomic insights that advance the species definition for prokaryotes. *Proceedings of the National Academy of Sciences* **102**, 2567–2572.

Konstantinidis, K. T. & Tiedje, J. M. (2007). Prokaryotic taxonomy and phylogeny in the genomic era. Advancements and challenges ahead. *Current Opinion in Microbiology* **10**, 504–509.

Korbel, J. O., **Doerks, T.**, **Jensen, L. J.**, **Perez-Iratxeta, C.**, **Kaczanowski, S.**, **Hooper, S. D.**, **Andrade, M. A. & Bork, P. (2005).** Systematic association of genes to phenotypes by genome and literature mining. *PLoS Biology* **3**, e134.

Kortebi, M., **Milohanic, E.**, **Mitchell, G.**, **Péchoux, C.**, **Prevost, M.-C.**, **Cossart, P. & Bierne, H. (2017).** *Listeria monocytogenes* switches from dissemination to persistence by adopting a vacuolar lifestyle in epithelial cells. *PLoS Pathogens* **13**, e1006734.

Kortman, G. A. M., **Raffatellu, M.**, **Swinkels, D. W. & Tjalsma, H. (2014).** Nutritional iron turned inside out. Intestinal stress from a gut microbial perspective. *FEMS Microbiology Reviews* **38**, 1202–1234.

Köster, W. (2001). ABC transporter-mediated uptake of iron, siderophores, heme and vitamin B_{12}. *Research in Microbiology* **152**, 291–301.

Krawczyk-Balska, A. & Bielecki, J. (2004). Molecular aspects of *Listeria monocytogenes* infection. *Polish Journal of Microbiology* **53 Suppl**, 17–22.

Kutzner, E., **Kern, T.**, **Felsl, A.**, **Eisenreich, W. & Fuchs, T. M. (2016).** Isotopologue profiling of the Listerial N-metabolism. *Molecular Microbiology* **100**, 315–327.

Lammerding, A. M., **Glass, K. A.**, **Gendron-Fitzpatrick, A. & Doyle, M. P. (1992).** Determination of virulence of different strains of *Listeria monocytogenes* and *Listeria innocua* by oral inoculation of pregnant mice. *Applied and Environmental Microbiology* **58**, 3991–4000.

Landstorfer, R., **Simon, S.**, **Schober, S.**, **Keim, D.**, **Scherer, S. & Neuhaus, K. (2014).** Comparison of strand-specific transcriptomes of enterohemorrhagic *Escherichia coli* O157:H7 EDL933 (EHEC) under eleven different environmental conditions including radish sprouts and cattle feces. *BMC Genomics* **15**, 353.

Lang Halter, E., **Neuhaus, K. & Scherer, S. (2013).** *Listeria weihenstephanensis* sp. nov., isolated from the water plant Lemna trisulca taken from a freshwater pond. *International Journal of Systematic and Evolutionary Microbiology* **63**, 641–647.

Langmead, B., **Trapnell, C.**, **Pop, M. & Salzberg, S. L. (2009).** Ultrafast and memory-efficient alignment of short DNA sequences to the human genome. *Genome Biology* **10**, R25.

Larsen, H. E. & Seeliger, H. P. (1966). A mannitol fermenting *Listeria*: *Listeria grayi* sp. n. *Proceedings of the Third International Symposium on Listeriosis, Bilthoven, The Netherlands*.

Lattmann, C., **Schwarzkopf, A. & Seeliger, H. P. (1989).** Pathogenicity testing of *Listeria* strains isolated from food in fertilized hen's eggs. *Zentralblatt fur Bakteriologie, Mikrobiologie, und Hygiene. Series A, Medical Microbiology, Infectious Diseases, Virology, Parasitology* **270**, 400–405.

Latunde-Dada, G. O. (2009). Iron metabolism. Microbes, mouse, and man. *BioEssays: News and Reviews in Molecular, Cellular and Developmental Biology* **31**, 1309–1317.

Lawan, F. A., **Tijjani, A. N.**, **Raufu, A. I.**, **Ameh, J. A.**, **Ngoshe, I. Y. & Auwal, M. S. (2013).** Isolation and characterisation of *Listeria* species from ruminants in Maiduguri north–eastern Nigeria. *African Journal of Biotechnology* **12**.

Lechowicz, J. & Krawczyk-Balska, A. (2015). An update on the transport and metabolism of iron in *Listeria monocytogenes*. The role of proteins involved in pathogenicity. *Biometals: an International Journal on the Role of Metal Ions in Biology, Biochemistry, and Medicine* **28**, 587–603.

Leclercq, A., **Clermont, D.**, **Bizet, C.**, **Grimont, P. A. D.**, **Le Flèche-Matéos, A.**, **Roche, S. M.**, **Buchrieser, C.**, **Cadet-Daniel, V. & Le Monnier, A. & other authors (2010).** *Listeria rocourtiae* sp. nov. *International Journal of Systematic and Evolutionary Microbiology* **60**, 2210–2214.

Lecuit, M., **Dramsi, S.**, **Gottardi, C.**, **Fedor-Chaiken, M.**, **Gumbiner, B. & Cossart, P. (1999).** A single amino acid in E-cadherin responsible for host specificity towards the human pathogen *Listeria monocytogenes*. *The EMBO Journal* **18**, 3956–3963.

Lecuit, M., **Ohayon, H.**, **Braun, L.**, **Mengaud, J. & Cossart, P. (1997).** Internalin of *Listeria monocytogenes* with an intact leucine-rich repeat region is sufficient to promote internalization. *Infection and Immunity* **65**, 5309–5319.

Lecuit, M., **Vandormael-Pournin, S.**, **Lefort, J.**, **Huerre, M.**, **Gounon, P.**, **Dupuy, C.**, **Babinet, C. & Cossart, P. (2001).** A transgenic model for listeriosis. Role of internalin in crossing the intestinal barrier. *Science (New York, N.Y.)* **292**, 1722–1725.

Ledala, N., **Pearson, S. L.**, **Wilkinson, B. J. & Jayaswal, R. K. (2007).** Molecular characterization of the Fur protein of *Listeria monocytogenes*. *Microbiology (Reading, England)* **153**, 1103–1111.

Ledala, N., **Sengupta, M.**, **Muthaiyan, A.**, **Wilkinson, B. J. & Jayaswal, R. K. (2010).** Transcriptomic response of *Listeria monocytogenes* to iron limitation and Fur mutation. *Applied and Environmental Microbiology* **76**, 406–416.

Lelouard, H., **Fallet, M.**, **Bovis, B.** de, **Méresse, S. & Gorvel, J.-P. (2012).** Peyer's patch dendritic cells sample antigens by extending dendrites through M cell-specific transcellular pores. *Gastroenterology* **142**, 592-601.e3.

Lelouard, H., **Henri, S.**, **Bovis, B.** de, **Mugnier, B.**, **Chollat-Namy, A.**, **Malissen, B.**, **Méresse, S. & Gorvel, J.-P. (2010).** Pathogenic bacteria and dead cells are internalized by a unique subset of Peyer's patch dendritic cells that express lysozyme. *Gastroenterology* **138**, 173-84.e1-3.

Li, H., **Handsaker, B.**, **Wysoker, A.**, **Fennell, T.**, **Ruan, J.**, **Homer, N.**, **Marth, G.**, **Abecasis, G. & Durbin, R. (2009).** The Sequence Alignment/Map format and SAMtools. *Bioinformatics (Oxford, England)* **25**, 2078–2079.

Linke, K., **Rückerl, I.**, **Brugger, K.**, **Karpiskova, R.**, **Walland, J.**, **Muri-Klinger, S.**, **Tichy, A.**, **Wagner, M. & Stessl, B. (2014).** Reservoirs of *Listeria* species in three environmental ecosystems. *Applied and Environmental Microbiology* **80**, 5583–5592.

Litwin, C. M. & Calderwood, S. B. (1993). Role of iron in regulation of virulence genes. *Clinical Microbiology Reviews* **6**, 137–149.

Liu, Y., **Leal, N. A.**, **Sampson, E. M.**, **Johnson, C. L. V.**, **Havemann, G. D. & Bobik, T. A. (2007).** PduL is an evolutionarily distinct phosphotransacylase involved in B_{12}-dependent 1,2-propanediol degradation by *Salmonella enterica* serovar Typhimurium LT2. *Journal of Bacteriology* **189**, 1589–1596.

Livak, K. J. & Schmittgen, T. D. (2001). Analysis of relative gene expression data using real-time quantitative PCR and the 2(-Delta Delta C(T)) Method. *Methods (San Diego, Calif.)* **25**, 402–408.

Lopetuso, L. R., **Scaldaferri, F.**, **Petito, V. & Gasbarrini, A. (2013).** Commensal *Clostridia*. Leading players in the maintenance of gut homeostasis. *Gut Pathogens* **5**, 23.

Lungu, B., **Ricke, S. C. & Johnson, M. G. (2009).** Growth, survival, proliferation and pathogenesis of *Listeria monocytogenes* under low oxygen or anaerobic conditions. A review. *Anaerobe* **15**, 7–17.

MacDonald, T. T. & Carter, P. B. (1980). Cell-mediated immunity to intestinal infection. *Infection and Immunity* **28**, 516–523.

MacGowan, A. P., **Bowker, K.**, **McLauchlin, J.**, **Bennett, P. M. & Reeves, D. S. (1994).** The occurrence and seasonal changes in the isolation of *Listeria* spp. in shop bought food stuffs, human faeces, sewage and soil from urban sources. *International Journal of Food Microbiology* **21**, 325–334.

Maier, E., **Anderson, R. C. & Roy, N. C. (2014).** Understanding how commensal obligate anaerobic bacteria regulate immune functions in the large intestine. *Nutrients* **7**, 45–73.

Mainou-Fowler, T., **MacGowan, A. P. & Postlethwaite, R. (1988).** Virulence of *Listeria* spp. Course of infection in resistant and susceptible mice. *Journal of Medical Microbiology* **27**, 131–140.

Marco, A. J., **Altimira, J.**, **Prats, N.**, **López, S.**, **Dominguez, L.**, **Domingo, M. & Briones, V. (1997).** Penetration of *Listeria monocytogenes* in mice infected by the oral route. *Microbial Pathogenesis* **23**, 255–263.

Marco, A. J., **Domingo, M.**, **Prats, M.**, **Briones, V.**, **Pumarola, M. & Dominguez, L. (1991).** Pathogenesis of lymphoid lesions in murine experimental listeriosis. *Journal of Comparative Pathology* **105**, 1–15.

Mariscotti, J. F., **García-del Portillo, F. & Pucciarelli, M. G. (2009).** The *Listeria monocytogenes* sortase-B recognizes varied amino acids at position 2 of the sorting motif. *The Journal of Biological Chemistry* **284**, 6140–6146.

Marr, A. K., **Joseph, B.**, **Mertins, S.**, **Ecke, R.**, **Müller-Altrock, S. & Goebel, W. (2006).** Overexpression of PrfA leads to growth inhibition of *Listeria monocytogenes* in glucose-containing culture media by interfering with glucose uptake. *Journal of Bacteriology* **188**, 3887–3901.

Marteyn, B., **Scorza, F. B.**, **Sansonetti, P. J. & Tang, C. (2011).** Breathing life into pathogens. The influence of oxygen on bacterial virulence and host responses in the gastrointestinal tract. *Cellular Microbiology* **13**, 171–176.

Marteyn, B., **West, N. P.**, **Browning, D. F.**, **Cole, J. A.**, **Shaw, J. G.**, **Palm, F.**, **Mounier, J.**, **Prévost, M.-C.**, **Sansonetti, P. & Tang, C. M. (2010).** Modulation of *Shigella* virulence in response to available oxygen *in vivo*. *Nature* **465**, 355–358.

Martin, F.-P. J., **Wang, Y.**, **Yap, I. K. S.**, **Sprenger, N.**, **Lindon, J. C.**, **Rezzi, S.**, **Kochhar, S.**, **Holmes, E. & Nicholson, J. K. (2009).** Topographical variation in murine intestinal metabolic profiles in relation to microbiome speciation and functional ecological activity. *Journal of Proteome Research* **8**, 3464–3474.

Matern, A., **Pedrolli, D.**, **Großhennig, S.**, **Johansson, J. & Mack, M. (2016).** Uptake and Metabolism of Antibiotics Roseoflavin and 8-Demethyl-8-Aminoriboflavin in Riboflavin-Auxotrophic *Listeria monocytogenes. Journal of Bacteriology* **198**, 3233–3243.

Matthysse, A. G., **Yarnall, H. A. & Young, N. (1996).** Requirement for genes with homology to ABC transport systems for attachment and virulence of *Agrobacterium tumefaciens*. *Journal of Bacteriology* **178**, 5302–5308.

Maury, M. M., **Chenal-Francisque, V.**, **Bracq-Dieye, H.**, **Han, L.**, **Leclercq, A.**, **Vales, G.**, **Moura, A.**, **Gouin, E. & Scortti, M. & other authors (2017).** Spontaneous Loss of Virulence in Natural Populations of *Listeria monocytogenes*. *Infection and Immunity* **85**.

McLauchlin, J. & Rees, C. *Listeria*. Pirie 1940a, 383AL. In *Bergey's Manual of Systematics of Archaea and Bacteria*.

Mekalanos, J. J. (1992). Environmental signals controlling expression of virulence determinants in bacteria. *Journal of Bacteriology* **174**, 1–7.

Mellin, J. R., **Koutero, M.**, **Dar, D.**, **Nahori, M.-A.**, **Sorek, R. & Cossart, P. (2014).** Riboswitches. Sequestration of a two-component response regulator by a riboswitch-regulated noncoding RNA. *Science (New York, N.Y.)* **345**, 940–943.

Mellin, J. R., **Tiensuu, T.**, **Bécavin, C.**, **Gouin, E.**, **Johansson, J. & Cossart, P. (2013).** A riboswitch-regulated antisense RNA in *Listeria monocytogenes*. *Proceedings of the National Academy of Sciences of the United States of America* **110**, 13132–13137.

Melton-Witt, J. A., **Rafelski, S. M.**, **Portnoy, D. A. & Bakardjiev, A. I. (2012).** Oral infection with signature-tagged *Listeria monocytogenes* reveals organ-specific growth and dissemination routes in guinea pigs. *Infection and Immunity* **80**, 720–732.

Mendum, M. L. & Smith, L. T. (2002). Characterization of glycine betaine porter I from *Listeria monocytogenes* and its roles in salt and chill tolerance. *Applied and Environmental Microbiology* **68**, 813–819.

Mengaud, J., **Chenevert, J.**, **Geoffroy, C.**, **Gaillard, J. L. & Cossart, P. (1987).** Identification of the structural gene encoding the SH-activated hemolysin of *Listeria monocytogenes*. Listeriolysin O is homologous to streptolysin O and pneumolysin. *Infection and Immunity* **55**, 3225–3227.

Mengaud, J., **Lecuit, M.**, **Lebrun, M.**, **Nato, F.**, **Mazie, J. C. & Cossart, P. (1996).** Antibodies to the leucine-rich repeat region of internalin block entry of *Listeria monocytogenes* into cells expressing E-cadherin. *Infection and Immunity* **64**, 5430–5433.

Menudier, A., **Bosiraud, C. & Nicolas, J.-A. (1991).** Virulence of *Listeria monocytogenes* Serovars and *Listeria* spp. in Experimental Infection of Mice. *Journal of Food Protection* **54**, 917–921.

Miethke, M. & Marahiel, M. A. (2007). Siderophore-based iron acquisition and pathogen control. *Microbiology and molecular biology reviews* **71**, 413–451.

Milohanic, E., **Glaser, P.**, **Coppée, J.-Y.**, **Frangeul, L.**, **Vega, Y.**, **Vázquez-Boland, J. A.**, **Kunst, F.**, **Cossart, P. & Buchrieser, C. (2003).** Transcriptome analysis of *Listeria monocytogenes* identifies three groups of genes differently regulated by PrfA. *Molecular Microbiology* **47**, 1613–1625.

Milohanic, E., **Jonquières, R.**, **Cossart, P.**, **Berche, P. & Gaillard, J. L. (2001).** The autolysin Ami contributes to the adhesion of *Listeria monocytogenes* to eukaryotic cells via its cell wall anchor. *Molecular Microbiology* **39**, 1212–1224.

Monk, I. R., **Casey, P. G.**, **Cronin, M.**, **Gahan, C. G. & Hill, C. (2008).** Development of multiple strain competitive index assays for *Listeria monocytogenes* using pIMC; a new site-specific integrative vector. *BMC Microbiology* **8**, 96.

Moreno, L. Z., **Paixão, R.**, **Gobbi, D. D. S.** de, **Raimundo, D. C.**, **Porfida Ferreira, T. S.**, **Micke Moreno, A.**, **Hofer, E.**, **dos Reis, C. M. F.**, **Matté, G. R. & Matté, M. H. (2014).** Phenotypic and genotypic characterization of atypical *Listeria monocytogenes* and *Listeria innocua* isolated from swine slaughterhouses and meat markets. *BioMed Research International* **2014**, 742032.

Mühlig, A., **Behr, J.**, **Scherer, S. & Müller-Herbst, S. (2014).** Stress response of **Salmonella enterica** serovar Typhimurium to acidified nitrite. *Applied and Environmental Microbiology* **80**, 6373–6382.

Müller-Herbst, S., **Wüstner, S.**, **Mühlig, A.**, **Eder, D.**, **M Fuchs, T.**, **Held, C.**, **Ehrenreich, A. & Scherer, S. (2014).** Identification of genes essential for anaerobic growth of *Listeria monocytogenes*. *Microbiology (Reading, England)* **160**, 752–765.

Murray, E.G.D., **Webb, R. A. & Swann, H.B.R. (1926).** A disease of rabbits characterized by a large mononuclear leucocytosis caused by a hitherto undescribed bacillus *Bacterium monocytogenes* (n.sp.). *The Journal of Pathology and Microbiology* **29**, 407–439.

Nakamura, S., **Kuda, T.**, **An, C.**, **Kanno, T.**, **Takahashi, H. & Kimura, B. (2012).** Inhibitory effects of *Leuconostoc mesenteroides* 1RM3 isolated from narezushi, a fermented fish with rice, on *Listeria monocytogenes* infection to Caco-2 cells and A/J mice. *Anaerobe* **18**, 19–24.

Nayak, D. N., **Savalia, C. V.**, **Kalyani, I. H.**, **Kumar, R. & Kshirsagar, D. P. (2015).** Isolation, identification, and characterization of *Listeria* spp. from various animal origin foods. *Veterinary World* **8**, 695–701.

Neuenhahn, M., **Kerksiek, K. M.**, **Nauerth, M.**, **Suhre, M. H.**, **Schiemann, M.**, **Gebhardt, F. E.**, **Stemberger, C.**, **Panthel, K. & Schröder, S. & other authors (2006).** CD8alpha+ dendritic cells are required for efficient entry of *Listeria monocytogenes* into the spleen. *Immunity* **25**, 619–630.

Neuhaus, K., **Satorhelyi, P.**, **Schauer, K.**, **Scherer, S. & Fuchs, T. M. (2013).** Acid shock of *Listeria monocytogenes* at low environmental temperatures induces *prfA*, epithelial cell invasion, and lethality towards Caenorhabditis elegans. *BMC Genomics* **14**, 285.

Newton, S. M. C., **Klebba, P. E.**, **Raynaud, C.**, **Shao, Y.**, **Jiang, X.**, **Dubail, I.**, **Archer, C.**, **Frehel, C. & Charbit, A. (2005).** The *svpA-srtB* locus of *Listeria monocytogenes*. Fur-mediated iron regulation and effect on virulence. *Molecular Microbiology* **55**, 927–940.

Nightingale, K. K., **Ivy, R. A.**, **Ho, A. J.**, **Fortes, E. D.**, **Njaa, B. L.**, **Peters, R. M. & Wiedmann, M. (2008).** *inlA* premature stop codons are common among *Listeria monocytogenes* isolates from foods and yield virulence-attenuated strains that confer protection against fully virulent strains. *Applied and Environmental Microbiology* **74**, 6570–6583.

Nikitas, G., **Deschamps, C.**, **Disson, O.**, **Niault, T.**, **Cossart, P. & Lecuit, M. (2011).** Transcytosis of *Listeria monocytogenes* across the intestinal barrier upon specific targeting of goblet cell accessible E-cadherin. *The Journal of Experimental Medicine* **208**, 2263–2277.

Nilsson, L., **Hansen, T. B.**, **Garrido, P.**, **Buchrieser, C.**, **Glaser, P.**, **Knøchel, S.**, **Gram, L. & Gravesen, A. (2005).** Growth inhibition of *Listeria monocytogenes* by a *nonbacteriocinogenic Carnobacterium piscicola*. *Journal of Applied Microbiology* **98**, 172–183.

Notermans, S., **Dufrenne, J.**, **Teunis, P. & Chackraborty, T. (1998).** Studies on the risk assessment of *Listeria monocytogenes*. *Journal of Food Protection* **61**, 244–248.

Notermans, S. H., **Dufrenne, J.**, **Leimeister-Wächter, M.**, **Domann, E. & Chakraborty, T. (1991).** Phosphatidylinositol-specific phospholipase C activity as a marker to distinguish between pathogenic and nonpathogenic *Listeria* species. *Applied and Environmental Microbiology* **57**, 2666–2670.

Ofer, A., **Kreft, J.**, **Logan, D. T.**, **Cohen, G.**, **Borovok, I. & Aharonowitz, Y. (2011).** Implications of the inability of *Listeria monocytogenes* EGD-e to grow anaerobically due to a deletion in the class III NrdD ribonucleotide reductase for its use as a model laboratory strain. *Journal of Bacteriology* **193**, 2931–2940.

Ooi, S. T. & Lorber, B. (2005). Gastroenteritis due to *Listeria monocytogenes*. *Clinical infectious diseases : an official publication of the Infectious Diseases Society of America* **40**, 1327–1332.

Orsi, R. H. & Wiedmann, M. (2016). Characteristics and distribution of *Listeria* spp., including *Listeria* species newly described since 2009. *Applied Microbiology and Biotechnology* **100**, 5273–5287.

Osaili, T. M., **Alaboudi, A. R. & Nesiar, E. A. (2011).** Prevalence of *Listeria* spp. and antibiotic susceptibility of *Listeria monocytogenes* isolated from raw chicken and ready-to-eat chicken products in Jordan. *Food Control* **22**, 586–590.

Osanai, A., **Li, S.-J.**, **Asano, K.**, **Sashinami, H.**, **Hu, D.-L. & Nakane, A. (2013).** Fibronectin-binding protein, FbpA, is the adhesin responsible for pathogenesis of *Listeria monocytogenes* infection. *Microbiology and Immunology* **57**, 253–262.

Overbeek, R., **Olson, R.**, **Pusch, G. D.**, **Olsen, G. J.**, **Davis, J. J.**, **Disz, T.**, **Edwards, R. A.**, **Gerdes, S. & Parrello, B. & other authors (2014).** The SEED and the Rapid Annotation of microbial genomes using Subsystems Technology (RAST). *Nucleic Acids Research* **42**, D206-14.

Palacios, S., **Starai, V. J. & Escalante-Semerena, J. C. (2003).** Propionyl coenzyme A is a common intermediate in the 1,2-propanediol and propionate catabolic pathways needed for expression of the

prpBCDE operon during growth of Salmonella enterica on 1,2-propanediol. *Journal of Bacteriology* **185**, 2802–2810.

Pamer, E. G. (2004). Immune responses to *Listeria monocytogenes*. *Nature Reviews: Immunology* **4**, 812–823.

Parida, S. K., **Domann, E.**, **Rohde, M.**, **Müller, S.**, **Darji, A.**, **Hain, T.**, **Wehland, J. & Chakraborty, T. (1998).** Internalin B is essential for adhesion and mediates the invasion of *Listeria monocytogenes* into human endothelial cells. *Molecular Microbiology* **28**, 81–93.

Patel, R. K. & Jain, M. (2012). NGS QC Toolkit: a toolkit for quality control of next generation sequencing data. *PloS One* **7**, e30619.

Pelaseyed, T., **Bergström, J. H.**, **Gustafsson, J. K.**, **Ermund, A.**, **Birchenough, G. M. H.**, **Schütte, A.**, **van der Post, S.**, **Svensson, F. & Rodríguez-Piñeiro, A. M. & other authors (2014).** The mucus and mucins of the goblet cells and enterocytes provide the first defense line of the gastrointestinal tract and interact with the immune system. *Immunological Reviews* **260**, 8–20.

Pentecost, M., **Kumaran, J.**, **Ghosh, P. & Amieva, M. R. (2010).** *Listeria monocytogenes* internalin B activates junctional endocytosis to accelerate intestinal invasion. *PLoS Pathogens* **6**, e1000900.

Pentecost, M., **Otto, G.**, **Theriot, J. A. & Amieva, M. R. (2006).** *Listeria monocytogenes* invades the epithelial junctions at sites of cell extrusion. *PLoS Pathogens* **2**, e3.

Perrin, M., **Bemer, M. & Delamare, C. (2003).** Fatal Case of *Listeria* innocua Bacteremia. *Journal of Clinical Microbiology* **41**, 5308–5309.

Pickard, J. M., **Zeng, M. Y.**, **Caruso, R. & Núñez, G. (2017).** Gut microbiota. Role in pathogen colonization, immune responses, and inflammatory disease. *Immunological Reviews* **279**, 70–89.

Picossi, S., **Belitsky, B. R. & Sonenshein, A. L. (2007).** Molecular mechanism of the regulation of Bacillus subtilis *gltAB* expression by GltC. *Journal of Molecular Biology* **365**, 1298–1313.

Pillich, H., **Puri, M. & Chakraborty, T. (2017).** ActA of *Listeria monocytogenes* and Its Manifold Activities as an Important *Listeria*l Virulence Factor. *Current topics in Microbiology and Immunology* **399**, 113–132.

Pine, L., **Kathariou, S.**, **Quinn, F.**, **George, V.**, **Wenger, J. D. & Weaver, R. E. (1991).** Cytopathogenic effects in enterocytelike Caco-2 cells differentiate virulent from avirulent *Listeria* strains. *Journal of Clinical Microbiology* **29**, 990–996.

Pirie, J. H. (1940). The Genus Listerella *pirie*. *Science (New York, N.Y.)* **91**, 383.

Pittman, M. S., **Corker, H.**, **Wu, G.**, **Binet, M. B.**, **Moir, A. J. G. & Poole, R. K. (2002).** Cysteine is exported from the *Escherichia coli* cytoplasm by CydDC, an ATP-binding cassette-type transporter required for cytochrome assembly. *The Journal of Biological Chemistry* **277**, 49841–49849.

Pittman, M. S., **Robinson, H. C. & Poole, R. K. (2005).** A bacterial glutathione transporter (*Escherichia coli CydDC*) exports reductant to the periplasm. *The Journal of Biological Chemistry* **280**, 32254–32261.

Pizarro-Cerdá, J., **Kühbacher, A. & Cossart, P. (2012).** Entry of *Listeria monocytogenes* in mammalian epithelial cells. An updated view. *Cold Spring Harbor Perspectives in Medicine* **2**.

Polissi, A., **Pontiggia, A.**, **Feger, G.**, **Altieri, M.**, **Mottl, H.**, **Ferrari, L. & Simon, D. (1998).** Large-scale identification of virulence genes from *Streptococcus pneumoniae*. *Infection and Immunity* **66**, 5620–5629.

Poole, R. K., **Gibson, F. & Wu, G. (1994).** The *cydD* gene product, component of a heterodimeric ABC transporter, is required for assembly of periplasmic cytochrome c and of cytochrome bd in *Escherichia coli*. *FEMS Microbiology Letters* **117**, 217–223.

Poole, R. K., **Hatch, L.**, **Cleeter, M. W.**, **Gibson, F.**, **Cox, G. B. & Wu, G. (1993).** Cytochrome bd biosynthesis in *Escherichia coli*. The sequences of the *cydC* and *cydD* genes suggest that they encode the components of an ABC membrane transporter. *Molecular Microbiology* **10**, 421–430.

Port, G. C. & Freitag, N. E. (2007). Identification of novel *Listeria monocytogenes* secreted virulence factors following mutational activation of the central virulence regulator, PrfA. *Infection and Immunity* **75**, 5886–5897.

Portnoy, D. A. (1992). Innate immunity to a facultative intracellular bacterial pathogen. *Current Opinion in Immunology* **4**, 20–24.

Premaratne, R. J., **Lin, W. J. & Johnson, E. A. (1991).** Development of an improved chemically defined minimal medium for *Listeria monocytogenes*. *Applied and Environmental Microbiology* **57**, 3046–3048.

Price-Carter, M., **Tingey, J.**, **Bobik, T. A. & Roth, J. R. (2001).** The alternative electron acceptor tetrathionate supports B_{12}-dependent anaerobic growth of *Salmonella enterica* serovar Typhimurium on ethanolamine or 1,2-propanediol. *Journal of Bacteriology* **183**, 2463–2475.

Pron, B., **Boumaila, C.**, **Jaubert, F.**, **Berche, P.**, **Milon, G.**, **Geissmann, F. & Gaillard, J. L. (2001).** Dendritic cells are early cellular targets of *Listeria monocytogenes* after intestinal delivery and are involved in bacterial spread in the host. *Cellular Microbiology* **3**, 331–340.

Pron, B., **Boumaila, C.**, **Jaubert, F.**, **Sarnacki, S.**, **Monnet, J. P.**, **Berche, P. & Gaillard, J. L. (1998).** Comprehensive study of the intestinal stage of listeriosis in a rat ligated ileal loop system. *Infection and Immunity* **66**, 747–755.

Qin, Q.-L., **Xie, B.-B.**, **Zhang, X.-Y.**, **Chen, X.-L.**, **Zhou, B.-C.**, **Zhou, J.**, **Oren, A. & Zhang, Y.-Z. (2014).** A proposed genus boundary for the prokaryotes based on genomic insights. *Journal of Bacteriology* **196**, 2210–2215.

Rajabian, T., **Gavicherla, B.**, **Heisig, M.**, **Müller-Altrock, S.**, **Goebel, W.**, **Gray-Owen, S. D. & Ireton, K. (2009).** The bacterial virulence factor InlC perturbs apical cell junctions and promotes cell-to-cell spread of *Listeria*. *Nature Cell Biology* **11**, 1212–1218.

Randle, C. L., **Albro, P. W. & Dittmer, J. C. (1969).** The phosphoglyceride composition of Gram-negative bacteria and the changes in composition during growth. *Biochimica et biophysica acta* **187**, 214–220.

Richter, M. & Rosselló-Móra, R. (2009). Shifting the genomic gold standard for the prokaryotic species definition. *Proceedings of the National Academy of Sciences of the United States of America* **106**, 19126–19131.

Robbe, C., **Capon, C.**, **Coddeville, B. & Michalski, J.-C. (2004).** Structural diversity and specific distribution of O-glycans in normal human mucins along the intestinal tract. *The Biochemical Journal* **384**, 307–316.

Robbins, J. R., **Barth, A. I.**, **Marquis, H.**, **Hostos, E. L.** de, **Nelson, W. J. & Theriot, J. A. (1999).** *Listeria monocytogenes* exploits normal host cell processes to spread from cell to cell. *The Journal of cell biology* **146**, 1333–1350.

Robbins, J. R., **Skrzypczynska, K. M.**, **Zeldovich, V. B.**, **Kapidzic, M. & Bakardjiev, A. I. (2010).** Placental syncytiotrophoblast constitutes a major barrier to vertical transmission of *Listeria monocytogenes*. *PLoS Pathogens* **6**, e1000732.

Robinson, M. D., **McCarthy, D. J. & Smyth, G. K. (2010).** edgeR: a Bioconductor package for differential expression analysis of digital gene expression data. *Bioinformatics (Oxford, England)* **26**, 139–140.

Robinson, M. D. & Oshlack, A. (2010). A scaling normalization method for differential expression analysis of RNA-seq data. *Genome Biology* **11**, R25.

Rocourt, J., **Boerlin, P.**, **Grimont, F.**, **Jacquet, C. & Piffaretti, J. C. (1992).** Assignment of *Listeria grayi* and *Listeria murrayi* to a single species, *Listeria grayi*, with a revised description of *Listeria grayi*. *International Journal of Systematic Bacteriology* **42**, 171–174.

Rocourt, J. & Grimont, P. A. D. (1983). *Listeria welshimeri* sp. nov. and *Listeria seeligeri* sp. nov. *International Journal of Systematic Bacteriology* **33**, 866–869.

Rocourt, J., **Hof, H.**, **Schrettenbrunner, A.**, **Malinverni, R. & Bille, J. (1986).** Méningite purulente aiguë à *Listeria seeligeri* chez un adulte immunocompétent. *Schweizerische medizinische Wochenschrift* **116**, 248–251.

Rocourt, J. & Seeliger, H. P. (1985). Distribution des espèces du genre *Listeria*. *Zentralblatt fur Bakteriologie, Mikrobiologie, und Hygiene. Series A, Medical Microbiology, Infectious Diseases, Virology, Parasitology* **259**, 317–330.

Rondon, M. R. & Escalante-Semerena, J. C. (1992). The poc locus is required for 1,2-propanediol-dependent transcription of the cobalamin biosynthetic (*cob*) and propanediol utilization (*pdu*) genes of *Salmonella* Typhimurium. *Journal of Bacteriology* **174**, 2267–2272.

Roth, J. R., **Lawrence, J. G. & Bobik, T. A. (1996).** Cobalamin (coenzyme B_{12}). Synthesis and biological significance. *Annual Review of Microbiology* **50**, 137–181.

Rutherford, K., **Parkhill, J.**, **Crook, J.**, **Horsnell, T.**, **Rice, P.**, **Rajandream, M. A. & Barrell, B. (2000).** Artemis: sequence visualization and annotation. *Bioinformatics (Oxford, England)* **16**, 944–945.

Ryan, S., **Begley, M.**, **Gahan, C. G. M. & Hill, C. (2009).** Molecular characterization of the arginine deiminase system in *Listeria monocytogenes*. Regulation and role in acid tolerance. *Environmental Microbiology* **11**, 432–445.

Ryan, S., **Begley, M.**, **Hill, C. & Gahan, C. G. M. (2010).** A five-gene stress survival islet (SSI-1) that contributes to the growth of *Listeria monocytogenes* in suboptimal conditions. *Journal of Applied Microbiology* **109**, 984–995.

Salazar, J. K., **Wu, Z.**, **McMullen, P. D.**, **Luo, Q.**, **Freitag, N. E.**, **Tortorello, M. L.**, **Hu, S. & Zhang, W. (2013).** PrfA-like transcription factor gene lmo0753 contributes to L-rhamnose utilization in *Listeria monocytogenes* strains associated with human food-borne infections. *Applied and Environmental Microbiology* **79**, 5584–5592.

Sallen, B., **Rajoharison, A.**, **Desvarenne, S.**, **Quinn, F. & Mabilat, C. (1996).** Comparative analysis of 16S and 23S rRNA sequences of *Listeria* species. *International Journal of Systematic Bacteriology* **46**, 669–674.

Sauders, B. D., **Overdevest, J.**, **Fortes, E.**, **Windham, K.**, **Schukken, Y.**, **Lembo, A. & Wiedmann, M. (2012).** Diversity of *Listeria* species in urban and natural environments. *Applied and Environmental Microbiology* **78**, 4420–4433.

Sauer, U. & Eikmanns, B. J. (2005). The PEP-pyruvate-oxaloacetate node as the switch point for carbon flux distribution in bacteria. *FEMS Microbiology Reviews* **29**, 765–794.

Schär, J., **Stoll, R.**, **Schauer, K.**, **Loeffler, D. I. M.**, **Eylert, E.**, **Joseph, B.**, **Eisenreich, W.**, **Fuchs, T. M. & Goebel, W. (2010).** Pyruvate carboxylase plays a crucial role in carbon metabolism of extra- and intracellularly replicating *Listeria monocytogenes*. *Journal of Bacteriology* **192**, 1774–1784.

Schardt, J. (2014). Further characterization of the nitrogen metabolism in *Listeria monocytogenes*. *Master's Thesis*.

Schauer, K., **Geginat, G.**, **Liang, C.**, **Goebel, W.**, **Dandekar, T. & Fuchs, T. M. (2010).** Deciphering the intracellular metabolism of *Listeria monocytogenes* by mutant screening and modelling. *BMC Genomics* **11**, 573.

Schauer, K., **Stolz, J.**, **Scherer, S. & Fuchs, T. M. (2009).** Both thiamine uptake and biosynthesis of thiamine precursors are required for intracellular replication of *Listeria monocytogenes*. *Journal of Bacteriology* **191**, 2218–2227.

Schlech, W. F., **Lavigne, P. M.**, **Bortolussi, R. A.**, **Allen, A. C.**, **Haldane, E. V.**, **Wort, A. J.**, **Hightower, A. W.**, **Johnson, S. E. & King, S. H. & other authors (1983).** Epidemic listeriosis--evidence for transmission by food. *The New England Journal of Medicine* **308**, 203–206.

Schmid, M. W., **Ng, E. Y. W.**, **Lampidis, R.**, **Emmerth, M.**, **Walcher, M.**, **Kreft, J.**, **Goebel, W.**, **Wagner, M. & Schleifer, K.-H. (2005).** Evolutionary history of the genus *Listeria* and its virulence genes. *Systematic and applied microbiology* **28**, 1–18.

Schneider, E. (2001). ABC transporters catalyzing carbohydrate uptake. *Research in Microbiology* **152**, 303–310.

Schuchat, A., **Deaver, K.**, **Hayes, P. S.**, **Graves, L.**, **Mascola, L. & Wenger, J. D. (1993).** Gastrointestinal Carriage of *Listeria monocytogenes* in Household Contacts of Patients with Listeriosis. *Journal of Infectious Diseases* **167**, 1261–1262.

Schuchat, A., **Swaminathan, B. & Broome, C. V. (1991).** Epidemiology of human listeriosis. *Clinical Microbiology Reviews* **4**, 169–183.

Schultze, T., **Hilker, R.**, **Mannala, G. K.**, **Gentil, K.**, **Weigel, M.**, **Farmani, N.**, **Windhorst, A. C.**, **Goesmann, A.**, **Chakraborty, T. & Hain, T. (2015).** A detailed view of the intracellular transcriptome of *Listeria monocytogenes* in murine macrophages using RNA-seq. *Frontiers in Microbiology* **6**, 1199.

Sears, C. L. (2005). A dynamic partnership. Celebrating our gut flora. *Anaerobe* **11**, 247–251.

Seeliger, H. P. (1961). Listeriosis. *Karger Verlag, Basel*.

Seeliger, H. P. (1981). Apathogene listerien. *L. innocua* sp. n. (Seeliger et Schoofs, 1977). *Zentralblatt fur Bakteriologie, Mikrobiologie und Hygiene. 1. Abt. Originale A, Medizinische Mikrobiologie, Infektionskrankheiten und Parasitologie* **249**, 487–493.

Seeliger, H. P., **Rocourt, J.**, **Schrettenbrunner, A.**, **Grimont, P. & Jones, D. A. (1984).** *Listeria ivanovii* sp. nov. *International Journal of Systematic Bacteriology* **34**, 336–337.

Sekirov, I., **Russell, S. L.**, **Antunes, L. C. M. & Finlay, B. B. (2010).** Gut microbiota in health and disease. *Physiological reviews* **90**, 859–904.

Sergeant, E. S., **Love, S. C. & McInnes, A. (1991).** Abortions in sheep due to *Listeria ivanovii*. *Australian Veterinary Journal* **68**, 39.

Seveau, S., **Pizarro-Cerda, J. & Cossart, P. (2007).** Molecular mechanisms exploited by *Listeria monocytogenes* during host cell invasion. *Microbes and Infection* **9**, 1167–1175.

Sewell, D., **Allen, S. C. & Phillips, C. A. (2015).** Oxygen limitation induces acid tolerance and impacts simulated gastro-intestinal transit in *Listeria monocytogenes* J0161. *Gut Pathogens* **7**, 11.

Shao, Y. (2007). Genetic and biochemical characterization of hydroxamate transporters in *Listeria monocytogenes*. *Dissertation*.

Shen, A. & Higgins, D. E. (2006). The MogR transcriptional repressor regulates nonhierarchal expression of flagellar motility genes and virulence in *Listeria monocytogenes*. *PLoS Pathogens* **2**, e30.

Shen, Y., **Kawamura, I.**, **Nomura, T.**, **Tsuchiya, K.**, **Hara, H.**, **Dewamitta, S. R.**, **Sakai, S.**, **Qu, H. & Daim, S. & other authors (2010).** Toll-like receptor 2- and MyD88-dependent phosphatidylinositol 3-kinase and Rac1 activation facilitates the phagocytosis of *Listeria monocytogenes* by murine macrophages. *Infection and Immunity* **78**, 2857–2867.

Shepherd, M. (2015). The CydDC ABC transporter of *Escherichia coli*. New roles for a reductant efflux pump. *Biochemical Society Transactions* **43**, 908–912.

Sicard, J.-F., **Le Bihan, G.**, **Vogeleer, P.**, **Jacques, M. & Harel, J. (2017).** Interactions of Intestinal Bacteria with Components of the Intestinal Mucus. *Frontiers in Cellular and Infection Microbiology* **7**, 387.

Sigrist, C. J. A., **Castro, E.** de, **Cerutti, L.**, **Cuche, B. A.**, **Hulo, N.**, **Bridge, A.**, **Bougueleret, L. & Xenarios, I. (2013).** New and continuing developments at PROSITE. *Nucleic Acids Research* **41**, D344-7.

Sigrist, C. J. A., **Cerutti, L.**, **Hulo, N.**, **Gattiker, A.**, **Falquet, L.**, **Pagni, M.**, **Bairoch, A. & Bucher, P. (2002).** PROSITE. A documented database using patterns and profiles as motif descriptors. *Briefings in Bioinformatics* **3**, 265–274.

Skovgaard, N. & Morgen, C. A. (1988). Detection of *Listeria* spp. in faeces from animals, in feeds, and in raw foods of animal origin. *International Journal of Food Microbiology* **6**, 229–242.

Sleator, R. D., **Francis, G. A.**, **O'Beirne, D.**, **Gahan, C. G. M. & Hill, C. (2003).** Betaine and carnitine uptake systems in *Listeria monocytogenes* affect growth and survival in foods and during infection. *Journal of Applied Microbiology* **95**, 839–846.

Sleator, R. D., **Gahan, C. G.**, **Abee, T. & Hill, C. (1999).** Identification and disruption of BetL, a secondary glycine betaine transport system linked to the salt tolerance of *Listeria monocytogenes* LO28. *Applied and Environmental Microbiology* **65**, 2078–2083.

Sleator, R. D. & Hill, C. (2010). Compatible solutes. The key to *Listeria*'s success as a versatile gastrointestinal pathogen? *Gut Pathogens* **2**, 20.

Sleator, R. D., **Wemekamp-Kamphuis, H. H.**, **Gahan, C. G. M.**, **Abee, T. & Hill, C. (2005).** A PrfA-regulated bile exclusion system (BilE) is a novel virulence factor in *Listeria monocytogenes*. *Molecular Microbiology* **55**, 1183–1195.

Sleator, R. D., **Wouters, J.**, **Gahan, C. G.**, **Abee, T. & Hill, C. (2001).** Analysis of the role of OpuC, an osmolyte transport system, in salt tolerance and virulence potential of *Listeria monocytogenes*. *Applied and Environmental Microbiology* **67**, 2692–2698.

Smith, M. A., **Takeuchi, K.**, **Anderson, G.**, **Ware, G. O.**, **McClure, H. M.**, **Raybourne, R. B.**, **Mytle, N. & Doyle, M. P. (2008).** Dose-response model for *Listeria monocytogenes*-induced stillbirths in nonhuman primates. *Infection and Immunity* **76**, 726–731.

Solovyev, V. & Salamov, A. (2011). Automatic annotation of microbial genomes and Metagenomic sequences. *Metagenomics and its Applications in Agriculture, Biomedicine and Environmental Studies. Nova Science Publishers, Hauppauge, NY*.

Soriano, J. M., **Rico, H.**, **Moltó, J. C. & Mañes, J. (2001).** *Listeria* species in raw and ready-to-eat foods from restaurants. *Journal of Food Protection* **64**, 551–553.

Srikumar, S. & Fuchs, T. M. (2011). Ethanolamine utilization contributes to proliferation of *Salmonella enterica* serovar Typhimurium in food and in nematodes. *Applied and Environmental Microbiology* **77**, 281–290.

Staib, L. & Fuchs, T. M. (2014). From food to cell. Nutrient exploitation strategies of enteropathogens. *Microbiology (Reading, England)* **160**, 1020–1039.

Staib, L. & Fuchs, T. M. (2015). Regulation of fucose and 1,2-propanediol utilization by *Salmonella enterica* serovar Typhimurium. *Frontiers in Microbiology* **6**, 1116.

Stea, E. C., **Purdue, L. M.**, **Jamieson, R. C.**, **Yost, C. K. & Truelstrup Hansen, L. (2015).** Comparison of the Prevalences and Diversities of *Listeria* Species and *Listeria monocytogenes* in an Urban and a Rural Agricultural Watershed. *Applied and Environmental Microbiology* **81**, 3812–3822.

Stecher, B. & Hardt, W.-D. (2011). Mechanisms controlling pathogen colonization of the gut. *Current Opinion in Microbiology* **14**, 82–91.

Stritzker, J., **Janda, J.**, **Schoen, C.**, **Taupp, M.**, **Pilgrim, S.**, **Gentschev, I.**, **Schreier, P.**, **Geginat, G. & Goebel, W. (2004).** Growth, virulence, and immunogenicity of *Listeria monocytogenes aro* mutants. *Infection and Immunity* **72**, 5622–5629.

Stritzker, J., **Schoen, C. & Goebel, W. (2005).** Enhanced synthesis of internalin A in *aro* mutants of *Listeria monocytogenes* indicates posttranscriptional control of the *inlAB* mRNA. *Journal of Bacteriology* **187**, 2836–2845.

Stuart, S. E. & Welshimer, H. J. (1974). Taxonomic reexamination of *Listeria Pirie* and transfer of *Listeria grayi* and *Listeria murrayi* to a new genus, *Murraya*. *International Journal of Systematic Bacteriology* **24**, 177–185.

Sue, D., **Fink, D.**, **Wiedmann, M. & Boor, K. J. (2004).** sigmaB-dependent gene induction and expression in *Listeria monocytogenes* during osmotic and acid stress conditions simulating the intestinal environment. *Microbiology (Reading, England)* **150**, 3843–3855.

Tamanai-Shacoori, Z., **Smida, I.**, **Bousarghin, L.**, **Loreal, O.**, **Meuric, V.**, **Fong, S. B.**, **Bonnaure-Mallet, M. & Jolivet-Gougeon, A. (2017).** *Roseburia* spp. A marker of health? *Future microbiology* **12**, 157–170.

Tamura, G. S., **Nittayajarn, A. & Schoentag, D. L. (2002).** A glutamine transport gene, *glnQ*, is required for fibronectin adherence and virulence of group B streptococci. *Infection and Immunity* **70**, 2877–2885.

Tamura, K., **Stecher, G.**, **Peterson, D.**, **Filipski, A. & Kumar, S. (2013).** MEGA6: Molecular Evolutionary Genetics Analysis version 6.0. *Molecular Biology and Evolution* **30**, 2725–2729.

Tang, S., **Orsi, R. H.**, **den Bakker, H. C.**, **Wiedmann, M.**, **Boor, K. J. & Bergholz, T. M. (2015).** Transcriptomic Analysis of the Adaptation of *Listeria monocytogenes* to Growth on Vacuum-Packed Cold Smoked Salmon. *Applied and Environmental Microbiology* **81**, 6812–6824.

Tatusova, T., **DiCuccio, M.**, **Badretdin, A.**, **Chetvernin, V.**, **Ciufo, S. & Stacy Li, S. (2013).** Prokaryotic Genome Annotation Pipeline. *The NCBI Handbook [Internet], 2nd ed., Bethesda (MD): National Center for Biotechnology Information (US)*.

Terplan, G. & Steinmeyer, S. (1989). Investigations on the pathogenicity of *Listeria* spp. by experimental infection of the chick embryo. *International Journal of Food Microbiology* **8**, 277–280.

Theriot, J. A., **Mitchison, T. J.**, **Tilney, L. G. & Portnoy, D. A. (1992).** The rate of actin-based motility of intracellular *Listeria monocytogenes* equals the rate of actin polymerization. *Nature* **357**, 257–260.

Thévenot, D., **Dernburg, A. & Vernozy-Rozand, C. (2006).** An updated review of *Listeria monocytogenes* in the pork meat industry and its products. *Journal of Applied Microbiology* **101**, 7–17.

Thiennimitr, P., **Winter, S. E.**, **Winter, M. G.**, **Xavier, M. N.**, **Tolstikov, V.**, **Huseby, D. L.**, **Sterzenbach, T.**, **Tsolis, R. M.**, **Roth, J. R. & Bäumler, A. J. (2011).** Intestinal inflammation allows *Salmonella* to use ethanolamine to compete with the microbiota. *Proceedings of the National Academy of Sciences of the United States of America* **108**, 17480–17485.

Toledo-Arana, A., **Dussurget, O.**, **Nikitas, G.**, **Sesto, N.**, **Guet-Revillet, H.**, **Balestrino, D.**, **Loh, E.**, **Gripenland, J. & Tiensuu, T. & other authors (2009).** The *Listeria* transcriptional landscape from saprophytism to virulence. *Nature* **459**, 950–956.

Tsai, H.-N. & Hodgson, D. A. (2003). Development of a synthetic minimal medium for *Listeria monocytogenes*. *Applied and Environmental Microbiology* **69**, 6943–6945.

Tsai, Y.-H., **Disson, O.**, **Bierne, H. & Lecuit, M. (2013).** Murinization of internalin extends its receptor repertoire, altering *Listeria monocytogenes* cell tropism and host responses. *PLoS Pathogens* **9**, e1003381.

Tsirigos, K. D., **Peters, C.**, **Shu, N.**, **Käll, L. & Elofsson, A. (2015).** The TOPCONS web server for consensus prediction of membrane protein topology and signal peptides. *Nucleic Acids Research* **43**, W401-7.

Tsoy, O., **Ravcheev, D. & Mushegian, A. (2009).** Comparative genomics of ethanolamine utilization. *Journal of Bacteriology* **191**, 7157–7164.

van de Velde, S., **Delaive, E.**, **Dieu, M.**, **Carryn, S.**, **van Bambeke, F.**, **Devreese, B.**, **Raes, M. & Tulkens, P. M. (2009).** Isolation and 2-D-DIGE proteomic analysis of intracellular and extracellular forms of *Listeria monocytogenes*. *Proteomics* **9**, 5484–5496.

van Netten, P., **Perales, I.**, **van de Moosdijk, A.**, **Curtis, G. D. & Mossel, D. A. (1989).** Liquid and solid selective differential media for the detection and enumeration of *L. monocytogenes* and other *Listeria* spp. *International Journal of Food Microbiology* **8**, 299–316.

Vance, J. E. (2008). Phosphatidylserine and phosphatidylethanolamine in mammalian cells. Two metabolically related aminophospholipids. *Journal of Lipid Research* **49**, 1377–1387.

Varghese, N. J., **Mukherjee, S.**, **Ivanova, N.**, **Konstantinidis, K. T.**, **Mavrommatis, K.**, **Kyrpides, N. C. & Pati, A. (2015).** Microbial species delineation using whole genome sequences. *Nucleic Acids Research* **43**, 6761–6771.

Vázquez-Boland, J. A., **Domínguez-Bernal, G.**, **González-Zorn, B.**, **Kreft, J. & Goebel, W. (2001a).** Pathogenicity islands and virulence evolution in *Listeria*. *Microbes and Infection* **3**, 571–584.

Vázquez-Boland, J. A., **Kuhn, M.**, **Berche, P.**, **Chakraborty, T.**, **Domínguez-Bernal, G.**, **Goebel, W.**, **González-Zorn, B.**, **Wehland, J. & Kreft, J. (2001b).** *Listeria* pathogenesis and molecular virulence determinants. *Clinical Microbiology Reviews* **14**, 584–640.

Vazquez-Torres, A., **Jones-Carson, J.**, **Bäumler, A. J.**, **Falkow, S.**, **Valdivia, R.**, **Brown, W.**, **Le, M.**, **Berggren, R.**, **Parks, W. T. & Fang, F. C. (1999).** Extraintestinal dissemination of *Salmonella* by CD18-expressing phagocytes. *Nature* **401**, 804–808.

Volokhov, D., **George, J.**, **Anderson, C.**, **Duvall, R. E. & Hitchins, A. D. (2006).** Discovery of natural atypical nonhemolytic *Listeria seeligeri* isolates. *Applied and Environmental Microbiology* **72**, 2439–2448.

Wallace, N., **Newton, E.**, **Abrams, E.**, **Zani, A. & Sun, Y. (2017).** Metabolic determinants in *Listeria monocytogenes* anaerobic listeriolysin O production. *Archives of Microbiology* **199**, 827–837.

Wang, Y., **Lu, L.**, **Lan, R.**, **Salazar, J. K.**, **Liu, J.**, **Xu, J. & Ye, C. (2017).** Isolation and characterization of *Listeria* species from rodents in natural environments in China. *Emerging Microbes & Infections* **6**, e44.

Weinberg, E. D. (1974). Iron and susceptibility to infectious disease. *Science (New York, N.Y.)* **184**, 952–956.

Weller, D., **Andrus, A.**, **Wiedmann, M. & den Bakker, H. C. (2015).** *Listeria booriae* sp. nov. and *Listeria newyorkensis* sp. nov., from food processing environments in the USA. *International Journal of Systematic and Evolutionary Microbiology* **65**, 286–292.

Wemekamp-Kamphuis, H. H., **Wouters, J. A.**, **Leeuw, P. P. L. A.** de, **Hain, T.**, **Chakraborty, T. & Abee, T. (2004).** Identification of sigma factor sigma B-controlled genes and their impact on acid stress, high hydrostatic pressure, and freeze survival in *Listeria monocytogenes* EGD-e. *Applied and Environmental Microbiology* **70**, 3457–3466.

Wemekamp-Kamphuis, H. H., **Wouters, J. A.**, **Sleator, R. D.**, **Gahan, C. G. M.**, **Hill, C. & Abee, T. (2002).** Multiple deletions of the osmolyte transporters BetL, Gbu, and OpuC of *Listeria monocytogenes* affect virulence and growth at high osmolarity. *Applied and Environmental Microbiology* **68**, 4710–4716.

Werbrouck, H., **Grijspeerdt, K.**, **Botteldoorn, N.**, **van Pamel, E.**, **Rijpens, N.**, **van Damme, J.**, **Uyttendaele, M.**, **Herman, L. & van Coillie, E. (2006).** Differential *inlA* and *inlB* expression and interaction with human intestinal and liver cells by *Listeria monocytogenes* strains of different origins. *Applied and Environmental Microbiology* **72**, 3862–3871.

Wiedmann, M. & Sauders, B. (2007). Ecology of *Listeria* Species and *L. monocytogenes* in the Natural Environment. In *Listeria, Listeriosis, and Food Safety, Third Edition*, pp. 21–53.

Wilkens, S. (2015). Structure and mechanism of ABC transporters. *F1000prime Reports* **7**, 14.

Williams, T., **Joseph, B.**, **Beier, D.**, **Goebel, W. & Kuhn, M. (2005).** Response regulator DegU of *Listeria monocytogenes* regulates the expression of flagella-specific genes. *FEMS Microbiology Letters* **252**, 287–298.

Winstedt, L., **Yoshida, K.**, **Fujita, Y. & Wachenfeldt, C.** von **(1998).** Cytochrome bd biosynthesis in *Bacillus subtilis*. Characterization of the *cydABCD* operon. *Journal of Bacteriology* **180**, 6571–6580.

Winter, S. E., **Thiennimitr, P.**, **Winter, M. G.**, **Butler, B. P.**, **Huseby, D. L.**, **Crawford, R. W.**, **Russell, J. M.**, **Bevins, C. L. & Adams, L. G. & other authors (2010).** Gut inflammation provides a respiratory electron acceptor for *Salmonella*. *Nature* **467**, 426–429.

Wollert, T., **Pasche, B.**, **Rochon, M.**, **Deppenmeier, S.**, **van den Heuvel, J.**, **Gruber, A. D.**, **Heinz, D. W.**, **Lengeling, A. & Schubert, W.-D. (2007).** Extending the host range of *Listeria monocytogenes* by rational protein design. *Cell* **129**, 891–902.

Wong, J. M. W., **Souza, R.** de, **Kendall, C. W. C.**, **Emam, A. & Jenkins, D. J. A. (2006).** Colonic health. Fermentation and short chain fatty acids. *Journal of Clinical Gastroenterology* **40**, 235–243.

Wright, M. L., **Pendarvis, K.**, **Nanduri, B.**, **Edelmann, M. J.**, **Jenkins, H. N.**, **Reddy, J. S.**, **Wilson, J. G.**, **Ding, X. & Broadway, P. R. & other authors (2016).** The Effect of Oxygen on Bile Resistance in *Listeria monocytogenes*. *Journal of Proteomics & Bioinformatics* **9**, 107–119.

Wu, R., **Skaar, E. P.**, **Zhang, R.**, **Joachimiak, G.**, **Gornicki, P.**, **Schneewind, O. & Joachimiak, A. (2005).** *Staphylococcus aureus* IsdG and IsdI, heme-degrading enzymes with structural similarity to monooxygenases. *The Journal of Biological Chemistry* **280**, 2840–2846.

Wurtzel, O., **Sesto, N.**, **Mellin, J. R.**, **Karunker, I.**, **Edelheit, S.**, **Bécavin, C.**, **Archambaud, C.**, **Cossart, P. & Sorek, R. (2012).** Comparative transcriptomics of pathogenic and non-pathogenic *Listeria* species. *Molecular Systems Biology* **8**, 583.

Xayarath, B., **Marquis, H.**, **Port, G. C. & Freitag, N. E. (2009).** *Listeria monocytogenes* CtaP is a multifunctional cysteine transport-associated protein required for bacterial pathogenesis. *Molecular Microbiology* **74**, 956–973.

Xiao, Q., **Jiang, X.**, **Moore, K. J.**, **Shao, Y.**, **Pi, H.**, **Dubail, I.**, **Charbit, A.**, **Newton, S. M. & Klebba, P. E. (2011).** Sortase independent and dependent systems for acquisition of haem and haemoglobin in *Listeria monocytogenes*. *Molecular Microbiology* **80**, 1581–1597.

Xu, J., **Bjursell, M. K.**, **Himrod, J.**, **Deng, S.**, **Carmichael, L. K.**, **Chiang, H. C.**, **Hooper, L. V. & Gordon, J. I. (2003).** A genomic view of the human-*Bacteroides thetaiotaomicron* symbiosis. *Science (New York, N.Y.)* **299**, 2074–2076.

Xue, J., **Murrieta, C. M.**, **Rule, D. C. & Miller, K. W. (2008).** Exogenous or L-rhamnose-derived 1,2-propanediol is metabolized via a *pduD*-dependent pathway in *Listeria innocua*. *Applied and Environmental Microbiology* **74**, 7073–7079.

Yamashita, M., **Shepherd, M.**, **Booth, W. I.**, **Xie, H.**, **Postis, V.**, **Nyathi, Y.**, **Tzokov, S. B.**, **Poole, R. K.**, **Baldwin, S. A. & Bullough, P. A. (2014).** Structure and function of the bacterial heterodimeric ABC transporter CydDC. Stimulation of ATPase activity by thiol and heme compounds. *The Journal of Biological Chemistry* **289**, 23177–23188.

Zeng, Z., **Surewaard, B. G. J.**, **Wong, C. H. Y.**, **Geoghegan, J. A.**, **Jenne, C. N. & Kubes, P. (2016).** CRIg Functions as a Macrophage Pattern Recognition Receptor to Directly Bind and Capture Blood-Borne Gram-Positive Bacteria. *Cell Host & Microbe* **20**, 99–106.

Zielińska, K., **Fabiszewska, A.**, **Świątek, M. & Szymanowska-Powałowska, D. (2017).** Evaluation of the ability to metabolize 1,2-propanediol by heterofermentative bacteria of the genus *Lactobacillus*. *Electronic Journal of Biotechnology* **26**, 60–63.

6 Supplement

Supplementary Table 1: Chemicals, enzymes and commercial kits used in this study

Chemicals

Supplier	Chemical	Molecular formula
Ambion - Thermo Fisher Scientific Waltham (MA), USA	Nuclease-free water	
Amresco Solon (OH), USA	Kanamycin	$C_{18}H_{36}N_4O_{11}$
AppliChem GmbH Darmstadt, Germany	Cyanocobalamin	$C_{72}H_{100}CoN_{18}O_{17}P$
Biochrom - Merck KGaA Darmstadt, Germany	Hanks balanced salt solution (1x)	
	Penicillin G	$C_{16}H_{18}N_2O_4S$
	Roswell Park Memorial Institute (RPMI) 1640 Medium	
Biotium Fremont (CA), USA	GelRed nucleic acid gel stain	
Biozym Scientific GmbH Hessisch Oldendorf, Germany	LE agarose	
Calbiochem San Diego (CA), USA	Erythromycin	$C_{37}H_{67}NO_{13}$
Carl Roth GmbH & Co. KG Karlsruhe, Germany	2,2'-dipyridyl	$C_{10}H_8N_2$
	4-(2-hydroxyethyl)-1-piperazineethanesulfonic acid (HEPES)	$C_8H_{18}N_2O_4S$
	Citric acid	$C_6H_8O_7$
	D-(+)-Sucrose	$C_{12}H_{22}O_{11}$
	Diethylpyrocarbonate	$C_6H_{10}O_5$
	Disodium phosphate	Na_2HPO_4
	Ethylenediaminetetraacetic acid dihydrate (EDTA)	$C_{10}H_{14}N_2Na_2O_8 \cdot 2H_2O$
	Glycerol	$C_3H_8O_3$
	Isopropanol	C_3H_8O
	Isopropyl β-D-1-thiogalactopyranoside	$C_9H_{18}O_5S$
	L-Histidine	$C_6H_9N_3O_2$
	Magnesium chloride hexahydrate	$MgCl_2 \cdot 6\ H_2O$
	Methanol	CH_3OH
	Monopotassium phosphate	KH_2PO_4
	NA_2-EDTA dihydrate	$C_{10}H_{14}N_2Na_2O_8 \cdot 2\ H_2O$
	Na-Acetate pH 8.0	$C_2H_3NaO_2$
	Paraffin oil	
	Potassium chloride	KCl
	Roti-Phenol	
	Sodium chloride	NaCl
	Sodium dodecylsulfate (SDS)	$C_{12}H_{25}NaO_4S$

	Trichlormethan/Chloroform	$CHCl_3$
	Tris base	C4H11NO3
	Tris Hydrochlorid	$C_4H_{11}NO_3 \cdot HCl$
	Triton X-100	$C_{14}H_{22}O(C_2H_4O)_n$ mit n = 9–10
Fermentas - Thermo Fisher Scientific Waltham (MA), USA	6x DNA loading dye	
	GeneRuler 1 kb DNA ladder	
	GeneRuler 100 bp DNA ladder	
Fluka - Sigma-Aldrich St. Loius (MO), USA	D-(+)-Glucose monohydrate	$C_6H_{12}O_6$
	Disodium phosphate dihydrate	$Na_2HPO_4 \cdot 2\ H_2O$
	Thiamine	$C_{12}H_{17}N_4OS^+$
Illumina San Diego (CA), USA	Custom RNA ladder	
	High resolution ladder	
J.T. Baker - Thermo Fisher Scientific Waltham (MA), USA	Ethanol absolute	C_2H_6O
Life Technolofies Carlsbad (CA), USA	6% Novex polyacrilamide gel	
	Novex TBE urea sample buffer	
	SYBR gold nucleic acid gel stain	
Merck KGaA Darmstadt, Germany	Boric acid	H_3BO_3
	Brain heart infusion broth	
	Calcium chloride	$CaCl_2$
	Ferric citrate	$C_6H_5FeO_7$
	Glycine	$C_2H_5NO_2$
	Iron (II) sulfate	$FeSO_4$
	L-Cysteine	$C_3H_7NO_2S$
	L-Isoleucine	$C_6H_{13}NO_2$
	L-Valine	$C_5H_{11}NO_2$
	Magnesium sulfate heptahydrate	$MgSO_4 \cdot 7\ H_2O$
	Peptone	
New England BioLabs GmbH Frankfurt am Main, Germany	Antarctic phosphatase buffer (10x)	
	ATP solution 10 mM	
	T4 polinucleotide kinase buffer (10x)	
Oxoid - Thermo Fisher Scientific Waltham (MA), USA	Agar bacteriological (Agar No. 1)	
	Tryptone	
	Yeast extract (YE)	
Qiagen GmbH Hilden, Germany	Buffer EB	
	QIAzol	
Serva Electrophoresis Heidelberg, Germany	L- Leucine	$C_6H_{13}NO_2$
Sifin Diagnostics GmbH Berlin, Germany	Palcam agar (basis)	
	Palcam selective supplement	
Sigma-Aldrich St. Louis (MO), USA	1,2-PD	$C_3H_8O_2$
	1,4-Dithiothreitol	$C_4H_{10}O_2S_2$
	Biotin	$C_{10}H_{16}N_2O_3S$

	Chloramphenicol	$C_{11}H_{12}Cl_2N_2O_5$
	DL-6,8-Thioctic acid	$C_8H_{14}O_2S_2$
	Glacial acetic acid	CH_3CO_2H
	L-Arginine	$C_6H_{14}N_4O_2$
	L-Methionine	$C_5H_{11}NO_2S$
	N-acetylcysteine	$C_5H_9NO_3S$
	Riboflavin	$C_{17}H_{20}N_4O_6$
	TRIzol/TRI reagent	
VWR Radnor (PA), USA	Sodium hydroxyde	NaOH

Enzymes

Supplier	**Enzyme**
Ambion - Thermo Fisher Scientific Waltham (MA), USA	SUPERase In RNA inhibitor
AppliChem GmbH Darmstadt, Germany	Proteinase K
Biochrom - Merck KGaA Darmstadt, Germany	1x Trypsin + 0.02% EDTA
New England BioLabs GmbH Frankfurt am Main, Germany	Antarctic phosphatase T4 polinucleotide kinase
Promega Madison (WI), USA	Rnase-free Dnase I
Qiagen GmbH Hilden, Germany	Lysozyme (NGS) Rnase-free Dnase
Quanta Biosciences Gaithersburg, MD, USA	PerfeCTA SYBR Green FastMix qScript cDNA Supermix
Self-produced	Taq polymerase
Sigma-Aldrich St. Louis (MO), USA	Lysozyme RNAse A
Thermo Fisher Scientific Waltham (MA), USA	*Bam*HI restriction enzyme *Bgl*II restriction enzyme *Eco*RI restriction enzyme *Kpn*I restriction enzyme *Pfu* Polymerase Shrimp alkaline phosphatase T4 DNA ligae *Xma*I restriction enzyme
Worthington Lakewood, NJ, USA	Collagenase IV DNAse I

Commercial kits

Supplier	**Kit**
Agilent Technologies	RNA 6000 Nano Kit

Santa Clara (CA), USA	RNA 6000 Pico Kit
Ambion - Thermo Fisher Scientific, Waltham (MA), USA	MICROBExpress Bacterial mRNA Enrichment Kit
Illumina San Diego (CA), USA	MiSeq Reagent Kit v2 50 cycles TruSeq DNA PCR-free LT library preparation Kit TruSeq Small RNA Library preparation kit
Invitrogen - Thermo Fisher Scientific, Waltham (MA), USA	GenElute HP plasmid miniprep kit
Omega Bio-Tek Norcross (GA), USA	E.Z.N.A. Cycle Pure Kit E.Z.N.A. Gel Extraction Kit
Qiagen GmbH Hilden, Germany	miRNeasy Mini Kit QIAamp DNA Mini Kit RNeasy Mini Kit
Sigma-Aldrich St. Louis (MO), USA	PureLink HiPure plasmid midiprep kit

Supplementary Table 2: Consumables, equipment and glass used in this study

Consumables

Supplier	Name
Bio-Rad Laboratories GmbH München, Germany	low-profile PCR-tube strips single PCR tubes
Brand GmbH & Co. KG Wertheim, Germany	Disposable cuvette 1.ml semi-micro
Corning Inc. Corning (NY), USA	0.22 µm Costar Spin-X plastic centrifuge tube filters
Covaris Woburn (MA), USA	microTUBE
Greiner Bio-One GmbH Frickenhausen, Germany	Petri dish (squared) Pipet tips (different volumina)
Millipore - Merck KGaA Darmstadt, Germany	Millex-GP syringe filter unit (0.22 µm)
MP Biomedicals Germany GmbH Eschwege, Germany	FastPrep cell disrupter
Nerbe Plus GmbH Winsen/Luhe, Germany	Falcon conical centrifuge tubes (15 ml or 50 ml) Serological pipet (different volumina)
Oy Growth Curves Ab Ltd Helsinki, Finnland	Bioscreen microtiterplates Honey Comb
Pechiney Plastic Packaging Chicago (IL), USA	Parafilm
Peqlab Life Science – VWR Radnor (PA), USA	2 mm gap electroporation cuvette
Sarstedt AG & Co. Nümbrecht, Germany	Cell culture flasks for adherent cells (25 cm^2, 75 cm^2 or 175 cm^2) Cell culture plates for adherent cells (24 well) Petri dish (round) Screw-capped 2 ml tube
Sigma-Aldrich St. Louis (MO), USA	Silica Beads, 0.1 mm
VWR Radnor (PA), USA	Latex gloves
Zefa-Laborservice GmbH Harthausen, Germany	Microcentrifuge tube (1.5 ml or 2.0 ml) Safe-Lock Microcentrifuge tube (1.5 ml or 2.0 ml)

Equipment

Supplier	Name
AEG Nümbrecht, Germany	Micromat_Duo microwave
Agilent Technologies Santa Clara (CA), USA	2100 Bioanalyzer
Analytik Jena AG Jena, Germany	TSC thermoshaker
Biometra GmbH Göttingen, Germany	TB 1Thermoblock UVsolo TS Imaging System
Bio-Rad Laboratories GmbH München, Germany	CFX96 Touch Gene Pulser

	MJ Mini Personal Therma Cycler
Brand GmbH & Co. KG Wertheim, Germany	Pipetting controler accu-jet Pro
Cepheid Inc Sunnyvale (CA), USA	Smartcycler System
Covaris Woburn (MA), USA	S220 focused-ultrasonication sytem
Eppendorff AG Hamburg, Germany	Concentrator 5301
Heidolph Instruments GmbH & Co. KG Schwabach, Germany	Reax 2000 Vortexer
Heraeus Holding Hanau, Germany	Freezer -80°C Microbiological safety cabinet HeraSafe
IKA Werke GmbH & Co. KG Staufen, Germany	PowerGen 1000 homogenizer RCT hot plate magnetic stirrer
Illumina San Diego (CA), USA	Miseq system
Kern & Sohn GmbH Balingen-Frommern, Germany	ALS 120-4 (Precision scale)
Liebherr International Deutschland GmbH Biberach an der Riß, Germany	Comfort refrigerator Premium freezer Premium frost KGN3446 refrigerator + freezer
Millipore - Merck KGaA Darmstadt, Germany	Milli-Q integral water purification system
MP Biomedicals Germany GmbH Eschwege, Germany	FastPrep®-24 Tissue and Cell Homogenizer
Olympus Deutschland GmbH Hamburg, Germany	BX 51 fluorescence microscope Bioscreen C Automated Microbiology Growth Curve Analysis System
Peqlab Life Science – VWR Radnor (PA), USA	PerfectBlue Gelsystem Mini Primus 96 advanced
PerkinElmer Life and Analytical Sciences Waltham (MA), USA	Lambda Bio+ Spectrophotometer
Sartorius AG Göttingen, Germany	Universal (Laboratory scale)
Süd-Laborbedarf GmbH Gauting, Germany	Homogenizer SL-Pette XE Pipets (different volumina)
Syngene Europe Cambridge, United Kingdom	UV table
Thermo Fisher Scientific Waltham (MA), USA	NanoDrop ND-1000 spectrophotometer Qubit® 2.0 Fluorometer
VELP Scientifica Usmate Velata, Italy	$2x^3$ Vortexer

Glass

Supplier	**Name**
Schott AG Mainz, Germany	100 ml Erlenmeyer flask 15 ml glass tubes 200 ml Erlenmeyer flask Glass tubes small

Supplementary Table 3: Chemicals, media, consumables and equipment used for cell culture experiments

Supplier	Name
AppliChem GmbH Darmstadt, Germany	Trypan blue
Binder GmbH Tuttlingen, Germany	CO2 incubator Serie CB
Biochrom - Merck KGaA Darmstadt, Germany	Dulbecco's modified Eagle medium (DMEM) Dulbecco's phosphate buffer saline (PBS) without Mg^{2+}/Ca^{2+} Gentamycin sulfate Roswell Park Memorial Institute (RPMI) 1640 Medium Trypsin 0.25% + EDTA 0.02%
Brand GmbH & Co. KG Wertheim, Germany	Neubauer-improved counting chamber
Carl Roth GmbH & Co. KG Karlsruhe, Germany	Dimethyl sulfoxide (DMSO)
GATC Biotech Konstanz, Germany	MYCOPLASMACHECK
Gesellschaft für Labortechnik (GFL) Burgwedel, Germany	Water bath
Heraeus Holding Hanau, Germany	HeraCell incubator
ILMVAC GmbH Ilmenau, Germany	biovac 102 vaccuum pump
Kendro Weaverville (NC), USA	Megafuge 1.o R
Leica Camera AG Wetzlar, Germany	DM IL microscope
Pan Biotech Aidenbach, Germany	Fetal calf serum
Sarstedt AG & Co. Nümbrecht, Germany	Cryotube 2 ml
Sigma-Aldrich St. Louis (MO), USA	Dulbecco's phosphate buffer saline (PBS) with Mg^{2+}/Ca^{2+}
Thermo Fisher Scientific Waltham (MA), USA	Mr. Frosty freezing container

Supplementary Table 4: Material and equipment used for mouse infection experiments

Supplier	Name
Abedd Vertriebs GmbH Wien, Austria	Bedding Nesting material
Carl Roth GmbH & Co. KG Karlsruhe, Germany	Dissecting instruments
Kroger Cincinatti (OH), USA	Salted butter White toast bread
REWE Köln, Germany	Salted butter White toast bread
Ssniff-Spezialdiäten GmbH Soest, Germany	Complete feed for mice breeding
Tecniplast Buggigate, Italy	Individually Ventilated Cages Sealsafe Plus Mouse house Water bottle

Supplementary Table 5: ANIb values from pairwise comparison of *Listeria* spp.

	***Listeria kieliensis* sp. nov.**	*L. aquatica* FSL S10-1188	*L. floridensis* FSL S10-1187	*L. fleischmannii* subsp. *coloradonensis* TTU M1-001	*L. fleischmanni* LU2006-1	*L. welshimeri* SLCC5334	*L. monocytogenes* F2365	*L. monocytogenes* EGDe	*L. monocytogenes* HCC23	*L. ivanovii* PAM 55	*L. seeligeri* SLCC3954	*L. marthii* FSL S4-120	*L. monocytogenes* FSL J1-208	*L. innocua* Clip11262	*L. grayi* DSM 20601	*L. grayi* subsp. *murrayi* FSL F6-1183	*L. cornellensis* FSL F6-969	*L. booriae* FSL A5-0281	*L. weihenstephanensis* DSM 24698	*L. grandensis* FSL F6-971	*L. newyorkensis* FSL M6-0635	*L. riparia* FSL S10-1204	*L. rocourtiae* FSL F6-920
***Listeria* kieliensis sp. nov.**	100.00	85.44	74.95	72.17	72.30	71.08	70.94	70.93	70.90	70.87	70.84	70.85	70.79	70.81	69.67	69.56	69.62	69.55	69.49	69.48	69.48	69.47	69.44
L. aquatica FSL S10-1188	85.55	100.00	75.07	72.36	72.42	71.22	70.65	70.67	70.73	70.59	71.13	71.09	70.63	71.07	69.81	69.13	69.66	69.70	69.62	69.49	69.52	69.77	69.70
L. floridensis FSL S10-1187	74.95	74.93	100.00	72.05	72.13	70.84	70.90	70.96	70.84	70.80	70.82	70.99	70.80	70.87	69.71	69.73	69.66	69.63	69.61	69.58	69.57	69.54	69.46
L. fleischmannii subsp. *coloradonensis* TTU M1-001	72.17	72.36	72.05	100.00	95.08	71.22	71.54	71.53	71.73	71.02	71.62	72.22	71.31	71.11	69.51	69.33	69.57	69.36	69.59	69.62	69.21	69.47	69.48
L. fleischmanni LU2006-1	72.43	72.42	72.23	95.08	100.00	71.83	71.65	71.68	71.64	71.68	71.65	71.59	71.37	71.76	69.72	69.68	69.66	69.71	69.84	69.61	69.57	69.84	69.92
L. welshimeri SLCC5334	71.26	71.29	71.22	71.22	71.91	100.00	86.26	86.33	86.22	82.55	82.71	86.02	85.82	86.74	71.03	70.94	71.15	71.22	71.25	71.09	71.01	71.32	71.37
L. monocytogenes F2365	71.08	71.16	70.90	71.54	71.65	86.17	100.00	94.50	94.40	82.36	82.59	88.84	92.79	88.07	70.88	70.85	71.03	71.32	71.18	70.95	70.91	71.13	71.13
L. monocytogenes EGDe	71.15	71.02	71.01	71.53	71.59	86.29	94.61	100.00	92.78	82.30	82.66	89.28	91.91	87.86	70.95	70.85	70.97	71.22	71.24	70.96	70.97	71.10	71.06
L. monocytogenes HCC23	71.16	71.01	71.23	71.73	71.82	86.23	94.47	92.78	100.00	82.53	82.69	89.04	95.17	88.10	70.92	70.94	71.29	71.36	71.40	71.18	71.20	71.33	71.22
L. ivanovii PAM 55	71.08	71.03	71.02	71.02	71.77	82.51	82.39	82.28	82.39	100.00	87.00	82.36	81.94	82.56	70.87	70.85	70.89	71.11	71.15	70.94	70.78	71.02	71.18
L. seeligeri SLCC3954	71.08	71.08	71.10	71.62	71.73	82.85	82.72	82.74	82.74	87.08	100.00	82.77	82.43	83.05	70.77	70.79	69.66	71.15	71.25	70.89	70.87	71.20	71.23
L. marthii FSL S4-120	70.85	71.09	70.99	71.59	71.59	86.02	88.84	89.28	89.04	82.36	82.77	100.00	88.65	87.24	70.58	70.56	70.79	70.99	71.08	70.86	70.71	71.14	70.86
L. monocytogenes FSL J1-208	70.65	70.60	70.80	71.31	71.59	85.87	92.82	91.98	95.15	82.04	82.32	88.65	100.00	87.26	70.46	70.49	70.62	70.90	70.83	70.63	70.56	70.81	70.80
L. innocua Clip11262	71.00	71.00	71.11	71.11	71.77	86.70	88.17	87.85	88.19	82.59	82.93	87.24	87.26	100.00	70.92	70.90	70.92	71.30	71.19	70.87	70.90	71.26	71.15
L. grayi DSM 20601	69.67	69.50	69.71	69.51	69.61	70.52	70.61	70.48	70.60	70.54	70.59	70.58	70.45	70.57	100.00	98.87	69.20	69.41	69.30	69.15	69.14	69.29	69.06
L. grayi subsp. *murrayi* FSL F6-1183	69.39	69.31	69.69	69.33	69.42	70.58	70.60	70.58	70.60	70.54	70.62	70.56	70.50	70.60	98.78	100.00	69.15	69.33	69.17	69.12	69.07	69.20	68.97
L. cornellensis FSL F6-969	69.58	69.26	69.58	69.57	69.57	70.61	70.62	70.72	70.61	70.39	70.51	70.79	70.48	70.50	69.11	68.96	100.00	78.97	82.41	82.87	89.42	78.80	83.11
L. booriae FSL A5-0281	69.55	69.70	69.63	69.86	69.71	71.22	71.32	71.22	71.36	71.11	71.15	72.09	70.90	71.30	69.41	69.33	78.97	100.00	78.64	78.70	79.02	91.31	78.12
L. weihenstephanensis DSM 24698	69.43	69.34	70.78	69.59	69.69	70.78	70.84	70.97	70.81	70.71	70.83	71.08	70.70	70.84	69.32	69.17	82.43	78.64	100.00	80.68	82.59	78.32	80.13
L. grandensis FSL F6-971	69.32	69.29	69.43	69.62	69.53	70.67	70.63	70.65	70.67	70.73	70.62	70.86	70.59	70.62	69.27	70.90	82.98	78.70	80.94	100.00	82.65	78.46	80.37
L. newyorkensis FSL M6-0635	69.29	69.12	69.36	69.21	69.24	70.33	70.53	70.56	70.56	70.22	70.29	70.71	70.36	70.44	69.05	68.91	89.06	79.02	82.45	82.41	100.00	78.44	83.17
L. riparia FSL S10-1204	69.48	69.23	69.42	69.47	69.59	70.86	70.96	71.00	70.92	70.86	71.04	71.14	70.85	70.96	69.35	69.03	78.58	91.31	78.16	78.37	78.59	100.00	77.64
L. rocourtiae FSL F6-920	69.18	69.22	69.37	69.48	69.52	70.84	70.76	70.77	70.72	70.63	70.84	70.86	70.73	70.68	69.05	68.85	83.14	78.12	80.38	80.60	83.57	77.69	100.00

Supplementary figure 1: Schematic representation of construction of deletion mutants by homologous recombination using the shuttle vector pLSV101.

Upstream and downstream flanking regions AB (dark grey) and CD (light grey) of the target gene (white arrow) are amplified using Pfu Polymerase and ligated via BglII restriction sites to yield a ~1,200 bp fragment containing a residual target gene sequence. Nested primers induce restriction sites for cloning of the nested PCR product into the multiple-cloning site (MCS) of pLSV101 (solid curved line), resulting in mutagenesis vector pLSV101lmoΔX (lmoX = gene to be deleted). The temperature-sensitive vector is integrated into the chromosome through a first recombination event to obtain erythromycin resistance (EmR). Positive clones are selected on erythromycin plates at the non-permissive temperature of 42°C. Recombination can occur between homologous sequences of either flank AB (crossed lines) or flank CD (not shown) and the corresponding chromosomal regions. Subsequent cultivation in medium without erythromycin results in deletion of the target gene from the chromosome (bold line) via a second recombination event over the second flank. Excision via the same flank restores the wildtype (not shown).

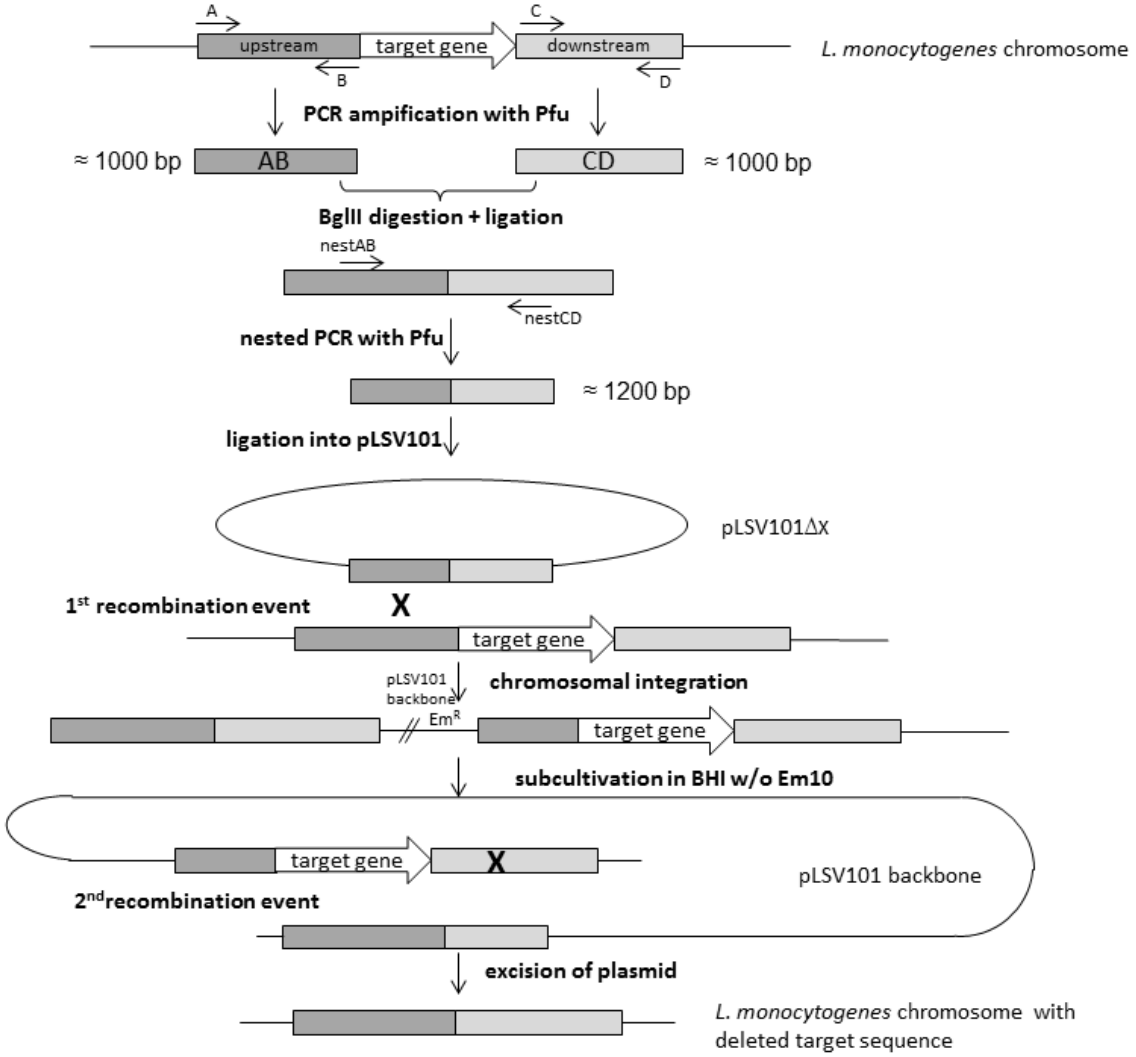

Supplementary figure 2: 1,2-PD does not improve aerobic growth of *L. monocytogenes*

Growth curves of *L. monocytogenes* EGDe (□) and *L. monocytogenes* EGDe *ΔpduD* (○) in MM and 0.5 % (w/v) YE cultivated at 37°C under aerobic conditions. MM was supplemented with 10 mM 1,2-PD and 25 nM cobalamin (filled symbols) or not supplemented (open symbols). OD_{600} was measured at the indicated intervals using Bioscreen C. Growth curves depict the calculated mean value of three independent biological experiments with technical duplicates, while error bars indicate the standard deviation.

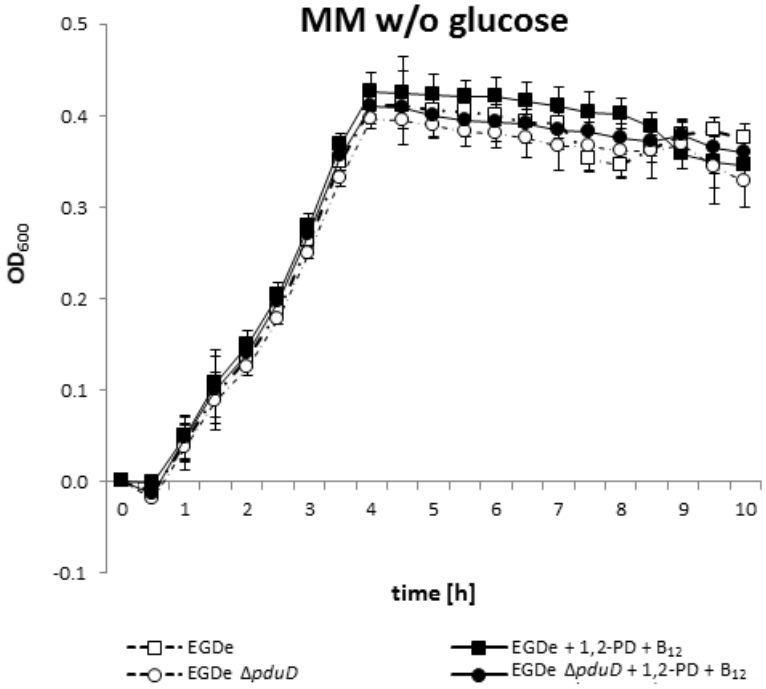

6.1 Acknowledgments

An dieser Stelle möchte ich mich bei allen Personen bedanken die mich während den vier Jahren meiner Dissertation auf verschiedenste Weise unterstützt haben:

Zu allererst möchte ich meinem Doktorvater Prof. Fuchs für die Möglichkeit danken, unter seiner Anleitung und Betreuung zu promovieren. Auf der einen Seite hatte ich viele Freiheiten, um mein Forschungsprojekt nach meinen Vorstellungen zu gestalten und mich in verschiedenen Dingen auszuprobieren, auf der anderen Seite standen Sie immer mit Rat und Tat zur Seite, um mich auf die richtige Bahn zu lenken und der Arbeit einen angemessenen Rahmen zu geben. Danke für die vielen anregenden Diskussionen und guten Ratschläge, unsere Zusammenarbeit verlief immer sehr angenehm und produktiv. Sie standen immer für Besprechungen zur Verfügung, auch nach Ihrem Umzug nach Jena. Vielen Dank auch für das Korrekturlesen der Arbeit und Ihre Verbesserungsvorschläge.

Mein Dank gilt auch Prof. Scherer, der mich diese Arbeit an seinem Lehrstuhl hat durchführen lassen und als Prüfungsvorsitzender zur Verfügung stand. Während meines Studium haben Ihre Vorlesungen meine Begeisterung für die Mikrobiologie geweckt und ich bin froh, dass ich die Möglichkeit hatte, die von Ihnen gelebte Begeisterung für Forschung zu erleben und zu verinnerlichen.

Ein herzliches Dankeschön an Prof. Zehn für die unkomplizierte Übernahme des Zweitprüfers trotz Ihres engen Terminplans.

Mein besonderer Dank gilt Dr. Stefanie Müller-Herbst. Du warst eine tolle Arbeitsgruppenleiterin, eine sehr angenehme Persönlichkeit und hast so viel zu meiner persönlichen und fachlichen Entwicklung beigetragen. Danke für all deine Hilfe und die vielen schönen Jahre!

Ich hatte die besondere Freude, Mitglied in gleich zwei Arbeitsgruppen zu sein, die beide wie eine kleine Familie waren: Danke an alle Personen aus der AG Müller-Herbst, insbesondere Anna Mühlig, bei der ich meine ersten Laborerfahrungen gemacht habe, und Elena Ferrari, die nicht nur eine tolle Unterstützung war, sondern auch eine gute Freundin ist. Ebenfalls Danke an die Füchse aus der AG Fuchs für fachliche Unterstützung und neue Freundschaften: Lena Staib, Tanja Kern, Nicoletta Nolle, Jessica Hellinckx und Katharina Springer. Ich bin auch dankbar für die vielseitige Unterstützung durch unsere TAs Katharina Sturm, Romy Wecko und Angela Felsl.

Das bringt mich zu den restlichen Mitarbeiten des Instituts: Danke für eine schöne Zeit und die tolle Hilfe. Tatkräftige Unterstützung erhielt ich auch durch meine Bachelorstudenten und Forschungspraktikanten, die an vielen Ergebnissen aus dieser Arbeit ihren Anteil hatten: Lena Riedl, Michael Schneider, Kevin Korfmann, Melanie Schoof, Regina Rettenmaier und Kerstin Schmidt.

A very special thank you to all the Kentuckians. Sarah D'Orazio, I am very grateful that you gave me the opportunity to come to Lexington, Kentucky and learn a completely new set of skills. I don't think my dissertation would've been successful without your help and the results that I obtained in your lab. A big thank you also to Michelle Pitts for the nice trips to the horse breeding farms and for the help with the liver and spleen samples! Most of all, I must thank Grant Jones for the help with the experiments and the linguistic corrections for my thesis. You dedicated so much time and effort to this project. You are an immense help and an even better friend, I had a wonderful time with you in Kentucky.

Eine besondere Erfahrung war auch die Mitgliedschaft im GRK 1482. Danke Dorothea Wörner für deine Hilfe bei allen organisatorischen und finanziellen Fragen und Problemen! Danke auch an alle Stipendiaten des GRKs, insbesondere Kathi, Maren, Patrick und Marcel.

Danke auch an meine Familie und Freunde, die mich auch in schlechten Zeiten immer unterstützt haben, insbesondere an meine Mama und mein Papa, sowie an meine Schwestern Sarah, Hannah und Dinah.

Zu guter Letzt: Danke Scharifa! Du hast mich vier Jahre lang in guten wie in schlechten Zeiten begleitet. Zusammen haben wir alle Hürden gemeistert. Ich bin dankbar für unsere gemeinsame Zeit und die Entwicklung die wir beide durchlaufen haben. Team Schakki for the win!

6.2 List of publications

Publications

- **Schardt, J.**, Jones G., Müller-Herbst S., Schauer K., D'Orazio S., Fuchs T. (2017): Comparison between *Listeria sensu stricto* and *Listeria sensu lato* strains identifies novel determinants involved in infection. *Scientific Reports*. Dec 19; 7(1):17821
- Kaspar D., Auer F., **Schardt J.**, Schindele F., Ospina A., Held C., Ehrenreich A., Scherer S., Müller-Herbst S. (2014): Temperature- and nitrogen source-dependent regulation of GlnR target genes in *Listeria monocytogenes*. *FEMS Microbiology Letters.* 355(2): 131-141
- Kabisch J., Schardt J., Brinks E., Rust F., Müller-Herbst S., Böhnlein C., Franz C., Habermann D. (2018): *Listeria kieliensis* sp. nov., isolated from a wastewater treatment plant in Germany. (Manuscript in preparation)
- Nolle, N., Clavel T., Zehn D., **Schardt J.**, Fuchs T. M. (2018): Influence of the host diet on the transcriptome of *Salmonella* Typhimurium and the microbiota of the mouse gut. (Manuscript in preparation)

Conference papers

- Poster presentation at the 7th Congress of European Microbiologists (FEMS), 09.07.-13.07.2017, Valencia (Spain):
  Schardt J., Scherer S., Müller-Herbst S., Fuchs T.: *Listeria sensu strictu* specific genes are important for *in vivo* colonization of *Listeria monocytogenes* in a foodborne mouse model.
- Oral presentation at the German Veterinary Society (DVG) Congress Section Bacteriology and Mycology, 31.08.-02.09.2016, Jena (Germany):
  Schardt J., Scherer S., Müller-Herbst S., Fuchs T: Vergleich der Kolonisierungsfähigkeit verschiedene *Listeria* Spezies im oralen Mausmodell.
- Poster presentation at the EMBO Conference "International Symposium on Problems of Listeriosis" (ISOPOL XIX), 14.06.-17.06.2016, Paris (France):
  Schardt J., Schindele F., Scherer S., Müller-Herbst S.: Temperature- and nitrogen source-dependent growth of *Listeria monocytogenes* implicates an important role of 2-oxoglutarate as internal signal during adaptation to changing environments.

- Poster presentation at the 6th Congress of European Microbiologists (FEMS), 07.06.-11.06.2015, Maastricht (Netherlands):

  Schardt J., Schindele F., Scherer S., Müller-Herbst S.: Temperature- and nitrogen source-dependent growth of *Listeria monocytogenes* implicates an important role of 2-oxoglutarate as internal signal during adaptation to changing environments.

- Poster presentation at the 4th Joint Conference of the Association for General and Applied Microbiology (VAAM) and the Society of Hygiene and Microbiology (DGHM), 5.10.-8.10. 2014, Dresden (Germany):

  Schardt J., Schindele F., Scherer S., Müller-Herbst S.: Temperature- and nitrogen source-dependent growth of *Listeria monocytogenes* implicates an important role of 2-oxoglutarate as internal signal during adaptation to changing environments.

Parts of this thesis have already been published in:

Schardt, J., Jones G., Müller-Herbst S., Schauer K., D'Orazio S., Fuchs T. (2017): Comparison between *Listeria sensu stricto* and *Listeria sensu lato* strains identifies novel determinants involved in infection. *Scientific Reports*. Dec 19; 7(1):17821

6.3 *Curriculum vitae*

Personal details

Name	Jakob Johannes Schardt
Address	Lerchenauerstraße 30b, 80809 Munich
Date of birth	11.11.1987
Place of birth	Munich
Nationality	German

Education

04/2014 – 12/2017	PhD candidate (Dr. rer. nat) at the Technical University Munich Chair for Microbial Ecology ZIEL - Institute for Food and Health Research Training Group GRK 1482
10/2011 – 03/2014	Molecular Biotechnology at the Technical University Munich Master of Science (M. Sc.)
10/2008 – 08/2011	Molecular Biotechnology at the Technical University Munich Bachelor of Science (B. Sc.)
08/1998 – 07/2007	Staatliches Gymnasium München-Moosach (High School) Staatliche Hochschulreife (Higher education entrance qualification)

Grants

04/2014	Scholarship in the Research Training Group (Graduiertenkolleg) GRK 1482: “Interface functions of the intestine between luminal factors and host signals.”

6.4 Eidesstattliche Erklärung

Ich erkläre an Eides statt, dass ich die bei der promotionsführenden Einrichtung

„Fakultät Wissenschaftszentrum Weihenstephan für Ernährung, Landnutzung und Umwelt“

der TUM zur Promotionsprüfung vorgelegte Arbeit mit dem Titel

“Characterization of *Listeria sensu stricto* specific genes involved in colonization of the gastrointestinal tract by *Listeria monocytogenes*”

am **Lehrstuhl für Mikrobielle Ökologie, Zentralinstitut für Ernährungs- und Lebensmittelforschung, Technische Universität München**

unter der Anleitung und Betreuung durch

Herrn Prof. Dr. Thilo M. Fuchs

ohne sonstige Hilfe erstellt und bei der Abfassung nur die gemäß § 6 Abs. 6 und 7 Satz 2 angegebenen Hilfsmittel benutzt habe.

Ich habe keine Organisation eingeschaltet, die gegen Entgelt Betreuerinnen und Betreuer für die Anfertigung von Dissertationen sucht, oder die mir obliegenden Pflichten hinsichtlich der Prüfungsleistungen für mich ganz oder teilweise erledigt.

Ich habe die Dissertation in dieser oder ähnlicher Form in keinem anderen Prüfungsverfahren als Prüfungsleistung vorgelegt.

Ich habe den angestrebten Doktorgrad noch nicht erworben und bin nicht in einem früheren Promotionsverfahren für den angestrebten Doktorgrad endgültig gescheitert.

Die öffentlich zugängliche Promotionsordnung der TUM ist mir bekannt, insbesondere habe ich die Bedeutung von § 28 (Nichtigkeit der Promotion) und § 29 (Entzug des Doktorgrades) zur Kenntnis genommen. Ich bin mir der Konsequenzen einer falschen Eidesstattlichen Erklärung bewusst.

Mit der Aufnahme meiner personenbezogenen Daten in die Alumni-Datei bei der TUM bin ich einverstanden.

München, den 15.01.2018

Jakob Schardt